

**The Role of the JNK/AP-1 Pathway in  
the Induction of iNOS and CATs in  
Vascular Cells**

**M Zamani**

**PhD**

**2011**

**The Role of the JNK/AP-1 Pathway in  
the Induction of iNOS and CATs in  
Vascular Cells**

**Marzieh Zamani**

**Submitted to the University of Hertfordshire in  
partial fulfilment of the requirements of the  
degree of PhD**

**August 2011**

## Abstract

Nitric oxide (NO) is an important biological molecule within the body, which over production of this molecule in response to different stimulations can cause various inflammatory diseases. Over production of this molecule is caused by the induction of the inducible nitric oxide synthase (iNOS) enzyme. This enzyme uses L-arginine as a substrate and therefore the presence and transport of this amino acid into the cells can be a key factor in regulating NO over production.

Different signalling mechanisms have been implicated in the regulation of this pathway and one of which involves the Mitogen Activated Protein Kinases (MAPK). This family of proteins respond to inflammatory conditions and may mediate effects induced by inflammatory mediators. Of the MAPKs, the role of the c-Jun-N-terminal kinase (JNK) pathway in the induction of iNOS is still controversial. JNK and its downstream target, the transcription factor Activator Protein-1 (AP-1), have shown contradictory effects on iNOS induction leading to controversies over their role in regulating iNOS expression in different cell systems or with various stimuli.

The studies described in this thesis have determined the role of JNK/AP-1 on iNOS expression, NO production, L-arginine uptake and also on the transporters responsible for L-arginine transport into the cells. The studies were carried out in two different cell types: rat aortic smooth muscle cells (RASMCs) and J774 macrophages which are both critically associated with the over production of NO in vascular inflammatory disease states.

The first approach was to block the expression of the inducible L-arginine-NO pathway using SP600125 and JNK Inhibitor VIII which are both pharmacological

inhibitors of JNK. The results from these studies showed that the pharmacological intervention was without effect in RASMCs, but inhibited iNOS, NO and L-arginine transport in J774 macrophages. In contrast, the molecular approach employed using two dominant negative constructs of AP-1 (TAM-67 and a-Fos) revealed a different profile of effects in RASMCs, where a-Fos caused an induction in iNOS and NO while TAM-67 had an inhibitory effect on iNOS, NO, L-arginine transport and CAT-2B mRNA expression. The latter was unaffected in RASMCs but suppressed in J774 macrophages by SP600125.

Examination of JNK isoforms expression showed the presence of JNK1 and 2 in both cell systems. Moreover, stimulation with LPS/IFN- $\gamma$  or LPS alone resulted in JNK phosphorylation which did not reveal any difference between smooth muscle cells and macrophages. In contrast, expression and activation of AP-1 subunits revealed differences between the two cell systems.

Activation of cells with LPS and IFN- $\gamma$  (RASMCs) or LPS alone (J774 macrophages) resulted in changes in the activated status of the different AP-1 subunit which was different for the two cell systems. In both cell types c-Jun, JunD and Fra-1 were increased and in macrophages, FosB activity was also enhanced. Inhibition of JNK with SP600125 caused down-regulation in c-Jun in both cell types. Interestingly this down-regulation was in parallel with increases in the subunits JunB, JunD, c-Fos and Fra-1 in RASMCs or JunB and Fra-1 in J774 macrophages. Since, SP600125 was able to exert inhibitory effects in the latter cell type but not in RASMCs, it is possible that the compensatory up-regulation of certain AP-1 subunits in the smooth muscle cells may compensate for c-Jun inhibition thereby preventing suppression of iNOS expression. This notion clearly needs to be confirmed but it is potentially likely that

hetero-dimers formed between JunB, JunD, c-Fos and Fra-1 could sustain gene transcription in the absence of c-Jun. The precise dimer required has not been addressed but unlikely to exclusively involve JunB and Fra-1 as these are up-regulated in macrophages but did not sustain iNOS, NO or induced L-arginine transport in the presence of SP600125.

To further support the argument above, the dominant negatives caused varied effects on the activation of the different subunits. a-Fos down-regulated c-Jun, c-Fos, FosB, Fra-1 whereas TAM-67 reduced c-Jun and c-Fos but marginally induced Fra-1 activity. Associated with these changes was an up-regulation of iNOS-NO by a-Fos and inhibition by TAM-67.

Taken together, the data proposes a complex mechanism(s) that regulate the expression of the inducible L-arginine-NO pathway in different cell systems and the complexity may reflect diverse intracellular changes that may be different in each cell type and not always be apparent using one experimental approach especially where this is pharmacological. Moreover, these findings strongly suggest exercising caution when interpreting pure pharmacological findings in cell-based systems particularly where these are inconsistent or contradictory.

## **Acknowledgements**

It would not have been possible to write this thesis without the help and support of the kind people around me, to only some of whom it is possible to give particular mention here.

I would like to express my deep and sincere gratitude to my principal supervisor, Professor Anwar Baydoun without whom this thesis would not have been possible and who tirelessly supported me through the ups and downs of this PhD. The friendship and support of my second supervisor Dr Shori Thakur has also been invaluable to me.

I wish to express my warm and sincere thanks to Professor Robert Slater, head of department of life sciences, for the support and the opportunity to conduct research at this institution.

I would also like to thank my colleagues with whom I have worked during the course of this PhD and I have many fond memories of working with them. To mention some of them, I'd like to thank Dr. Alexandra Nunes Costa, Dr. Peter Humphrey, Dr. Tamer Rabie, Edmund Garr, Hema pramod, Ashish Patidar, Sanil Bhatia, Yogesh Kamra and also to all the Technicians in the Life Science Department.

I would like to dedicate this work to my parents who supported and encouraged me throughout my life. Also special thanks to my beloved husband Daniel Bassiri for his encouragement, support and patience throughout the course of this PhD.

I thank you all and will always keep you in my heart and in my life.

## Table of contents

<b>Abbreviations.....</b>	<b>1</b>
<b>Chapter 1, Introduction.....</b>	<b>5</b>
1.1 Characteristics of nitric oxide .....	6
1.2 Physiological properties of Nitric oxide.....	9
1.3 Pathophysiological properties of Nitric oxide .....	10
1.4 Physiological and pathophysiological target for NO.....	12
1.5 Biosynthesis of Nitric oxide from L-arginine .....	14
1.6 Nitric oxide synthase.....	17
1.7 Inducible nitric oxide synthase (iNOS).....	19
1.8 Importance of altered NO production in human diseases and therapeutic strategies based on regulation of NO production.....	21
1.9 Regulation of iNOS activity .....	26
1.10 L-arginine.....	26
1.11 L-arginine transport system.....	29
1.12 Cationic amino acid transporters (CATs).....	29
1.13 Regulation of iNOS and CAT gene expression .....	32
1.14 c-Jun-N-terminal kinase (JNK) pathway .....	34
1.15 AP-1.....	42
1.16 Transcriptional Regulation of AP-1 family members.....	45
1.17 Aims.....	48
<b>Chapter 2, Methods.....</b>	<b>50</b>

2.1	Cell Culture.....	51
2.1.1	Preparation of complete cell culture growth medium .....	51
2.1.2	Culture of J774 macrophages .....	51
2.1.3	Isolation of Rat Aortic Smooth Muscle Cells (RASMCs) .....	51
2.1.4	Sub-culturing of rat aortic smooth muscle cells.....	52
2.1.5	Identification of Smooth Muscle Cells .....	52
2.1.6	Determination of cell number.....	53
2.1.7	Plating of cells for experimentation.....	54
2.2	Experimental Protocols .....	55
2.2.1	Regulation of nitric oxide production by drug treatment.....	56
2.2.2	Determination of nitrite production by the Griess assay .....	56
2.2.3	Protein quantification using Bicinchoninic acid (BCA) .....	59
2.2.4	Measurement of [ <sup>3</sup> H]L-arginine transport .....	62
2.2.5	Determination of cell viability by the MTT assay .....	63
2.2.6	Western blotting .....	65
2.2.7	Stripping the western blot membrane .....	67
2.2.8	Preparation of DH5-α Competent <i>E.coli</i> .....	67
2.2.9	Transformation of <i>E.Coli</i> DH5-α with dominant negative GFP-a-Fos or GFP-TAM-67.....	68
2.2.10	Mini-scale preparation of plasmid DNA (mini-preps) .....	69
2.2.11	Preparation of 0.8% agarose for mini-gel .....	70

2.2.12 Determination of DNA yield .....	70
2.2.13 Digestion of plasmids by restriction enzymes .....	71
2.2.14 Transfection of RASMCs with dominant negative GFP-a-Fos and GFP-TAM-67 .....	71
2.2.15 Isolation of total RNA .....	72
2.2.16 RNA treatment and purification .....	73
2.2.17 Quantification of isolated RNA .....	74
2.2.18 Reverse Transcription .....	75
2.2.19 PCR Primer design .....	77
2.2.20 Polymerase Chain Reaction (PCR) .....	80
2.2.21 Analysing PCR data .....	82
2.2.22 Preparation of Nuclear Extract .....	90
2.2.23 Analysis of AP-1 activation using the TransAM AP-1 kit .....	90
2.3 Analysis of data .....	93

**Chapter 3, Results.....95**

**Effects of JNK/AP-1 inhibition on the expression profile of the inducible L-arginine-nitric oxide pathway in rat cultured aortic smooth muscle cells and the murine J774 macrophages**

<b>3.1 Introduction .....</b>	<b>96</b>
<b>3.2 Methods .....</b>	<b>99</b>
3.2.1 Time course of iNOS gene expression, protein induction and NO production in RASMCs and J774 macrophages.....	99

3.2.2 Effect of different stimuli on iNOS gene expression, protein induction and NO production in J774 macrophages.....	100
3.2.3 Effect of SP600125 and JNK inhibitor VIII on nitric oxide production, iNOS expression and L-arginine transport in RASMCs and J774 macrophage.	100
3.2.4 Effect of SP600125 and JNK inhibitor VIII on cell viability in RASMCs and J774 macrophages.....	101
3.2.5 Generation of Mini-preps of pGFP-a-Fos and pGFP-TAM-67.....	101
3.2.6 Expression profile of p-GFP-a-Fos and pGFP-TAM-67 transfected into RASMCs.....	102
3.2.7 Effect of pGFP-a-Fos and p-GFP-TAM-67 on LPS and IFN- $\gamma$ induced nitric oxide production, iNOS expression and L-[ $^3$ H]-arginine transport in RASMCs.....	102
3.2.8 The effect of SP600125 on iNOS mRNA expression in RASMCs and J774 macrophages.....	103
3.2.9 Effect of a-Fos and TAM-67 on iNOS mRNA expression in RASMCs...	103
<b>3.3 Results.....</b>	<b>104</b>
3.3.1 Identification and biochemical characterization of Rat Aortic Smooth Muscle Cells (RASMCs).....	104
3.3.2 Time course of iNOS gene and protein expression and NO production in RASMCs and J774 macrophages.....	106
3.3.3 Effect of different stimuli on iNOS gene and protein expression and NO production in J774 macrophages.....	113
3.3.4 Effect of SP600125 on nitric oxide production in RASMCs.....	117
3.3.5 Effect of SP600125 on iNOS expression in RASMCs.....	117
3.3.6 Effect of SP600125 on L-[ $^3$ H]-arginine transport in RASMCs.....	117

3.3.7 Effect of SP600125 on Cell viability in RASMCs.....	118
3.3.8 Effect of SP600125 on NO production in J774 macrophages.....	123
3.3.9 Effect of SP600125 on iNOS expression in J774 macrophages.....	123
3.3.10 Effect of SP600125 on L-[ <sup>3</sup> H]-arginine transport in J774 macrophages.	123
3.3.11 Effect of SP600125 on Cell viability in J774 macrophages.....	124
3.3.12 Effect of JNK Inhibitor VIII on NO production in RASMCs.....	129
3.3.13 Effect of JNK Inhibitor VIII on iNOS expression in RASMCs.....	129
3.3.14 Effect of JNK Inhibitor VIII on L-arginine transport in RASMCs.....	130
3.3.15 Effect of JNK Inhibitor VIII on Cell viability in RASMCs.....	130
3.3.16 Effect of JNK Inhibitor VIII on NO production in J774 macrophages.....	135
3.3.17 Effect of JNK Inhibitor VIII on iNOS expression in J774 macrophages..	135
3.3.18 Effect of JNK Inhibitor VIII on L-arginine transport in J774 macrophages.....	135
3.3.19 Effect of JNK Inhibitor VIII on Cell viability in J774 macrophages.....	136
3.3.20 Mini-preps of a-Fos and TAM-67 characterised by restriction digest.....	141
3.3.21 Expression profile of transfected pGFP-a-Fos and pGFP-TAM-67 plasmide in RASMCs.....	141
3.3.22 Effect of pGFP-a-Fos and pGFP-TAM-67 on LPS and IFN- $\gamma$ induced NO production in RASMCs.....	147
3.3.23 Effect of pGFP-a-Fos and pGFP-TAM-67 on LPS and IFN- $\gamma$ induced iNOS expression in RASMCs.....	147
3.3.24 Effect of pGFP-a-Fos and pGFP-TAM-67 on LPS and IFN- $\gamma$ induced L- arginine transport in RASMCs.....	148

3.3.25 Effect of SP600125 on iNOS gene expression in RASMCs.....	155
3.3.26 Effect of SP600125 on iNOS gene expression in J774 macrophages....	155
3.3.27 Effect of pGFP-a-Fos and pGFP-TAM-67 on LPS and IFN- $\gamma$ induced iNOS gene expression in RASMCs.....	156
<b>3.4 Discussion.....</b>	<b>161</b>
<b>3.5 Summary.....</b>	<b>171</b>
<b>Chapter 4, Results.....</b>	<b>172</b>
<b>The expression profile of Cationic Amino acid Transporters and their regulation by JNK/AP-1 inhibition</b>	
<b>4.1 Introduction.....</b>	<b>174</b>
<b>4.2 Methods.....</b>	<b>176</b>
4.2.1 Time course of CAT gene expression in RASMCs and J774 macrophages.....	176
4.2.2 Effect of different stimuli on CAT gene expression in J774 macrophages.....	176
4.2.3 Effect of SP600125 on CAT gene expression in RASMCs and J774 macrophages.....	177
4.2.4 Effect of a-Fos and TAM-67 on CAT gene expression in RASMCs.....	177
<b>4.3 Results.....</b>	<b>178</b>
4.3.1 Time course of CAT mRNA expression induced by LPS and IFN- $\gamma$ in RASMCs.....	178
4.3.2 Time course of CAT mRNA expression induced by LPS in J774 macrophages.....	179

4.3.3	Effect of different stimuli on CATs mRNA expression in J774 macrophages.....	180
4.3.4	Effect of SP600125 on CAT gene expression in RASMCs and J774 macrophages.....	193
4.3.5	Effect of a-Fos and TAM-67 on CAT gene expression in RASMCs.....	200
4.4	<b>Discussion</b> .....	<b>207</b>
4.5	<b>Summary</b> .....	<b>215</b>
 <b>Chapter 5, Results</b> .....		<b>216</b>
 <b>The expression and activation profile of JNK isoforms and AP-1 subunits in RASMCs and J774 macrophages</b>		
5.1	<b>Introduction</b> .....	<b>217</b>
5.2	<b>Methods</b> .....	<b>211</b>
5.2.1	Detection of JNK1, JNK2 and phospho-JNK expression in RASMCs and J774 macrophages.....	219
5.2.2	Effect of SP600125 on JNK phosphorylation status in RASMCs and J774 macrophages.....	219
5.2.3	Expression profile of AP-1 subunits in RASMCs and J774 macrophages stimulated with LPS/IFN- $\gamma$ or LPS.....	220
5.2.4	The effect of JNK inhibitor (SP600125) on the activity of AP-1 subunits in RASMCs and J774 macrophages.....	220

5.2.5 The effect of pGFP-a-Fos and pGFP-TAM-67 on the activation of AP-1 subunits in RASMCs.....	221
<b>5.3 Results.....</b>	<b>232</b>
5.3.1 Detection of JNK1, JNK2 and phospho-JNK expression in RASMCs.....	232
5.3.2 Effect of SP600125 on JNK phosphorylation status in RASMCs.....	232
5.3.3 Detection of JNK1, JNK2 and phospho-JNK in J774 macrophages.....	233
5.3.4 The effect of SP600125 on JNK phosphorylation status in J774 macrophages.....	233
5.3.5 Expression profile of AP-1 subunits in activated RASMCs and J774 macrophages.....	234
5.3.6 The effect of JNK inhibition on AP-1 subunits activity in RASMCs and J774 macrophages.....	248
The effect of a-Fos and TAM-67 on activation of AP-1 subunits in RASMCs....	263
<b>5.4 Discussion.....</b>	<b>278</b>
<b>5.5 Summary.....</b>	<b>299</b>
<b>Chapter 6, General Discussion .....</b>	<b>300</b>
<b>Future Work.....</b>	<b>317</b>
<b>References .....</b>	<b>318</b>
<b>Appendix.....</b>	<b>376</b>

## List of figures

### Introduction

Figure 1.1 Chemistry of nitric oxide.....	8
Figure 1.2 Physiological and pathophysiological effects of nitric oxide.....	11
Figure 1.3 Physiological and deleterious effects of the NO–sGC–cGMP signalling pathway .....	13
Figure 1.4 Synthesis of nitric oxide from L-arginine.....	16
Figure 1.5 Beneficial and detrimental effects of iNOS.....	20
Figure 1.6 Arginine metabolism.....	28
Figure 1.7 JNK and AP-1 activation.....	41
Figure 1.8 AP-1 transcription dimmers.....	44
Figure 1.9 Activation of activator protein-1 (AP-1) and its potential actions.....	47

### Methods

Figure 2.1 Detection of $\text{NO}_2^-$ in solution by the Griess assay .....	57
Figure 2.2 A representative nitrite standard curve.....	58
Figure 2.3 Protein detection by the BCA method.....	60
Figure 2.4 A representative protein standard curve.....	61
Figure 2.5 Detection of formazan by viable cells.....	64
Figure 2.6 Agarose gel electrophoresis of RNA isolates from RASMCs and J774 macrophages.....	76

Figure 2.7 Structure of SYBR green.....	81
Figure 2.8 The standard curve, amplification curve and crossing points of the PCR.....	85
Figure 2.9 The dissociation curve and background correction.....	87
Figure 2.10 Amplification curve.....	89
Figure 2.11 The mechanism of TransAM AP-1 family kit.....	92

### **Chapter 3, Results**

#### **The expression profile of inducible L-arginine-nitric oxide pathway and effect of JNK/AP-1 inhibition**

Figure 3.1.1 AP-1 Dominant negatives constructs .....	98
Figure 3.1 Morphology and $\alpha$ -actin staining of RASMCs.....	105
Figure 3.2 iNOS gene expression profile in RASMCs.....	107
Figure 3.3 iNOS protein expression profile in RASMCs.....	108
Figure 3.4 Nitrite production profile in RASMCs.....	109
Figure 3.5 iNOS gene expression profile in J774 macrophages .....	110
Figure 3.6 iNOS induction profile in J774 macrophages .....	111
Figure 3.7 Nitrite production profile in J774 macrophages.....	112
Figure 3.8 Effects of LPS, IFN- $\gamma$ and a combination of both on iNOS gene expression in J774 macrophages .....	114
Figure 3.9 Effects of LPS, IFN- $\gamma$ and a combination of both on iNOS protein expression in J774 macrophages .....	115

Figure 3.10 Effects of LPS, IFN- $\gamma$ and a combination of both on Nitrite production in J774 macrophages .....	116
Figure 3.11 Effect of SP600125 on NO production in RASMCs .....	117
Figure 3.12 Effect of SP600125 on iNOS expression in RASMCs .....	120
Figure 3.13 Effect of SP600125 on L-[ <sup>3</sup> H]-arginine transport in RASMCs .....	121
Figure 3.14 Effect of SP600125 on Cell viability in RASMCs .....	122
Figure 3.15 Effect of SP600125 on NO production in J774 macrophages .....	123
Figure 3.16 Effect of SP600125 on iNOS expression in J774 macrophages.....	124
Figure 3.17 Effect of SP600125 on L-arginine transport in J774 macrophages....	125
Figure 3.18 Effect of SP600125 on Cell viability in J774 macrophages.....	128
Figure 3.19 Effect of JNK Inhibitor VIII on NO production in RASMCs.....	131
Figure 3.20 Effect of JNK Inhibitor VIII on iNOS expression in RASMCs.....	132
Figure 3.21 Effect of JNK Inhibitor VIII on L-arginine transport in RASMCs.....	133
Figure 3.22 Effect of JNK Inhibitor VIII on Cell viability in RASMCs.....	134
Figure 3.23 Effect of JNK Inhibitor VIII on NO production in J774 macrophages..	137
Figure 3.24 Effect of JNK Inhibitor VIII on iNOS expression in J774 macrophages.....	138
Figure 3.25 Effect of JNK Inhibitor VIII on L-arginine transport in J774 macrophages.....	139
Figure 3.26 Effect of JNK Inhibitor VIII on Cell viability in J774 macrophages.....	140
Figure 3.27 Mini-preps of non-restricted and restricted $\alpha$ -Fos and TAM-67.....	141
Figure 3.28 Expression of GFP in time course study of transfected pGFP- $\alpha$ -Fos and pGFP-TAM-67 in RASMCs.....	143

Figure 3.29 Visualisation of Transfected RASMCs with pGFP-a-Fos and pGFP-TAM-67 at 18 hours.....	136
Figure 3.30 Effect of pGFP-a-Fos and pGFP-TAM-67 on LPS and IFN- $\gamma$ induced NO production in RASMCs.....	150
Figure 3.31 Effect of pGFP-a-Fos and pGFP-TAM-67 on LPS and IFN- $\gamma$ induced iNOS expression in RASMCs.....	152
Figure 3.32 Effect of pGFP-a-Fos and pGFP-TAM-67 on LPS and IFN- $\gamma$ induced L-arginine transport in RASMCs.....	154
Figure 3.33 The effect of SP600125 on iNOS gene expression in RASMCs.....	157
Figure 3.34 The effect of SP600125 on iNOS gene expression in J774 macrophages.....	158
Figure 3.35 The effect of pGFP-a-Fos construct on iNOS expression in LPS/IFN- $\gamma$ stimulated RASMCs.....	159
Figure 3.36 The effect of pGFP-TAM-67 construct on iNOS expression in LPS/IFN- $\gamma$ stimulated RASMCs.....	160

## **Chapter 4, Results**

### **The expression profile of Cationic Amino acid Transporters and effect of JNK/AP-1 inhibition**

Figure 4.1 Representative association curves for CAT-1, CAT-2A and CAT-2B....	182
Figure 4.2 CAT-1 gene expression profile in RASMCs following treatment with LPS and IFN- $\gamma$ .....	183
Figure 4.3 Time course of CAT-2A gene expression induced by LPS and IFN- $\gamma$ in RASMCs.....	184

Figure 4.4 Time course of CAT-2B gene expression induced by LPS and IFN- $\gamma$ in RASMCs.....	185
Figure 4.5 Representative association curves for CAT-1, CAT-2A and CAT-2B....	187
Figure 4.6 CAT-1 gene expression profile in J774 macrophages following treatment with LPS.....	188
Figure 4.7 CAT-2A gene expression profile in J774 macrophages following treatment with LPS.....	189
Figure 4.8 CAT-2B gene expression profile in J774 macrophages following treatment with LPS.....	190
Figure 4.9 Effect of different stimuli on CAT gene expression in J774 macrophages.....	192
Figure 4.10 Effect of SP600125 on CAT-1 expression in RASMCs.....	194
Figure 4.11 Effect of SP600125 on CAT-2A expression in RASMCs.....	195
Figure 4.12 Effect of SP600125 on CAT-2B expression in RASMCs.....	196
Figure 4.13 Effect of SP600125 on CAT-1 expression in J774 macrophages.....	197
Figure 4.14 Effect of SP600125 on CAT-2A expression in J774 macrophages.....	198
Figure 4.15 Effect of SP600125 on CAT-2B expression in J774 macrophages.....	199
Figure 4.16 Effect of a-Fos and TAM-67 on CAT-1 gene expression in RASMCs..	202
Figure 4.17 Effect of a-Fos and TAM-67 on CAT-2A gene expression in RASMCs	204
Figure 4.18 Effect of a-Fos and TAM-67 on CAT-2B gene expression in RASMCs	206

## Chapter 5, Results

### The expression and activation profile of JNK isoforms and AP-1 subunits in RASMCs and J774 macrophages

Figure 5.1	Expression and activation of JNK in control and LPS/IFN- $\gamma$ activated RASMCs.....	225
Figure 5.2	The effect of SP600125 on JNK phosphorylation in RASMCs.....	227
Figure 5.3	The time point study of JNK phosphorylation following LPS activation of J774 macrophages.....	229
Figure 5.4	The effect of SP600125 on JNK phosphorylation in J774 macrophages.....	231
Figure 5.5	The effect of LPS/IFN- $\gamma$ stimulation on c-Jun activation in RASMCs.....	234
Figure 5.6	The effect of LPS/IFN- $\gamma$ stimulation on JunB activation in RASMCs.....	235
Figure 5.7	The effect of LPS/IFN- $\gamma$ stimulation on JunD activation in RASMCs.....	236
Figure 5.8	The effect of LPS/IFN- $\gamma$ stimulation on c-Fos activation in RASMCs.....	237
Figure 5.9	The effect of LPS/IFN- $\gamma$ stimulation on FosB activation in RASMCs.....	238
Figure 5.10	The effect of LPS/IFN- $\gamma$ stimulation on Fra-1 activation in RASMCs....	239
Figure 5.11	The effect of LPS/IFN- $\gamma$ stimulation on Fra-2 activation in RASMCs....	240
Figure 5.12	The effect of LPS stimulation on c-Jun activation in J774 macrophages.....	241
Figure 5.13	The effect of LPS stimulation on JunB activation in J774 macrophages.....	242
Figure 5.14	The effect of LPS stimulation on JunD activation in J774 macrophages.....	243
Figure 5.15	The effect of LPS stimulation on c-Fos activation in J774 macrophages.....	244

Figure 5.16 The effect of LPS stimulation on FosB activation in J774 macrophages.....	245
Figure 5.17 The effect of LPS stimulation on Fra-1 activation in J774 macrophages.....	246
Figure 5.18 The effect of LPS stimulation on Fra-2 activation in J774 macrophages.....	247
Figure 5.19 Effect of SP600125 on activation of c-Jun in RASMCs.....	249
Figure 5.20 Effect of SP600125 on activation of JunB in RASMCs.....	250
Figure 5.21 Effect of SP600125 on activation of JunD in RASMCs.....	251
Figure 5.22 Effect of SP600125 on activation of c-Fos in RASMCs.....	252
Figure 5.23 Effect of SP600125 on activation of FosB in RASMCs.....	253
Figure 5.24 Effect of SP600125 on activation of Fra-1 in RASMCs.....	254
Figure 5.25 Effect of SP600125 on activation of Fra-2 in RASMCs.....	255
Figure 5.26 Effect of SP600125 on activation of c-Jun in J774 macrophages.....	256
Figure 5.27 Effect of SP600125 on activation of JunB in J774 macrophages.....	267
Figure 5.28 Effect of SP600125 on activation of JunD in J774 macrophages.....	258
Figure 5.29 Effect of SP600125 on activation of c-Fos in J774 macrophages.....	259
Figure 5.30 Effect of SP600125 on activation of FosB in J774 macrophages.....	260
Figure 5.31 Effect of SP600125 on activation of Fra-1 in J774 macrophages.....	261
Figure 5.32 Effect of SP600125 on activation of Fra-2 in J774 macrophages.....	262
Figure 5.33 Effects of a-Fos on c-Jun activation in RASMCs.....	263
Figure 5.34 Effects of a-Fos on JunB activation in RASMCs.....	264
Figure 5.35 Effects of a-Fos on JunD activation in RASMCs.....	265

Figure 5.36 Effects of a-Fos on c-Fos activation in RASMCs.....	267
Figure 5.37 Effects of a-Fos on FosB activation in RASMCs.....	268
Figure 5.38 Effects of a-Fos on Fra-1 activation in RASMCs.....	269
Figure 5.39 Effects of a-Fos on Fra-2 activation in RASMCs.....	270
Figure 5.40 Effects of TAM-67 on c-Jun activation in RASMCs.....	271
Figure 5.41 Effects of TAM-67 on JunB activation in RASMCs.....	272
Figure 5.42 Effects of TAM-67 on JunD activation in RASMCs.....	273
Figure 5.43 Effects of TAM-67 on c-Fos activation in RASMCs.....	274
Figure 5.44 Effects of TAM-67 on FosB activation in RASMCs.....	275
Figure 5.45 Effects of TAM-67 on Fra-1 activation in RASMCs.....	276
Figure 5.46 Effects of TAM-67 on Fra-2 activation in RASMCs.....	277

## **Chapter6, General discussion**

Figure 6.1 The proposed role of different AP-1 subunits in the induction of iNOS expression in RASMCs and J774 macrophages.....	312
---	-----

## **List of Tables**

Table 1.1 iNOS isozymes.....	18
Table 1.2 Charasteristic of cationic amino acid transporters.....	31
Table 2.1 Rat primer sequences used in PCR analysis.....	78
Table 2.2 Mouse primer sequences used in PCR analysis.....	79

Table 5.1 The summary of subunits activation and their effect on iNOS expression and L-arginine transport in RASMCs.....	290
Table 5.2 The summary of subunits activation and their effect on iNOS expression and L-arginine transport in J774 macrophages.....	292

## **Abbreviations**

**Ab** – Antibody

**Abs** – Absorbance

**Akt** – Protein Kinase B

**AP-1** – Activator protein-1

**APS** – Ammonium persulfate

**ASL** – argininosuccinate lyase

**ASS** – argininosuccinate synthetase

**ATP** – Adenosine 5'-triphosphate

**ATF2** – Activating Transcription factor 2

**BCA** – Bicinchoninic Acid

**BH4** – Tetrahydrobiopterin

**BSA** – Bovine Serum Albumin

**CAM** – Calmodulin

**CAT** – Cationic Amino acid Transporter

**cDNA** – Complementary Deoxyribonucleic Acid

**cGMP** – cyclic adenosine monophosphate

**CREB** – cAMP responsive element binding protein

**Ct** – threshold cycle

**DDW** – Double Distilled Water

**DMEM** – Dulbecco's Modified Eagle's Medium

**DNA** – Deoxyribonucleic acid

**DPM** – Disintegrations Per Minute

**EDRF** – endothelium-derived relaxation factor

**ECL** – Enhanced chemiluminescence

**EDTA** – Ethylene Diamine Tetra Acetic Acid

**EGF** – epidermal growth factor

**eNOS** – endothelial Nitric Oxide Synthase

**ERK** – Extracellular signal Regulated Kinases

**FAD** – Flavin Adenine Nucleotide

**FBS** – Foetal Bovine Serum

**FITC** – Fluorescein isothiocyanate

**FMN** – Flavin Mononucleotide

**GTP** – Guanosine 5'-Triphosphate

**HEPES** – 4-(2-hydroxyethyl)-1-piperazine ethanesulphonic acid

**HRP** – Horse Radish Peroxidase

**IEGs** – immediate-early genes

**IFN- $\gamma$**  – Interferon-gamma

**IgG** – Immunoglobulin

**IK-BK** – inhibitory protein- $\kappa$ B

**IKK-1 and 2** – Cytokine-activated IKappa B Kinases

**IL-1** – Interleukin-1

**IL-18** – Interleukin-18

**IL-1 $\beta$**  – Interleukin-1beta

**iNOS** – inducible Nitric Oxide Synthase

**IRF** – IFN- $\gamma$  regulatory factor

**ISRE** – IFN-stimulated response element

**JNK** – c-Jun N-terminal Kinases

**Km** – Affinity constant (half maximal saturation constant)

**LPS** – Lipopolysaccharide

**MAPK** – Mitogen Activated Protein Kinases

**MEK** – Mitogen-activated ERK Kinase

**mRNA** – messenger Ribonucleic Acid

**MTT** – 3-(4,5-Dimethylthiazol-2-yl)-2,5-diphenyltetrazolium bromide

**NADPH** – Nicotinamide Adenine Dinucleotide Phosphate

**NCBI** – National Center for Biotechnology Information

**NF- $\kappa$ B** – Nuclear Factor-kappa B

**nNOS** – neuronal Nitric Oxide Synthase

**NOS** – Nitric Oxide Synthase

**PAK** – P21-Activated Kinase

**PBS** – Phosphate Buffered Saline

**PCR** – Polymerase Chain Reaction

**PDGF** – platelet-derived growth factor

**PI3K** – Phosphoinositide-3 Kinase

**PKC** – Protein Kinase C

**PMSF** – phenyl methyl sulfonyl fluoride

**PS** – Penicillin/Streptomycin

**PTPs** – protein tyrosine phosphatase

**PVDF** – Polyvinylidene difluoride

**p38 MAPK** – p38 Mitogen Activated Protein Kinase

**RASMC** – Rat Aortic Smooth Muscle Cells

**Ras** – family of genes encoding small GTPases

**RNA** – Ribonucleic Acid

**RPM** – Revolutions per minutes

**SAPK** – Stress Activated Protein Kinases

**S.E.M.** – Standard Error Mean

**SDS** – Sodium Dodecyl Sulphate

**SDS-PAGE** – Sodium Dodecyl Sulphate – Poly Acrylamide Gel Electrophoresis

**sGC** – soluble Guanylyl Cyclase

**SMC** – Smooth Muscle Cells

**TEMED** – NNN'N'-Tetramethylethylenediamine

**TF** – tissue factor

**TLR-4** – Toll-like receptor-4

**TNF- $\alpha$**  – Tumor Necrosis Factor-alpha

**TPA** – 12-O-tetradecanoylphorbol 13-acetate

**TRE** – TPA Responsive Elements

**TRIS Base** – Tris(hydroxymethyl)aminoethane

**U.V.** – Ultra Violet

**VSMC** – Vascular Smooth Muscle Cells

# **Chapter 1**

## **Introduction**

## Introduction

### 1.1 Characteristics of nitric oxide

Nitric oxide or nitrogen monoxide (NO) is an important intermediate in the chemical industry and a toxic air pollutant, as well as being an important signalling molecule in the body of mammals (Hou *et al.*, 1999).

Nitric oxide is probably one of the most studied molecules of the last 20 years. It is an important messenger molecule involved in many physiological and pathological conditions with both beneficial and detrimental role. The first biological role described for NO was as endothelial-derived relaxation factor in 1987 (Ignarro *et al.*, 1987; Palmer *et al.*, 1987). Nitric oxide is an uncharged molecule with an unpaired electron (Figure 1.1), which does not need any 'pharmacological' receptors for its actions and can diffuse freely across membranes. Its unpaired electron makes it a highly reactive molecule (Stamler *et al.*, 1992).

Nitric oxide has a short half life of between 4 and 50 seconds and due to its high reactivity forms intermediate molecules such as nitrogen dioxide (NO<sub>2</sub>), nitrite (NO<sub>2</sub><sup>-</sup>), and nitrate (NO<sub>3</sub><sup>-</sup>). It also reacts with free radicals such as superoxide (O<sub>2</sub><sup>-</sup>) to form other highly reactive species such as peroxynitrite (ONOO<sup>-</sup>) (Beckman *et al.*, 1990).

Nitric oxide is well known for its major roles in many physiological systems, for example, as a messenger and as a defence molecule in the immune system (Ignarro, 2000). Moreover, any abnormalities in NO synthesis may be associated with some disorders such as septic shock, high blood pressure, diabetes and neurodegenerative diseases (Hughes *et al.*, 2008).

While appropriate level of NO production may be critical in protecting organs such as the heart and liver from ischemic damage, its over production may result in direct tissue toxicity and contribute to the vascular collapse associated with, for instance, septic shock. Overproduction of NO may also be associated with various carcinomas and inflammatory conditions including diabetes, multiple sclerosis and arthritis (Taylor *et al.*, 1997).

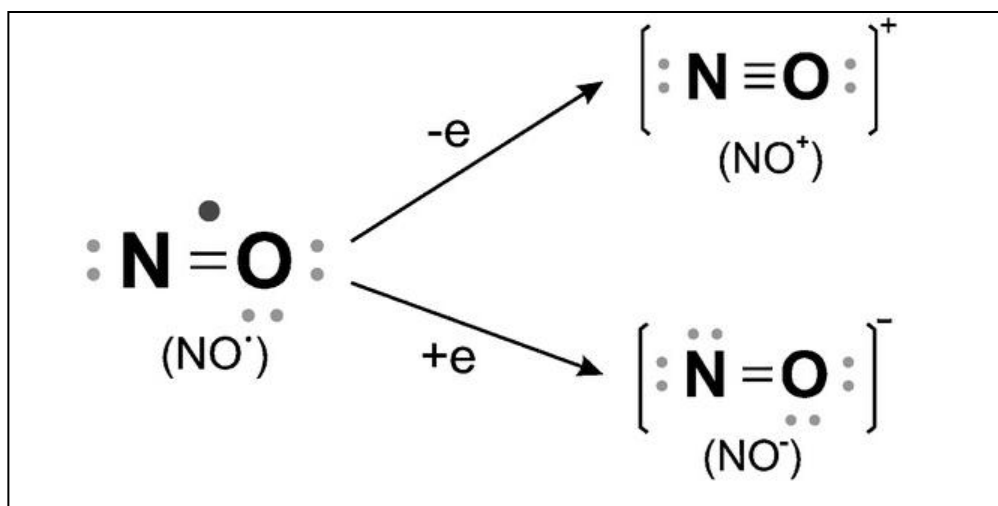


**Figure 1.1 Chemistry of nitric oxide**

Nitric oxide is rapidly oxidized by the removal of one electron to give nitrosonium cation ( $\text{NO}^+$ ), or reduced by the addition of one electron to form nitroxyl anion ( $\text{NO}^-$ ), which are important intermediates in the biochemistry of NO (Lamattina *et al.*, 2003).

## **1.2 Physiological properties of nitric oxide**

After the discovery of NO, there was a huge increase in our knowledge on the role of endothelium and nitric oxide in cardiovascular diseases. It is now accepted that NO derived from the vascular endothelium maintains a vasodilator tone which is essential for the regulation of blood flow and pressure. NO also has a role in the control of platelet aggregation and the regulation of cardiac development. Moreover NO also acts as a mediator in cell-cell communication in the brain. In the peripheral nervous system, release of NO from nerves classified as non-adrenergic and non-cholinergic maintains various gastrointestinal, respiratory and genitourinary tract functions (Moncada, 1997).

Most of the positive physiological functions of NO include regulation of vascular smooth muscle tone and vascular resistance. Low physiological concentration of NO has been shown to relax blood vessels, reduce vascular resistance and thus lower blood pressure (Rees *et al.*, 1989). Additionally, constitutively derived NO has also been shown to have a role in the protection against apoptosis (Kim *et al.*, 1991), wound repair (Frank *et al.*, 2002), contraction of skeletal muscle and cardiac development (Stamler *et al.*, 2001).

## **1.3 Pathophysiological properties of Nitric oxide**

While the physiological effects of NO like vasorelaxation and neuronal signalling are mostly mediated by the activation of guanylate cyclase, NO can also have damaging, even fatal effects. In the often fatal condition of septic shock, excessive production of NO in blood vessels can lead to vascular leakage and drop in blood pressure

(Maeda *et al.*, 1994; Nava *et al.*, 1991). In chronic diseases such as rheumatoid arthritis, NO contributes to tissue damage caused by an inappropriate inflammatory response (Bernardeau *et al.*, 2001; Sakurai *et al.*, 1995; St Clair *et al.*, 1996). In stroke, NO also contributes to brain damage (Iadecola *et al.*, 1997; Iadecola *et al.*, 1995; Nanri *et al.*, 1998).

In cytotoxic condition, it seems that NO directly or indirectly exerts its effect through the formation of more reactive oxidative species such as  $\text{ONOO}^-$ . This molecule is a powerful oxidant that exhibits a wide range of tissue damaging effects including nitration of proteins, inactivation of various enzymes and ion channels via protein oxidation (Beckman *et al.*, 1996).

The different physiological and pathophysiological effects of NO may be dependent on its concentration in the tissue. At low concentrations, those normally achieved after stimulation of constitutively expressed isoforms (NOS1 and NOS3), NO can modulate the activity of heme-containing proteins, such as guanylyl cyclase, and also important proteins of the mitochondria including the cytochromes. It is also able to regulate certain transcription factors like hypoxia inducible factor (HIF-1). At higher concentrations, usually produced by the inducible isoform (NOS2) NO can nitrosylate cysteine residues or produce tyrosine nitration in different proteins. In some cases, DNA deamination have been observed (Agulló; 2007). These effects are summarised in Figure 1.2.

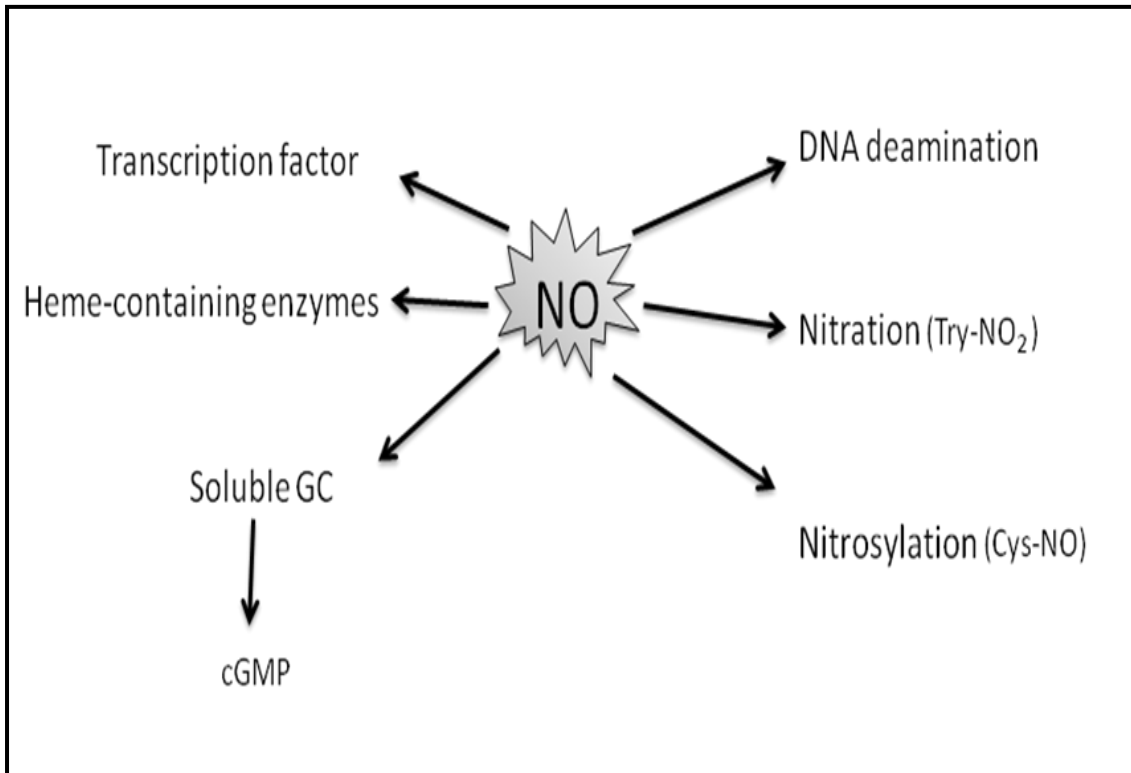


**Figure 1.2 Physiological and pathophysiological effects of nitric oxide**

#### 1.4 Physiological and pathophysiological target for NO

Nitric oxide has been shown to have several targets in biological system. Among these targets, soluble guanylate cyclase (sGC) may be the most important (Ignarro, 1991; Ishii *et al.*, 1990; Russwurm *et al.*, 2002) and converts GTP to cyclic GMP (cGMP), mediating various physiological and tissue protective effects (Arnold *et al.*, 1977; Durner *et al.*, 1998; Stamler, 1994). NO–sGC–cGMP signalling can be compromised either by reducing the bioavailability of NO or by altering the activity of sGC. The latter could be mediated through oxidative stress or the action of ONOO<sup>-</sup> which could make sGC unresponsive to endogenous NO (Evgenov *et al.*, 2006). Some of the physiological and adverse effects of NO are summarised in Figure 1.3 and Figure 1.5 below.

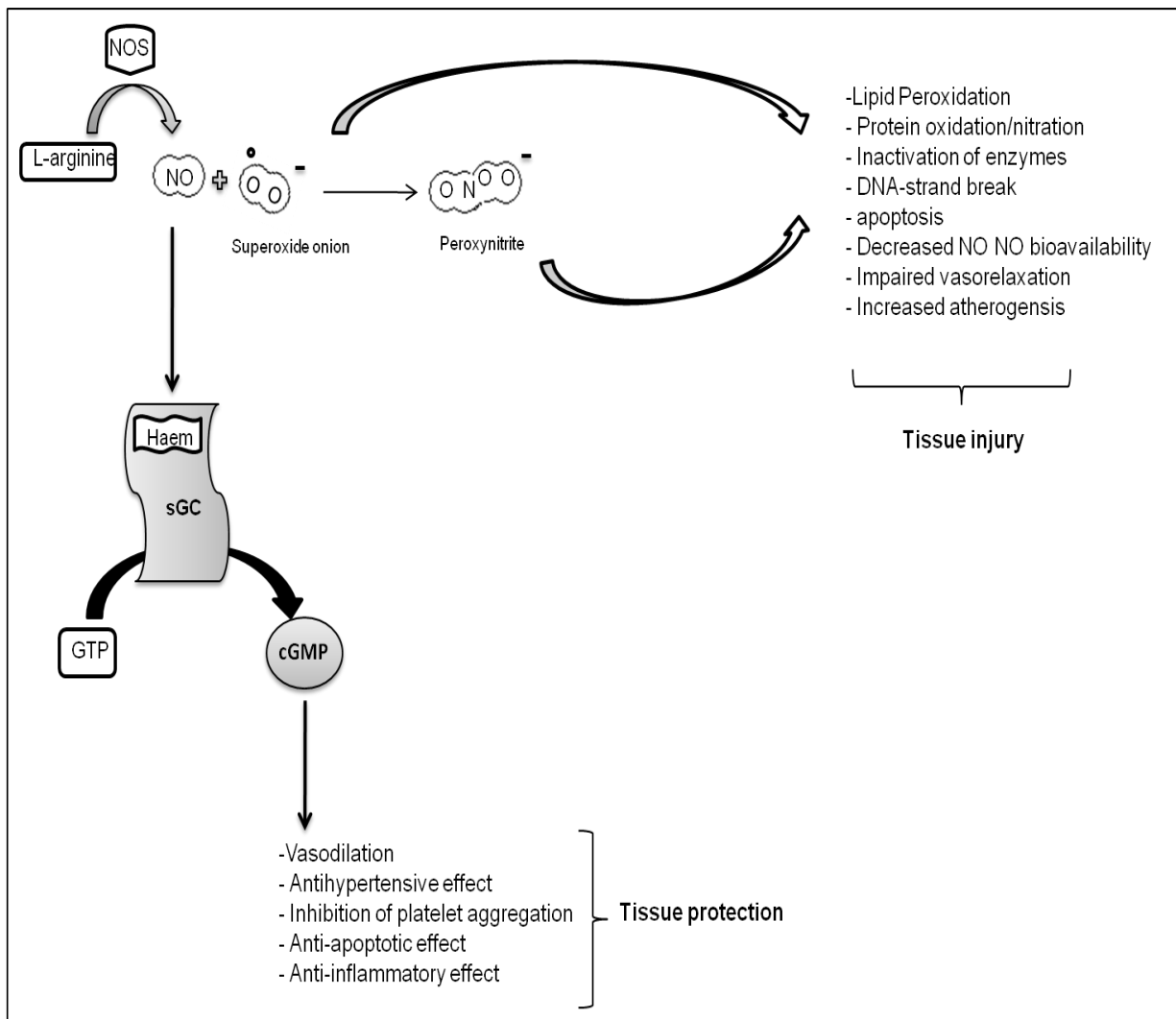


**Figure 1.3 Physiological and deleterious effects of the NO signalling pathway**

Nitric oxide activates guanylate cyclase by combining with the haem group in the enzyme. Activation of sGC would convert GTP to cGMP and increase cGMP in vessel walls which will result in the various physiological effects shown in the diagram. In contrast, interaction of NO with  $O_2^-$  results in the formation of peroxynitrite which can induce a multitude of deleterious effects in cells and tissues (Evgenov *et al.*, 2006).

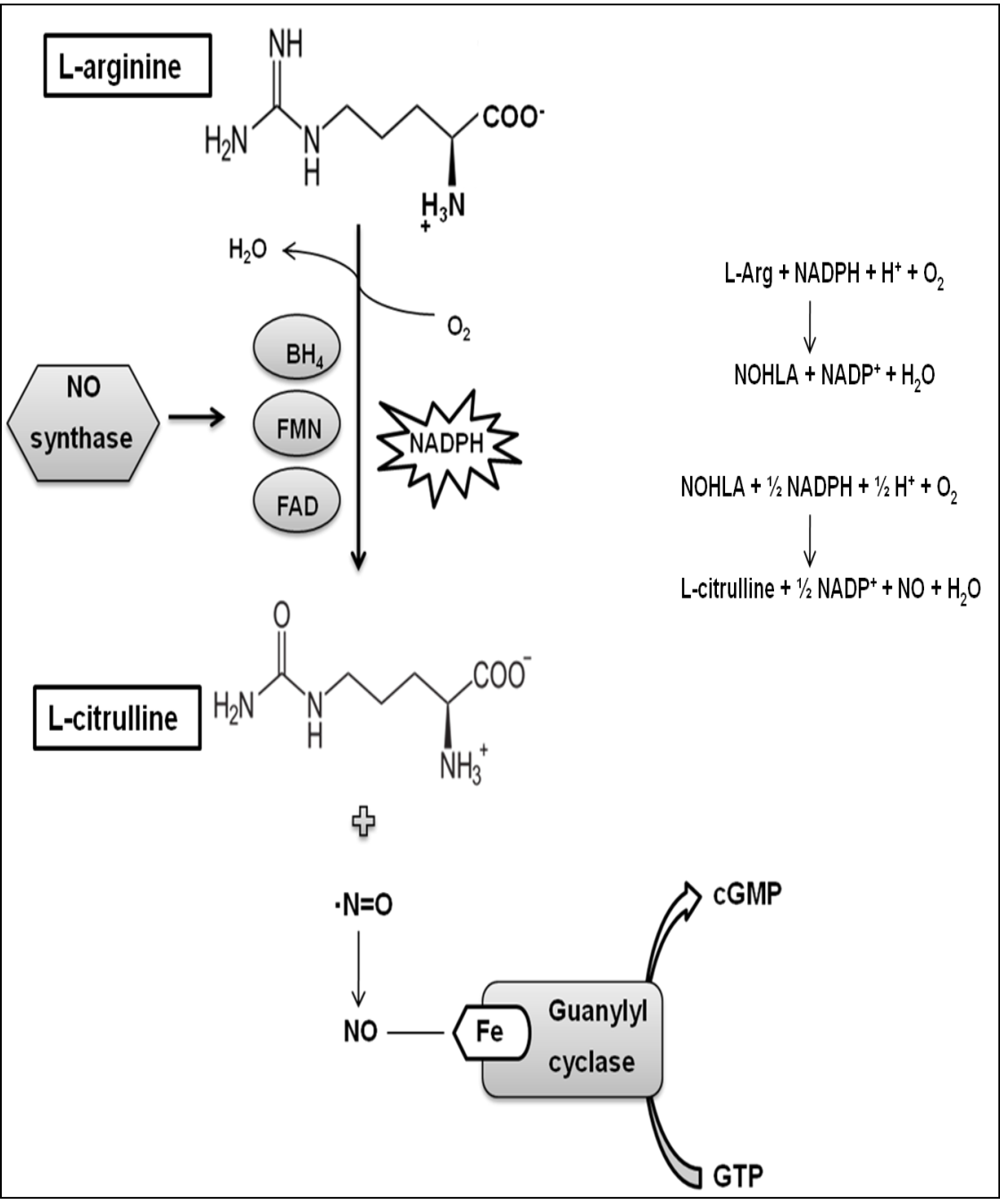
## 1.5 Biosynthesis of Nitric oxide from L-arginine

Nitric oxide is formed by the oxidation of the amino acid L-arginine and results in NO and citrulline production in a reaction that is catalyzed by the nitric oxide synthase (NOS) enzymes (Hughes, 2008; Ishimura *et al.*, 2005).

The NOS enzyme produces NO by a five-electron oxidation catalysis reaction of guanidino nitrogen from the cationic amino acid L-arginine (L-Arg). L-Arginine to L-citrulline oxidation takes place via mono-oxygenation reactions which utilises molecular O<sub>2</sub> and cofactors such as NADPH. The product of this reaction is the intermediate *N*<sup>ω</sup>-hydroxy-L-arginine (NOHLA). NOHLA is subsequently converted to L-citrulline and NO with NOS again utilising cofactors including NADPH (Korth *et al.*, 1994; Schmidt *et al.*, 2001). The reaction is summarised in Figure 1.4.

#### Figure 1.4 Synthesis of nitric oxide from L-arginine

Endogenous NO is formed from the amino acid L-arginine through a catalyzed reaction by the NOS family of enzymes, which convert L-arginine into NO and L-citrulline, requiring two co-substrates: oxygen and reduced nicotinamide adenine dinucleotide (NADPH). This reaction also needs FMN, FAD, tetrahydrobiopterin (BH<sub>4</sub>) as the cofactors. L-arginine is first converted to *N*<sup>ω</sup>-hydroxy-L-arginine (NOHLA) by NOS which utilises molecular O<sub>2</sub> and cofactors such as NADPH. NOHLA is then converted to L-citrulline and NO with NOS again employing cofactors including NADPH. It is estimated that 2 mol of O<sub>2</sub> and 1.5 mol of NADPH are consumed per mole of NO produced (Andrew *et al.*, 1999; Knowles *et al.*, 1989; Moncada *et al.*, 2006; Palacios *et al.*, 1989).



## 1.6 Nitric oxide synthase

There are three NOS isoforms referred to as neuronal (nNOS or NOS I), inducible NOS (iNOS or NOS II) and endothelial (eNOS or NOS III) (Alderton *et al.*, 2001; Stuehr *et al.*, 2004). These enzymes share 50-60% homology and are the product of different genes. All NOS isoforms are homodimeric enzymes which as explained above, require L-arginine and molecular oxygen as the substrate. All three enzymes utilise NADPH, FMN, FAD and tetrahydrobiopterin (BH<sub>4</sub>) as the cofactors. The enzyme functions as a dimer consisting of two identical monomers, which functionally and structurally is divided into two major domains: a C-terminal reductase domain, and an N-terminal oxygenase domain. The C-terminal reductase domain contains binding sites for NADPH, FAD, and FMN while N-terminal oxygenase domain which binds heme, BH<sub>4</sub> and arginine (Andrew *et al.*, 1999).

The isoforms are different with regards to their main mode of regulation, tissue expression pattern and the average amount of NO produced as summarised in Table 1.1. The eNOS and nNOS enzymes are constitutively expressed in many tissues, regulated mainly by Ca<sup>2+</sup>/Calmodulin and produce low concentrations of NO (Chin *et al.*, 1999; Furchgott *et al.*, 1980). The inducible isoform is associated with the immune system, independent of elevated Ca<sup>2+</sup> and already has calmodulin tightly bound to its structure during synthesis (Alderton *et al.*, 2001). Moreover, iNOS catalyzes the production of high concentrations of NO in response to various stimuli such as cytokines (Cross *et al.*, 2002; Ghosh *et al.*, 2003; Hughes, 2008; Newman *et al.*, 2004). As this thesis is focused on iNOS, the rest of the section below will concentrate on this enzyme.

Table 1.1 The NOS isozymes

NOS isozyme	Alternative descriptions	Mr [kDa]	Distinctive properties	Subcellular localization	Tissue expression
Neuronal	type I, nNOS, ncNOS, bNOS	160	Ca <sup>2+</sup> -dependent, constitutively expressed	binds to specific membrane proteins through an N-terminal PDZ domain	neuronal cells, skeletal muscle
Endothelial	type III, eNOS, ecNOS	134	Ca <sup>2+</sup> -dependent, constitutively expressed	targets to the Golgi and to caveoli through N-terminal myristoylation and palmitoylation	endothelial cells, epithelial cells, cardiomyocytes, some neurons
Inducible	type II, iNOS, macNOS	130	Ca <sup>2+</sup> -independent, induced by inflammatory stimuli (cytokines, LPS)	Soluble	macrophages, hepatocytes, astrocytes, smooth muscle cells, and many more

(Pfeiffer et al., 1999)

## 1.7 Inducible nitric oxide synthase (iNOS)

The inducible nitric oxide synthase is normally expressed only in the presence of stress stimuli, such as bacterial endotoxin and/or cytokines. In the cardiovascular system, it can be induced in smooth muscle cells, endothelial cells, and endocardial cells. In immune cells iNOS plays an active role in host defence during enteric bacterial pathogen infections thus contributing to the host defence mechanisms in man. However, its induction in several diseases is believed to contribute to the pathogenesis of the disease state. There is strong evidence, for instance, that expression of iNOS within the vasculature may play a major role in conditions such as septic shock (Albuszies *et al.*, 2007; Bultinck *et al.*, 2006).

Moreover it is reported to have an important role along with other pro-inflammatory mediators in the pathogenesis of inflammatory bowel disease (Dijkstra *et al.*, 1998) and intestinal inflammation (Marion *et al.*, 2003). A role for iNOS in inflammatory conditions is supported by the fact that pro-inflammatory mediators that increase cAMP (an intercellular mediator of pro-inflammatory mediators) levels also increase iNOS expression and therefore NO production (Cavicchi *et al.*, 1999). Some of the functional properties of iNOS are summarised in Figure 1.5.

This enzyme functions as a dimer consisting of two identical monomers with two major domains: a C-terminal reductase domain (contains binding sites for one molecule each of NADPH, FAD, and FMN) and an N-terminal oxygenase domain (which binds haem and BH<sub>4</sub>, as well as the substrate L-arginine) (Andrew *et al.*, 1999).

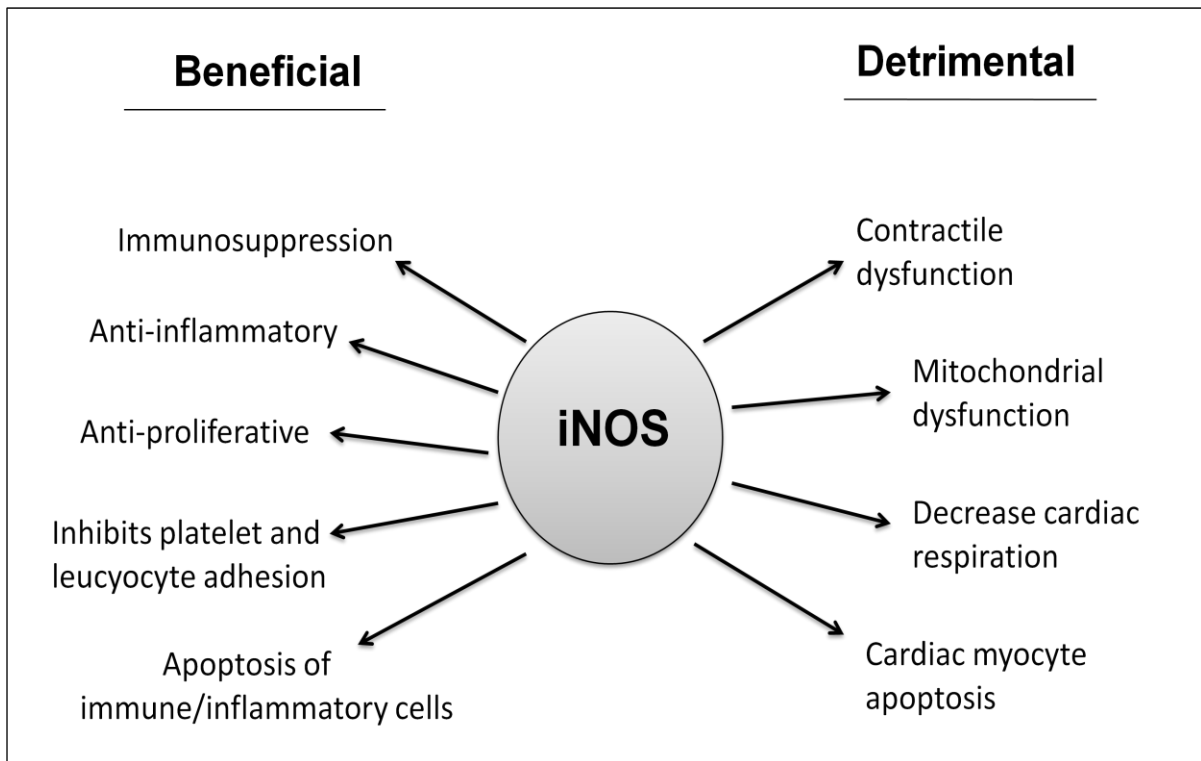


**Figure 1.5 Beneficial and detrimental effects of iNOS**

iNOS is induced in several disease states and plays a major role in conditions with both beneficial and detrimental effects as indicated in the diagram. (Pieper *et al.*, 2008).

## **1.8 Importance of altered NO production in human diseases and therapeutic strategies based on regulation of NO production**

Nitric oxide plays a critical role in the physiological regulation of blood flow, regulation of integrated cardiac and vascular function, homeostasis and is required for normal cardiac physiology. Nitric oxide may also exert a protective role in the ischemic heart via different mechanisms such as stimulation of sGC to reduce intracellular  $\text{Ca}^{2+}$  concentration (Jones *et al.*, 2006; Shah *et al.*, 2000). Nitric oxide may act as a physiological regulator of cell respiration and a modulator of the generation of reactive oxygen species by mitochondria via interactions with components of the mitochondrial respiratory chain and therefore modulates mechanisms of cell survival or death (Moncada *et al.*, 2002). At physiological concentrations, NO relaxes smooth muscle cells in the walls of the vasculature. At each cardiac cycle, in systole, the endothelial cells that line the blood vessels release NO which diffuses into the underlying smooth muscle cells causing relaxation and therefore facilitate blood flow (Champion *et al.*, 2003; De Belder *et al.*, 1997; Dusting., 1996; Haywood *et al.*, 1996; Starling., 2005).

In addition to the above beneficial effects of constitutively derived NO, NO produced from iNOS has been shown to have a protective role in cell-mediated oxidative modification of LDL (Buttery *et al.*, 1996). Studies have shown that in an *in vivo* model, iNOS reduced the development of atherosclerosis after immune injury. In addition, iNOS enhanced endothelial integrity, survival and protection against apoptotic or necrotic cell death (Hemmrich *et al.*, 2003; Rikitake *et al.*, 1998). Similarly, in hepatocytes, enhanced NO generation through iNOS has been reported to be a protective mechanism under inflammatory conditions (Kuo *et al.*, 1997).

Nevertheless, NO has an important pathophysiological role in various diseases both in animal experimental models as well as in different human pathologies, with harmful consequences leading to cardiovascular diseases (Champion *et al.*, 2003), chronic liver disease (Kirkali *et al.*, 2000), neurodegenerative disease (Titheradge., 1999), inflammatory bowel disease (Grisham *et al.*, 2002) and ulcerative colitis (Middleton *et al.*, 1993). In addition, ONOO<sup>-</sup> formation under these conditions may contribute to the pathology (Singer *et al.*, 1996) and can affect the viability and function of cells (Szabo *et al.*, 2007).

Within the cardiovascular system iNOS derived NO may cause excessive vasodilatation, cytotoxicity, inflammation and cardiovascular dysfunction such as that seen in septic shock (Smith *et al.*, 1992; Petros *et al.*, 1994). In heart failure and in myocardial infarction over-production of NO and superoxide radical generation also leads to injury to the coronary endothelium and myocytes, compromising ventricular contractile function (Horton *et al.*, 2000; Pacher *et al.*, 2007). Furthermore, NO derived from iNOS has been implicated in neurodegenerative diseases like Alzheimer's and Parkinson's disease and stroke where NO acts as a neurotoxin, inhibiting the main enzymes of energy metabolism. Nitric oxide may also damages the DNA and reacts with superoxide to form ONOO<sup>-</sup> (Schulz *et al.*, 1995).

The potential mechanisms underlying these harmful effects may involve an interaction of NO with a wide variety of proteins and enzymes through their amino, thiol (SH), diazo, tyrosyl, heme, Fe<sup>2+</sup> and sulfur centres (Angeloni *et al.*, 2012). Unregulated NO production is also associated with oxidative stress which can result in the generation of peroxynitrite and other reactive species that alter protein function via nitration and oxidation reactions (Arstall *et al.*, 1999; Lapu-bula *et al.*, 2007;

Searles., 2002). Nitric oxide can also lead to apoptosis via activation of mitochondrial pro-apoptotic pathways, and mitogen activated protein kinases (MAPK) which then results in cell death (Oyama *et al.*, 2002).

All the observations above support a role for excessive NO production in various pathologies. Disease development may also occur under conditions of impaired NO bioavailability which can result from reduced NO release from the endothelial cells or through amplified inactivation of NO by reactive oxygen species (ROS). This is in fact the case with atherosclerosis where endothelial impairment together with oxidative stress reduce bioavailable NO resulting in various deleterious effects including impaired vascular function (Kolluru *et al.*, 2012). Kashyab *et al.* (1990), also demonstrated that impaired NO synthase activity in skeletal muscle can contribute to insulin resistance in type 2 diabetes. Thus, it is clear that maintaining NO production at the physiological concentration range is critical in preventing disease development. However, where there is an imbalance, restoring NO production or in the case of iNOS, understanding the mechanisms that regulate expression and activity of the enzyme would be essential for developing novel strategies in controlling disease states.

Different therapeutic strategies to control diseases associated with changes in NO production have been considered. These include the use of NO donor compounds, stimulating the receptors linked to the L-arginine-NO pathway, increasing the action of endogenous NO, inhibiting substrate supply for iNOS or even inhibiting its expression and activity. The NO donor compounds are distributed into diverse classes such as organic nitrates (glyceryl trinitrate) and nitrites (amyl nitrite), inorganic nitroso compounds (sodium nitroprusside), sydnonimines (molsidomine),

and S-nitrosothiols (S-nitroso-N-acetyl-D, L-penicillamine). Most of these compounds exert their effect after being metabolised to release NO (Moncada *et al.*, 1995). Donors such as nitroglycerin are used to control high blood pressure (Agvald *et al.*, 2002) and to restore blood flow in conditions such as arterial or myocardial ischaemia (Karlberg *et al.*, 1998; Varughese *et al.*, 2001). However, one of the limitations of using this compound is the development of tolerance after a few weeks of continued usage (Agvald *et al.*, 2002).

In contrast to up-regulation NO production, inhibition of NO synthesis can be used as a therapeutic strategy under conditions associated with enhanced NO production via iNOS. In many different diseases NO is considered as a target for therapeutic strategy, for instance in Alzheimer's disease acetylcholinesterase inhibitors and N-methyl-D-aspartate (NMDA) receptor antagonists are the only recognised treatment for managing the cognitive deficits. However, elevated NOS activity has been shown to increase the amount of NO which may contribute to the progression of the disease. Therefore, a likely approach to regulate disease progression must include inhibitors which targets NOS isoforms associated with damage to brain cells (Fernandez *et al.*, 2010). There are, however, contradictory reports as to whether there is more or less NO synthesis in these diseases. These discrepancies may be due to the fact that the method for the direct detection of NO levels in the brain is still not difficult. Most studies use various biomarkers and metabolites (such as biomarkers of arginine) produced via the NO pathway as an indirect measurement for identifying the role of NO, and for this reason it is not clear whether NO plays a neuroprotective or cytotoxic role. However, using NOS inhibitors such as L-NAME has helped provide a better understanding of the role of NO in diseases such as

acute liver injury (Adawi *et al.*, 1997) and gastrointestinal diseases (Wang *et al.*, 2002). These inhibitors which also include other analogs of L-arginine such as NG monomethyl-L-arginine (L-NMMA) act as competitive inhibitors of NOS enzymes (Moncada *et al.*, 1995) and may therefore have some potential therapeutic benefits in disease states associated with the over production of NO. As an example L-NMMA has been shown to be effective in reversing hypotension in human with septic shock (Schilling *et al.*, 1993; Watson *et al.*, 2004). Similarly, the use of L-NAME as a treatment for conditions such as cardiogenic shock has been proposed (Avontuur *et al.*, 1998; Cotter *et al.*, 2003; Kiehl; 1998). Despite these reports; the clinical exploitation of NOS inhibitors is still limited. This is mainly because the compounds mentioned above lack selectivity and inhibit all known NOS isoforms which is not desirable. For this reason, many studies have suggested that general NOS inhibition is not beneficial in conditions like septic shock and selective inhibition of iNOS was suggested. Liaudet *et al.*, 1998 compared the selective inhibitor of iNOS (L-canavanine) and non-selective inhibitor of NOS (L-NAME) in endotoxemia. Both compounds managed to reduce the amount of nitrite. However L-NAME caused liver damage and was detrimental in endotoxic shock, while L-canavanine considerably reduced mortality with no fatal effects on the liver. Su *et al.* (2010) compared the selective iNOS inhibitor BYK191023 with norepinephrine in septic shock condition and showed that selective iNOS inhibition had a more profound and beneficial effect on blood pressure and flow. Thus there is promise from these observations to develop NOS inhibitors that could be exploited clinically in the future.

## 1.9 Regulation of iNOS activity

Induced iNOS can generate high nM to  $\mu$ M amounts of NO over prolonged periods but this may be critically dependent on the availability of exogenous substrate. Moreover, its activity may be directly related to the rate of transport of exogenous arginine (Assreuy *et al.*, 1992; Bogle *et al.*, 1992) and could be inhibited following blockade of L-arginine transport into cells expressing the enzyme (Bogle *et al.*, 1992). Interestingly, this dependency of iNOS on exogenous L-arginine occurs despite the fact that cells contain concentrations of L-arginine of between 0.1 to 0.8 mM (Baydoun *et al.*, 1990; Mitchell *et al.*, 1990) which are well above the reported  $K_m$  of iNOS for L-arginine of around 1-20  $\mu$ M (Knowles *et al.*, 1994). These observations indicate a critical role of L-arginine supply and potentially provide an alternative novel target for regulating overproduction of NO in disease states beyond targeting the enzyme itself.

## 1.10 L-arginine

L-arginine is a semi-essential amino acid that is synthesized from citrulline (Figure 1.6) by the actions of argininosuccinate synthetase (AS) and argininosuccinate lyase (AL), the third and fourth enzymes of the urea cycle (ornithine cycle) (Chin-Dusting *et al.*, 2007; Mori *et al.*, 2000). L-arginine participates in a variety of key biochemical and physiological activities. Other than for NO synthesis, L-arginine is a precursor for urea, polyamines, creatine phosphate and various proteins. It is transported from the blood circulation into cells via different carrier systems including the cationic amino acid transporters (CAT) which are discussed below. When iNOS is induced in

various cells stimulated by bacterial lipopolysaccharide (LPS) and/or cytokines, AS and sometimes AL are induced (Figure 1.6). iNOS and AS were first found to be co-induced in murine macrophage after stimulation with LPS and interferon- $\gamma$  (IFN- $\gamma$ ) (Nussler *et al.*, 1994), also in cultured rat aortic smooth muscle cells stimulated by LPS and IFN- $\gamma$  (Hattori *et al.*, 1994), and cultured rat and human pancreatic  $\beta$ -cells treated with cytokines (Flodstrom *et al.*, 1995; Hattori *et al.*, 1994; Mori, 2007; Mori *et al.*, 2004).

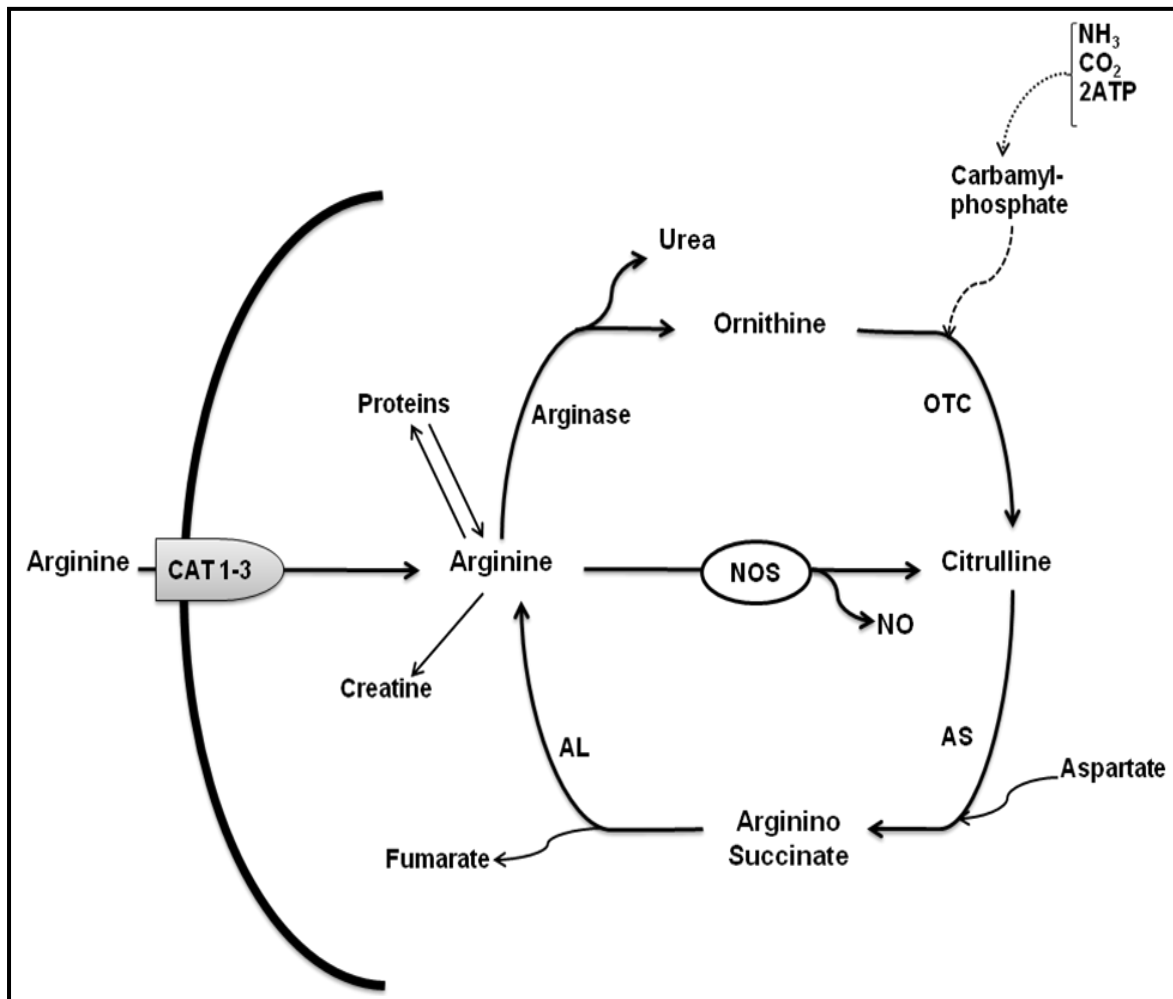


**Figure 1.6 Arginine metabolism**

The urea cycle is composed of carbamylphosphetase I (CPS I), ornithine transcarbamylase (OTC), argininosuccinate synthetase (AS), argininosuccinate lyase (AL), and arginase. The citrulline–NO cycle is composed of nitric oxide synthase (NOS), AS, and AL. CPS I and OTC are present only in hepatocytes and small intestinal epithelial cells. CAT-1–3: cationic amino acid transporter-1–3 (Mori *et al.*, 2000).

### 1.11 L-arginine transport system

Entry of L-arginine and other cationic amino acids (CAAs) into cells is mediated by at least one of four transport systems referred to as systems  $y^+$ ,  $y^+L$ ,  $b^{0,+}$  and  $B^{0,+}$  which are characterised according to their affinity for CAAs and by their dependence on sodium (Deves *et al.*, 1998). Of these, systems  $y^+$  is perhaps the most diverse and widespread classical system, transporting CAAs  $Na^+$  independently and with high affinity ( $K_m$  in the micro-molar range) (Closs *et al.*, 1999; White *et al.*, 1982). By comparison, systems  $b^{0,+}$ ,  $B^{0,+}$  and  $y^+L$ , also carry a range of other amino acids, including neutral amino acids and do so in a  $Na^+$ -dependent manner, thus making the CATs the only truly selective transporters of CAAs expressed in vascular cells (Deves *et al.*, 1998). The discussion below will therefore concentrate on the CATs as these are the other main focus of the studies conducted in this thesis.

### 1.12 Cationic amino acid transporters (CATs)

The CAT family of proteins include CAT-1, CAT-2A, CAT-2B, and CAT-3. Of these, CAT-1 is a high affinity carrier cloned by scientists searching for the ecotropic murine leukemia virus receptor (ecoR). The protein they cloned was expressed in *Xenopus* oocytes and shown to mediate cationic amino acid transport (Kim *et al.*, 1991). The *Cat-2* gene was cloned shortly after *Cat-1* and initially named Tea (T-cell early activation receptor) related to its early induction in the response of normal T cells to mitogens. The full length cDNA was subsequently isolated and shown to have 61 % homology with CAT-1 (Closs *et al.*, 1993a; Dall'Asta *et al.*, 2000). Both CAT-2A and CAT-2B are products of the same gene produced by alternative splicing with 98%

homology with each other (Closs *et al.*, 1993a). CAT-1 is expressed ubiquitously while CAT-2B is apparently expressed in most cells, including cultured rat astrocytes (Gill *et al.*, 1996), J774 macrophages (Baydoun *et al.*, 1994; Closs *et al.*, 2000) and cardiac myocytes (Simmons *et al.*, 1996a; Simmons *et al.*, 1996b) following its induction by various stimuli. Interestingly, previous studies from our group has revealed the expression of CAT-2A and CAT-2B in control non-activated cultured vascular smooth muscle cells (Baydoun *et al.*, 1999) suggesting that these carriers may be expressed constitutively in certain cell systems. Some of the characteristics of these carriers are summarised in Table 1.

**Table 1.2 Characteristics of cationic amino acid transporters**

	<b>CAT-1</b>	<b>CAT-2A</b>	<b>CAT-2B</b>	<b>CAT-3</b>
K <sub>m</sub> (mM)	0.1-0.2	2.1-5.2	0.04-0.3	0.1-0.15
Na <sup>+</sup> -independent	Yes	Yes	Yes	Yes
Amino acids	622	657	658	619
MW (kDa)	67	72	72	67
N-glycosylation	Yes	Yes	Yes	Yes
Expression	Constitutive	Constitutive	inducible	Constitutive
Key cell type	Ubiquitous Except liver	Liver, muscle, skin	T-cells, Macrophages	Brain

Adopted from (Closs *et al.*, 1993c; Kakuda *et al.*, 1999)

### 1.13 Regulation of iNOS and CAT gene expression

Since both iNOS and CATs can be induced, it is evident that their induction requires the activation of specific signalling pathways within the cells. Considerable progress has been made in unravelling those involved for iNOS which can be regulated largely at the transcriptional level (Hecker *et al.*, 1999; Kolyada *et al.*, 1996; Matsumura *et al.*, 2001; Walker *et al.*, 1997; Wong *et al.*, 1996; Xie *et al.*, 1993). In addition, there is some evidence for the possibility of post-transcriptional regulation (Korhonen *et al.*, 2007) in rat mesangial cells (Kunz *et al.*, 1996), in RAW 264.7 macrophages (Walker *et al.*, 1997) and in human chondrocytes (Schmidt *et al.*, 2010) in which different stimulations regulate the translational rate of iNOS.

Studies on the 5'-upstream sequence of the iNOS gene (considered as the promoter region) have shown that this region contains a number of transcription factor binding sites including those for IFN- $\gamma$  regulatory factor (IRF), nuclear factor- $\kappa$ B (NF- $\kappa$ B), IFN-stimulated response element (ISRE), activating protein-1 (AP-1), tumor necrosis factor (TNF) response element and CAAT box element (Beck *et al.*, 1998; Lowenstein *et al.*, 1993; Yang *et al.*, 1998; Zhang *et al.*, 1996).

Activation of NF- $\kappa$ B is being reported as essential for iNOS expression (Forstermann *et al.*, 1995; Goldring *et al.*, 1995; Martin *et al.*, 1994; Xie *et al.*, 1993) but NF- $\kappa$ B alone may not be sufficient for full induction of the iNOS gene (Adcock *et al.*, 1994; Beck *et al.*, 1996; Ding *et al.*, 1995; Zhang *et al.*, 1998). Other transcription factors involved include AP-1 which is claimed to regulate iNOS expression either positively (Kristof *et al.*, 2006; Won *et al.*, 2004) or negatively (Kleinert *et al.*, 1998; Mendes *et al.*, 2003). Alternative studies suggested that CAAT box/ enhancer binding protein

(C/EBP) and cAMP responsive element binding protein (CREB) may have synergistic effects on iNOS induction via the CAAT box (Hecker *et al.*, 1997; Kinugawa *et al.*, 1997).

It should be noted that activation of these nuclear factors is usually associated with exposure of tissue or cells to pro-inflammatory mediators including LPS and/or cytokines (Beasley *et al.*, 1991; Nussler *et al.*, 1992; Rees *et al.*, 1990; Stuehr *et al.*, 1989). These pro-inflammatory mediators often act synergistically, activating a series of signalling pathways which may include the mitogen activated protein kinases (MAPKs) (Chen *et al.*, 1999; Guan *et al.*, 1999; Singh *et al.*, 1996), protein kinase C (PKC) (Paul *et al.*, 1995; Scott-Burden *et al.*, 1994), the phosphoinositide-3 kinases (PI3Ks) (Matsuzaki *et al.*, 1999) and the c-Jun-N-terminal kinase (JNKs) (Chan *et al.*, 2001; Chan *et al.*, 1998; Pawate *et al.*, 2006) of which the last is the main focus of this thesis and discussed in more detail below.

In contrast to the vast literature on the regulation of iNOS expression, relatively little is known about the signalling that regulates CAT induction. Limited reports have suggested that neither tyrosine kinases nor Protein kinase C (PKC) may mediate the induction of L-arginine transport by LPS and IFN- $\gamma$  in smooth muscle cells (Baydoun *et al.*, 1999). These observations indicate a difference in the mechanisms responsible for the induction of iNOS and CATs when cells are exposed to inflammatory mediators. It was shown that the p38 MAPK pathway could regulate both iNOS and CAT function and expression (Baydoun *et al.*, 1999) suggesting a critical role for this kinase family in the production of not only NO but also in the enhancement of L-arginine transport into cells. Furthermore, the ERKs and p38 have been shown to act at the post transcriptional level in controlling CAT-2B synthesis

(Caivano, 1998) but at least one other study has suggested no involvement of MAPKs in L-arginine transport (Visigalli *et al.*, 2004), thus again highlighting the inconsistencies in the current literature. In addition to the kinase signalling, it has been shown that NF- $\kappa$ B can act as an essential transcription factor for CAT-2B up-regulation (Hammermann *et al.*, 2000; Visigalli *et al.*, 2004) but again the data are limited and it is not clear what role other elements such as AP-1 play in controlling CAT expression and function. The p38 MAPK also seems to be related for up-regulation of CAT expression and function which leads to enhancing the transporter activity and induction of transcript for CAT-1, CAT-2A and CAT-2B (Baydoun *et al.*, 1999). Indeed, in preliminary studies, our research group has obtained data suggesting that JNK (and thus AP-1) may not be involved in the induction of CATs. Interestingly, the studies also showed opposing actions on iNOS induction and NO production with the potent JNK inhibitor SP600125 when compared to AP-1 dominant negatives, TAM-67 and a-Fos. Thus, it is unclear what role the JNK pathway plays in the induction of iNOS and/or CATs and this has been the major focus of the studies carried out for this thesis.

#### **1.14 c-Jun-N-terminal kinase (JNK) signalling pathway**

The JNKs, also called stress activated protein kinase (SAPK) belong to the mitogen-activated protein (MAP) kinases family of signalling proteins. Three different MAPK pathways have been described in mammalian cells: the extracellular signal regulated kinase (ERK), JNK and the p38 MAPK pathways. The ERKs are activated by mitogenic stimuli, and the JNKs and p38 MAPKs respond to environmental stress,

including ultraviolet light, heat, osmotic shock and inflammatory cytokines. The molecular cloning of human (Derijard *et al.*, 1994; Kallunki *et al.*, 1994) and rat JNK (Kyriakis *et al.*, 1994) has led to the identification of JNK as a member of MAPK family.

These MAP kinases are activated by dual phosphorylation within their protein kinase subdomain VIII. This phosphorylation is mediated by a protein kinase cascade that consists of a MAP kinase kinase kinase, a MAP kinase kinase, and a MAP kinase. Individual MAP kinases are activated by diverse signalling molecules that are regulated by various stimuli. For instance, the ERKs are activated by the MAP kinase kinases MKK1 and MKK2; the p38 MAP kinases are activated by MKK3, MKK4, and MKK6 (Mercer *et al.*, 2006). The JNKs are activated by upstream protein kinases that include two dual specificity MAP kinase kinases (MKK4 and MKK7) and multiple MAP kinase kinase kinases (MKKKs) (Widmann *et al.*, 1999). The MKKKs phosphorylate and activate MKK4 and MKK7 which then cause the activation of JNKs by dual phosphorylation on threonine and tyrosine residues within a Thr–Pro–Tyr motif in protein kinase subdomain VIII (Bode *et al.*, 2007; Boutros *et al.*, 2008; Davis, 2000a; Wang *et al.*, 2007) (Figure 1.7). While MKK7 is a specific activator of JNKs, MKK4 can also phosphorylate the Thr–Gly–Tyr motif of p38 MAPKs (Derijard *et al.*, 1995; Sanchez *et al.*, 1994; Tournier *et al.*, 1997). Interestingly, JNK activation in the liver (*in vivo* model) correlates with decreased p38 MAPK activity (Mendelson *et al.*, 1996) suggesting that the two pathways may be regulated differentially.

The JNKs are encoded by three genes: *jnk1*, *jnk2*, *jnk3*. JNK1 and JNK2 are expressed ubiquitously and show variances in their ability to interact with c-Jun.

JNK2 in comparison with JNK1, seem to have a much greater affinity to bind with c-Jun (Bode *et al.*, 2007; Kallunki *et al.*, 1994; Sabapathy *et al.*, 2004).

JNKs have an important role in the induction of apoptosis, but are also involved in enhancing cell survival and proliferation. The divergent roles of JNKs are related to the fact that they activate a large number of different substrates which are dependent on specific stimulus and cell type (Bode *et al.*, 2007; Gupta *et al.*, 1996). Studies on different animal disease models demonstrated specific roles of JNK genes in a huge numbers of pathologic conditions including neurodegenerative disorders such as Parkinson's and Alzheimer's disease (Hunot *et al.*, 2004; Peng *et al.*, 2003), arthritis (Han *et al.*, 2002), asthma (Nath *et al.*, 2005; Sumara *et al.*, 2005), as well as in cancer development (Kennedy *et al.*, 2003). In relation to the latter, many tumour cell lines have been shown to have constitutively active JNK. Moreover, a decline in the transforming potential of a number of oncogenes was observed when an anti-sense JNK oligonucleotides or dominant negative constructs were employed (Potapova *et al.*, 1997; Potapova *et al.*, 2000). The JNK pathway has also been shown to play a critical role in Type 1 diabetes (Hirosumi *et al.*, 2002), and in other cardiovascular complications such as heart failure as well as mediating hypertrophic responses to various forms of cardiac stress (Adams *et al.*, 1998; Kim *et al.*, 1998; Liang *et al.*, 1997).

Most of the evidence in support of the above observations has been obtained from animal and experimental models. For instance the abolition of JNK expression in mice (i.e. JNK deficient mice) with Parkinson's disease prevents neurodegeneration (Hunot *et al.*, 2004). Similarly, inhibition of the JNK pathway with compounds such as CEP-1347 exerts neuro-protection potentially through inhibition of JNK but not p38 or

ERK1/2 activation. CEP-1347 is now in clinical trials for Parkinson's disease treatment (Peng *et al.*, 2003).

With regards to cardiovascular diseases, the role of the JNK pathway has also been established using various approaches. For instance, overexpression of JNK contributes to the development of pathological cardiac hypertrophy (Heineke *et al.*, 2006). Furthermore, inhibition of endogenous JNK signalling using dominant negative JNK1/2 or JNK1/2<sup>-/-</sup> in mice has been shown to be augmented cardiac growth supporting that JNK1/2 inhibits cardiac hypertrophy (Liang *et al.*, 2003). In another study in JNK1/2/3<sup>-/-</sup> mice, pressure overload resulted in cardiac hypertrophy which was not seen in the wildtype (Tachibana *et al.*, 2006). Additionally, it has been suggested that pharmacological inhibition of JNK1/2 decreases pathological cardiac remodeling after myocardial infarction in humans (Muslin 2008) and treatment of mice with SP600125, a potent JNK inhibitor, inhibited the development of atherosclerosis (Ricci *et al.*, 2004).

The effects highlighted above may be mediated by different JNK which may vary in their functions (Chen *et al.*, 2002; Singh *et al.*, 2009). For instance, JNK2 has been shown to have a 25-fold higher binding affinity (with lower K<sub>m</sub>) for c-Jun (the main substrate for JNK) than JNK1 and it has been proposed that JNK2 is the key c-Jun activator (Kallunki *et al.*, 1994). Kallunki *et al.*, 1994, also suggested that both efficient c-Jun binding and c-Jun phosphorylation are determined by a short region on the catalytic c-terminal of the enzyme, which is different between JNK1 and JNK2. As a result, c-Jun is more likely to be phosphorylated by JNK2 than by JNK1. This is however contradicted by at least one report which suggested that the JNK1 isoform may be slightly more efficient in phosphorylating c-Jun (Gupta *et al.*, 1996;

Hochedlinger *et al.*, 2002) since there is reduced c-Jun phosphorylation in JNK1 deficient fibroblast. Moreover these cells had higher resistance to UV-induced cell death (Hochedlinger *et al.*, 2002). However JNK2 deficient cells revealed elevated sensitivity to UV light and had an increase c-Jun phosphorylation. Thus, the two isoforms clearly act in opposing ways and there are indications that the specific biological functions may probably depend on the stimulation and responding tissue/cell type (Sabapathy *et al.*, 2004).

Depending on the stimulus and cell type, JNKs can phosphorylate a number of activator protein-1 (AP-1) components, including c-Jun, JunD, and activating transcription factor 2 (ATF2) (Davis, 2000b; Fuchs *et al.*, 1997) which may be required, for maximal induction of iNOS, independently or in conjunction with NF- $\kappa$ B.

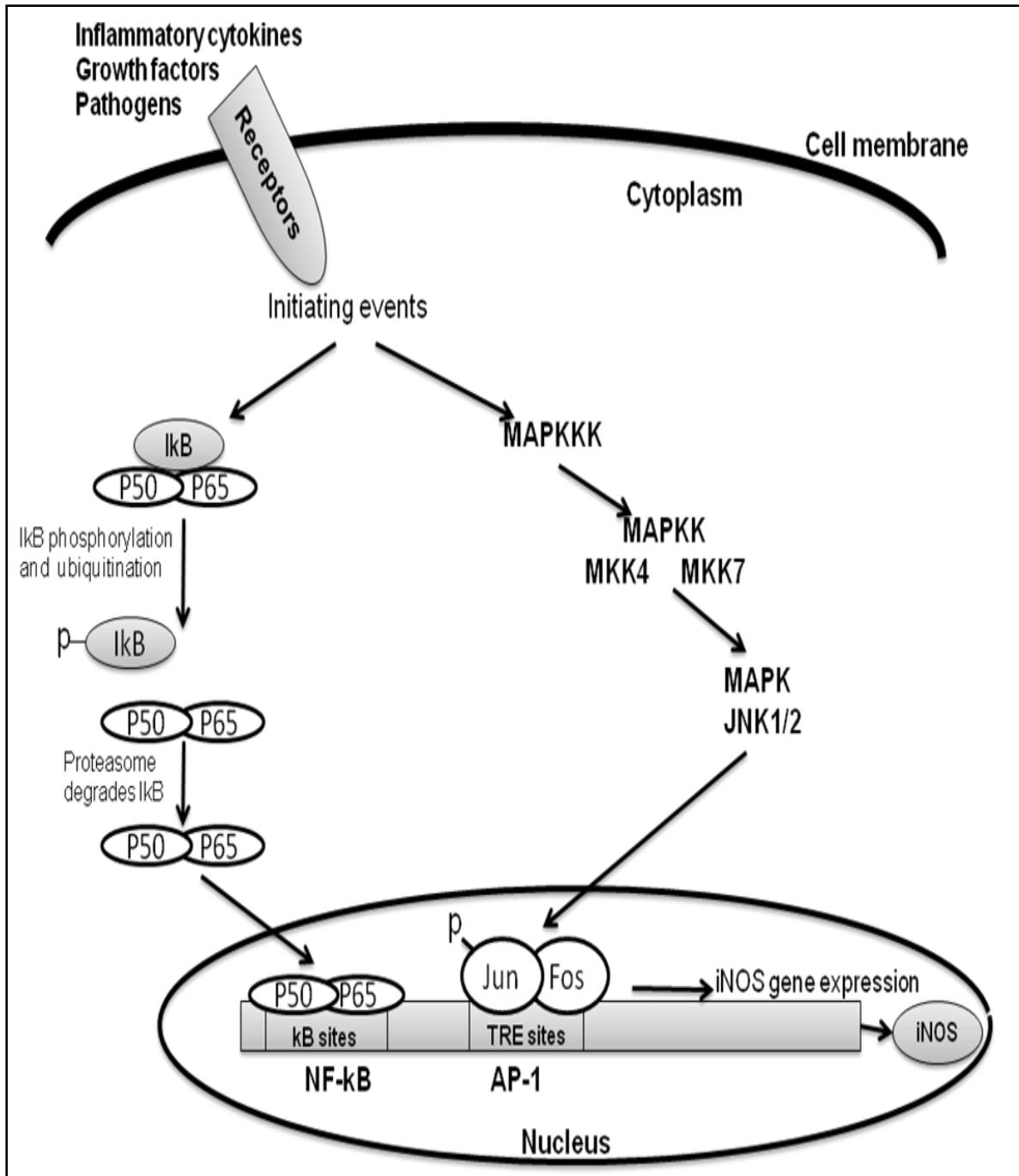
Activator Protein-1 (AP-1) is a downstream target for JNK and its activity is directly increased following phosphorylation of c-Jun by JNKs. This activation augments stabilization and overall transcriptional activation (Bode *et al.*, 2007). Furthermore, JNKs directly up-regulate c-Jun expression which results in activated AP-1 complex and its translocation into the nucleus to initiate gene expression. Other MAPKs may be able to up-regulate the Fos family genes by phosphorylation of JNK. The ERKs in particular are one of the potential upstream for Fos activation which act through ETS-like transcription factor-1 (Elk-1) activation (Kaminska *et al.*, 1999; Whitmarsh *et al.*, 1996). This would suggest a complex network of signalling cross-talk which can activate AP-1 and subsequent gene transcription (Figure 1.7).

There is some evidence revealing an important role for JNK in the induction of iNOS (Chan *et al.*, 1998; Chiu *et al.*, 2008; Lee *et al.*, 2010; Pawate *et al.*, 2006; Rodriguez

*et al.*, 2008). For example in human astrocyte, dominant negative of JNK inhibited interleukin-1 (IL-1)-induced iNOS expression (Hua *et al.*, 2002), however this dominant negative construct did not show any effect on bovine type I collagenstimulated iNOS expression in RAW264.7 murine macrophages (Cho *et al.*, 2002). The effects of JNK on iNOS expression may be via a post transcriptional mechanism through stabilization of iNOS mRNA (Korhonen *et al.*, 2007; Lahti *et al.*, 2003). Lahti *et al.*, 2003 used the specific JNK inhibitor, SP600125, on LPS-activated J77 murine macrophages. The experiments showed this inhibitor has no effect on iNOS mRNA expression after 4 hours but reduced transcript levels by up to 90% after 8 hours of incubation suggesting that it may be altering the stability on the induced mRNA.

**Figure 1.7 Representation of the activation of the NF- $\kappa$ B and JNK/AP-1 pathways.**

Both the NF- $\kappa$ B and JNK/AP-1 pathways are activated by upstream mitogen-activated protein kinases. AP-1 is formed through activation of a family of Jun/Fos proteins. The activated AP-1 complex translocates into the nucleus, initiating gene expression. Some of the signalling that activates AP-1 may also activate NF- $\kappa$ B and each transcription factor has a specific recognition binding site ( $\kappa$ B for NF- $\kappa$ B and TRE for AP-1) on the iNOS gene promoter which can be activated to induce iNOS (Herlaar *et al.*, 1999; Rahman, *et al.*, 1998).



### 1.15 AP-1

Activator Protein-1 (AP-1) is a transcription factor complex composed of homo- and/or hetero-dimers of Jun (c-Jun, JunB and JunD) and Fos (c-Fos, FosB, Fra-1 and Fra-2) proteins. Fos proteins cannot form homo-dimers but can hetero-dimerize with members of the Jun family. The Jun proteins can both homo-dimerize and hetero-dimerize with other Jun or Fos members to form transcriptionally active complexes (Angel *et al.*, 1991) as shown in Figure 1.8.

Additionally, Jun proteins can also hetero-dimerize with other transcription factors, such as members of the activator transcription factor (ATF) family. The Jun and Fos proteins contain a basic-region leucine zipper (bZIP) domain, and are therefore able to bind to other bZIP proteins including those from the ATF, MAF, CNC and C/EBP (CCAAT/enhancer-binding protein) subfamilies (Chinenov *et al.*, 2001).

Generally, enhanced expression of *c-jun* gene, protein and function can be maintained by an induction of transcription factors that are related to c-Jun (e.g. Jun-B, Jun-D), the Fos family members (Fos, FosB, Fra-1/2), or the ATF-family members, allowing the formation of functionally different hetero-dimers. Additionally, some members of the activating transcription factor and cAMP response element-binding protein families also dimerize with the core members of the AP-1 family to regulate a broad variety of genes by binding to their promoter and enhancer regions. Jun and Fos proteins, after dimerization, bind to so-called TPA (12-O-tetradecanoylphorbol 13-acetate) responsive elements (TRE's; TGAC/GTCA) in the promoter and enhancer regions of target genes (Miller *et al.*, 1984; Mitchell *et al.*, 1989; Nakamura *et al.*, 1991; Smeal *et al.*, 1989; van Dam *et al.*, 2001).

Activation of AP-1 occurs both transcriptionally and post-translationally, and is signalled mostly through the mitogen-activated protein kinase (MAPK). The diversity of AP-1 proteins and other interacting factors appears to have effect on how specific cell types respond to a stimulus (Young *et al.*, 2003).

AP-1 regulates a variety of cellular processes summarised in Figure 1.9, including proliferation, differentiation and apoptosis, and contributes to both basal and stimulus-activated gene expression. It is activated by growth factors, hormones, stress, cytokines, Reactive Oxygen Species (ROS) and ultraviolet radiation (Vesely *et al.*, 2009) (Figure 1.10). Regulation of AP-1 activity is critical in deciding cell fate and occurs at various levels, including dimer-composition, transcriptional and post-translational events, and interaction with the other proteins (Eferl *et al.*, 2003).

It has been demonstrated that the promoter region of iNOS gene from different species contain binding site for AP-1 (Lowenstein *et al.*, 1993) and there is evidence for an important role of JNK in the induction of iNOS (Chan *et al.*, 1998; Chiu *et al.*, 2008; Lee *et al.*, 2010; Pawate *et al.*, 2006; Rodriguez *et al.*, 2008) which could be mediated through activation of AP-1. Additionally, the JNKs may also regulate iNOS expression via post transcriptional mechanism through stabilization of iNOS mRNA (Korhonen *et al.*, 2007; Lahti *et al.*, 2003). The role of JNK/AP-1 on iNOS expression may however be different in various systems and this will be discuss later in the thesis.

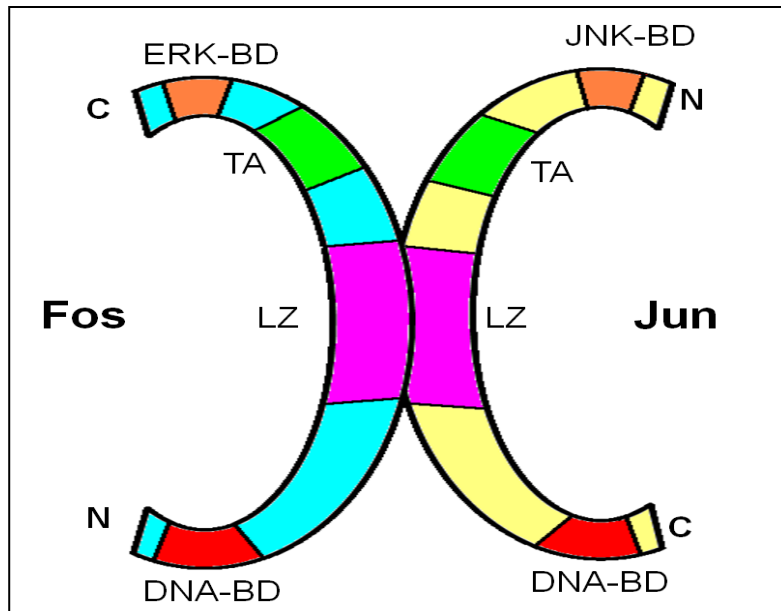


**Figure 1.8 AP-1 transcription dimers**

A cartoon depicting dimerisation of Jun\Fos to form an active AP-1 complex. Although members of the Jun and Fos families share a high degree of structural homology, the individual AP-1 dimers show significant differences in their DNA binding affinity and their capability to activate or suppress gene expression (Wagner *et al.*, 2005). TA: transactivating domain; LZ: Leucine Zipper domain; DNA-BD: DNA binding domain (Raivich *et al.*, 2006).

## 1.16 Transcriptional regulation of AP-1 family members

Increasing evidence has suggested the important roles of different AP-1 proteins and/or AP-1 dimer formation in various cell systems and their effect in controlling diverse cellular functions. ERK, p38, and JNK each selectively regulated AP-1 subcomponent expression and DNA binding activity (Ding *et al.*, 2008).

Extracellular stimuli including stress, growth factors, mechanical stretch, G protein-coupled receptor agonists, cytokines, psychotropic drugs, etc., lead to a wide variety of cellular responses such as cellular phenotypic change, growth, apoptosis, migration, or gene expressions (Figure 1.9). Most genes that regulate components of AP-1 are known as "immediate-early genes" (IEGs), and are induced in response to these stimuli (Kim *et al.*, 2003).

Various toxic and mitogenic stimuli can also induce *jun* and *fos* mRNA expression rapidly and by several fold above the basal level in a wide variety of tissues and/or cell types. In general, the mRNA levels of *c-jun*, *junB*, *junD*, *c-fos*, and *fosB* peak within 15-30 min of stimulation and return to basal level within 1-2 hours.

Jun–Jun and Jun–Fos dimers bind with highest affinity to the phorbol 12-O-tetradecanoate-13-acetate (TPA) response element (TRE) with the consensus sequence 5'-TGAG/CTCA-3' (Angel *et al.*, 1991); although many other 'AP-1-like sites' have been reported. Binding to any of these sites can be (1) tissue-specific, (2) affected by neighbouring sequences, and (3) dependent on interactions with other transcription factors or cofactors (Angel *et al.*, 1987).

Although Jun and Fos proteins are rapidly induced by various stimuli, most cells possess a certain amount of pre-existing Jun and Fos proteins that are initial targets

for JNK and ERK, MAPKs. Upon their activation, ERKs and JNKs phosphorylate both pre-existing and newly synthesized AP-1 proteins. The activated JNKs bind to the docking site located in the NH<sub>2</sub>-terminal region of c-Jun and phosphorylates Ser63 and -73 located within its transactivation domain (Whitmarsh *et al.*, 1996). Due to its higher affinity to the docking site, JNK2 phosphorylates c-Jun with more efficiency than JNK1 (Gupta *et al.*, 1996). JunB also contains the JNK docking site but lacks NH<sub>2</sub>-terminal acceptor serine residues and therefore appears to be poorly activated by JNKs. However, a recent study shows phosphorylation of Thr102 and -104 of JunB by JNKs in some cell type (Li *et al.*, 1999).

In contrast to Jun proteins, which are mainly phosphorylated by JNKs within their NH<sub>2</sub>-terminal region, Fos proteins are mainly phosphorylated by ERKs on serine and/or threonine residues located within their COOH-terminal domain. Upon activation, ERKs translocate into the nuclei and phosphorylate c-Fos on Ser374 (Chen *et al.*, 1996; Karin, 1996).

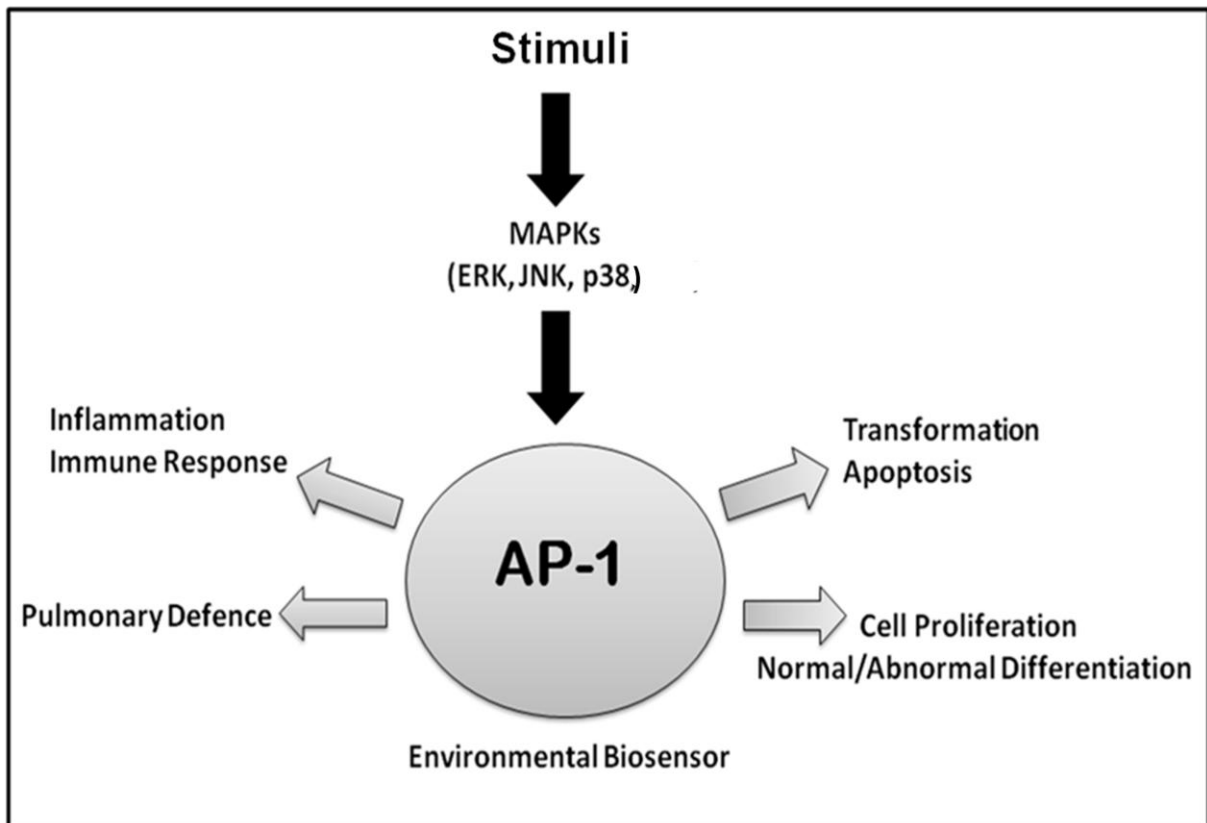


**Figure 1.9 Activation of activator protein-1 (AP-1) and its potential actions**

Various toxins, after interacting with cells, activate different mitogen-activated protein kinase (MAPK) signalling pathways, which in turn activate the AP-1 transcription factor. Upon activation, AP-1 binds to its target sites located in the promoter regions to regulate expression of a wide variety of genes involved in various biological processes. ERK, extracellular signal-regulated kinase; JNK, c-Jun NH<sub>2</sub>-terminal kinase (Reddy *et al.*, 2002).

### 1.17 Aims

The aim of this study is to determine the role of the JNK-AP-1 pathway in the induction of iNOS, NO synthesis and L-arginine transport in J774 macrophages and rat aortic smooth muscle cells (RASMCs) which both play a critical role in disease states associated with over production of NO by iNOS in the body.

The rationale for wanting to conduct these studies is the fact that preliminary studies in our group revealed opposing actions of the JNK inhibitor SP600125 when compared to dominant negatives  $\alpha$ -Fos and TAM-67. In addition the literature also indicates inconclusive and contradictory findings about the role of the JNK/AP-1 pathway on iNOS induction in different cell systems and there are no studies that have explored their critical requirement in the regulating L-arginine transport into cells. Thus, it is unclear whether the JNKs and/or AP-1 are required for either induced NO synthesis and/or L-arginine transport. Moreover, it is not clear whether the discrepancies we and others have observed are due to differences in cell types and/or experimental approaches using pharmacological vs molecular approaches to regulate iNOS induction.

Studies have therefore been carried out to investigate the critical role of JNK/AP-1 in the expression of the inducible L-arginine-NO pathway in both J774 macrophages and RASMCs. The planned experiments will use pharmacological inhibitors and the dominant negative constructs TAM-67 and  $\alpha$ -Fos to confirm previous findings. More importantly, the studies will be expanded to include a detailed investigation of the activated status of different AP-1 subunits under various experimental conditions. This would be with the aim of establishing whether the discrepancies and current

controversies relating to the role of JNK/AP-1 in the induction of iNOS/CATs are indeed associated with differences in the patterns of activation of various AP-1 subunits; some of which may be without effect while others may positively or negatively regulate iNOS and/or CAT gene expression.

# **Chapter 2**

## **Methods**

## **Methods**

### **2.1 Cell Culture**

#### **2.1.1 Preparation of complete cell culture growth medium**

Dulbecco's Modified Eagle's Medium (DMEM, low glucose- i.e. 1000 mg/ml, without sodium pyruvate) supplemented with 10% foetal bovine serum (FBS), 100 units ml<sup>-1</sup> penicillin plus 100 µg ml<sup>-1</sup> streptomycin, was used as cultured medium. Once prepared, the complete growth medium was kept at 4 °C and used within a period of 2 weeks.

#### **2.1.2 Culture of J774 macrophages**

The murine monocytic macrophage cell line J774 was obtained from the European Collection of Animal Cell Cultures and maintained in continuous culture at 37 °C and 5% CO<sub>2</sub> in T-75 tissue culture flasks containing complete growth medium. When necessary cells were harvested by gentle scraping and passage every 3-5 days by dilution of the suspension of the cells in fresh medium.

#### **2.1.3 Isolation of Rat Aortic Smooth Muscle Cells (RASMCs)**

Vascular smooth muscle cells were isolated from the aorta of male Weister rats (250-300g) as described (Wileman *et al.*, 1995) and cultured in complete growth medium. Briefly, each aorta was cleaned off fat and other tissues before cutting open to expose the lumen, which was gently scraped to remove the endothelial layer.

Each aorta was then cut into small (2 mm) segments and transferred into a T-25 flasks containing complete medium. Segments were allowed to attach to the plastic by keeping each flask in the upright position for 6-12 h in a cell culture incubator at 37 °C/5% CO<sub>2</sub>. Flasks were then placed flat, allowing the medium to cover the tissue explants and observed over 7-14 days. Migrating and proliferating cells were harvested and sub-cultured as described below.

#### **2.1.4 Sub-culturing of rat aortic smooth muscle cells**

Proliferating cells that had migrated from the explants were harvested with Trypsin-EDTA (0.01/0.02 %) made up in Phosphate Buffer Saline (PBS). At first, the culture medium was aspirated from flasks and the cells washed with PBS (3 times) to remove all the media containing FBS. Trypsin-EDTA was added to the cell monolayer and incubated for 5 min in a cell culture incubator. Cells were then observed under the microscope to ensure detachment. Five ml of complete growth medium was added to the flasks to inactive the trypsin and the cells were dispersed into single cultures with a Pasteur Pipette before being transferred into sterile T-75 tissue culture flasks. Cells were passaged weekly and used between passage 3 and 6.

#### **2.1.5 Identification of Smooth Muscle Cells**

Cells isolated were identified as being smooth muscle by immunostaining using a monoclonal anti- $\alpha$  smooth muscle actin antibody and anti-mouse IgG FITC

conjugated secondary antibody (Skalli *et al.*, 1986). Cells were plated in Lab Tec wells at sub-confluent density and allowed to grow to 50% - 60% confluency. The cells were washed twice with PBS (1X) fixed with ice-cold methanol for 45 sec and rinsed with ice-cold PBS before blocking for 20 min with a solution that contain 5% Bovine Serum Albumin (BSA) in 10 ml of 1X PBS. A 1:50 dilution of the anti- $\alpha$ -actin antibody was made up in blocking buffer and incubated with cells for 1 h at 37°C. Cells were washed four times with PBS changing the wash buffer every 5 min. The secondary antibody was diluted 1:50 in blocking buffer and incubated with the cells for 1 h at 37°C. Cells were then treated for 15 sec with 30% glycerol. This procedure was repeated using 50% and 80% glycerol solution respectively. Finally, the cells were mounted in 2-3 drop of glycerol (100%) solution and a cover slip was placed on top of the cells. A seal was made using nail varnish and visualised under the UV microscope at a magnification of 100x.

#### **2.1.6 Determination of cell number**

Cell number was determined using a haemocytometer with the Trypan Blue exclusion assay. Monolayers of cells were trypsinized as described above and resuspended in 10 ml of DMEM. 100 $\mu$ l of the cell suspension was mixed with an equal volume of Trypan blue and then a total volume of 10  $\mu$ l was used to fill the chamber on both side of the haemocytometer with the cover slip placed on top. The haemocytometer was then placed on the microscope stage and viewed. The total number of cells was determined by counting the cells in each large square (1mm) on both side of the haemocytometer ensuring that only cells touching the two borders

were counted. Moreover, cells outside the large square even if they were within the field of view were not counted. The cell count per millilitre was determined as follows

$$\text{Cells/ml} = \frac{\text{Number of the cells counted}}{\text{Square counted}} \times \text{conversion factor}$$

Where:

Number of the cells = total cell counted

Square = the four squares counted on the haemocytometer

Conversion factor =  $10^4$ , as each square is equal to  $10^{-4}$  ml

To get the total number of cells harvested, the number of cells determined per millilitre was multiplied by the original volume of medium in which the cells were suspended:

$$\text{Total Cells} = \text{cells/ml} \times \text{total volume of cell suspension}$$

### **2.1.7 Plating of cells for experimentation**

When required, confluent monolayer of J774 macrophages were scraped with the rubber scraper while RASMCs were trypsinised as described above. Cells were then

plated at the appropriate density and allowed to grow to the required confluency by incubating plates at 37°C/ 5% CO<sub>2</sub> in a tissue culture incubator.

## **2.2 Experimental Protocols**

### **2.2.1 Regulation of nitric oxide production by drug treatment**

Effects of the selected drugs on NO production were investigated on confluent monolayers of cells. When present, drugs were added for 30 min prior to activation of cells with LPS and/or IFN- $\gamma$  for the required time period.

### **2.2.2 Determination of nitrite production by the Griess assay**

Nitric oxide production was measured by the standard Griess assay as described by Wileman et al., (1995). This assay relies on a diazotization reaction that was originally described by Griess in 1879 and detects NO<sub>2</sub><sup>-</sup> in solution as shown in Figure 2.1(Green *et al.*, 1982).

A 100  $\mu$ l aliquot of media was removed from each well and transferred to new 96 well plates. Sodium nitrite standards (1 to 10 pmoles/well) made up in complete culture medium were transfer to the outer wells on the same plate and all samples were incubated at room temperature for 15 min with 100  $\mu$ l of Griess reagent (Appendix 1). The absorbance of each well was read at 540 nm on a Multiscan Ascent (Lab-system) plate reader and the level of nitrite determined using the

sodium nitrite standard curve constructed. Figure 2.2 shows an example of a nitrite standard curve that was used to determine nitrite concentration.

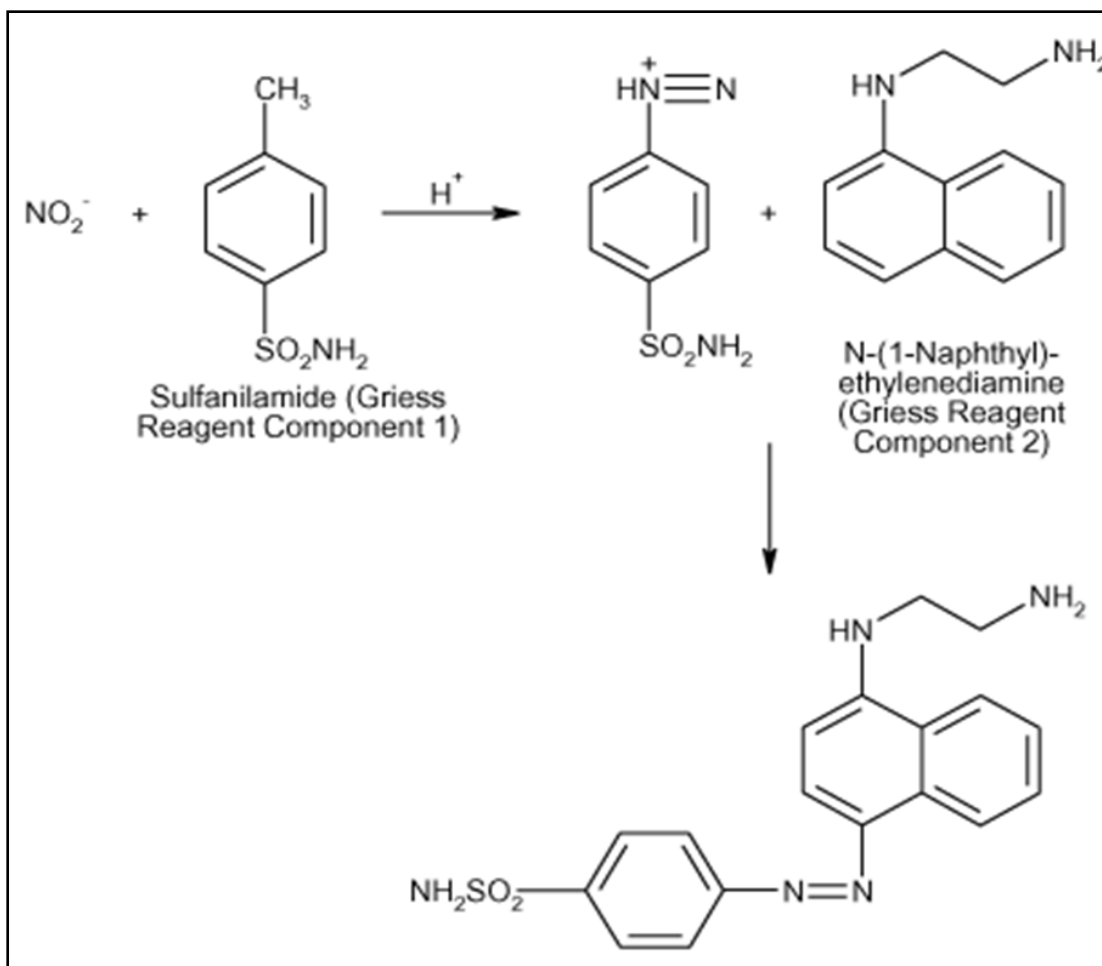


Figure 2.1 **Detection of  $\text{NO}_2^-$  in solution by the Griess assay**

Under acidic conditions nitrite reacts with the amino group of sulfanilic acid to form the diazonium cation, which couples to  $\alpha$ -naphthylamine in the *para*-position to form the azo dye (Green *et al.*, 1982).

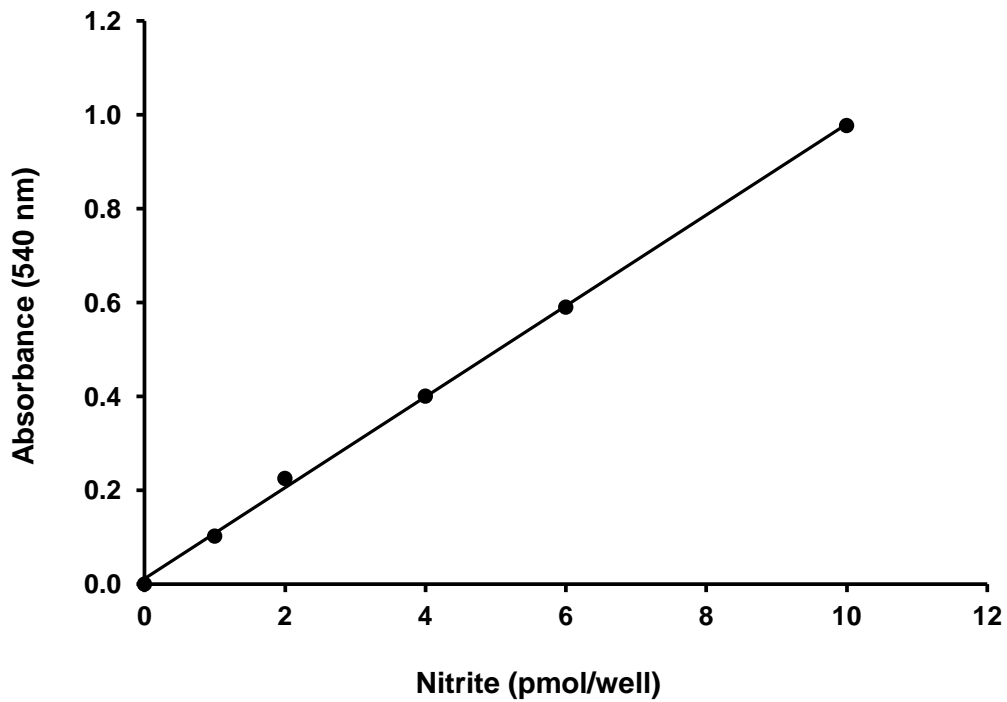


Figure 2.2 **A representative nitrite standard curve**

Sodium nitrite standard were prepared in complete culture medium. A 100  $\mu$ l aliquot from each standard was added in triplicate to the 96 well plates and incubated for 15 min with an equal volume of the Griess reagents. Absorbance values were taken at 540 nm on a Multiskan Ascent plate reader.

### 2.2.3 Protein quantification using Bicinchoninic acid (BCA)

Total cell protein was determined by the BCA assay which is based on the Biuret reaction as shown in Figure 2.3. This is a detergent-compatible formulation for the colorimetric detection and quantification of total proteins. This method is a combination of the reduction of cupric ions [Cu (II)] to cuprous ions [Cu (I)] by proteins in an alkaline medium (i.e. biuret reaction) and a selective and sensitive colorimetric detection of the cuprous ions. The purple-coloured product is formed by the chelation of one Cu (I) ion by two molecules of BCA (Smith *et al.*, 1985; Wiechelman *et al.*, 1988)

For the determination of total cell protein, 10 µl of Double distilled water (DDW) or lysis buffer was added to each well containing cells. Protein standards (1-30 µg/ml) were made from a 1 mg/ml bovine serum albumen (BSA) stock solution in DDW. 10 µl of each standard was added in triplicate to wells. The BCA reagent was prepared as instructed by the manufactures by mixing reagent A with reagent B at the ratio of 1:50 volume. [Pierce BCA assay reagent A contains sodium carbonate, sodium bicarbonate, bicinchoninic acid and sodium tartrate in 0.1M sodium hydroxide. Reagent B contains 4 % (w/v) Copper (II) sulfate pentahydrate (CuSO<sub>4</sub> • 5H<sub>2</sub>O)]

A 100 µl aliquot of the BCA reagents was added to each well and the plates incubated at room temperature on a shaker for 40 minutes. The absorbance was read at 620 nm on a Multiscan Ascent plate reader. The absorbance values of samples were then converted to protein using a BSA standards curve (Figure 2.4) constructed with each assay.

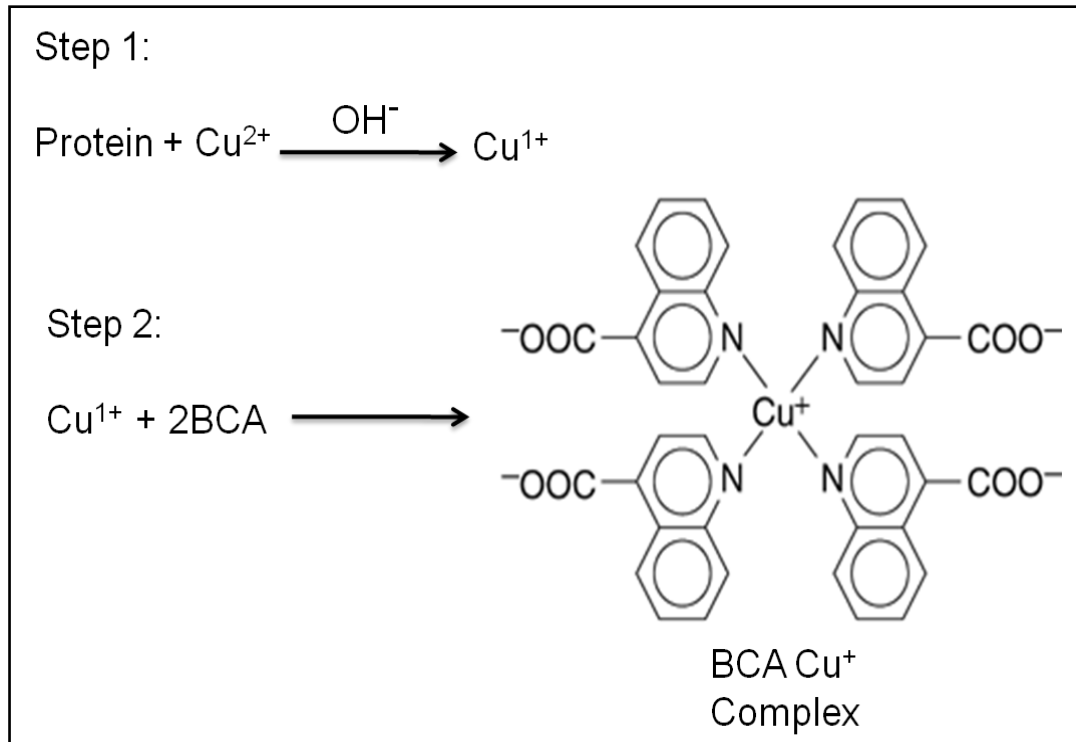


Figure 2.3 **Protein detection by the BCA method**

The method combines the reduction of  $\text{Cu}^{+2}$  to  $\text{Cu}^{+1}$  by protein in an alkaline medium with the highly sensitive and selective colorimetric detection of the chelation of  $\text{Cu}^{+1}$  by the BCA reagent to form a BCA  $\text{Cu}^{+}$  complex.

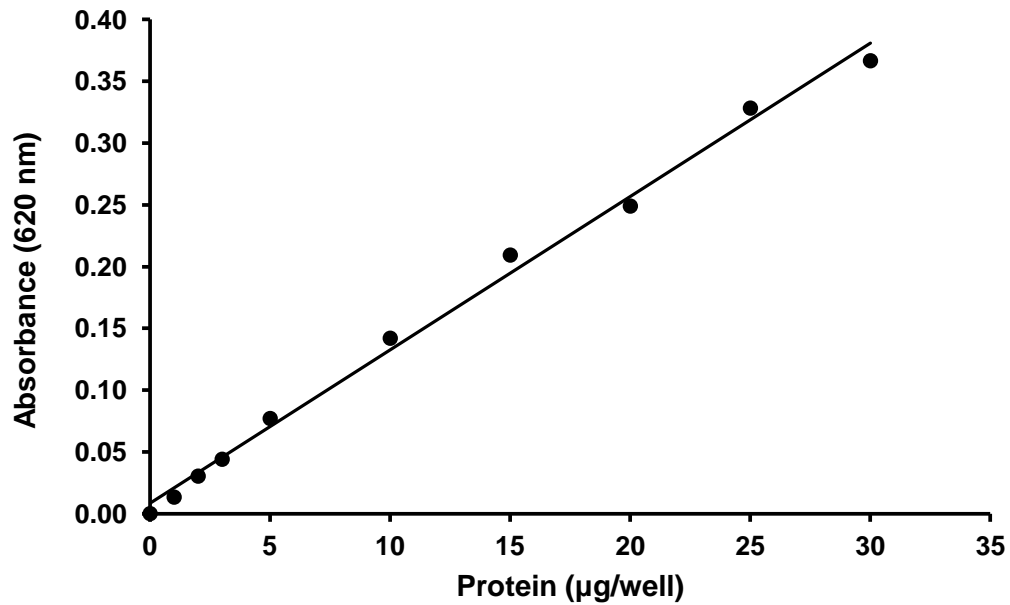


Figure 2.4 **A representative protein standard curve**

Bovine serum albumin standards were prepared in lysis buffer/water. 10 µl of each was added in triplicate to the plates. 100 µl of BCA reagent was added to each well and incubated for 40 minutes at room temperature. Absorbance values were then read at 620 nm using a Multiscan II plate reader and the readings used to construct the standard graph.

## 2.2.4 Measurement of [<sup>3</sup>H]-L-arginine transport

Transport of [<sup>3</sup>H]-L-arginine was performed as described (Wileman *et al.*, 1995). Cells were washed twice with 200 µl Kreb's buffer (NaCl, 131 mM; KCl, 5.6 mM; NaHCO<sub>3</sub>, 25 mM; NaH<sub>2</sub>PO<sub>4</sub>, 1 mM; D-glucose, 5.5 mM; HEPES, 20 mM; MgCl<sub>2</sub>, 1 mM; CaCl<sub>2</sub>, 2.5 mM) at 37°C. Transport was initiated by the addition of transport buffer (Kreb's buffer containing 1 µCi/ml [<sup>3</sup>H]-L-arginine plus 100 µM unlabelled L-arginine) to the cells at 37°C. The reaction was stopped after 2 min by incubating plates on ice and washing cells twice with ice cold Kreb's buffer containing 10 mM non-radioactive L-arginine.

Total cell protein was determined as described above and the content of each well transferred into scintillation vials. 4 ml of scintillation fluid was added to each vial, vortexed and counted on a Beckman LS6500 β-scintillation counter. The standard vials were prepared using 50 µl of Kreb's buffer alone and 50 µl of Kreb's buffer containing 100 µM L-arginine plus 1 µM Ci/ml [<sup>3</sup>H]L-arginine. Blank Disintegrations Per Minute (DPMs) were subtracted from each sample and the remaining DPMs converted to pmoles of L-arginine/µg protein/minute using the equation:

$$R = \frac{(5000 \times C) / X}{2 \times Y}$$

**R** is the amount of L-arginine in cell lysates expressed in pmoles

**5000** is the amount of cold arginine in pmoles in 50 µl of 100 µM solution

**C** is DPM in cell lysates

**X** is DPM in 50  $\mu$ l aliquot of 100  $\mu$ M L-arginine solution containing 1  $\mu$  Ci/ml [ $^3$ H]-arginine

**Y** is total protein content of cell lysates counted

**2** is for 2 minutes incubation time with [ $^3$ H]-L-arginine

### **2.2.5 Determination of cell viability by the MTT assay**

Cell viability was determined by monitoring the metabolism of 3-(4,5-Dimethylthiazol-2-yl)-2,5-diphenyltetrazolium bromide (MTT) to purple formazan by viable cells (Figure 2.5). This reaction takes place only when mitochondrial reductase enzymes are active, and so conversion is directly related to the number of viable cells. The production of purple formazan in cells treated with an agent was compared to its production in control cells. Toxic concentrations of a compound would lead to a reduction in the mitochondrial dehydrogenase ability to metabolise (MTT) to formazan and therefore produce a reduced absorbance in the MTT assay.

For the assay, confluent monolayers of cells were treated according to the experimental protocol. After the incubation time, fresh medium containing 0.5 mg/ml of MTT was added to the cells and incubated for 4 h at 37°C in a tissue culture incubator. The MTT solution was removed and 100  $\mu$ l Isopropanol was added to the cells and the plate incubated on an orbital shaker for 10 minutes or until all the formazan crystals had dissolved. The plates were read on Ascent multiscan plate reader at 540 nm. The cell viability in the control cells (untreated cells) was considered as 100% and cell viability at each drug concentration was calculated as a percentage of the control.

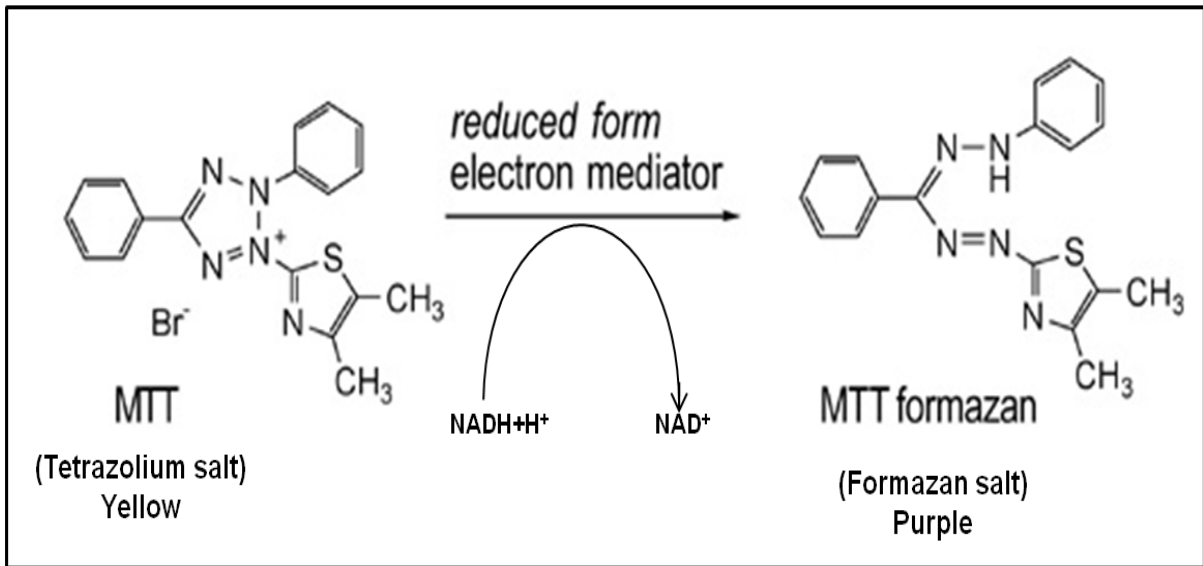


Figure 2.5 **Detection of formazan by viable cells**

Water soluble tetrazolium salt is converted into an insoluble purple compound, formazan, by cleavage of the tetrazolium ring by mitochondrial dehydrogenases into purple formazan in viable cells (Mosmann, 1983).

## **2.2.6 Western blotting**

### **Preparation of cell extracts for Western blot analysis**

Confluent monolayers of cells were incubated under different experimental conditions. At the end of each treatment time, wells were washed twice with ice-cold PBS and the cells lysed using hot lysis buffer containing TRIS 100 mM (pH 7.4) and 10% SDS. The lysates were scraped and transferred into eppendorf tubes. The samples were heated for 5 minutes at 95°C and sonicated three times for 30 seconds each time. Lysis of phospho-proteins was performed using ice-cold lysis buffer plus the EDTA-free protease inhibitor cocktail containing: AEBSF, 100 mM/ml; Arotinin, 80 µM/ml; Bestatin, 5 mM/ml, E64 protease inhibitor, 1.5 mM/ml; Leupeptin, 2mM/ml; Pepstatin A, 1 mM/ml diluted 1:200 in lysis buffer.

Protein quantification was performed as described in the BCA assay and samples were kept in the freezer at -20 °C until analysed.

### **SDS-PAGE electrophoresis**

Various target protein were identified from cell lysis by Western blot analysis using specific antibodies. Samples were diluted with a 1:1 volume of loading buffer (TRIS 250 µM; SDS 4%; glycerol 10%, β-mercaptoethanol 2%; bromophenol blue 0.006%; pH 6.8) and heated for 5 minutes at 90 °C prior to loading. Resolving and stacking gels and buffers were prepared as described in appendix 2.

Samples were loaded into the wells on the stacking gel and run at a constant voltage of 100V in a Bio-Rad Mini-PROTEAN II (Bio-Rad, UK) electrophoresis tank until the bromophenol blue front had migrated to the bottom of the gel. The proteins in the gel

were transferred to a polyvinylidene difluoride (PVDF) blotting membrane that was pre-soaked in methanol (99.8%) for 15 seconds prior to blotting. The membrane was placed in a transfer cell on 3 blotting filter paper and followed by gel and 3 filter papers on top. The proteins were transferred in an electroblotter (semi-dry transfer systems) (Bio-Rad, UK) for 120 min at 1mA per cm<sup>2</sup> of membrane. The gels were stained in Coomassie blue reagent after the transferring stage to check the efficiency of the protein transferred to the membrane followed by de-staining using a solution of methanol (455 ml), DDW (455 ml) and glacial acetic acid (90 ml). The membrane was blocked in blocking buffer (washing buffer (1x), 0.1% Tween20 and 5% fat free milk or BSA for phospho-proteins) for 1 hour at room temperature to prevent nonspecific antibody binding to charged and other molecules on the membrane, thus preventing or reducing background noise.

The membrane was then incubated with the appropriate primary antibody for the target protein and for  $\beta$ -actin, which was used to standardise for loading. On the following day, the membrane was washed with 1x washing buffer (200ml of 10X washing buffer (Appendix 2.7) + 2ml Tween-20 + 1800 ml of DDW) for 30 minutes, changing the buffer every 5 minutes. This was followed by a further 90 minute incubation of the membrane with the secondary antibody and the antibody for the molecular weight marker in blocking buffer. The membrane was washed for another 30 minutes, changing the wash buffer every 5 minutes. Proteins were detected by the enhanced chemiluminescence detection method following the manufacturer's protocol. The membrane was covered with ECL reagent and then exposed to photosensitive film for 1 to 5 minutes. The photosensitive film was developed and fixed. The developed protein bands on the film were scanned using an Epson

(Perfection 2480 Photo) Scanner and the intensities of the protein bands on the scanned image were measured using the densitometry software, Syngene Gene Tools (version 3.00) and the data expressed as the percentage of the value obtained for Control samples.

### **2.2.7 Stripping the western blot membrane**

If a membrane was needed for another probe after ECL treatment, it was washed for 10 min with washing buffer prior to incubation with a stripping buffer (2 g SDS in 62.5 mM Tris-HCl pH 6.7 plus 700  $\mu$ l mercaptoethanol) at 50°C for 30 min (on shaker). The blotting procedure was repeated and the primary and secondary antibody incubations carried out as described above.

### **2.2.8 Preparation of DH5- $\alpha$ Competent E.coli**

Using a loop, DH5- $\alpha$  cells were transferred directly from frozen stock to growth media (TYM; Tryptone, 20 g/l; Yeast Extract, 5 g/l; MgSO<sub>4</sub>.7H<sub>2</sub>O, 2.5 g/l; NaCl, 5.8 g/l; dissolved in DDW) and incubate overnight at 37°C. The following day, 2 ml of an overnight culture was incubated with 200 ml TYM. Cells were grown to a density of approximately 10<sup>8</sup> cells/ml for 3 hours at 37°C in a microbiological shaker. The cultures were cooled on ice for 10 minutes and recovered by centrifugation at 4100 rpm for 10 minutes. The supernatant was removed and the pellet re-suspended in 20 ml of ice-cold frozen storage buffer (potassium acetate, 1M pH 7.5; MnCl<sub>2</sub>.4H<sub>2</sub>O, 8.91 g; CaCl<sub>2</sub>.2H<sub>2</sub>O, 1.47 g; potassium chloride, 7.46 g; hexaminecobalt chloride, 0.80 g; glycerol, 100 ml; DDW, 1 L). Re-suspended cells were then placed on ice for

10 minutes before centrifuging at 4100 rpm for 10 minutes. The supernatant was removed and the pellet re-suspended in 14 ml of ice-cold storage buffer containing 140  $\mu$ l DMSO per 5 ml of re-suspended cells. Cells were incubated on ice for 15 minutes before being aliquot into eppendorf tubes and stored at -70°C until needed.

### **2.2.9 Transformation of *E.Coli* DH5- $\alpha$ with dominant negative GFP-a-Fos or GFP-TAM-67**

Aliquots of competent DH5- $\alpha$  cells were thawed on ice for 15 minutes. Under aseptic condition, 200  $\mu$ l of DH5- $\alpha$  cells were transferred into three vials, labelled and kept on ice. Vial 1 contained no plasmid, vial 2 contained the positive control vector (PUC19: small, high copy number E.coli plasmid cloning vector) and vial 3 contained the plasmid. The suspension in the vials were mixed and incubated on ice for 30 minutes. Following heat shock for 30-45 seconds at 37°C (in water bath), the competent cells were immediately placed on ice for 5 min. 800  $\mu$ l of liquid broth (LB without antibiotics) was added and then cultures incubated for 1 hours in 37°C. Cultures were centrifuged at 14,000 rpm for 1 minutes and the supernatant discarded. The pellet was re-suspended in 100  $\mu$ l of LB and transferred on the agar plates containing 50  $\mu$ g/ml Kanamycin. Plates were allowed to stand at room temperature for 1 hour before incubating at 37°C overnight for colony growth. A mature single colony, resistance to Kanamycin was used to inoculate sterile bottle containing 10 ml of LB (with 50  $\mu$ g/ml Kanamycin). The cultures were incubated overnight at 37°C in an orbital shaker. It should be noted that the colour of L-Broth

should change from a clear yellow to a cloudy solution indicating the growth of bacteria in suspension.

#### **2.2.10 Mini-scale preparation of plasmid DNA (mini-preps)**

A single colony of transformed DH5- $\alpha$  cells from a fresh plate was picked using a flamed sterile loop and inoculated into 10 ml LB containing Kanamycin. This was then left to incubate in an orbital shaker for 24 hours at 37°C. An aliquot of 1 to 5 ml of an overnight recombinant *E.Coli* culture was pelleted at 12,000 rpm for 1 minute. The supernatant was discarded and the pellet re-suspended in 200  $\mu$ l re-suspension solution (Tris-Cl, 50 mM; pH 8.0; EDTA, 10 mM; RNase A, 100  $\mu$ g/ml) by vortexing in order to thoroughly re-suspend the cells. Cells were lysed with 200  $\mu$ l of lysis solution (NaOH, 200mM; SDS, 1%) and mixed immediately by gentle inversion until the mixture become clear and viscous. 350  $\mu$ l of neutralization/binding solution (Potassium acetate, 3.0 M; pH 5.5) was added to precipitate the cell debris. Tubes were then gently inverted and the debris pelleted by centrifuge at 12,000 rpm for 10 minutes. Each tube was washed twice with 750  $\mu$ l wash solution and centrifuged at 12,000 rpm for 30 seconds to 1 minute to remove residual salts and other contaminants. The supernatant was discarded and re-centrifuged again at 12,000 rpm for 1 to 2 minutes to remove excess ethanol. Finally the DNA was eluted by the addition of 100  $\mu$ l of elution solution (NaCl, 1.6 M; MOPS, 50 mM; pH 7.0; Isopropanol, 15%) and centrifuged at 12,000 rpm for 1 minute. The elute containing the DNA was collected and stored at -20°C for future use.

### 2.2.11 Preparation of 0.8% agarose for mini-gel

The quality of the DNA generated was determined on an agarose gel. The gel was prepared by dissolving 0.4 g of agarose in 50 ml of 1X gel running buffer (Tris, 90 mM; EDTA 2.5 mM; Boric acid, 90 mM) and dissolved in a microwave. The mixture was poured in the gel tray after being slightly cool and well forming comb inserted and left to set properly. The gel was placed in the tank and covered with gel running buffer. Plasmid DNA was loaded into the wells and run for 2 hours at 80 volts. The gel was stained with ethidium bromide (5µg/ml) added to the running buffer for 1 hour. Plasmid DNA was visualized in a UV chamber and captured using a Bio Imaging System and Gene Genius software program.

### 2.2.12 Determination of DNA yield

The quantification of DNA was performed spectrophotometrically. Two micro litres of plasmid DNA was diluted in 998 µl of sterile double distilled water and placed in a quartz cuvette. The spectrophotometer was blanked against 1 ml of water and the optical density of the DNA read at 260 nm. The concentration of DNA was determined using the following equation:

$$\text{DNA concentration } (\mu\text{g/ml}) = \text{OD}_{\lambda 260} \times \text{Dilution factor} \times 50$$

$\text{OD}_{\lambda 260}$  is the absorbance of the DNA measured

**50** is concentration in µg/ml of DNA in a solution with an  $\text{OD}_{\lambda 260}$  of 1

### **2.2.13 Digestion of plasmids by restriction enzymes**

Plasmids (GFP-a-Fos and GFP-TAM-67) were digested with the restriction enzymes BamHI and HindIII for a-Fos or BamHI and XhoI for TAM-67 to confirm the presence of the inserted fragment. Restriction enzyme digestion was performed in a volume of 20  $\mu$ l on 0.2- 1.5  $\mu$ g of substrate DNA. The mixture was prepared in an eppendorf tube with sterile deionised water at a ratio of 16.3  $\mu$ l; digestion buffer 2  $\mu$ l; acetylated BSA 0.2  $\mu$ l and DNA at the concentration of 1  $\mu$ g/ml. This was mixed by gentle pipetting and 0.5  $\mu$ l of restriction enzyme (10 U/ $\mu$ l) added, mixed by a further gentle pipetting and centrifuged for a few seconds at 2000 rpm. The tube was incubated in a water bath at 37°C for 4 hours before mixing with loading buffer and loaded on to the mini gel. (The maps for each plasmid are attached in appendix 4)

### **2.2.14 Transfection of RASMCs with dominant negative GFP-a-Fos and GFP-TAM-67**

Rat aortic smooth muscle cell were transfected using a polycationic peptide (Peptide 6; Hart *et al.*, 1998) as described by Cui et al (2005). Cells were seeded at a density of  $4 \times 10^4$  cells per well in 24-well plates and allowed to reach a confluency of 50-70%. The transfection mixture was prepared by adding 0.75  $\mu$ l, Lipofectin (stock of 1mg/ml) to 100  $\mu$ l of OptiMEM followed by 40  $\mu$ l of Peptide 6 (stock 0.1 mg/ml). In a different tube, 1  $\mu$ l of 1 mg/ml DNA stock was added to 100  $\mu$ l OptiMEM which was then added to the content of the first mixture and incubated at room temperature in the cell culture hood for 3 hours to let the DNA-Peptide 6 complex form. After the incubation period the solution was diluted (1:2) to give 2  $\mu$ g/ml DNA concentration in

OptiMEM. The culture medium was removed from each well and replaced with 500  $\mu$ l of complex mixture containing the DNA of interest. Plates were incubated for 3 hours at 37°C in the cell culture incubator to allow the DNA to internalise. After this stage, the transfection mixture was removed and cells incubated in fresh culture medium for periods of 3, 6, 9, 12, 18 and 24 hours in order to determine the maximum transfection efficiency. After establishing the optimum time for transfection, transfected cells were activated with LPS and IFN- $\gamma$  for a further 24 hours. Controls were cultured in normal complete growth medium without transfection mixture in the presence or absence of LPS and IFN- $\gamma$ . The transfected cells were observed under UV microscope, which showed the green fluorescent colour and also by western blotting using a Green Fluorescent Protein (GFP) antibody.

#### **2.2.15 Isolation of total RNA**

Total RNA was prepared from confluent monolayers of cells using the RNA STAT-60 reagent (AMC Biotechnology) according to the manufacturer's instructions. 1 ml of RNA STAT-60 was added to each T-25 plate and incubated at room temperature for 3 min to allow lysis and complete dissociation of nucleoprotein complexes. Cell lysates were scrapped using a sharp sterile scrapper and transferred into eppendorf tubes and 200  $\mu$ l of chloroform per ml of RNA STAT-60 added to each tube. The mixture was then incubated for a further 5 min at room temperature. Each tube was vortexed for 15-20 seconds and incubated for 10 min at room temperature before centrifugation at 4°C for 10 min at 10,000 rpm. The upper clear aqueous phase containing RNA was removed and transferred into a new eppendorf tube. Total RNA

was precipitated by adding 500 µl of isopropyl alcohol per ml of RNA STAT-60 to the clear supernatant and samples incubated at room temperature for 10 min before centrifuging at 4°C for 10 min at 10,000 rpm. The RNA pellet was washed three times with 75% ethanol, centrifuged for 2 min at 8,000 rpm and then air dried in the fume cupboard before re-dissolving in 50 µl of DNase free treated water. The samples were frozen down at -20 °C for future use.

#### **2.2.16 RNA treatment and purification**

Ribonucleases are ubiquitous and are often the leading cause of RNA degradation during RNA isolation. Before the resulting RNA could be used it must be ensured that the extracted RNA is of high quality, intact and is free of DNA contamination. To achieve this, the extracted RNA was initially treated with RNase-free DNase to eliminate DNA from the RNA sample. This was carried out using the TURBO DNA-free DNase kit (Applied Biosystems) according to the manufacturer's protocol. Briefly, the RNA was mixed with DNase enzyme in a DNase buffer (Turbo DNase free buffer) and incubated in 37 °C for 30 min. After incubation time, DNase inactivation reagent was added and mixed properly. The RNA was then centrifuged at 10,000 rpm for 3 min and supernatant transferred into fresh ependorh tubes. The samples were then freeze in -20 °C.

### 2.2.17 Quantification of isolated RNA

The RNA concentration was assessed using a UV spectrophotometer (Eppendorf Biophotometer, Germany) by measuring the absorbance at 260 (OD<sub>260</sub>) and 280 (OD<sub>280</sub>) nm and calculating the concentration as follows:

$$\text{RNA concentration } (\mu\text{g/ml}) = A_{\lambda 260} \times 40 \mu\text{g/ml} \times \text{Dilution Factor}$$

Where

$A_{\lambda 260}$  is Absorbance of RNA

40 represents the concentration in  $\mu\text{g ml}^{-1}$  of RNA in a solution with an OD <sub>$\lambda 260$</sub>  of 1.

Measurements were carried out in triplicate, and the average value was used. Also RNA purity was determined using the ratio of absorbance at 260 nm to the absorbance at 280 nm ( $A_{260}/A_{280}$ ).

RNA quality was assessed by gel electrophoresis, in order to visualize the discrete and intact ribosomal bands of 28S and 18S respectively. Sharp and non-smearing bands of the latter will confirm the quality and degree of RNA degradation. Figure 2.6 is a sample of agarose gel and ribosomal band for both RASMCs and J774 macrophages.

### 2.2.18 Reverse Transcription

To quantify the level of gene expression, reverse transcription in combination with polymerase chain reaction (Horikoshi *et al.*, 1992; Murphy *et al.*, 1990) was carried

out using the high capacity RNA to cDNA Reverse Transcription kit (Applied Biosystems). 2 µg of total RNA was used per 20 µl reaction mix containing RT buffer (10 µl), RT enzyme mix (1 µl) plus Nuclease-free H<sub>2</sub>O to reach to the volume of 20 µl. The tubes were briefly centrifuged and incubate in a thermal cycler at 37°C for 60 min. The reaction stopped by heating at 95°C for 5 min and the samples held at 4°C. The cDNA was either analysed or frozen down at -20°C until required.

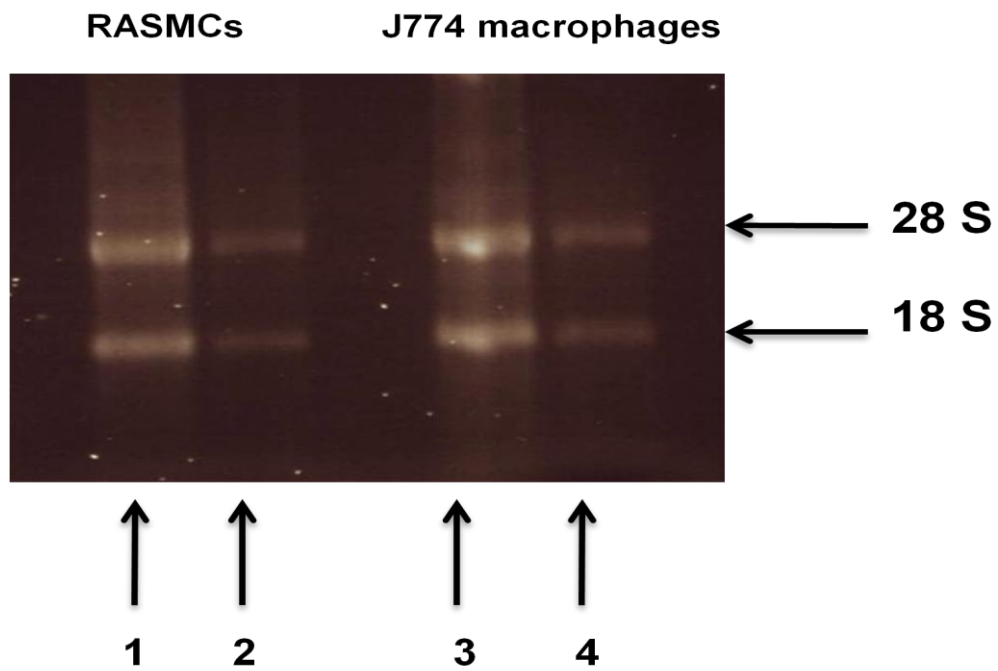


Figure 2.6 **Agarose gel electrophoresis of RNA isolates from RASMCs and J774 macrophages**

The gel is representative of at least five independent isolations and shows 28s and 18s ribosomal bands. Panel 1 and 3 representing the RNA before DNase treatment and Panel 2 and 4 represent the RNA after treatment.

### **2.2.19 PCR primer design**

Primers for use in PCR analysis of iNOS and CATs (Tables 2.1 and 2.2) were designed from respective published sequences obtained from the murine database with cross-reference to the National Center for Biotechnology Information (NCBI). The sequences retrieved were: iNOS [NOS II – RefSeq; NM\_010927.3], CAT-1 [SLC7A1 – RefSeq; NM\_007513.3], CAT-2 [SLC7A2] (gene encoding the spliced variants of CAT-2A - RefSeq; NM\_001044740.1 and CAT-2B- RefSeq; NM\_007514.3). Housekeeping genes, glyceraldehyde phosphate dehydrogenase (GAPDH- RefSeq; NM\_008084.2) for mouse and Ribosomal protein L13a (RPL13a- RefSeq; NM\_009438) for rat were chosen. Primers were designed with a melting temperature ( $T_m$ ) of  $60^\circ\text{C} \pm 2^\circ\text{C}$  using FASTPCR and Molecular Beacon programs. The primer sequences generated (Table 2.1 and 2.2) were checked for hairpins and self-complementarity using the Oligonucleotide Properties calculator software and specificity was assessed using BLAST and/or ClustaW.

**Table 2.1: Rat primer sequences used in PCR analysis**

<b>GENES</b>	<b>FORWARD PRIMER</b> 5'-sequence-3'	<b>REVERSE PRIMERS</b> 5'-sequence-3'
<b>i-NOS</b>	<b>CTGGCTCGCTTGGCCACGGA</b>	<b>GCTCGACAGCAGGAAGGCA</b>
<b>rCat1</b>	<b>TCGCTGCTGTGA TGGCCTTCC</b>	<b>ATCGGTGGTCTGGCCATCTGG</b>
<b>rCat2A</b>	<b>ATGTTCCCTTACCCCGCATTTCTG</b>	<b>TGGCAGCAA CGGGTGACTG</b>
<b>rCat2B</b>	<b>TCGTGTAATCTA TGC TATGGC GGA</b>	<b>TGC CAC TGC ACC CGA TGA C</b>
<b>RPL 13a</b>	<b>CCTGGAGGAGAAGAGAAAGAGA</b>	<b>TTGAGGACCTCTGTGTA TTTGTCAA</b>

**Table 2.2: Mouse primer sequences used in PCR analysis**

<b>GENES</b>	<b>FORWARD PRIMER</b> 5'-sequence-3'	<b>REVERSE PRIMERS</b> 5'-sequence-3'
<b>m-iNOS</b>	<b>CTGGCTCGCTTTGCCACGGA</b>	<b>GCTGGACAGCAGGAGGCA</b>
<b>mCat1</b>	<b>CAGCTCGTCAA AGTTGCACTCC</b>	<b>CAGCTCGTCAA AGTTGCACTCC</b>
<b>mCat2A</b>	<b>ATGTTCCCTTACCCCGCATCTG</b>	<b>TGGCAGCAACGGGTGACTG</b>
<b>mCat2B</b>	<b>TCGTGTAATCTATGCTATGGCGGA</b>	<b>TGCCACTGCCACCCGATGA</b>
<b>GAPDH</b>	<b>TGGCGTTCACCACCATGG</b>	<b>TGAGTGGCAGTGTGGCATGG</b>

### 2.2.20 Polymerase Chain Reaction (PCR)

Following the reverse transcription, quantitative Polymerase Chain Reaction (qPCR) was carried out using the fluorogenic minor groove binding dye, SYBR green (Figure 2.7), the most commonly used dye for a variety of detections. It is a double-stranded DNA intercalating dye which fluoresces, bound to the DNA. A pair of specific primers is required to amplify the target gene with this chemistry. The amount of dye incorporated is proportional to the amount of generated target. The dye emits at 520 nm and this can be detected and related to the amount of target gene (Kubista *et al.*, 2006; Scipioni *et al.*, 2008).

The experiments were performed in a reaction mixture (20µl) consisting of 10µl Power SYBR green master mix, 2µl each of sense and antisense primers (Forward and reverse), 2 µl of template cDNA (1µg/µl cDNA) and 4µl of DNA free water.

PCRs were performed using a Quantica real time machine (Techne) using the 'hot-start' approach as follows:

AmpliTaq Gold polymerase activation at 95°C for 10 min

Template cDNA denaturing at 95°C for 15 secs

Annealing between 59 to 61°C depending on the primer used for 30 secs

Extension at 72°C for 45 secs

The annealing/extension were allowed to progress through a maximum of 45 cycles.

This was followed by:

Dissociation at 56°C - 95°C and Final hold at 4°C

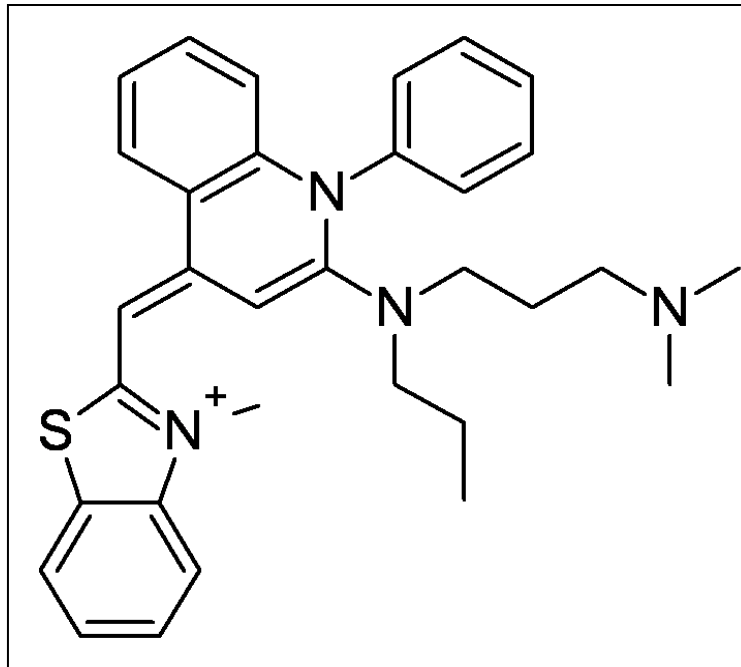


Figure 2.7 **Structure of SYBR green**

Asymmetric cyanines have two aromatic systems containing nitrogen, one of which is positively charged and connected by a methine bridge. The dye has virtually no fluorescence when it is free in solution due to vibrations engaging both aromatic systems, which convert electronic excitation energy into heat that dissipates to the surrounding solvent. On the other hand the dye becomes brightly fluorescent when it binds to DNA, presumably due to the minor channel, and to the fact that rotation around the methine bond is restricted (Bengtsson *et al.*, 2003; Zipper *et al.*, 2004).

### 2.2.21 Analysing PCR data

To investigate physiological changes in gene expression levels, relative quantification was used to analyse the data generated from qPCR results. This is based on the expression level of a target gene versus a housekeeping gene (reference or control gene). The relative quantities can thus be compared across multiple real time PCR experiments (Orlando *et al.*, 1998). The q-PCR results were analysed by the comparative CT method also known as the Delta-Delta CT method ( $2^{-\Delta\Delta CT}$ ). This method involves comparing threshold cycle (Ct) values of both the target gene and the housekeeping gene. The latter was used to normalize the expression results in both control and activated or treated samples. It is therefore necessary that reliable housekeeping genes having minimal variation in expression irrespective of the treatment strategies are employed. To further improve our amplification profile, we incorporate a mathematical model and analyze our data by adjusting for PCR efficiency differences as described (Pfaffl, 2001).

Figure 2.8 shows a sample of standard curve (panel A) which should be plotted for each samples and housekeeping gene. Preparing a standard curve for each gene, which needs to be analysed, can provide a good idea of the performance of the qPCR. The standard curve should include at least 5 points of dilution. Plotting these points on a standard curve, determine the linearity, efficiency, sensitivity and reproducibility of the assay. The slope of the standard curve gives the efficiency of the PCR reaction by the following equations:

$$\text{Exponential amplification} = 10^{(-1/\text{slope})}$$

$$\text{Efficiency} = 10^{(-1/\text{slope})} - 1$$

If the slope of the standard curve is -3.32 then the PCR is 100 % efficient.

With 100 % efficiency, a 2x dilution gives a  $\Delta Ct$  of 1 between each dilution (each cycle the amount of amplification is doubled).

With 100 % efficiency, a 10x dilution gives a  $\Delta Ct$  of 3.2 values between each dilution (every 3.2 cycles the amount of amplification is 10 fold higher).

PCR efficiency between 90 %-110 % is acceptable (slope between 3.1 and 3.58) (Kubista *et al.*, 2006; Schmittgen *et al.*, 2008).

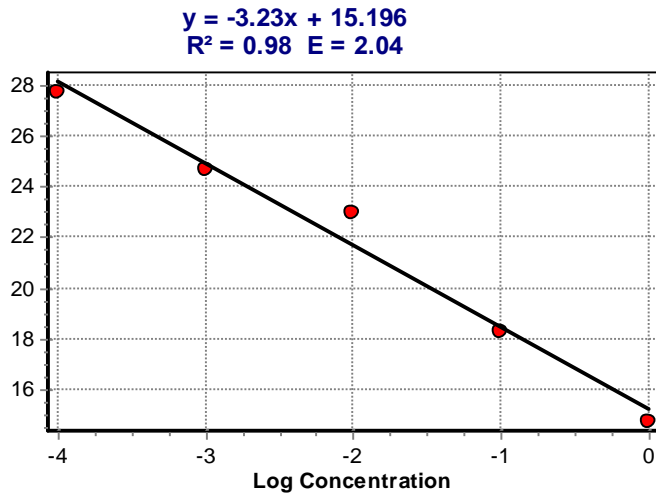
Panel B, an amplification curve, reveals the number of cycles for amplification in which the lower a cycle the higher expression. Panel C is the crossing point, which shows the CT value.

Figure 2.9 panel A and B, shows the dissociation peak and background correction respectively.

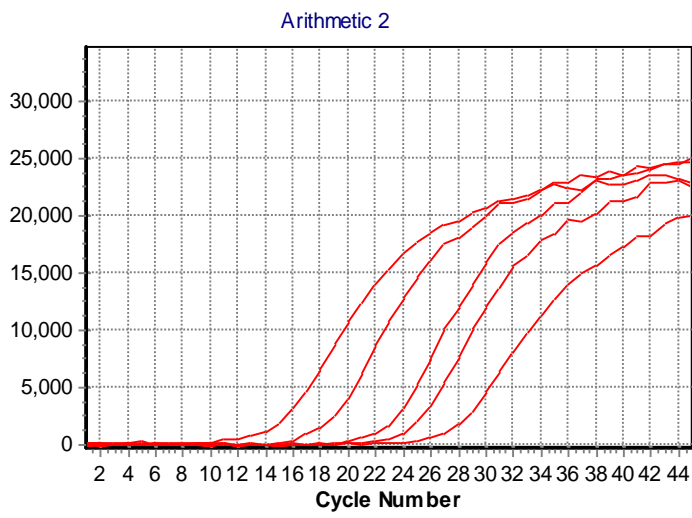
Figure 2.10 is an example of comparison between control and activated samples for iNOS expression.

**Figure 2.8 The standard curve, amplification curve and crossing points of the PCR**

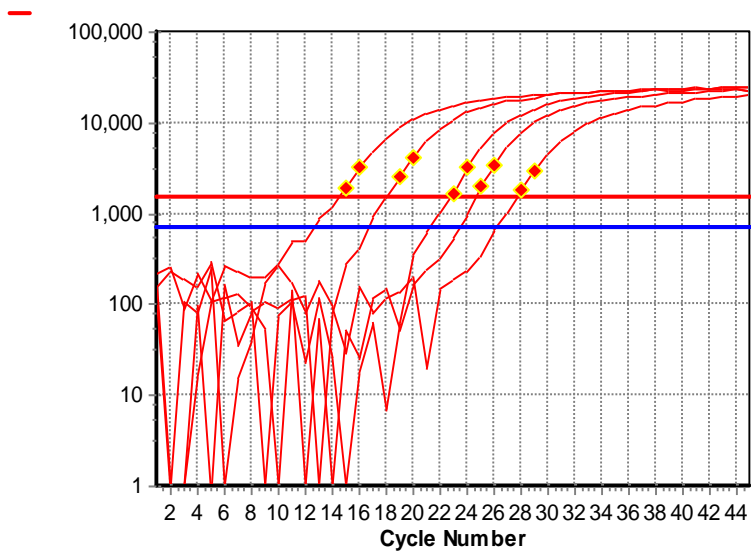
Panel A is an example of a standard curve and Panel B is demonstrates the cycle for the same standard to be amplified. Panel C shows the same cycle with the baseline and the threshold cycle (Ct) value. The blue colour line is the baseline which is the average background. It is calculated according to the noise level in the early cycles, when there is no detectable increase in fluorescence, due to PCR products. The threshold (the red colour line) is the level of fluorescence above the baseline, at which the signal is not considered to be background. The Ct value is defined as the cycle in which there is a significant increase in reporter signal, above the threshold. It is consequently related to the initial amount of DNA and shows also the sensitivity of the assay. The Ct value is consequently in inverse proportion to the expression level of the gene. If the Ct value is low, it means the fluorescence crosses the threshold early, meaning that the amount of target in the sample is high.



(A)



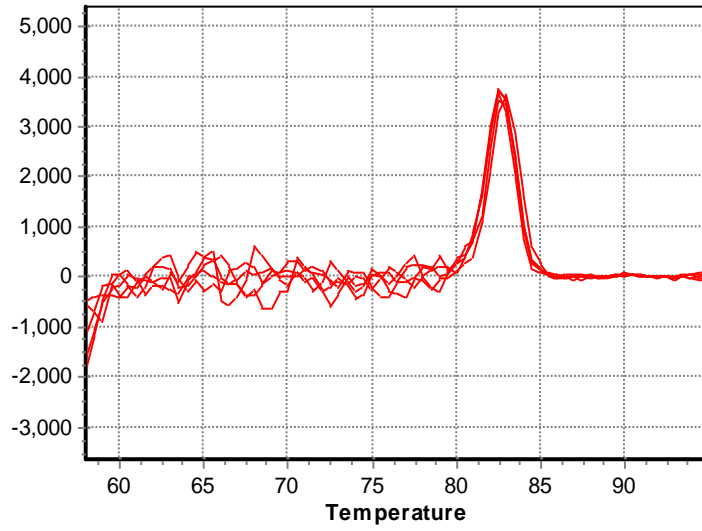
(B)



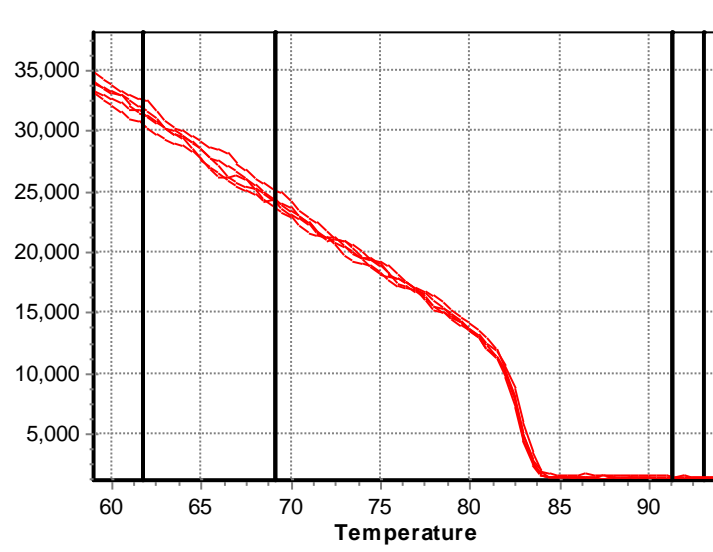
(C)

### **Figure 2.9 The dissociation curve and background correction**

An example of a dissociation curve which demonstrates the peak temperature for dissociation of DNA ladder is shown in Panel A. As the temperature of dissociation depend on the length and composition of the amplicon, it is consequently possible to check how many products of amplification are present in the well. A nice meltcurve should show a unique dissociation peak. This temperature is specific for each product (primer). Panel B is a sample of background correction.



(A)

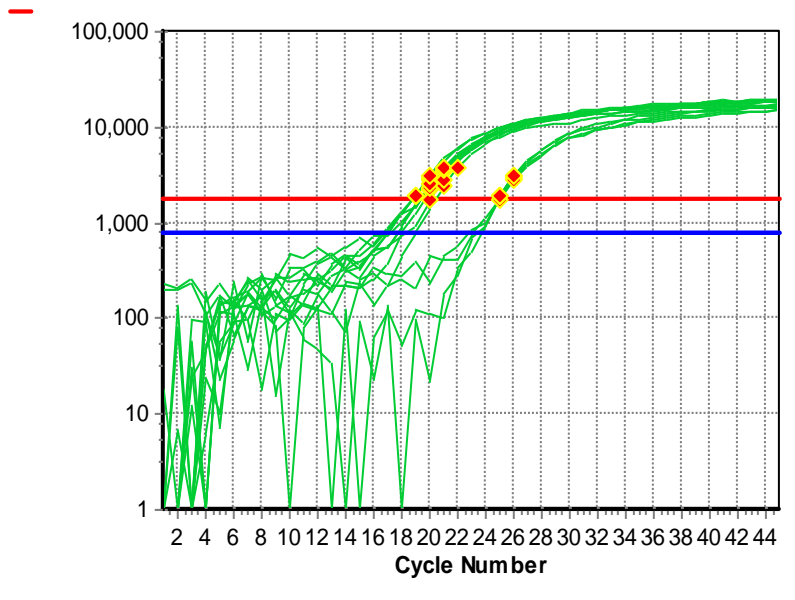
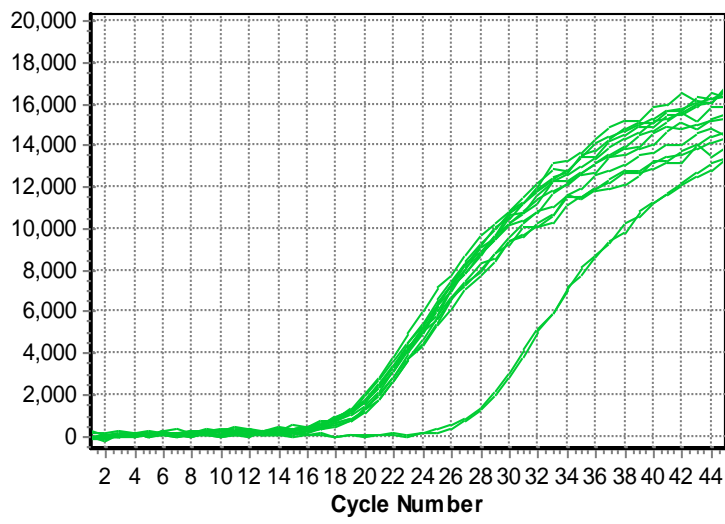


(B)

### **Figure 2.10 Amplification curve**

An example of expression cycle with different samples (control and activated for iNOS). The control expression is in the later cycles (26) and activated cells expressed iNOS in the earlier cycles (18-22 according to the treatment).

Arithmetic 2



### **2.2.22 Preparation of Nuclear Extract for ELISA**

Confluent monolayer of RASMCs or J774 macrophages in T-75 flasks were washed with 10 ml of ice-cold PBS/PIB (Protease Inhibitor Buffer) [125mM NaF (Sodium Fluoride), 250mM  $\beta$ -glycerophosphate, 250mM p-nitrophenyl phosphate (PNPP), 25mM NaVO<sub>3</sub> (Sodium metavanadate) ]. The PBS/PIB was discarded and another 10 ml of this solution added to cell which were then scraped with a cell scraper. Cells were subsequently transferred to pre-chilled 15 ml falcon tube and centrifuge at 300 rpm for 5 min at 4°C. Supernatants were removed and pellets resuspended in 1 ml of ice-cold hypotonic buffer (HB) (20mM Hepes, pH 7.5, 5mM NaF, 1 $\mu$ M Na<sub>2</sub>MoO<sub>4</sub>, 0.1mM EDTA). The mixture was transferred into a pre-chilled 1.5 ml eppendorf tube and left on ice for 15 min for cells to swell. After this stage 50  $\mu$ l 10% Nonidet P-40 (0.5% final) was added and tubes vortexed vigorously for 10 sec.

The homogenates were centrifuge for 30 sec at 4°C in a microcentrifuge and the supernatant (cytoplasmic fraction) removed, while the pellet was resuspended in 50  $\mu$ l complete lysis buffer and left on ice for 30 min on a shaking platform. The tubes were centrifuged at 4°C for 10 min at 12,000 rpm and the supernatant (Nuclear Extract) transferred to a fresh tube and stored in -80°C until analysed.

### **2.2.23 Analysis of AP-1 activation using the TransAM AP-1 kit**

To determine the effect of various experimental procedures on AP-1 activity, a TransAM AP-1 kit (Active Motif, Belgium) was used to assess the activated status of different AP-1 subunits. This kit contains a 96 well ELISA plate with immobilized double-stranded oligonucleotide that contains a TPA Response Element (TRE; 5'-

TGAGTCA-3') which specifically binds to phospho subunits of AP-1 in the nuclear extract. Phosphorylated and bound to DNA epitopes of AP-1 subunits (c-Jun, JunB, JunD, c-Fos, FosB, Fra-1 and Fra-2) were subsequently identified using a primary antibody. A secondary HRP-conjugated antibody provides a sensitive colorimetric read-out which could be quantified by spectrophotometry.

For each assay, 10 µg of nuclear extract was diluted in complete lysis buffer (the total volume of 20 µl) and added to the binding buffer (30 µl) which was added to the wells previously. After one hour incubation at room temperature, plates were washed with washing buffer and the primary antibody specific for each subunit, diluted (1:500 for c-Jun and 1:1000 for the rest of antibodies) and added to the wells. Each plate was incubated at room temperature with mild agitation for another hour before washing three times with wash buffer. The procedure was followed by the incubation with the HRP- conjugated secondary antibody (1:1000 dilution) for a further one hour. The wells were washed three times before adding 100 µl developing solution. The reaction was stopped after 10 min using 100 µl stop solution and the absorbance read on a spectrophotometer in 450 nm. The complete procedure is summarised in Figure 2.11.

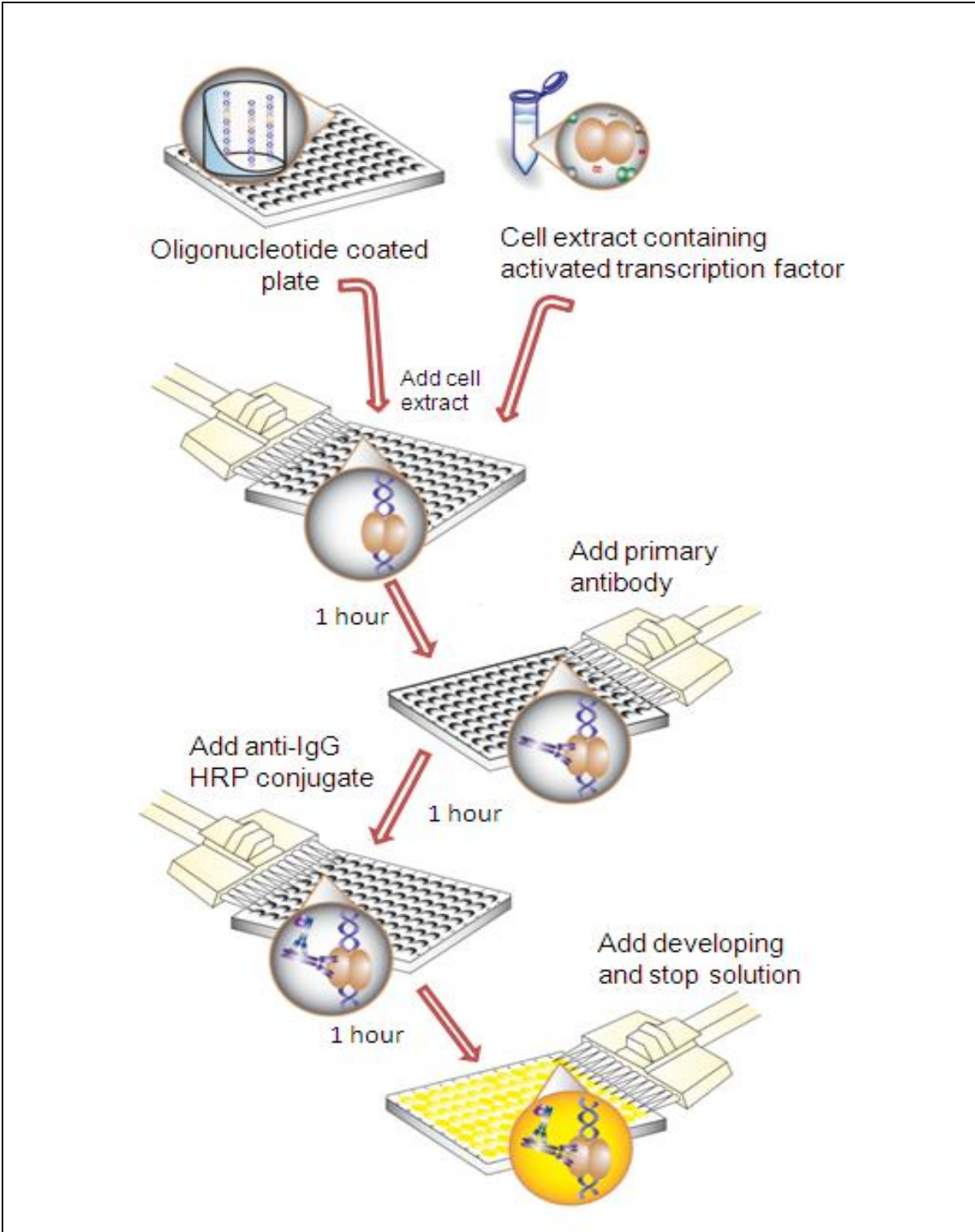


Figure 2.8 The mechanism of TransAM AP-1 family kit

### **2.3 Analysis of data**

All values are expressed as means  $\pm$  S.E.M of measurement of at least three different experiments with replicates in each. Statistics applied to data was one way Anova followed by Dunnett's Multiple Comparison Test for the experiment in which one control was compared Treatment conditions. Two way Anova, was used to compare multiple data complex in which various concentrations of drugs were compared over different time point.

# Results

## **Chapter 3**

**Effects of JNK/AP-1 inhibition on the expression profile of the inducible L-arginine-nitric oxide pathway in rat cultured aortic smooth muscle cells and the murine J774 macrophages.**

### 3.1 Introduction

The role of the JNK signalling pathway in the induction of iNOS in different cell systems has been controversial and inconclusive as highlighted in Chapter 1. Even in our group it has been difficult to ascertain the critical role of the JNKs in regulating either induced NO synthesis or L-arginine transport. In preliminary unpublished observations, it would appear SP600125 regulates the expression of the inducible L-arginine-NO pathway in J774 macrophages but not in RASMCs even though the latter can be regulated by dominant negatives of AP-1 which again show opposing effects (unpublished observations). It is not clear whether this could be due, at least in part, to the experimental approaches used and/or the cell systems being investigated. To ascertain the precise role of the JNK/AP-1 pathway and establish whether the discrepancies are due to cell type differences or to limitations of using SP600125 as a pharmacological inhibitor, studies have been conducted in this chapter that examined the concentration-dependent effects of an additional potent JNK inhibitor referred to as JNK inhibitor VIII (N-(4-Amino-5-cyano-6-ethoxypyridin-2-yl)-2-(2,5-dimethoxyphenyl) in comparison with SP600125.

Studies were carried out in both RASMCs and J774 macrophages to ensure we could identify potential cell type differences. Although additional studies were planned for using freshly isolated peritoneal rat macrophages, these were eventually not conducted because of the lack of adequate facilities for obtaining these cells from infection-free animals. The experiments were intended to eliminate inconsistencies that may arise from species as opposed to cell type differences.

In addition to the pharmacological approach, other experiments were conducted exploiting dominant negative constructs for AP-1, which are  $\alpha$ -Fos and TAM-67.

These constructs contain a transactivation domain, in addition to the bZIP domain, that is phosphorylated or dephosphorylated in response to various stimuli. Deletion of the major transactivation domain of c-Jun (amino acids 3–122) results in TAM-67 being produced as a dominant-negative mutant of c-Jun and blocks AP-1 activity (Young *et al.*, 1999; Li *et al.*, 2000). a-Fos which is a chimeric protein belongs to the c-Fos leucine zipper family and has a designed 25 amino acid acidic protein sequence which replaces the DNA-binding region. It heterodimerizes with c-Fos dimerization partners, preventing AP-1-DNA binding and as a result blocks the activity of AP-1 (Gerdes *et al.*, 2006). Figure 1.10 presents the schematic structure of the two dominant negatives.

Induction of the L-arginine-NO pathway in RASMCs consistently requires LPS and IFN- $\gamma$  in our laboratory while J774 macrophages require LPS alone. In fact, it would appear that the induction of transporter activity in particular is independent of IFN- $\gamma$  signalling in J774 cells (Baydoun *et al.*, 1993), suggesting a difference in the signalling for the two processes (i.e. induced NO synthesis and induced L-arginine transport). As an expansion of these previous observations additional studies have been carried out exploring the effects of LPS, IFN- $\gamma$  and a combination of both on iNOS and CAT mRNA expression to determine whether the divergence between these agents is reflected at the nuclear and thus functional levels.

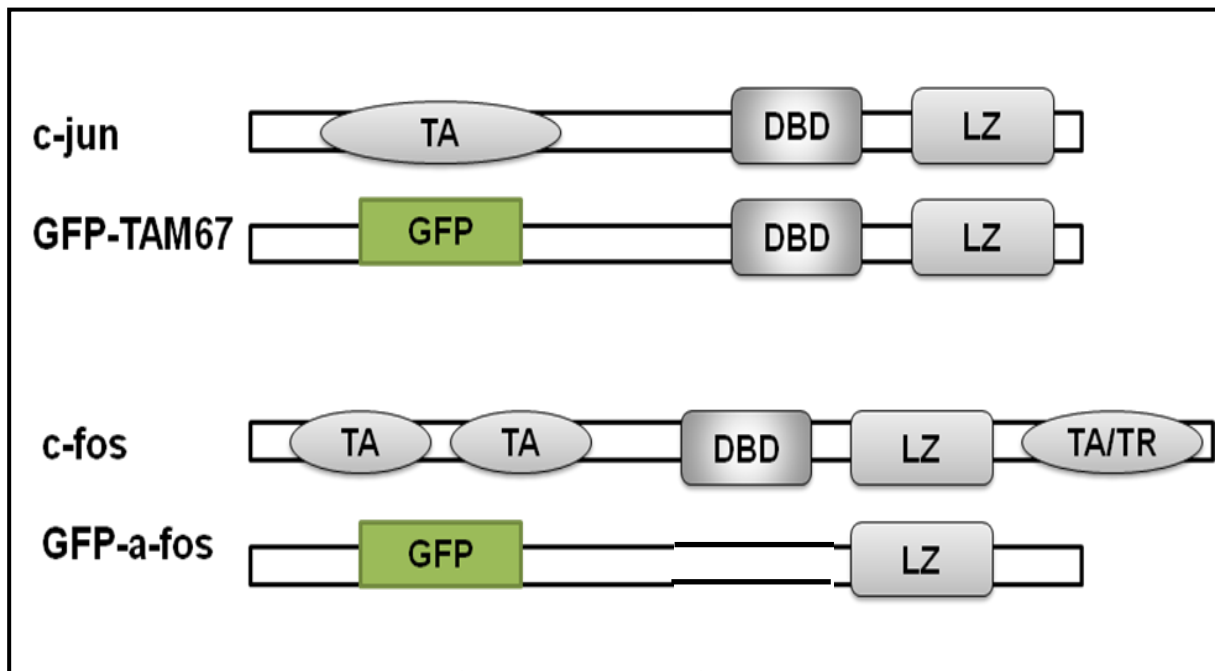


**Figure 3.1.1 AP-1 Dominant negatives constructs**

The schematic presents the structure of GFP-aFos and GFP-TAM67 mutants. TA: transactivating domain; TR: transrepressing domain; DBD: DNA binding domain; LZ: leucine zipper dimerization domain; GFP: green fluorescent protein (Bahassi *et al.*, 2004).

## **3.2 Methods**

All general protocols have been described in Chapter 2 and the methods outlined in this section highlight specific details relevant to the experiments carried out for this chapter. In all the experiments, control cells were harvested at the maximum time course without addition of any inflammatory stimulator or any drug incubation.

### **3.2.1 Time course of iNOS gene expression, protein induction and NO production in RASMCs and J774 macrophages**

Cells were cultured to confluency in T-25 flasks and treated either with LPS (100  $\mu\text{g ml}^{-1}$ )/ IFN- $\gamma$  (100 U  $\text{ml}^{-1}$ ) (RASMCs) or LPS (1  $\mu\text{g ml}^{-1}$ ) alone (J774 macrophages) for periods of either 3, 6, 12, 18 and 24 hours (RNA analysis) or 0.5, 1, 2, 6, 12, 18 and 24 hours (protein analysis). Control cells were incubated with complete culture medium alone. Total RNA was subsequently extracted, cDNAs generated by reverse transcription and analysed by qPCR using 1  $\mu\text{g/ml}$  of cDNA template together with rat iNOS specific primers (Tables 2.1 and 2.2).

For Western blotting, cells were cultured in 6 well plates and treated as above before generating lysates for analysis. The medium was used to measure the amount of nitrite produced using the Griess assay.

### **3.2.2 Effect of different stimuli on iNOS gene expression, protein induction and NO production in J774 macrophages**

Monolayers of J774 macrophages were plated in T-25 culture flasks and incubated for 24 hours with either LPS ( $1 \mu\text{g ml}^{-1}$ ), IFN- $\gamma$  ( $1 \text{ U ml}^{-1}$ ) or LPS plus IFN- $\gamma$  together. Changes in iNOS mRNA expression were determined on isolated RNA by RT-qPCR analysis as described above using murine iNOS specific primers (Tables 2.1 and 2.2). Parallel studies were carried out on 6-well plates and lysates generated for western blotting using a monoclonal anti-iNOS antibody.

### **3.2.3 Effect of SP600125 and JNK inhibitor VIII on nitric oxide production, iNOS expression and L-arginine transport in RASMCs and J774 macrophages**

Confluent monolayer of cells in 96- or 6-well plates were respectively activated for 24 hours with LPS ( $100 \mu\text{g ml}^{-1}$ ) and IFN- $\gamma$  ( $100 \text{ U ml}^{-1}$ ) (RASMCs) or LPS ( $1 \mu\text{g ml}^{-1}$ ) alone (J774 macrophages) following a 30 min pre-treatment period with either SP600125 ( $0.1\text{-}10 \mu\text{M}$ ) or JNK inhibitor VIII ( $0.1\text{-}10 \mu\text{M}$ ). Controls were incubated with culture medium alone. Incubations were terminated 24 hours after activation, the medium was removed for nitrite measurement and cell monolayers washed three times with ice cold PBS. Lysate were prepared and sample subjected to western blotting. In parallel study, confluent monolayers of cells in 96 well plates were used to determine the transport of L- $^3\text{H}$ -arginine.

### **3.2.4 Effect of SP600125 and JNK inhibitor VIII on cell viability in RASMCs and J774 macrophages**

To examine any potential cytotoxic action of each drug, confluent monolayers of the cells in 96 well plates were treated with different concentration of SP600125 (0.1-30  $\mu\text{M}$ ) or JNK inhibitor VIII (0.1-30  $\mu\text{M}$ ) for 30 min prior to a 24 hours activation with LPS (100  $\mu\text{g ml}^{-1}$ ) and IFN- $\gamma$  (100 U  $\text{ml}^{-1}$ ) for RASMCs or LPS (1  $\mu\text{g ml}^{-1}$ ) alone for J774 macrophages. Cells were then incubated for a further 4 hours with MTT (0.5 mg/ml) and assayed for formazan production and analysis.

### **3.2.5 Generation of Mini-preps of pGFP-a-Fos and pGFP-TAM-67**

Mini-preps of pGFP-a-Fos and pGFP-TAM-67 were produced from transformed DH5- $\alpha$  *E. Coli*. The quality of DNA isolated was determined using a 0.8% agarose mini-gel and the quantity estimated spectrophotometrically. Plasmids were digested with the restriction enzymes BamHI and HindIII for a-Fos or BamHI and XhoI for TAM-67 and then analysed as described in the methods. Restriction enzyme digest was performed in a volume of 20  $\mu\text{l}$  on 1  $\mu\text{g}$  of DNA. The mixture was prepared with sterile deionised water, digestion buffer, acetylated BSA and DNA at the concentration of 1  $\mu\text{g/ml}$ . Restriction enzymes were added and incubated in a water bath at 37°C for 4 hours before mixing with loading buffer and then ran on the mini gel.

### **3.2.6 Expression profile of p-GFP-a-Fos and pGFP-TAM-67 transfected into RASMCs**

Partially confluent (60-70%) monolayers of RASMCs in 24 well plates transfected with pGFP-a-Fos or pGFP-TAM-67 were visualised under the UV microscope at the different time point of 3, 6, 18 and 24 hours. Lysates were also prepared at the end of each time point and subjected to western blotting for the detection of GFP using an anti-GFP primary antibody.

### **3.2.7 Effect of pGFP-a-Fos and p-GFP-TAM-67 on LPS and IFN- $\gamma$ induced nitric oxide production, iNOS expression and L-[ $^3$ H]-arginine transport in RASMCs**

Partially confluent (60-70%) monolayers of RASMCs were transfected with either pGFP-a-Fos or pGFP-TAM-67 before being activated for 24 hours with LPS (100  $\mu$ g ml $^{-1}$ ) and IFN- $\gamma$  (100 U ml $^{-1}$ ) at 18 hours post transfection as this was the optimum time for incubation that did not result in significant cell loss but gave good expression of GFP. Cells incubated with culture medium alone or with transfection mix containing peptide 6 (to increase the transfection efficiency) were used as respective control. Nitric oxide production was determined by the nitrite assay and lysates from cell monolayers subjected to western blotting. In parallel plates, uptake of L-[ $^3$ H]-arginine was monitored in cell monolayers using transport buffer containing 100  $\mu$ M unlabelled L-arginine plus 1  $\mu$ Ci ml $^{-1}$  of L-[ $^3$ H]-arginine.

### **3.2.8 The effect of SP600125 on iNOS mRNA expression in RASMCs and J774 macrophages**

Confluent monolayers of cells were treated with SP600125 (0.3 and 3  $\mu\text{M}$ ) for 30 min prior to activation with LPS (100  $\mu\text{g ml}^{-1}$ ) and IFN- $\gamma$  (100 U  $\text{ml}^{-1}$ ) for RASMCs or LPS (1  $\mu\text{g ml}^{-1}$ ) alone for macrophages for a further 18 hours. The control cells were incubated in complete culture medium in the absence or presence of SP600125 for the same period of time but without activation with LPS and IFN- $\gamma$ . The incubations were terminated at the end of this time, total RNA extracted and analysed using iNOS specific primers in the qPCR reaction.

### **3.2.9 Effect of a-Fos and TAM-67 on iNOS mRNA expression in RASMCs**

Because of the difficulties encountered in transfecting macrophages, studies using the dominant negatives were limited to RASMCs which were grown to partial confluency (60-70%) before being transfected with pGFP-aFos or pGFP-TAM-67 for 18 hours and then activated with LPS (100  $\mu\text{g ml}^{-1}$ ) and IFN- $\gamma$  (100 U  $\text{ml}^{-1}$ ) for a further 18 hours. The total RNA was extracted and analysed using iNOS specific primers.

### **3.3 Results**

#### **3.3.1 Identification and biochemical characterization of Rat Aortic Smooth Muscle Cells (RASMCs)**

The characteristics of the cells isolated from rat aorta were determined morphologically and biochemically to ensure that studies were carried out on the required cell types. Cultures isolated exhibited the characteristic spindly morphology and Figure 3.1, shows the labelling of the  $\alpha$ -actin filaments positively identifying smooth muscle cells.

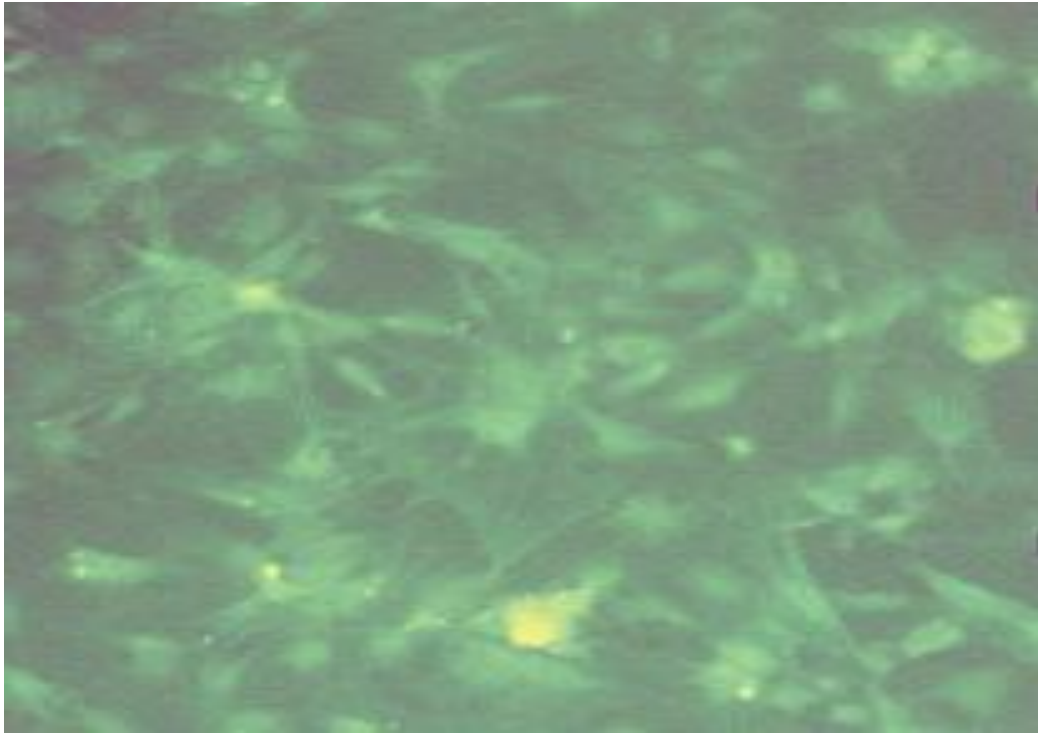


**Figure 3.1 Morphology and  $\alpha$ -actin staining of RASMCs**

Smooth muscle cells were isolated from rat aorta as described in the methods (section 1.2.5) and plated at a density of 50-60% in Lab-Tec wells. Cells were allowed to establish over 2 days before staining for  $\alpha$ -actin as described in the methods (Section 2.1.5). This figure is representative of at least five experiments carried out at random on various isolates.

### **3.3.2 Time course of iNOS gene and protein expression and NO production in RASMCs and J774 macrophages**

Gene expression of iNOS in both RASMCs (Figure 3.2) and J774 macrophages (Figure 3.5) was detectable as early as 3 h after activation and increased time-dependently, reaching a peak at 18 to 24 hours after induction. Similarly, iNOS protein was also detectable early and was marginally present in controls which would indicate some basal expression even before activation of cells. The levels however remained low and stable at the earlier time points increasing significantly at 12 hours in RASMCs (Figure 3.3) and 6 hours in macrophages (Figure 3.6), reaching peak levels in both cell types at 18 to 24 hours after activation. Nitrite production reflected the trends seen for iNOS gene and protein expression in both cell systems (Figures 3.4 for RASMCs and 3.7 for J774 macrophages)

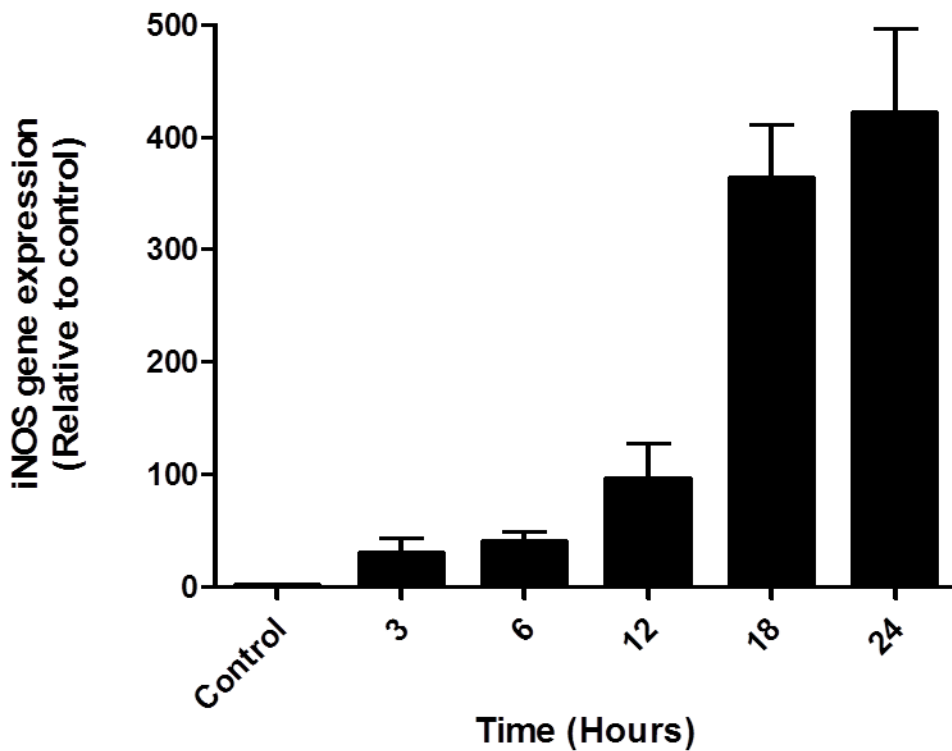


**Figure 3.2 iNOS gene expression profile in RASMCs**

Confluent monolayers of RASMCs were incubated in culture medium alone or in medium containing LPS ( $100 \mu\text{g ml}^{-1}$ ) and IFN- $\gamma$  ( $100 \text{ U ml}^{-1}$ ) for different time periods. Total RNA was isolated from cells and the cDNA prepared before analysing by quantitative PCR using iNOS specific primers. The graph reflects fold changes in iNOS level in activated cells relative to control. The results are the mean  $\pm$  SEM of 3 independent experiments with 3 replicates in each.

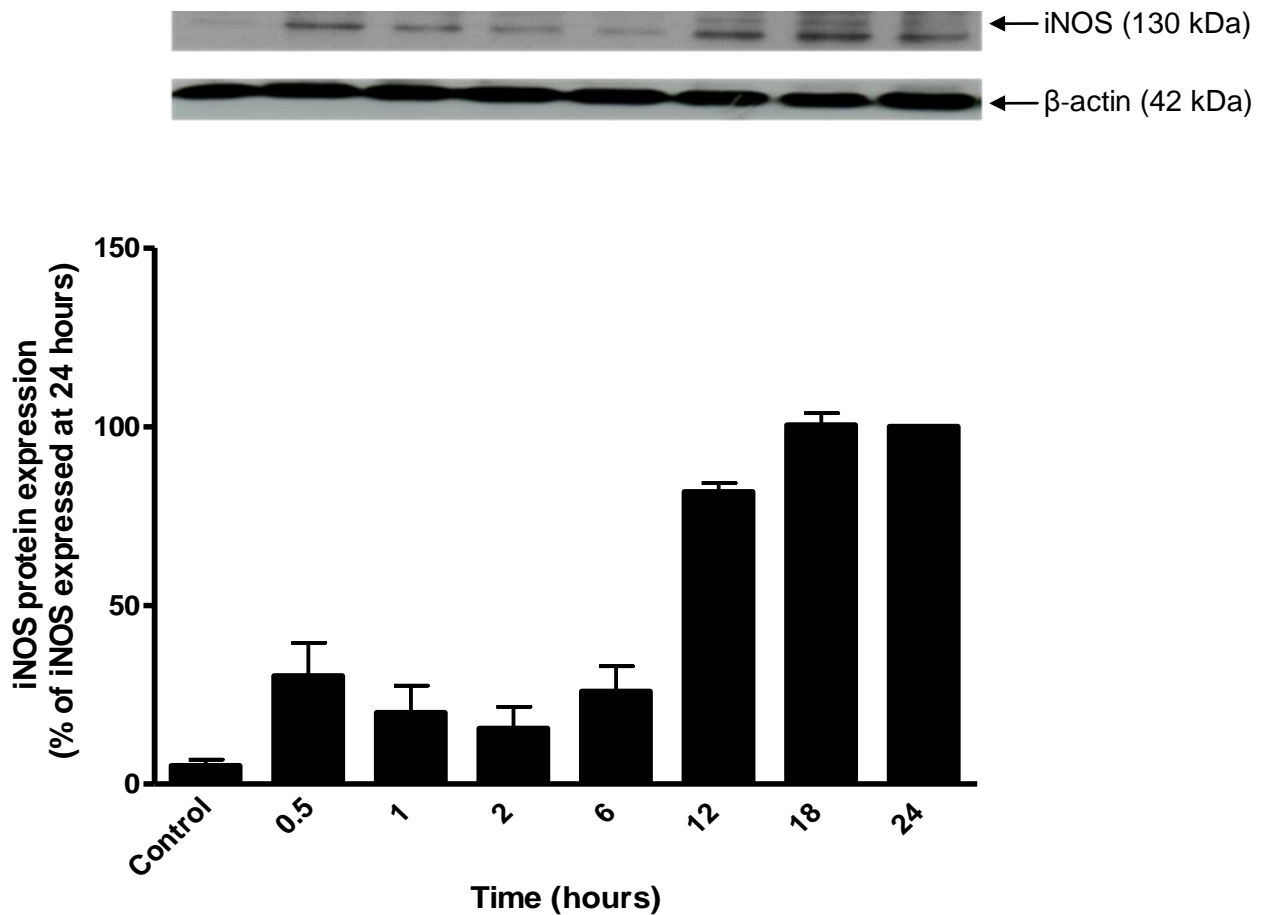


**Figure 3.3 iNOS protein expression profile in RASMCs**

Confluent monolayers of RASMCs were incubated in culture medium alone or in medium containing LPS ( $100 \mu\text{g ml}^{-1}$ ) and IFN- $\gamma$  ( $100 \text{ U ml}^{-1}$ ) for different time points. Lysates were generated at the end of each incubation and subjected to western blotting using an anti-iNOS selective antibody. Expression of  $\beta$ -actin was also determined and used to standardise the loading and expression levels of iNOS. The bar graph is a scanning densitometry obtained using a Bio Imaging System and the Gene Genius software program (Gene Snap). The results represent percentage change in iNOS expression relative to the 24 h activation time point and are the mean  $\pm$  SEM of three separate experiments. Statistical analysis was carried out using a one way Anova followed by Dunnett's multiple comparison test.

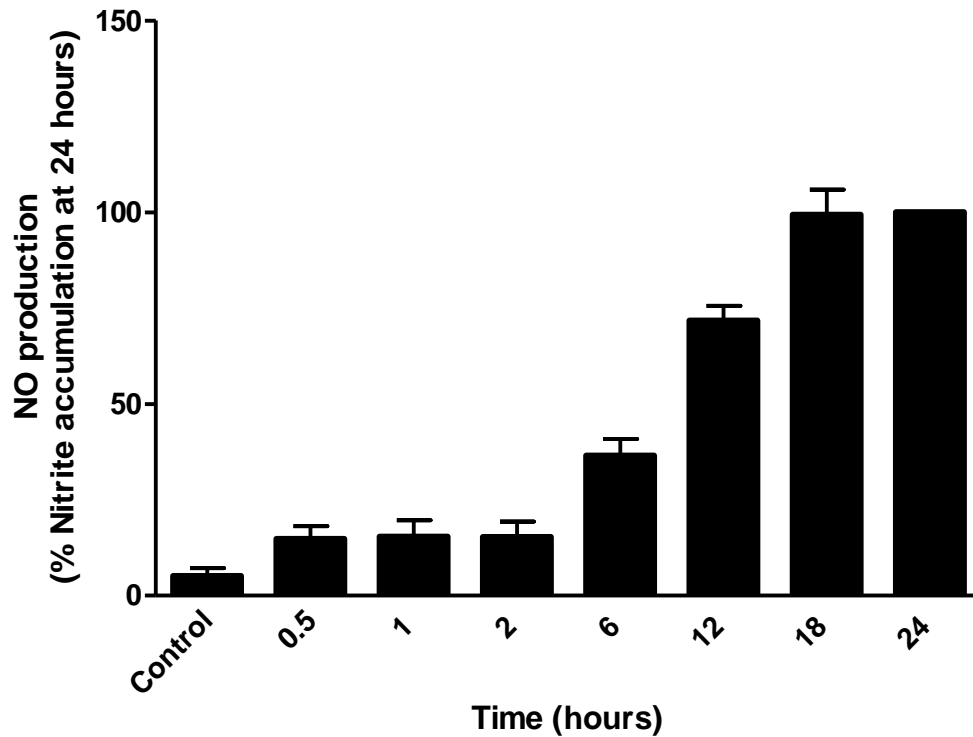


**Figure 3.4 Nitrite production profile in RASMCs**

Confluent monolayers of RASMCs were incubated in culture medium alone or in medium containing LPS ( $100 \mu\text{g ml}^{-1}$ ) and IFN- $\gamma$  ( $100 \text{ U ml}^{-1}$ ) for different time points. Accumulated nitrite was determined by the Griess assay as described in the methods (Section 2.2.2) and standardised for total protein present in each well. The result is expressed as a percentage of the total amount of nitrite accumulated at 24 h and is the mean  $\pm$  SEM of 3 independent experiments with 3 replicates in each.

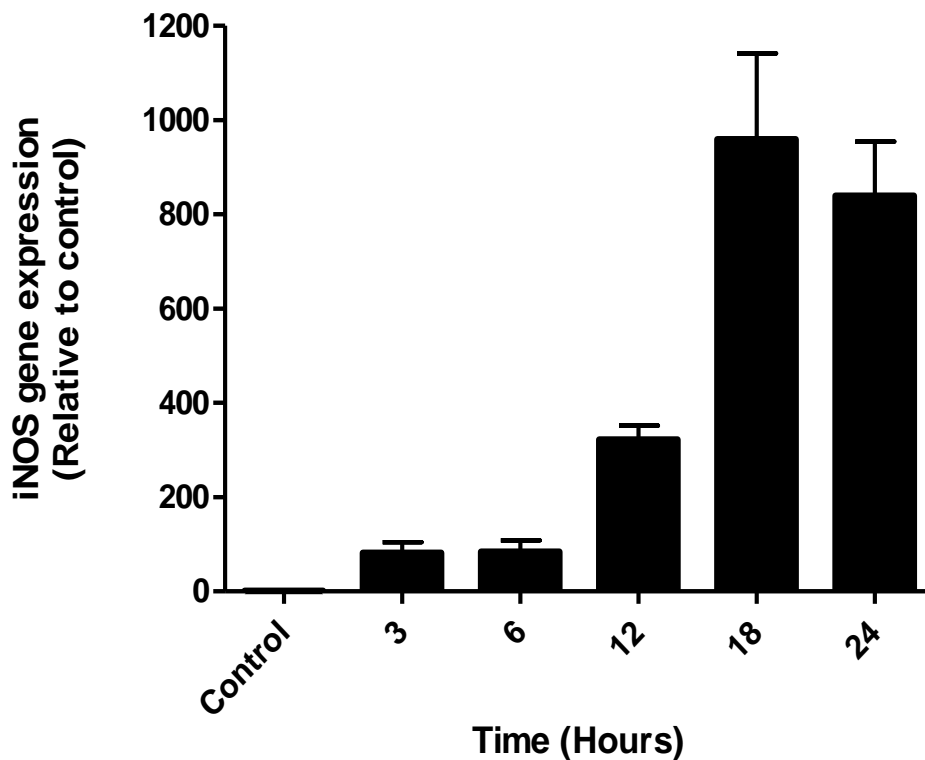


**Figure 3.5 iNOS gene expression profile in J774 macrophages**

Confluent monolayers of J774 macrophages were incubated in culture medium alone or in medium containing LPS ( $1\mu\text{g ml}^{-1}$ ) for different time periods. Total RNA was isolated from cells and the cDNA prepared before analysing by quantitative PCR using iNOS specific primers. The graph reflects fold changes in iNOS level in activated cells relative to control. The results are the mean  $\pm$  SEM of 3 independent experiments with 3 replicates in each.

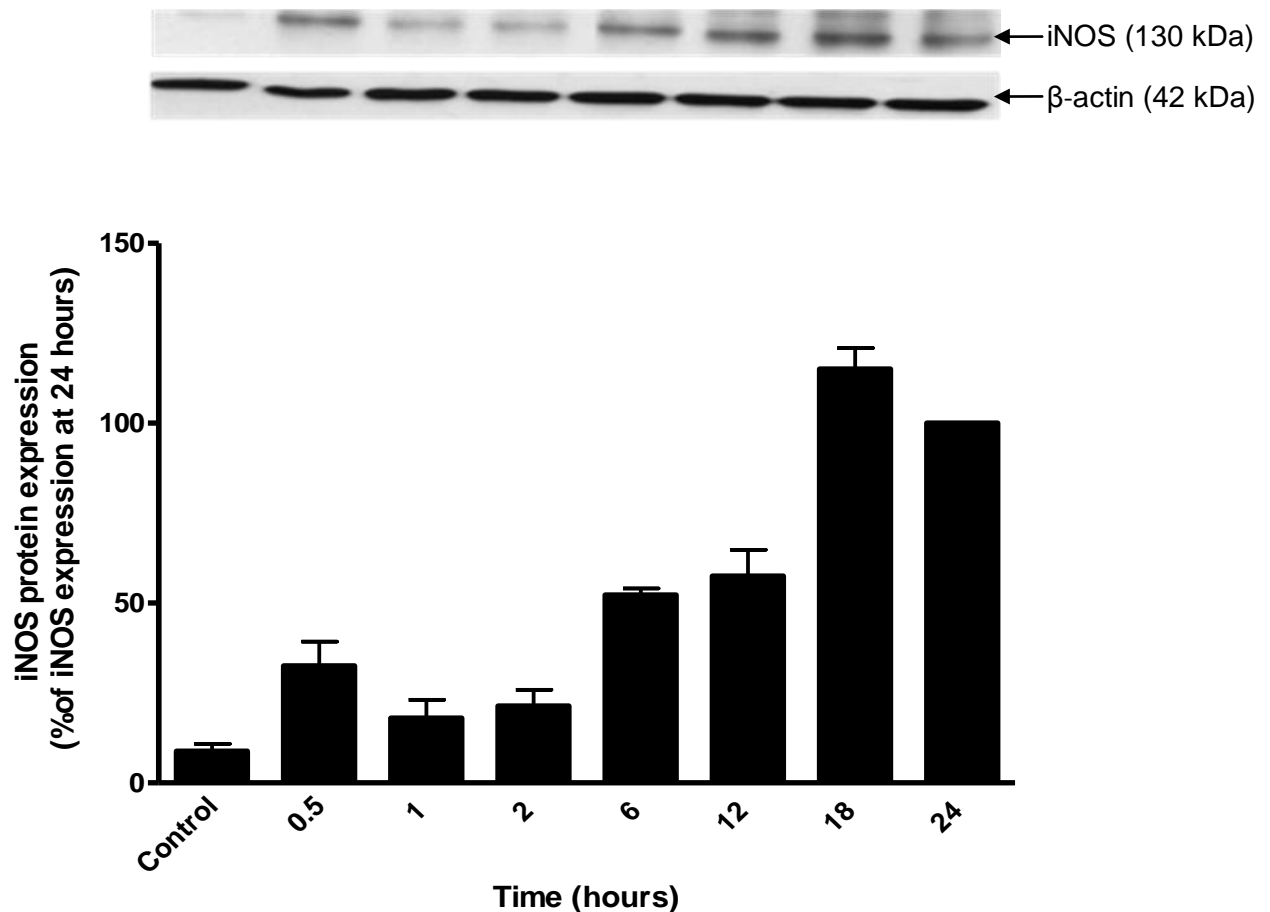


**Figure 3.6 iNOS induction profile in J774 macrophages**

Confluent monolayers of J774 macrophages were incubated in culture medium alone or in medium containing LPS ( $1\mu\text{g ml}^{-1}$ ) for different time points. Lysates were generated at the end of each incubation and subjected to western blotting using an anti-iNOS selective antibody. Expression of  $\beta$ -actin was also determined and used to standardise the loading and expression levels of iNOS. The bar graph is a scanning densitometry obtained using a Bio Imaging System and the Gene Genius software program (Gene Snap). The results represent percentage change in iNOS expression relative to the 24 h activation time point and are the mean  $\pm$  SEM of three separate experiments. Statistical analysis was carried out using a one way Anova followed by Dunnett's multiple comparison test.

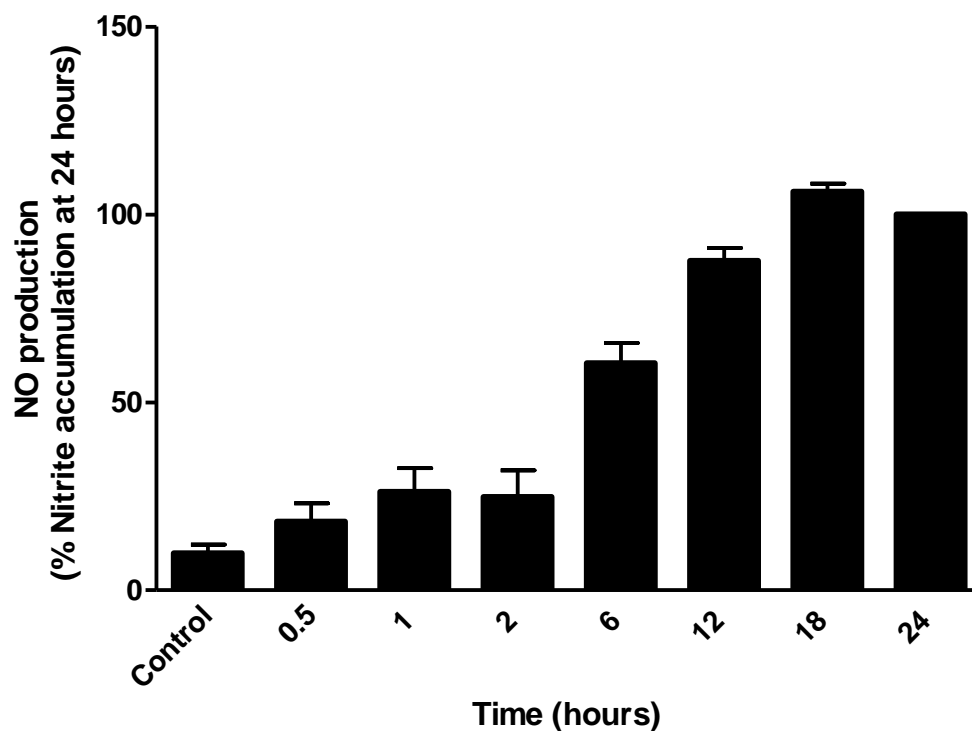


**Figure 3.7 Nitrite production profile in J774 macrophages**

Confluent monolayers of J774 macrophages were incubated in culture medium alone or in medium containing LPS ( $1\mu\text{g ml}^{-1}$ ) for different time points. Accumulated nitrite was determined by the Griess assay as described in the methods (Section 2.2.2) and standardised for total protein present in each well. The result is expressed as a percentage of the total amount of nitrite accumulated at 24 h and is the mean  $\pm$  SEM of 3 independent experiments with 3 replicates in each.

### **3.3.3 Effect of different stimuli on iNOS gene and protein expression and NO production in J774 macrophages**

In order to determine whether J774 macrophages respond differently to LPS or IFN- $\gamma$  in expressing iNOS and NO, cells were incubated with LPS ( $1 \mu\text{g ml}^{-1}$ ), IFN- $\gamma$  ( $1 \text{ U ml}^{-1}$ ) or both for 18 hours and qPCR, Western blotting and the Griess assays were performed to detect changes in iNOS gene expression, protein induction and nitrite production respectively. As shown in Figure 3.8, levels of iNOS mRNA were marginal in controls but significantly elevated by up to 800-fold following activation with LPS. IFN- $\gamma$  also induced iNOS mRNA but to a much lesser extent (only 160-fold) than that seen with LPS alone. Both LPS and IFN- $\gamma$  together increase the level of gene induction by up to 1000 fold.

The result of the western blots and Griess assays reflected a similar pattern in that LPS caused a higher induction of iNOS protein expression (Figure 3.9) and NO production (Figure 3.10) than IFN- $\gamma$  but together produced an even more pronounced change than either agent alone.

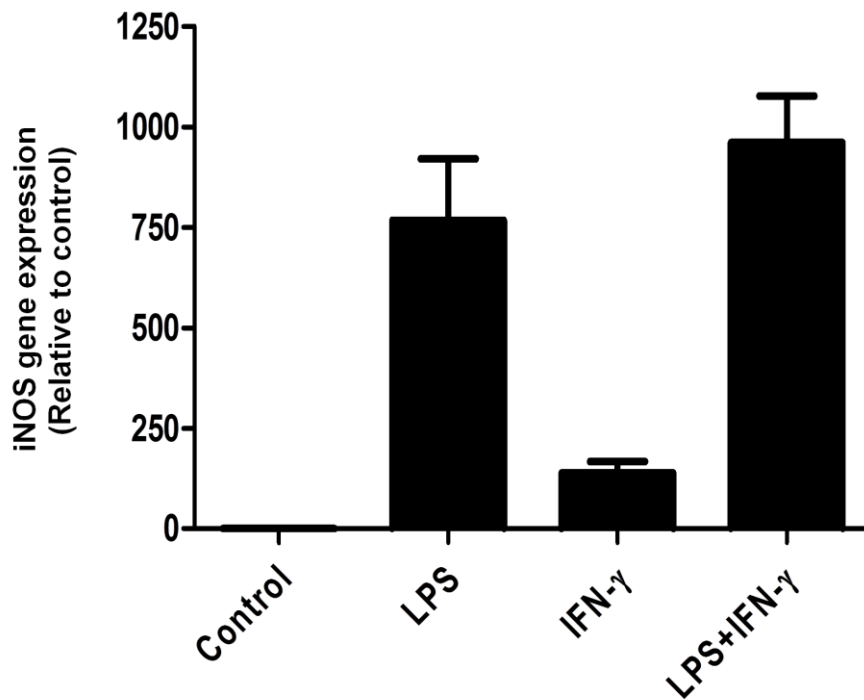


**Figure 3.8 Effects of LPS, IFN- $\gamma$  and a combination of both on iNOS gene expression in J774 macrophages**

Confluent monolayer of J774 macrophages were stimulated with either LPS ( $1 \mu\text{g ml}^{-1}$ ), IFN- $\gamma$  ( $1 \text{ unit ml}^{-1}$ ) or both for 18 hours. Total RNA was isolated from cells and the cDNA prepared and analysed by quantitative PCR using iNOS specific primers. The graph reflects fold changes in iNOS level in activated cells compared to control. The results are representative of 3 independent experiments with 3 replicates in each.

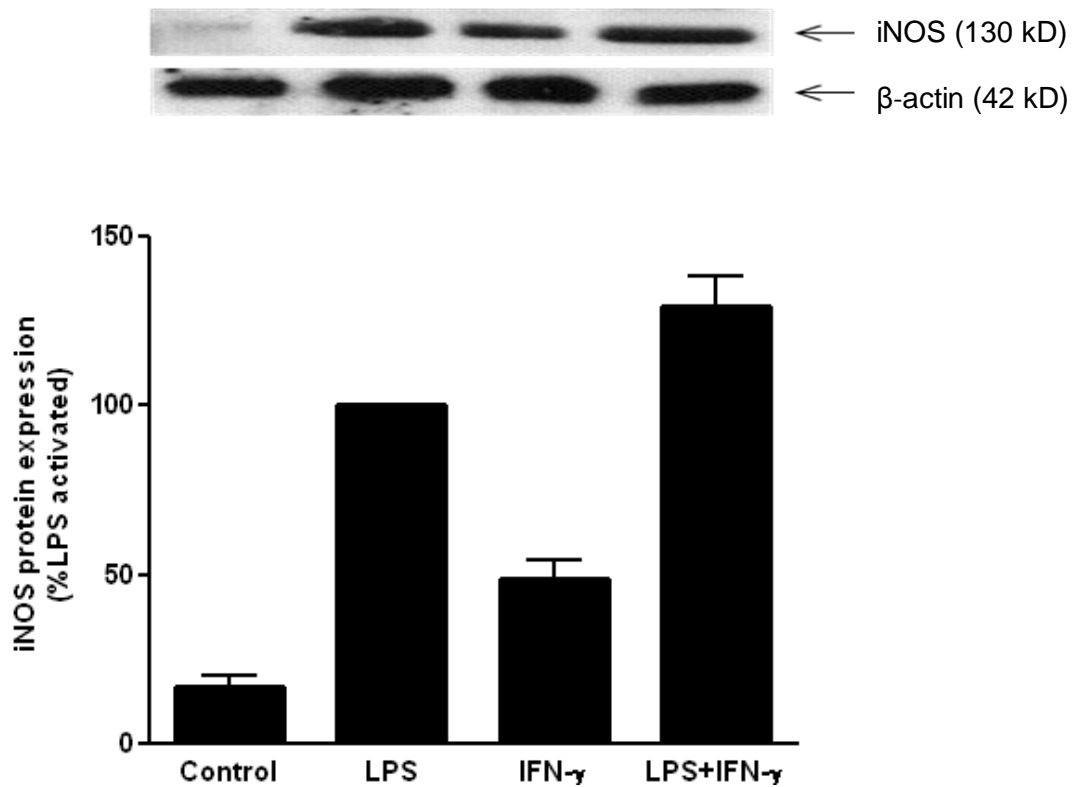


**Figure 3.9 Effects of LPS, IFN- $\gamma$  and a combination of both on iNOS protein expression in J774 macrophages**

Confluent monolayer of J774 macrophages in 6 well plate were incubated with either LPS ( $1 \mu\text{g ml}^{-1}$ ), IFN- $\gamma$  ( $1 \text{ unit ml}^{-1}$ ) or a mixture of both for 18 hours. Lysates were generated at the end of the incubation period and subjected to western blotting using an anti-iNOS selective antibody. Expression of  $\beta$ -actin was also determined and used to standardise the loading and expression levels of iNOS. Protein bands were quantified by scanning densitometry using a Bio Imaging System and the Gene Genius software program. The data is expressed as a percentage of levels detected at 24 h post activation and is the mean  $\pm$  SEM of three separate experiments.

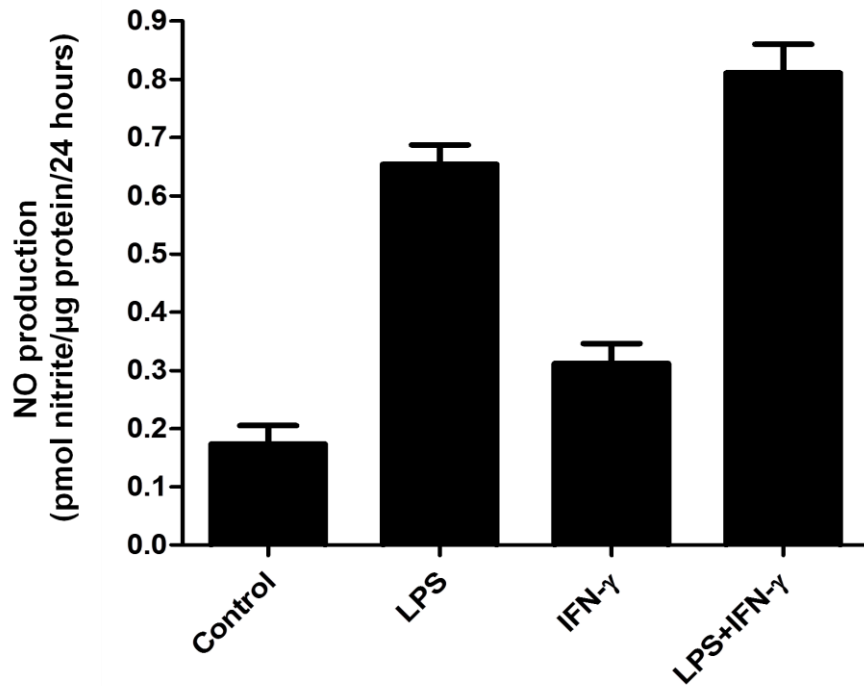


**Figure 3.10 Effects of LPS, IFN- $\gamma$  and a combination of both on Nitrite production in J774 macrophages**

Confluent monolayers of J774 macrophages were incubated with either LPS ( $1 \mu\text{g ml}^{-1}$ ), IFN- $\gamma$  ( $1 \text{ unit ml}^{-1}$ ) or a mixture of both for 18 hours. Accumulated nitrite was determined by the Griess assay and standardised for total protein present in the well. The result is expressed as pmol nitrite/ $\mu\text{g}$  protein/24 hours and is the mean  $\pm$  SEM of 3 independent experiments with 3 replicates in each.

### **3.3.4 Effect of SP600125 on nitric oxide production in RASMCs**

Consistent with all our studies, treatment of RASMCs with LPS ( $100 \mu\text{g ml}^{-1}$ ) and IFN- $\gamma$  ( $100 \text{ U ml}^{-1}$ ) for 24 h, resulted in the production of NO, which was not detectable in control non-activated cells. Under these conditions, activated cells produced  $0.4 \pm 0.01 \text{ pmole nitrite } \mu\text{g protein}^{-1} 24 \text{ h}^{-1}$ . As seen in Figure 3.11, NO production was increased marginally by SP600125 at  $0.3 \mu\text{M}$ , declining thereafter to the LPS/IFN- $\gamma$  stimulated levels. SP600125 ( $0.1\text{-}10 \mu\text{M}$ ) however failed to cause any significant inhibition in either basal or activated nitrite release when incubated with cells for 30 min prior to activation (Figure 3.11).

### **3.3.5 Effect of SP600125 on iNOS expression in RASMCs**

To determine the effect of SP600125 on iNOS protein expression, western blot analysis was performed on lysates obtained from control and activated cells in the absence and presence of increasing concentration of SP600125 ( $0.1\text{-}10 \mu\text{M}$ ). There was no detectable expression of iNOS in control non-activated cells. In contrast, activation with LPS and IFN- $\gamma$  caused the expected induction of iNOS protein which remained unaltered in cells treated with increasing concentrations of SP600125 of up to  $10 \mu\text{M}$  (Figure 3.12).

### **3.3.6 Effect of SP600125 on L-[ $^3\text{H}$ ]-arginine transport in RASMCs**

Consistent with previous findings (Baydoun, 1999), basal rates of L-[ $^3\text{H}$ ]-arginine transport were increased in RASMCs exposed to LPS ( $100 \mu\text{g ml}^{-1}$ ) and IFN- $\gamma$  ( $100 \text{ U}$

mi<sup>-1</sup>). In these experiments, L-[<sup>3</sup>H]-arginine transport increased from control values of 1 pmoles µg protein<sup>-1</sup> min<sup>-1</sup> (n=3) to 1.4 ± 0.05 pmole µg protein<sup>-1</sup> min<sup>-1</sup> (n=3) in activated cells. SP600125 at the full concentration range of 0.1 µM to 10 µM failed to cause any significant changes in either basal or activated transport rates (Figure 3.13).

### **3.3.7 Effect of SP600125 on Cell viability in RASMCs**

Viability studies carried out in parallel with experiments outlined above revealed that SP600125 did not cause any significant degrees of cytotoxicity in RASMCs over the concentration range of 0.1 µM to 3 µM. At 10 µM, the activated cells reveal a decline in viability of 18%, with the higher concentration of 30 µM showing a more significant increase in cell toxicity (Figure 3.14). As a result all experiments using SP600125 were limited to a maximum concentration of 10 µM.

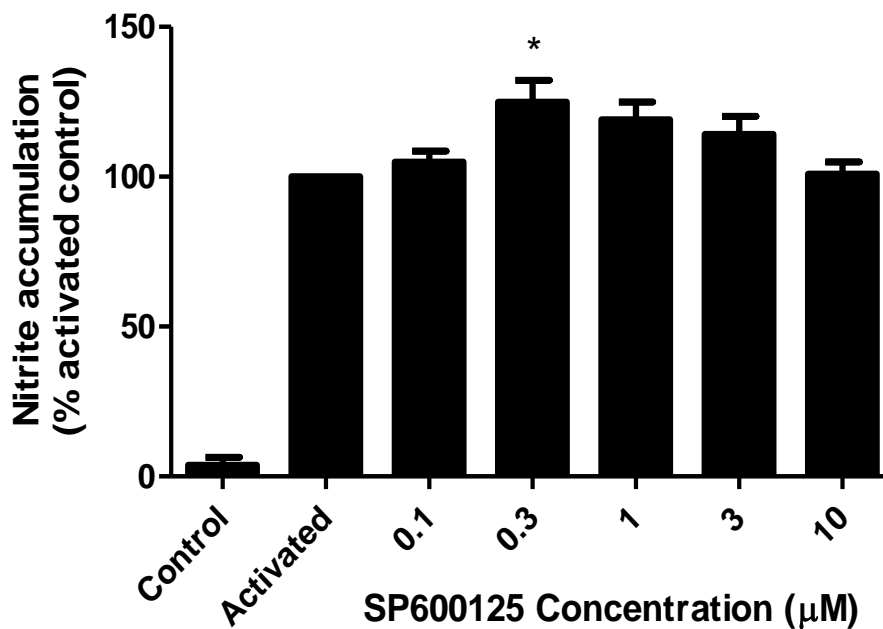


**Figure 3.11 Effect of SP600125 on NO production in RASMCs**

Confluent monolayers of RASMCs were incubated with increasing concentrations of SP600125 for 30 min prior to a further 24 h incubation in culture medium alone or in medium containing LPS ( $100 \mu\text{g ml}^{-1}$ ) and IFN- $\gamma$  ( $100 \text{ U ml}^{-1}$ ). Accumulated nitrite was determined by the Griess assay and standardised for total protein present in the well. The results are expressed as a percentage of the total amount of nitrite accumulated at 24 h and are the mean  $\pm$  SEM of 3 independent experiments with 3 replicates in each. Statistical analysis was carried out using a one way Anova followed by Dunnett's multiple comparison test. \* $p < 0.05$  compared to activated non-drug treated cells.

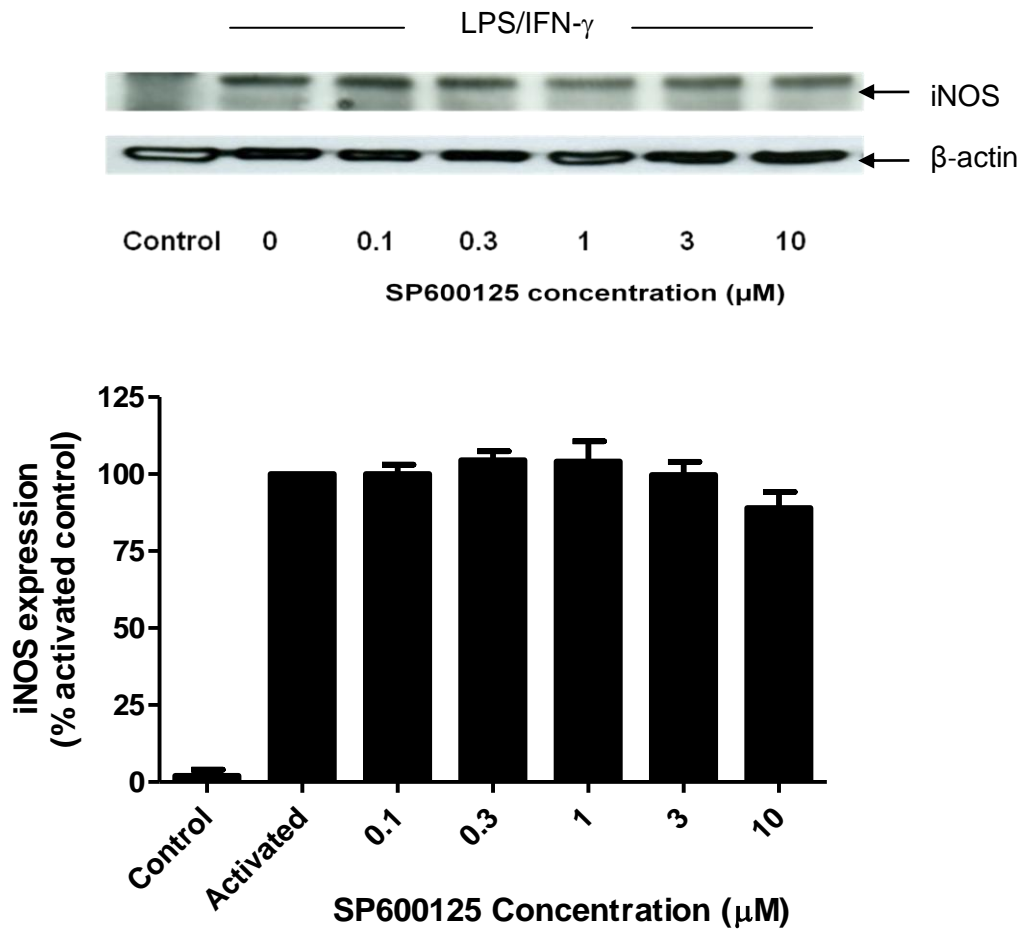


**Figure 3.12 Effect of SP600125 on iNOS expression in RASMCs**

Confluent monolayers of RASMCs were incubated with increasing concentrations of SP600125 for 30 min prior to a further 24 h incubation in culture medium alone or in medium containing LPS ( $100 \mu\text{g ml}^{-1}$ ) and IFN- $\gamma$  ( $100 \text{ U ml}^{-1}$ ). Lysates were generated at the end of the incubation period and subjected to western blotting using an anti-iNOS selective antibody. Expression of  $\beta$ -actin was also determined and used to standardise the loading and expression levels of iNOS. The bar graph is a scanning densitometry of iNOS expression as a percentage of the levels detected at 24 h post activation and is the mean  $\pm$  SEM of three separate experiments. Statistical analysis was carried out using a one way Anova followed by Dunnett's multiple comparison test.

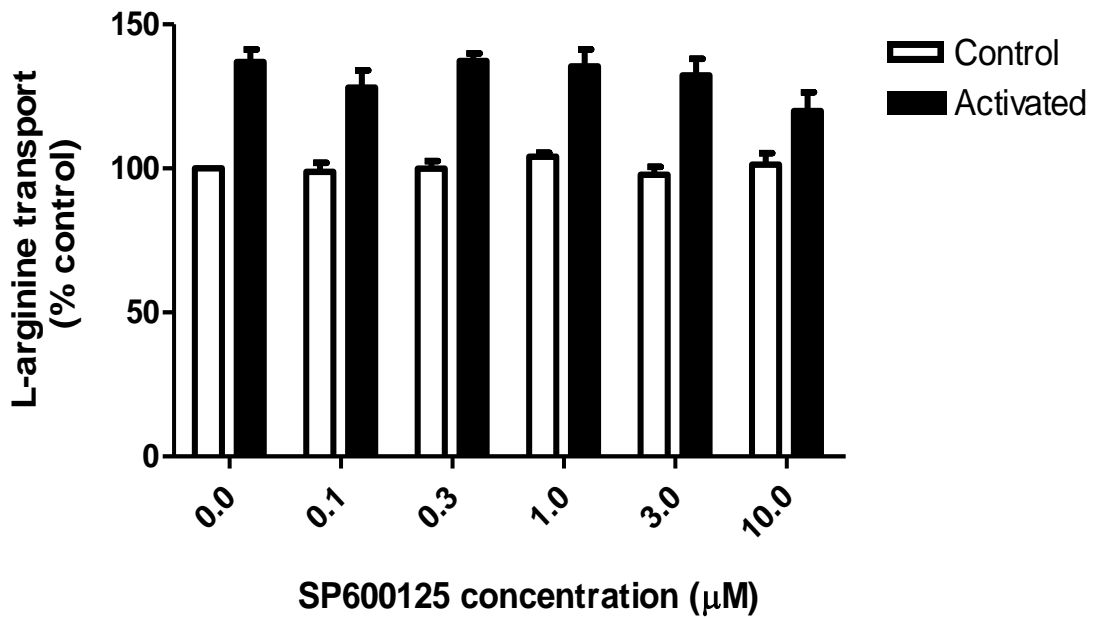


**Figure 3.13 Effect of SP600125 on L-[<sup>3</sup>H]-arginine transport in RASMCs**

Confluent monolayers of RASMCs were incubated with increasing concentrations of SP600125 for 30 min prior to a further 24 h incubation in culture medium alone or in medium containing LPS (100 µg ml<sup>-1</sup>) and IFN-γ (100 U ml<sup>-1</sup>). L-arginine transport was monitored over 2 min in Krebs buffer containing 1µCi ml<sup>-1</sup> L-[<sup>3</sup>H]arginine plus 100 µM unlabelled L-arginine. The data is expressed as percentage of the transport rates in the control non treated samples. The results are representative of 3 independent experiments with 5 replicates in each. Statistical analysis was carried out using a one way Anova followed by Dunnett's multiple comparison test.

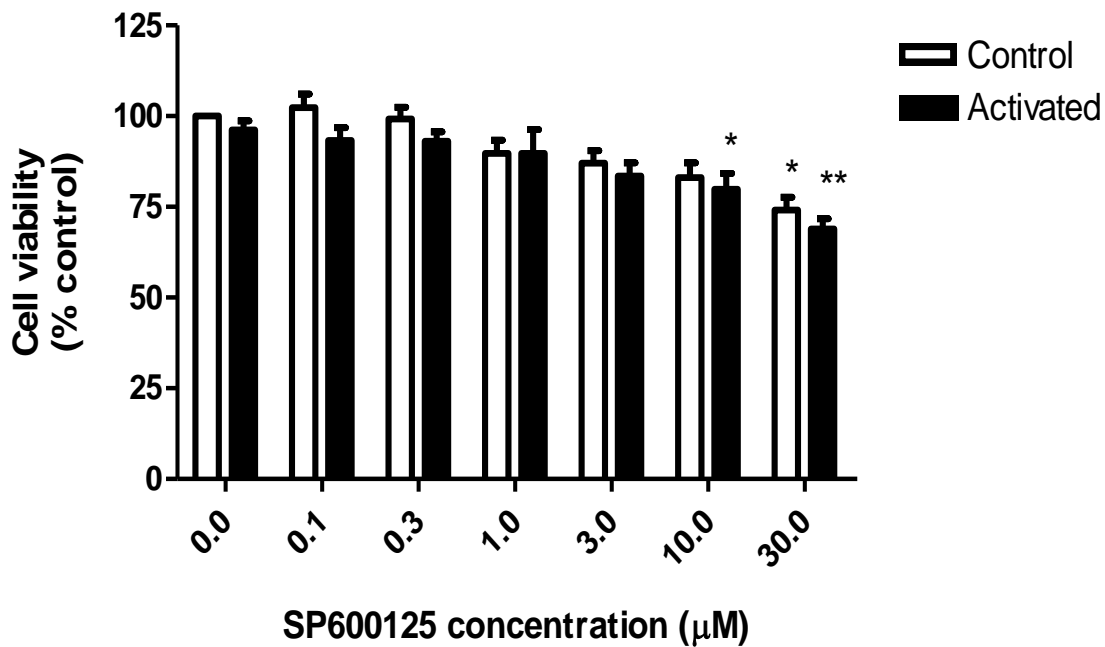


**Figure 3.14 Effect of SP600125 on Cell viability in RASMCs**

Cells were pre-incubated with SP600125 for 30 min prior to incubated in culture medium alone or activation with LPS ( $100 \mu\text{g ml}^{-1}$ ) and  $\text{INF-}\gamma$  ( $100 \text{ U ml}^{-1}$ ) for 24 h. The culture medium was removed at the end of this period and cells were incubated with MTT ( $0.5 \text{ mg/ml}$ ) in  $200 \mu\text{l}$  fresh medium per well at  $37^\circ\text{C}$  for 4h. The formazan crystals produced from the metabolism of MTT were subsequently solubilised in  $100 \mu\text{l}$  of Isopropanol. Plates were read at  $540 \text{ nm}$  using a Multiscan II plate reader. All values are a percentage of formazan production in the control non-activated cells and are expressed as the mean  $\pm$  S.E.M of 4 separate experiments with 5 replicate in each. Statistical analysis was carried out using a one way Anova followed by Dunnett's multiple comparison test. \*  $p < 0.05$  and \*\*  $p < 0.01$  compared to activated non-inhibitor cells.

### **3.3.8 Effect of SP600125 on NO production in J774 macrophages**

Exposure of J774 macrophages to LPS ( $1 \mu\text{g ml}^{-1}$ ) resulted in the induction of NO production with nitrite levels increasing from none detectable amount under control conditions to  $0.6 \pm 0.01 \text{ pmoles nitrite } \mu\text{g protein}^{-1} 24 \text{ h}^{-1}$  in activated cells. When applied, SP600125 caused a biphasic effect which was a significant up-regulation of accumulated nitrite levels at concentrations of 0.3 to  $1 \mu\text{M}$  and a significant concentration-dependent inhibition at 3 to  $10 \mu\text{M}$  (Figure 3.15).

### **3.3.9 Effect of SP600125 on iNOS expression in J774 macrophages**

To verify whether SP600125 affect the level of iNOS expression in J774 macrophages, western blot analysis was performed on lysates obtained from control and activated cells in the absence and presence of increasing concentration of the drug. There was no detectable expression of iNOS in control non-activated cells. In contrast, activation with LPS caused the induction of iNOS protein which, as seen with nitrite production, was enhanced at 0.1 to  $0.3 \mu\text{M}$  SP600125 and decreased thereafter with  $10 \mu\text{M}$  reducing accumulated nitrite levels by 50% (Figure 3.16).

### **3.3.10 Effect of SP600125 on L-[ $^3\text{H}$ ]-arginine transport in J774 macrophages**

Activation of J774 macrophages resulted in a significant increase in L-[ $^3\text{H}$ ]-arginine transport which was elevated from  $1.2 \text{ pmoles } \mu\text{g protein}^{-1} \text{ min}^{-1}$  (control;  $n=3$ ) to  $1.7 \text{ pmoles } \mu\text{g protein}^{-1} \text{ min}^{-1}$  ( $n=3$ ) following LPS treatment. SP600125 did not cause

any significant changes on L-arginine transport except at 10  $\mu$ M where transport rate in activated but not controls was reduced by 24% (n=3) (Figure 3.17).

### **3.3.11 Effect of SP600125 on Cell viability in J774 macrophages**

Similar to the findings in RASMCs, viability studies carried out to determine the toxicity of SP600125 in J774 macrophages showed that the compound was only cytotoxic at concentrations above 10  $\mu$ M and as can be seen in Figure 3.18, there was a significant reduction in cell viability when SP600125 was used at the concentration of 30  $\mu$ M. Thus, when used, the maximum concentration of the drug was limited to 10  $\mu$ M.

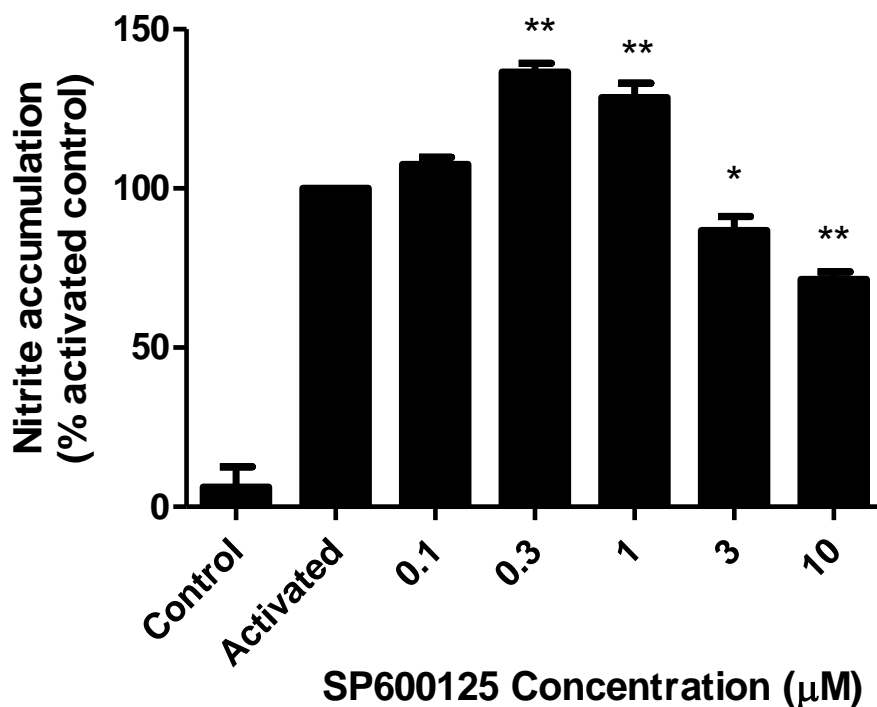


**Figure 3.15 Effect of SP600125 on NO production in J774 macrophages**

Confluent monolayers of J774 macrophages were incubated with increasing concentrations of SP600125 for 30 min prior to a further 24 h incubation in culture medium alone or in medium containing LPS ( $1 \mu\text{g ml}^{-1}$ ). Accumulated nitrite was determined by the Griess assay and standardised for total protein present in the well. Values are expressed as the mean  $\pm$  S.E.M of 3 separate experiments with 3 replicate in each. Statistical analysis was carried out using a one way Anova followed by Dunnett's multiple comparison test. \*  $p < 0.05$  and \*\*  $p < 0.01$  compared to activated non-inhibitor cells.

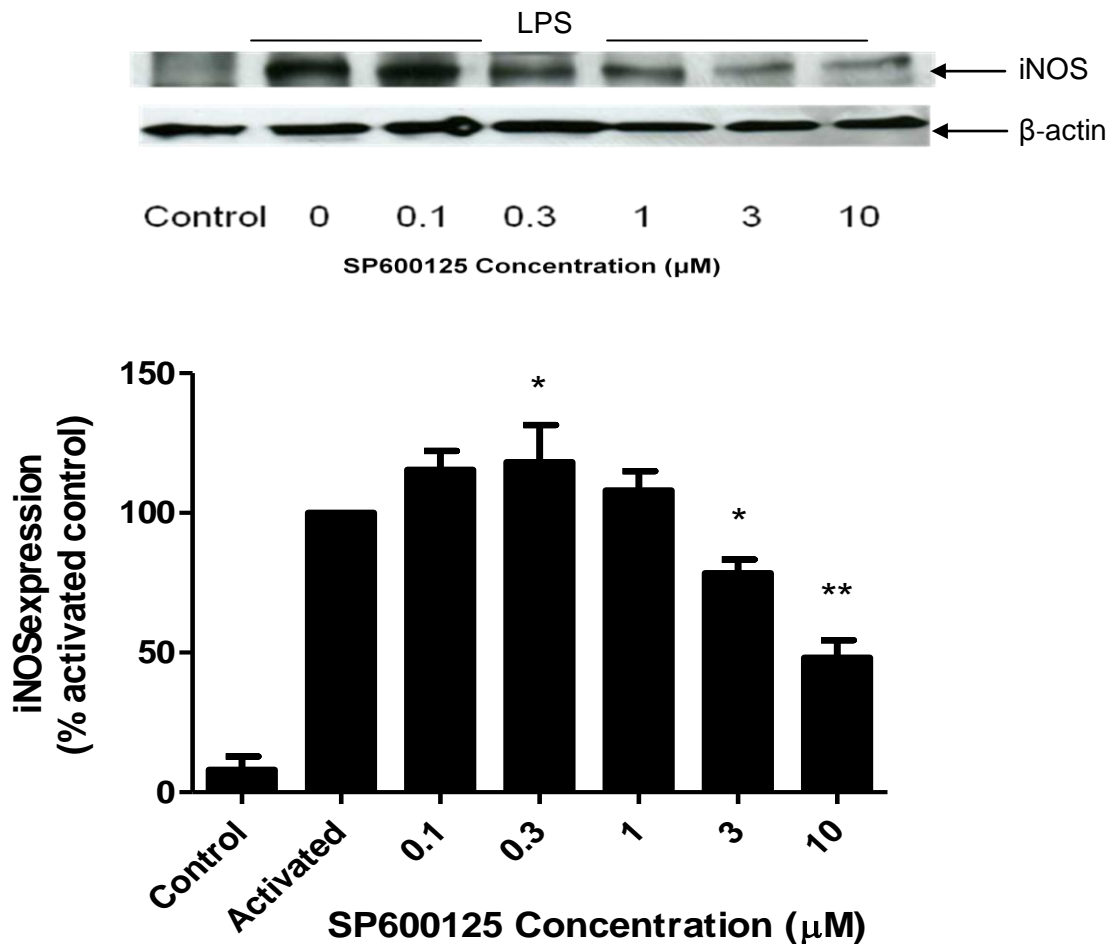


**Figure 3.16 Effect of SP600125 on iNOS expression in J774 macrophages**

Confluent monolayers of J774 macrophages were incubated with increasing concentrations of SP600125 for 30 min prior to a further 24 h incubation in culture medium alone or in medium containing LPS ( $1 \mu\text{g ml}^{-1}$ ). Lysates were generated at the end of the incubation period and subjected to western blotting using an anti-iNOS selective antibody. Expression of  $\beta$ -actin was also determined and used as a loading control in the assay. The bar graph is a scanning densitometry of iNOS expression as a percentage of the levels detected at 24 h post activation and is the mean  $\pm$  SEM of three separate experiments. Statistical analysis was carried out using a one way Anova followed by Dunnett's multiple comparison test. \* $p < 0.05$  and \*\* $p < 0.01$  compared to activated, non-inhibitor cells.

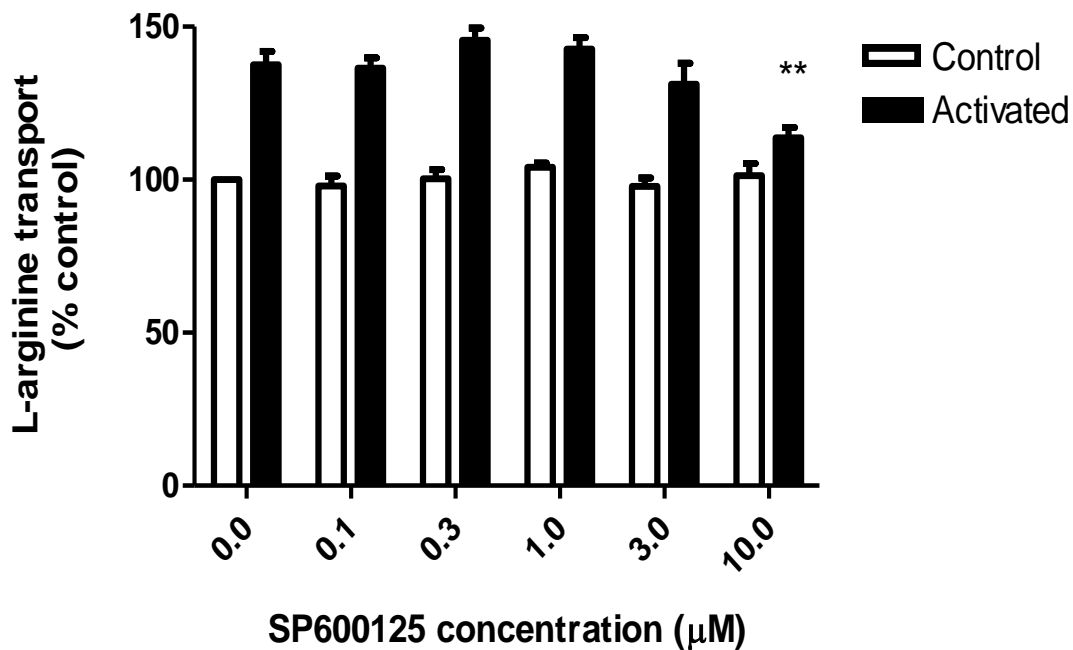


**Figure 3.17 Effect of SP600125 on L-arginine transport in J774 macrophages**

Confluent monolayers of J774 macrophages were incubated with increasing concentrations of SP600125 for 30 min prior to a further 24 h incubation in culture medium alone or in medium containing LPS ( $1 \mu\text{g ml}^{-1}$ ). L-arginine transport was monitored over 2 min in Krebs buffer containing  $1 \mu\text{Ci ml}^{-1}$  L- $^3\text{H}$ -arginine plus  $100 \mu\text{M}$  unlabelled L-arginine. Values are expressed as the mean  $\pm$  S.E.M of 3 separate experiments with 5 replicate in each. Statistical analysis was carried out using a one way Anova followed by Dunnett's multiple comparison test. \*\*  $p < 0.01$  compared to activated non-inhibitor cells

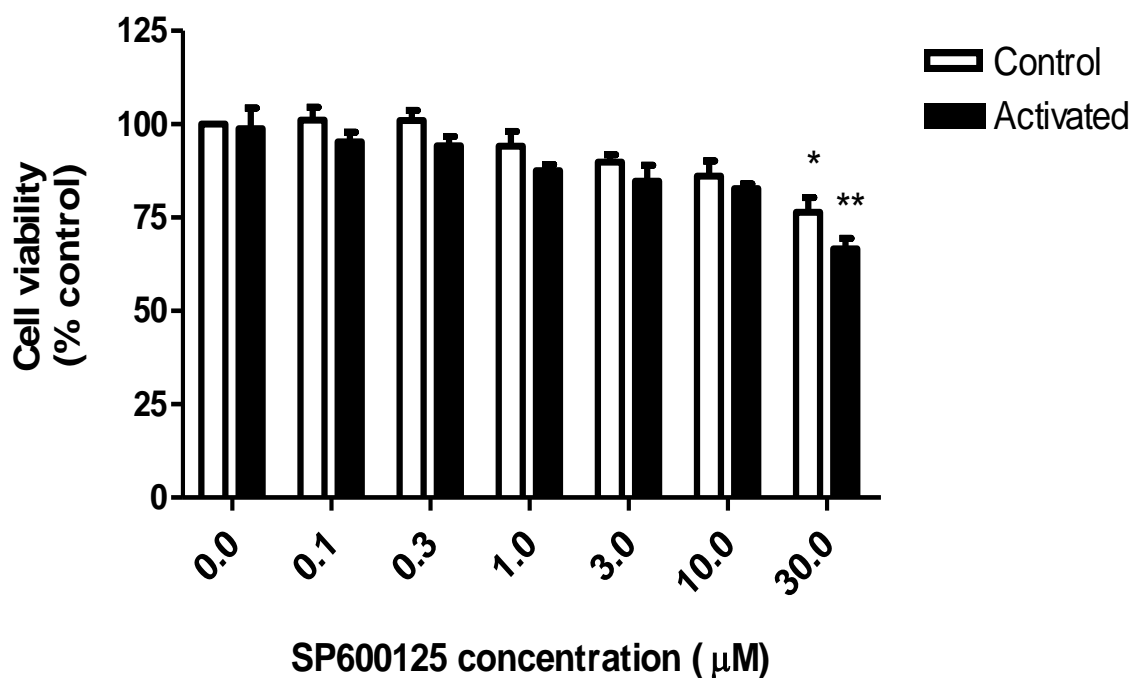


**Figure 3.18 Effect of SP600125 on Cell viability in J774 macrophages**

Cells were pre-incubated with SP600125 for 30 min prior to activation with LPS ( $1 \mu\text{g ml}^{-1}$ ). After 24 h activation, the culture medium was removed and cells were incubated with MTT (concentration of  $0.05 \text{ mg/ml}$ ) in  $200 \mu\text{l}$  fresh medium per well at  $37^\circ\text{C}$  for 4h. The medium was removed and the formazan crystals produced from the metabolism of MTT solubilised in  $100 \mu\text{l}$  of Isopropanol. Plates were read at  $540 \text{ nm}$  using a Multiscan II plate reader. All values are expressed as a percentage of the control non-activated cells. Values are expressed as the mean  $\pm$  S.E.M of 4 separate experiments with 5 replicate in each. Statistical analysis was carried out using a one way Anova followed by Dunnett's multiple comparison test. \*  $p < 0.05$  and \*\*  $p < 0.01$  compared to activated non-inhibitor cells.

### **3.3.12 Effect of JNK Inhibitor VIII on NO production in RASMCs**

To confirm the role or lack of involvement of JNK in the induction of iNOS and NO production in RASMCs further experiments were carried out using an additional inhibitor of the JNK pathway. The compound used, referred to as JNK inhibitor VIII, is known to block JNK I, II and III ( $K_i = 2 \text{ nM}$ ,  $4 \text{ nM}$  and  $52 \text{ nM}$  for JNK1, 2 and 3, respectively;  $EC_{50}$  of  $920 \text{ nM}$ ) (Ogino *et al.*, 2009; Kluwe *et al.*, 2010). This inhibitor however failed to cause any significant changes in either basal or activated nitrite release when incubated with cells at concentrations of  $0.1 \text{ }\mu\text{M}$  to  $10 \text{ }\mu\text{M}$  for 30 min prior to activation (Figure 3.19). This finding, together with the data from the SP600125 studies, seems to further support a lack of involvement of the JNK pathway in the induction of iNOS in RASMCs.

### **3.3.13 Effect of JNK Inhibitor VIII on iNOS expression in RASMCs**

To determine the effects of JNK Inhibitor VIII on iNOS protein expression, western blot analysis was performed on lysates obtained from control and activated cells in the absence and presence of increasing concentration of JNK Inhibitor VIII ( $0.1\text{-}10 \text{ }\mu\text{M}$ ). There was no detectable expression of iNOS in control non-activated cells. In contrast, activation with LPS and IFN- $\gamma$  caused the expected induction of iNOS protein which remained unaltered in cells treated with JNK inhibitor VIII as shown in figure 3.20.

### **3.3.14 Effect of JNK Inhibitor VIII on L-arginine transport in RASMCs**

Following the nitrite assay, transport of L-[<sup>3</sup>H]-arginine was conducted on the underlying cell monolayers. In these experiments, L-[<sup>3</sup>H]-arginine transport increased from control values of 1 pmoles  $\mu\text{g protein}^{-1} \text{ min}^{-1}$  (n=3) to 1.4 pmoles  $\mu\text{g protein}^{-1} \text{ min}^{-1}$  (n=3) in the cells activated with LPS/IFN- $\gamma$ . Treatment with JNK inhibitor VIII at the full concentration range of 0.1  $\mu\text{M}$  to 10  $\mu\text{M}$  failed to cause any significant changes in either basal or activated transport rates (Figure 3.21).

### **3.3.15 Effect of JNK Inhibitor VIII on Cell viability in RASMCs**

Viability studies carried out in parallel with experiments outlined above, revealed that JNK Inhibitor VIII did not cause any significant degrees of cytotoxicity in RASMCs over the concentration range of 0.1  $\mu\text{M}$  to 10  $\mu\text{M}$ ; however at 30  $\mu\text{M}$  the drug did appear cytotoxic, decreasing cell viability by 26% in control and 40% in activated cells (treated with LPS and INF- $\gamma$ ) as shown in Figure 3.22. As a result all experiments using JNK inhibitor VIII limited the concentration used to a maximum of 10  $\mu\text{M}$ .

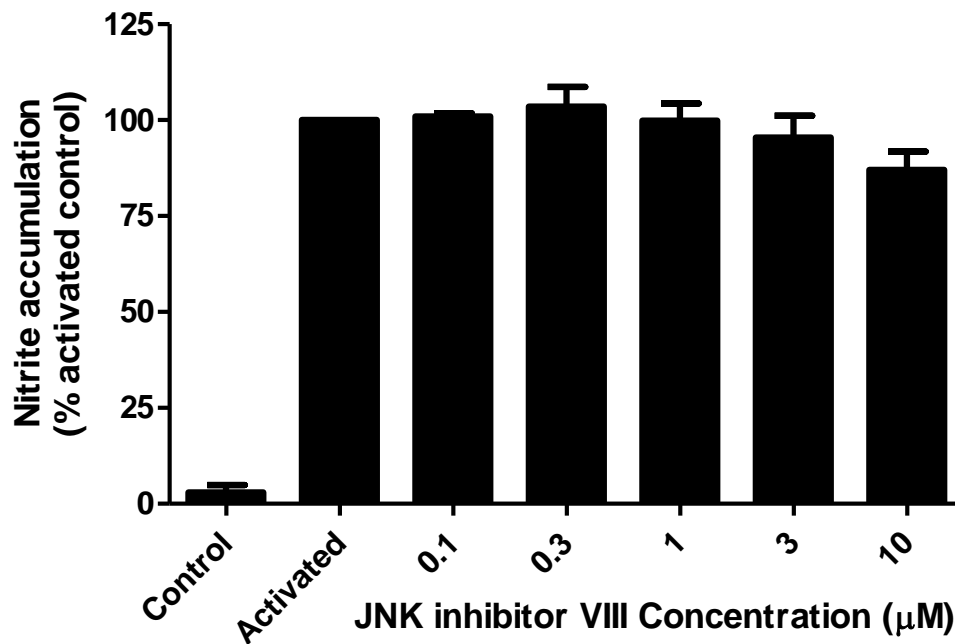


**Figure 3.19 Effect of JNK Inhibitor VIII on NO production in RASMCs**

Confluent monolayers of RASMCs were incubated with increasing concentrations of JNK inhibitor VIII for 30 min prior to a further 24 h incubation in culture medium alone or in medium containing LPS ( $100 \mu\text{g ml}^{-1}$ ) and IFN- $\gamma$  ( $100 \text{ U ml}^{-1}$ ). Accumulated nitrite was determined by the Griess assay and standardised for total protein present in the well. The results are expressed as a percentage of the total amount of nitrite accumulated at 24 h and are the mean  $\pm$  SEM of 3 independent experiments with 3 replicates in each. Statistical analysis was carried out using a one way Anova followed by Dunnett's multiple comparison test.

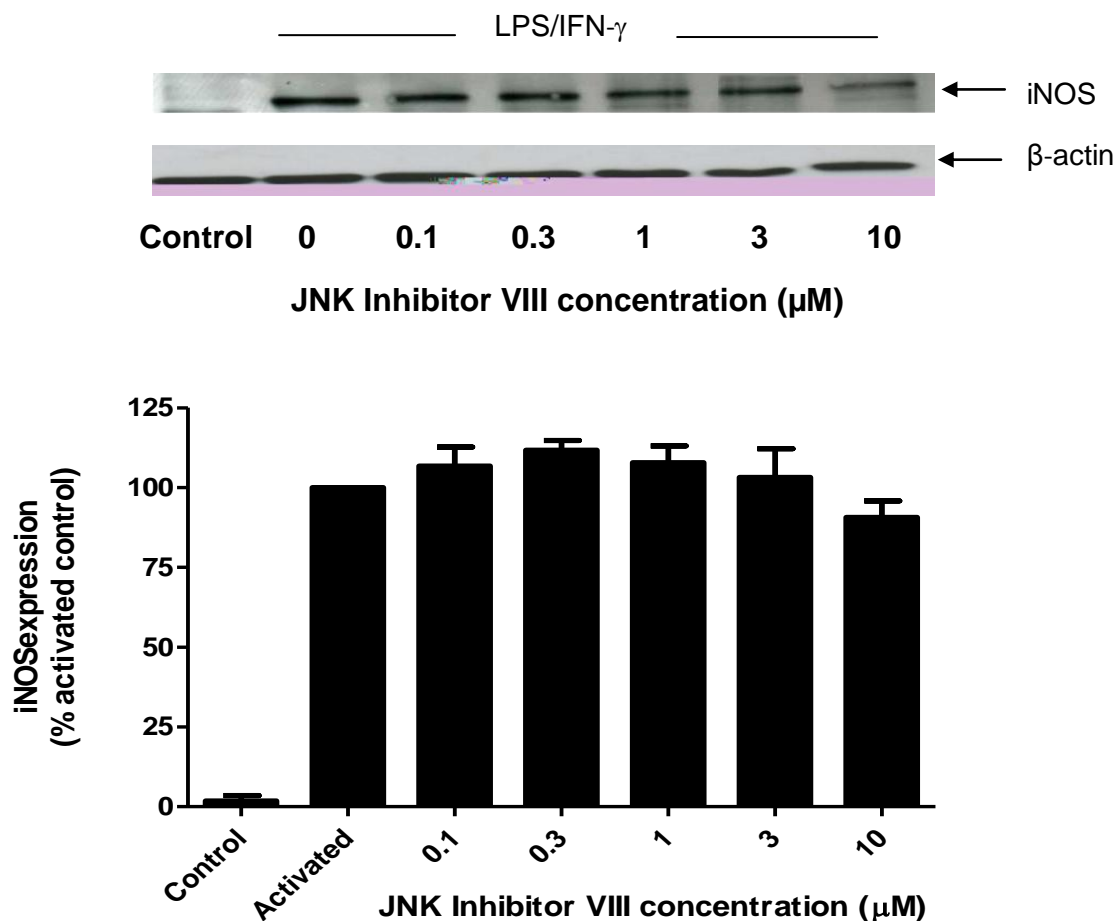


**Figure 3.20 Effect of JNK Inhibitor VIII on iNOS expression in RASMCs**

Confluent monolayers of RASMCs were incubated with increasing concentrations of JNK inhibitor VIII for 30 min prior to a further 24 h incubation in culture medium alone or in medium containing LPS ( $100 \mu\text{g ml}^{-1}$ ) and IFN- $\gamma$  ( $100 \text{ U ml}^{-1}$ ). Lysates were generated at the end of the incubation period and subjected to western blotting using an anti-iNOS selective antibody. Expression of  $\beta$ -actin was also determined and used to standardise the loading and expression levels of iNOS. The bar graph is a scanning densitometry of iNOS expression as a percentage of the levels detected at 24 h post activation and is the mean  $\pm$  SEM of three separate experiments. Statistical analysis was carried out using a one way Anova followed by Dunnett's multiple comparison test.

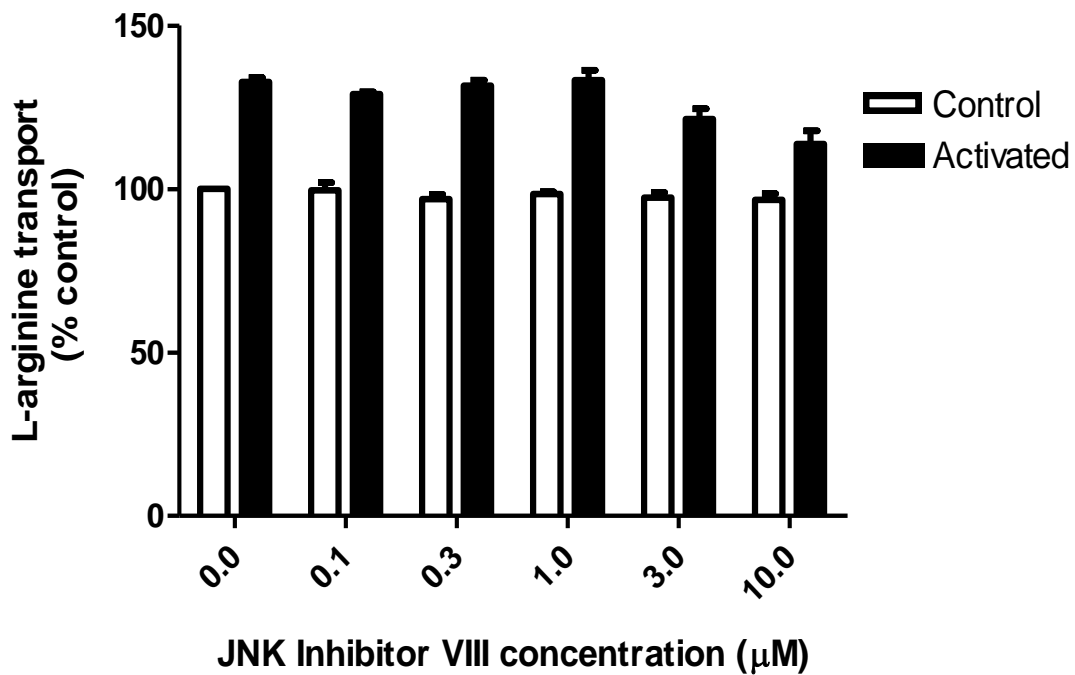


**Figure 3.21 Effect of JNK Inhibitor VIII on L-arginine transport in RASMCs**

Confluent monolayers of RASMCs were incubated with increasing concentrations of JNK Inhibitor VIII for 30 min prior to a further 24 h incubation in culture medium alone or in medium containing LPS ( $100 \mu\text{g ml}^{-1}$ ) and IFN- $\gamma$  ( $100 \text{ U ml}^{-1}$ ). L-arginine transport was monitored over 2 min in Krebs buffer containing  $1 \mu\text{Ci ml}^{-1}$  L- $[\text{}^3\text{H}]$ -arginine plus  $100 \mu\text{M}$  unlabelled L-arginine. The results are representative of 3 independent experiments with 5 replicates in each. Statistical analysis was carried out using a one way Anova followed by Dunnett's multiple comparison test.

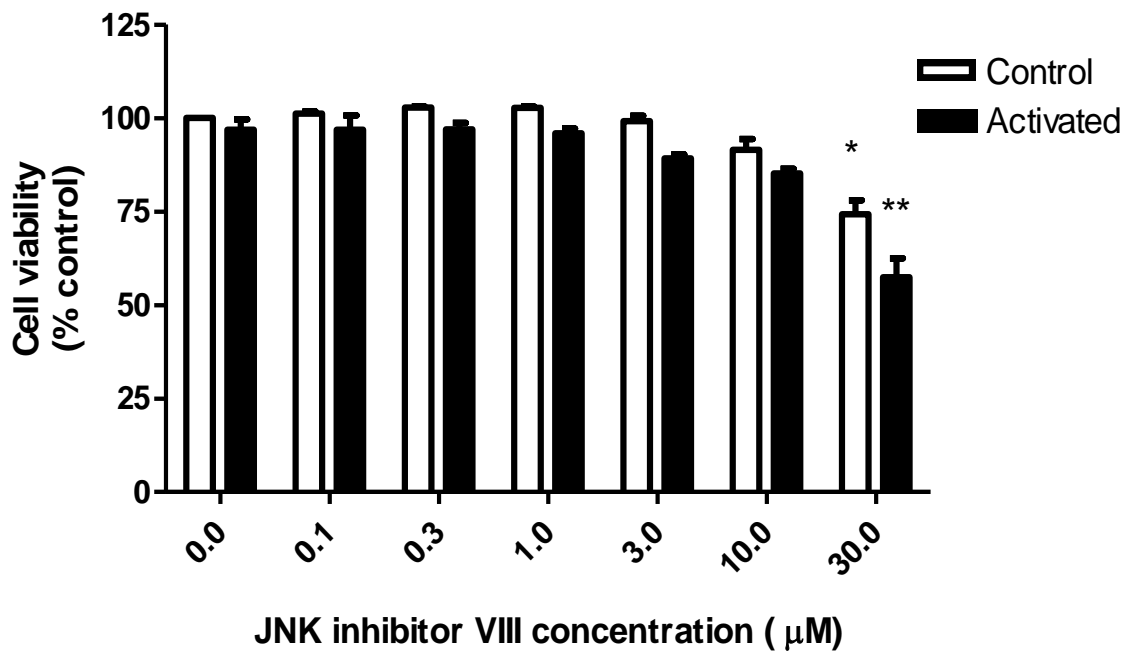


**Figure 3.22 Effect of JNK Inhibitor VIII on Cell viability in RASMCs**

Cells were pre-incubated with JNK Inhibitor VIII for 30 min prior to activation with LPS ( $100 \mu\text{g ml}^{-1}$ ) and  $\text{INF-}\gamma$  ( $100 \text{ U ml}^{-1}$ ). After 24 h activation, the culture medium was removed and cells were incubated with MTT (concentration of  $0.5 \text{ mg/ml}$ ) in  $200 \mu\text{l}$  fresh medium per well at  $37^\circ\text{C}$  for 4h. The medium was removed and the formazan crystals produced from the metabolism of MTT solubilised in  $100 \mu\text{l}$  of Isopropanol. Plates were read at  $540 \text{ nm}$  using a Multiscan II plate reader. All values are expressed as a % of the control non-activated cells. Values are expressed as the mean  $\pm$  S.E.M of 3 separate experiments with 5 replicate in each. Statistical analysis was carried out using a one way Anova followed by Dunnett's multiple comparison test. \*  $p < 0.05$  and \*\*  $p < 0.01$  compared to activated non-inhibitor cells.

### **3.3.16 Effect of JNK Inhibitor VIII on NO production in J774 macrophages**

In contrast to its lack of effect in RASMCs, but consistent with the actions of SP600125 in J774 macrophages, JNK inhibitor VIII initially marginally enhanced LPS-induced nitrite accumulation at 0.1  $\mu\text{M}$  and 0.3  $\mu\text{M}$ , inhibiting by 23 % and 38% at concentrations of 3  $\mu\text{M}$  and 10  $\mu\text{M}$  respectively (Figure 3.23).

### **3.3.17 Effect of JNK Inhibitor VIII on iNOS expression in J774 macrophages**

Parallel studies were also carried out in J774 macrophages to verify whether JNK inhibitor VIII affect the level of iNOS expression in J774 macrophages. Western blot analysis was performed on lysates obtained from control and activated cells in the absence and presence of increasing concentration of the drug. In these studies, JNK inhibitor VIII was without significant effect at concentrations of  $\leq 1$   $\mu\text{M}$  but inhibited iNOS expression by 29% and 44% at 3  $\mu\text{M}$  and 10  $\mu\text{M}$  respectively (Figure 3.24).

### **3.3.18 Effect of JNK Inhibitor VIII on L-arginine transport in J774 macrophages**

Consistent with the observations in RASMCs, activation of J774 macrophages resulted in a significant increase in L-arginine transport which was elevated from 1.2 pmoles  $\mu\text{g protein}^{-1} \text{ min}^{-1}$  (in control; n=3) to 1.7 pmoles  $\mu\text{g protein}^{-1} \text{ min}^{-1}$  (n=3) following LPS treatment. JNK inhibitor VIII at concentrations of 3 and 10  $\mu\text{M}$  caused a significant down regulation in L-arginine transport in the J774 macrophages activated with LPS but not in controls (Figure 3.25).

### **3.3.19 Effect of JNK Inhibitor VIII on Cell viability in J774 macrophages**

Viability studies carried out to determine the toxicity of JNK inhibitor VIII in J774 macrophages showed that the compound was cytotoxic particularly at 30  $\mu\text{M}$  as shown in Figure 3.26. As a result all experiments using JNK inhibitor VIII in J774 macrophages limited the concentration used to a maximum of 10  $\mu\text{M}$ .

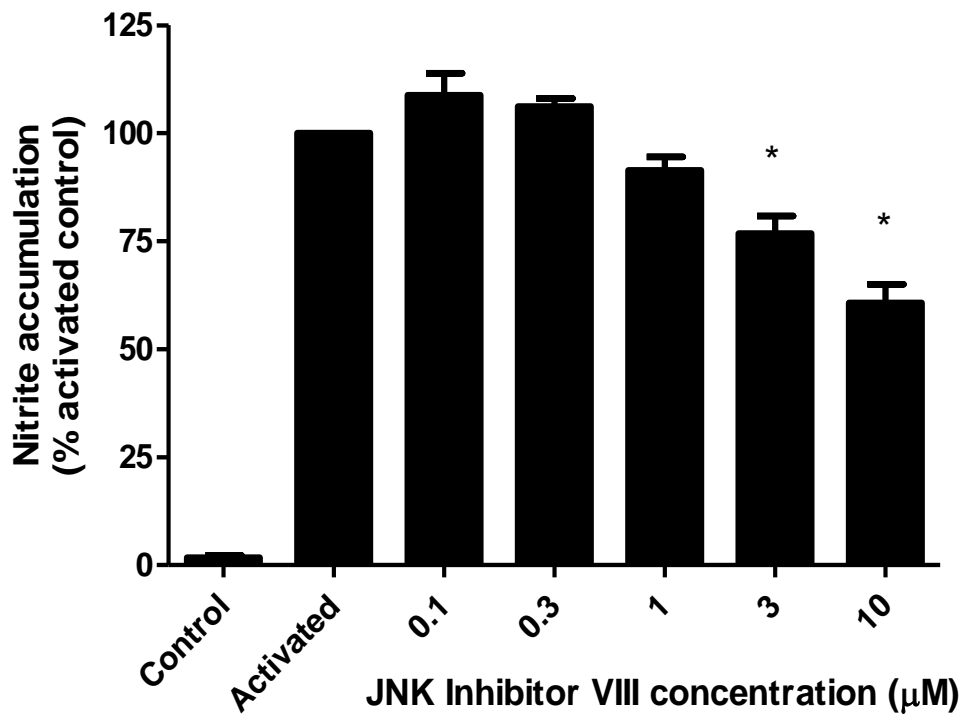


**Figure 3.23 Effect of JNK Inhibitor VIII on NO production in J774 macrophages**

Confluent monolayers of J774 macrophages were incubated with increasing concentrations of JNK Inhibitor VIII for 30 min prior to a further 24 h incubation in culture medium alone or in medium containing LPS ( $1 \mu\text{g ml}^{-1}$ ). Accumulated nitrite was determined by the Griess assay and standardised for total protein present in the well. Values are expressed as the mean  $\pm$  S.E.M of 3 separate experiments with 3 replicate in each. Statistical analysis was carried out using a one way Anova followed by Dunnett's multiple comparison test. \*  $p < 0.05$  compared to activated non-inhibitor cells.

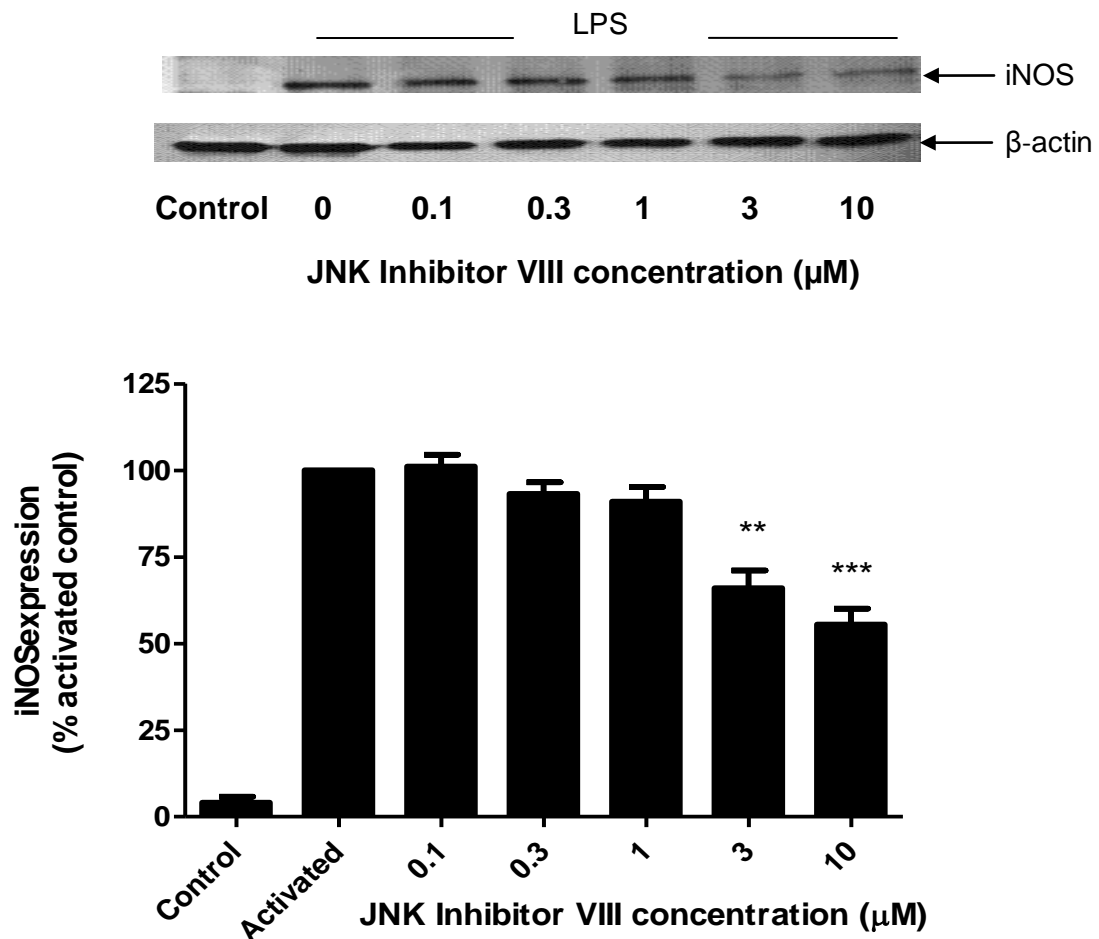


**Figure 3.24 Effect of JNK Inhibitor VIII on iNOS expression in J774 macrophages**

Confluent monolayers of J774 macrophages were incubated with increasing concentrations of JNK inhibitor VIII for 30 min prior to a further 24 h incubation in culture medium alone or in medium containing LPS ( $1 \mu\text{g ml}^{-1}$ ). Lysates were generated at the end of the incubation period and subjected to western blotting using an anti-iNOS selective antibody. Expression of  $\beta$ -actin was also determined and used as a loading control in the assay. The bar graph is a scanning densitometry of iNOS expression as a percentage of the levels detected at 24 h post activation and is the mean  $\pm$  SEM of three separate experiments. Statistical analysis was carried out using a one way Anova followed by Dunnett's multiple comparison test. \*\* $p < 0.01$  and \*\*\* $p < 0.001$  compared to activated, non-inhibitor cells.

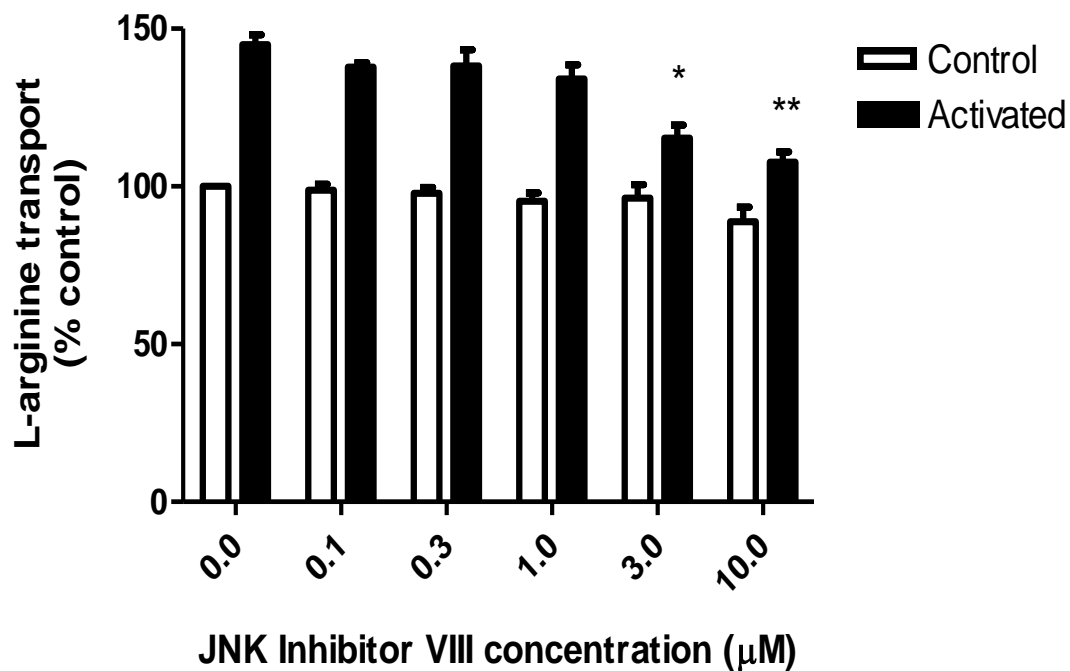


**Figure 3.25 Effect of JNK Inhibitor VIII on L-arginine transport in J774 macrophages**

Confluent monolayers of J774 macrophages were incubated with increasing concentrations of JNK Inhibitor VIII for 30 min prior to a further 24 h incubation in culture medium alone or in medium containing LPS ( $1 \mu\text{g ml}^{-1}$ ). L-arginine transport was monitored over 2 min in Krebs buffer containing  $1 \mu\text{Ci ml}^{-1}$  L- $^3\text{H}$ -arginine plus  $100 \mu\text{M}$  unlabelled L-arginine. Values are expressed as the mean  $\pm$  S.E.M of 3 separate experiments with 5 replicate in each. Statistical analysis was carried out using a one way Anova followed by Dunnett's multiple comparison test.

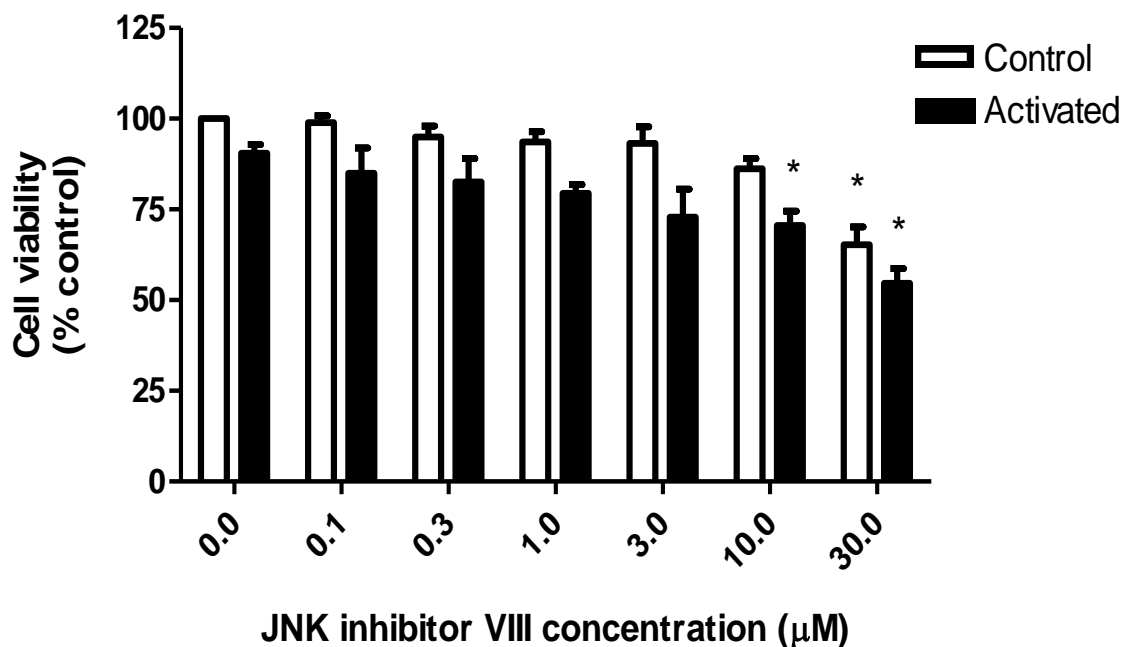


**Figure 3.26 Effect of JNK Inhibitor VIII on Cell viability in J774 macrophages**

Cells were pre-incubated with JNK Inhibitor VIII for 30 min prior to activation with LPS ( $1 \mu\text{g ml}^{-1}$ ). After 24 h activation, the culture medium was removed and cells were incubated with MTT (concentration of 0.5 mg/ml) in 200  $\mu\text{l}$  fresh medium per well at 37°C for 4h. The medium was removed and the formazan crystals produced from the metabolism of MTT solubilised in 100  $\mu\text{l}$  of Isopropanol. Plates were read at 540 nm using a Multiscan II plate reader. All values are expressed as a percentage of the control non-activated cells. Values are expressed as the mean  $\pm$  S.E.M of 3 separate experiments with 5 replicate in each. Statistical analysis was carried out using a one way Anova followed by Dunnett's multiple comparison test. \*  $p < 0.05$  compared to activated non-inhibitor cells.

### **3.3.20 Mini-preps of a-Fos and TAM-67 characterised by restriction digest**

DH5- $\alpha$  competent cells, were generated as described in the methods (Section 2.2.9) and transformed with pGFP-a-Fos and pGFP-TAM-67 (Section 2.2.10). The cultures were isolated and purified by mini-prep (Section 2.2.11) and a mini-gel was run to observe the purity of the plasmids isolated which as shown in Figures 3.27 (Panel A) appears as smear-free bands confirming that the isolates were not degraded.

Restricting the plasmids with BamHI and HindIII for a-Fos (Figure 3.27, panel B) or BamHI and XhoI for TAM-67 (Figure 3.27, panel C) produced single bands of 250 and 700 kb respectively which correspond to their insert sizes.

Ladder a-Fos TAM-67

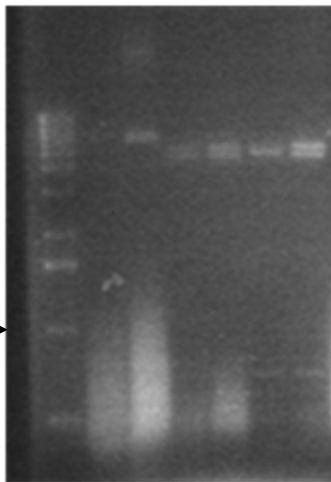
(A)

5090 kb →



(B)

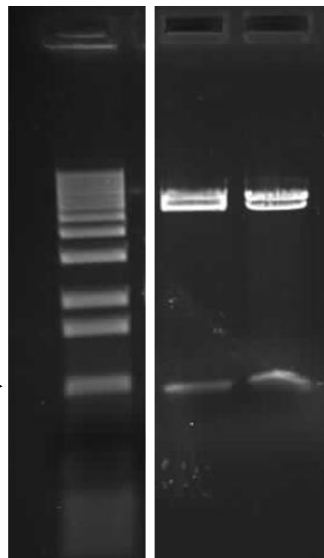
506 kb →



← a-Fos (250 bp)

(C)

1008 kb →



← TAM-67 (700 bp)

**Figure 3.27 Mini-preps of non-restricted and restricted a-Fos and TAM-67**

The plasmids were either left intact or restricted and then separated on a mini-gel to ensure they possessed the correct insert as well as observe their purity. The figures show the unrestricted plasmid (Panel A), plasmids restricted using BamHI & HindIII for a-Fos (Panel B) or BamHI and XhoI for TAM-67 (Panel C). The first columns in the panels represent the DNA ladder (1kb) and in Panel B the next 2 column are undigested plasmid and the rest are digested plasmids showing fragments of 250 bp which corresponds to the a-Fos insert. Panel C shows a band of 700 bp corresponding to the insert size of TAM-67.

### **3.3.21 Expression profile of transfected pGFP-a-Fos and pGFP-TAM-67 plasmide in RASMCs**

The optimum transfection time was first established prior to examining the effect of plasmids on NO production, iNOS expression and L-arginine uptake. This was carried out by examining the expression of each plasmid at various time points after the transfection using the GFP-antibody. Lysates from transfected cells were analysed by western blot analysis as described, using a primary GFP-antibody as an indicator of the expression of GFP. The expression of  $\beta$ -actin was also determined in parallel (Figure 3.28) and used to confirm the loading efficiency. Western blotting confirmed successful transfection of RASMCs with both a-Fos and TAM-67 as expression of the GFP tagged to a-Fos and TAM-67 (panel A and B respectively) was detectable over the time course examined, albeit marginally, at 6 hrs reaching a peak at 24 hrs. It is worth noting however that incubations of 24 hours cause cytotoxicity to cells with many lifting off from the monolayers. To ensure the planned experiments could be carried out we did the study for an 18 hour transfection time period which as shown in Figure 3.29 revealed high transfection efficiency but with little change in either cell morphology or density.

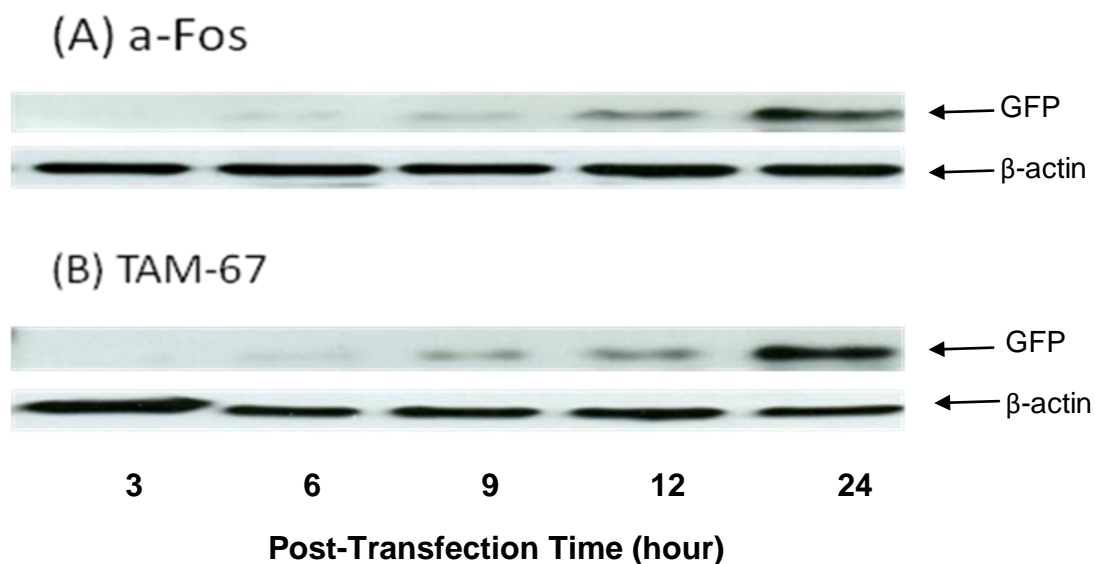


**Figure 3.28 Expression of GFP in time course study of transfected pGFP-a-Fos and pGFP-TAM-67 in RASMCs**

Partially confluent RASMCs were transfected with pGFP-a-Fos or pGFP-TAM-67 in 24 well plates as described in the methods (Section 2.2.14). Lysate of transfected cells were analysed by western blotting using a primary GFP-antibody to detect pGFP-a-Fos (Panel A) or pGFP-TAM-67 (Panel B). The expression of  $\beta$ -actin was also determined in parallel and used to determine the loading efficiency. The blots are representative of 2 individual experiments.

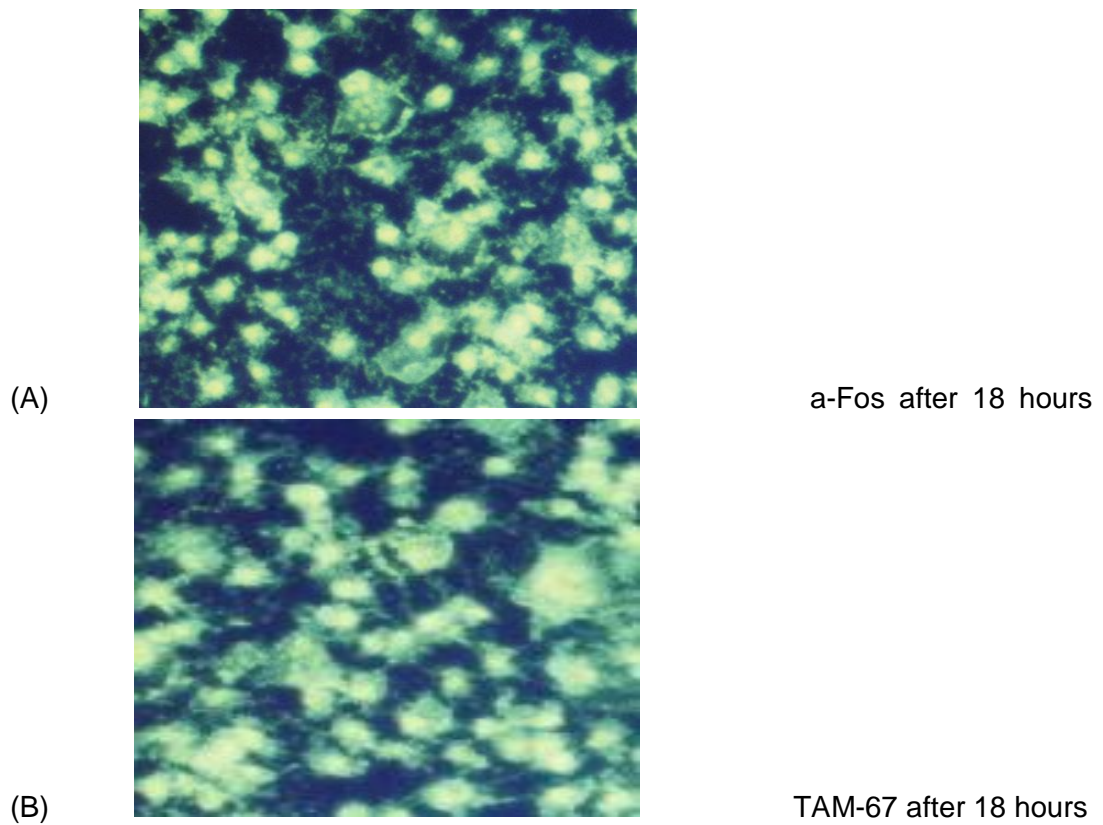


**Figure 3.29 Visualisation of Transfected RASMCs with pGFP-a-Fos and pGFP-TAM-67 at 18 hours**

Partially confluent RASMCs were transfected with pGFP-a-Fos (panel A) or pGFP-TAM-67 (panel B) in 24 well plates as described in the methods (Section 2.2.15). Cells were visualised under UV light 18 hours post transfection using a Nikon EFD3, LABOPHOT-2 fluorescence microscope at 40x magnifications. The photographs are representative of 3 individual experiments.

### **3.3.22 Effect of pGFP-a-Fos and pGFP-TAM-67 on LPS and IFN- $\gamma$ induced NO production in RASMCs**

Partially confluent monolayers of RASMCs were transfected with pGFP-a-Fos or pGFP-TAM-67 for 18 hours and activated for 24 h with LPS ( $100 \mu\text{g ml}^{-1}$ ) and IFN- $\gamma$  ( $100 \text{ U ml}^{-1}$ ). Nitric oxide production was determined by the nitrite assay as described in the methods (section 2.2.2). The data obtained from these studies suggest opposing effects of the dominant constructs in that pGFP-a-Fos caused a marginal but significant increase (18%) of NO production in activated cells, while pGFP-TAM-67 significantly suppressed induced NO production, reducing the later by 45% (Figure 3.30). Neither pGFP-a-Fos nor pGFP-TAM-67 caused any significant changes in basal nitrite levels in control non-activated cells.

### **3.3.23 Effect of pGFP-a-Fos and pGFP-TAM-67 on LPS and IFN- $\gamma$ induced iNOS expression in RASMCs**

To determine whether the changes on NO production observed above were associated with changes in iNOS expression, partially confluent monolayers of RASMCs transfected with pGFP-a-Fos or pGFP-TAM-67 for 18 h and activated for 24 h with LPS ( $100 \mu\text{g ml}^{-1}$ ) and IFN- $\gamma$  ( $100 \text{ U ml}^{-1}$ ) were lysed and subjected to western blotting. As shown in Figure 3.31 iNOS bands were not detectable in control non-activated cells but present in cells exposed to LPS and IFN- $\gamma$ . More importantly,

level of the enzyme increased by 24% in cells expressing pGFP-a-Fos but reduced by 27% in cells expressing pGFP-TAM-67.

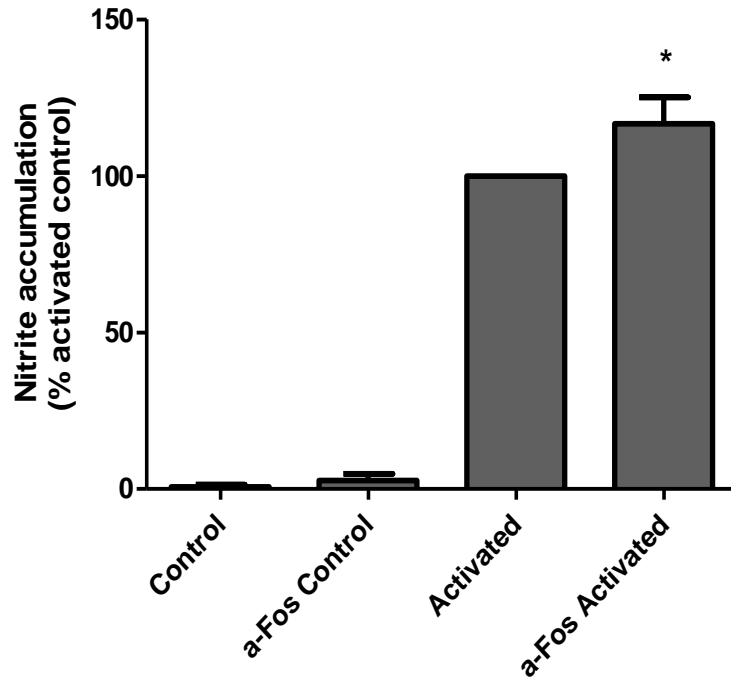
### **3.3.24 Effect of pGFP-a-Fos and pGFP-TAM-67 on LPS and IFN- $\gamma$ induced L-arginine transport in RASMCs**

In parallel with the study on NO production and iNOS expression, experiments were also carried out examining the effect of either pGFP-a-Fos or pGFP-TAM-67 on L-arginine transport in both control and activated RASMCs. The data shown in Figure 3.32 reveal that transport of L-arginine was not altered in a-Fos transfected cells when compared to the controls. In contrast, activated cells expressing TAM-67 showed a significant reduction in L-arginine transport, with the induced rates decreasing from  $1.6 \pm 0.01$  pmoles  $\mu\text{g protein}^{-1} \text{ min}^{-1}$  (n=3) to the basal control rates of  $1.3 \pm 0.015$  pmoles  $\mu\text{g protein}^{-1} \text{ min}^{-1}$  (n=3). Transport into control cells was unaffected suggesting a selective action of TAM-67 on the induction process.

**Figure 3.30 Effect of pGFP-a-Fos and pGFP-TAM-67 on LPS and IFN- $\gamma$  induced NO production in RASMCs**

50- 70% confluent monolayers of RASMCs were transfected with pGFP-a-Fos (panel A) or pGFP-TAM-67 (panel B) and activated for 24 h with LPS ( $100 \mu\text{g ml}^{-1}$ ) and IFN- $\gamma$  ( $100 \text{ U ml}^{-1}$ ). Cells incubated with culture medium alone or with transfection mix containing peptide 6 were used as controls. Nitric oxide production was determined by the nitrite assay. Values are expressed as the mean  $\pm$  S.E.M of 3 separate experiments with 3 replicate in each. Statistical analysis was carried out using a one way Anova followed by Dunnett's multiple comparison test. \*  $p < 0.05$  and \*\*\*  $p < 0.01$  compared to activated non-transfected cells.

### a-Fos



### TAM-67

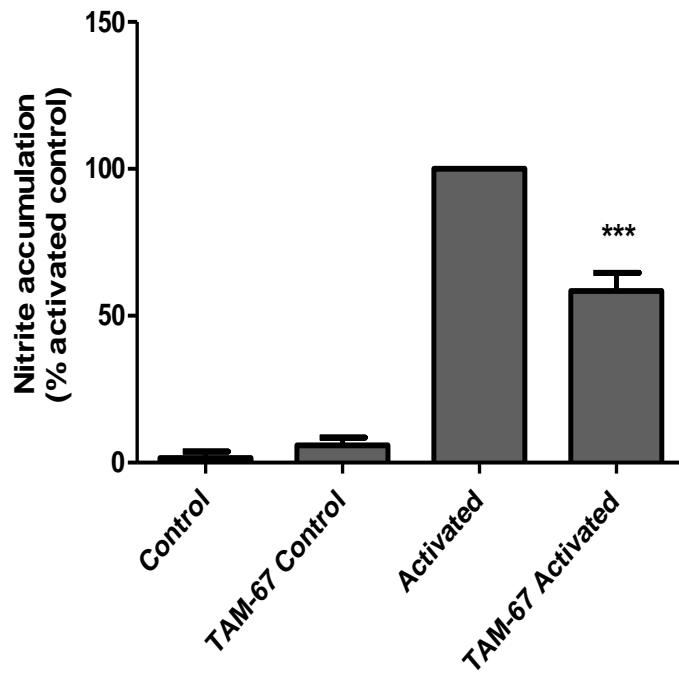


**Figure 3.31 Effect of pGFP-a-Fos and pGFP-TAM-67 on LPS and IFN- $\gamma$  induced iNOS expression in RASMCs**

50-70% confluent monolayers of RASMCs were transfected with pGFP-TAM-67 or pGFP-a-Fos and activated for 24 h with LPS (100  $\mu\text{g ml}^{-1}$ ) and IFN- $\gamma$  (100 U  $\text{ml}^{-1}$ ). iNOS expression was determined by western blotting using a specific anti-iNOS monoclonal antibody as described in the methods. Expression of  $\beta$ -actin was also determined and used to standardise the loading and expression levels of iNOS.

Protein bands were quantified by scanning densitometry using a Bio Imaging System and the Gene Genius software program. The data is expressed as a percentage of value obtained for samples from activated cells and is the mean  $\pm$  SEM of three separate experiments. Statistical analysis was carried out using a one way Anova followed by Dunnett's multiple comparison test. \*\*  $p < 0.01$  compared to activated non-transfected cells.

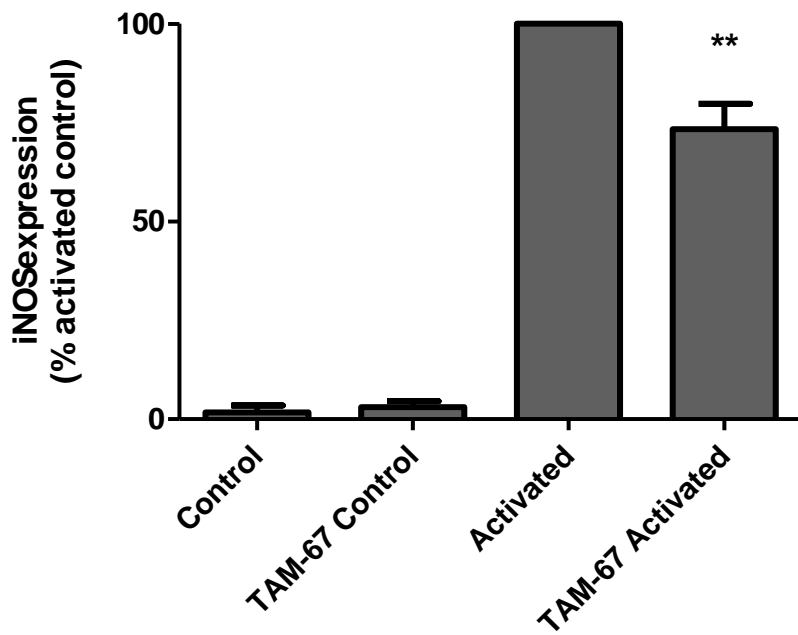
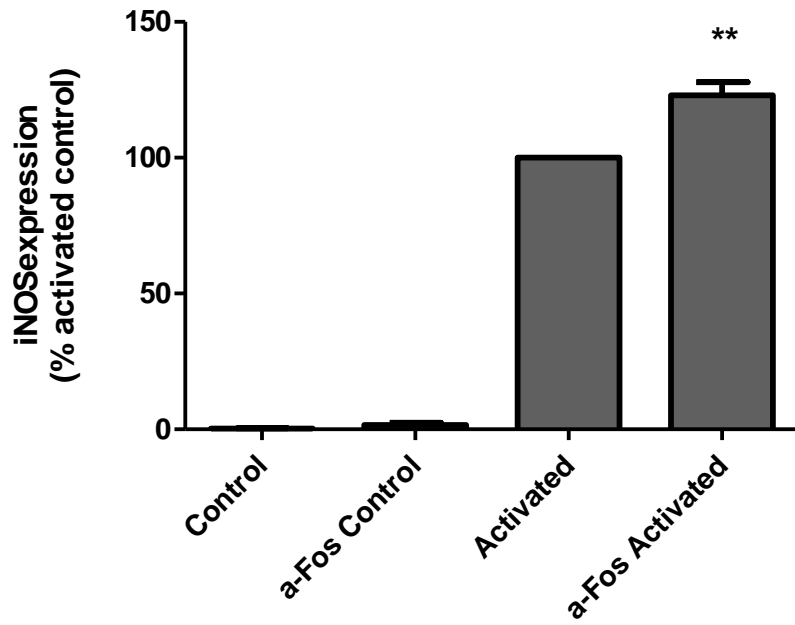
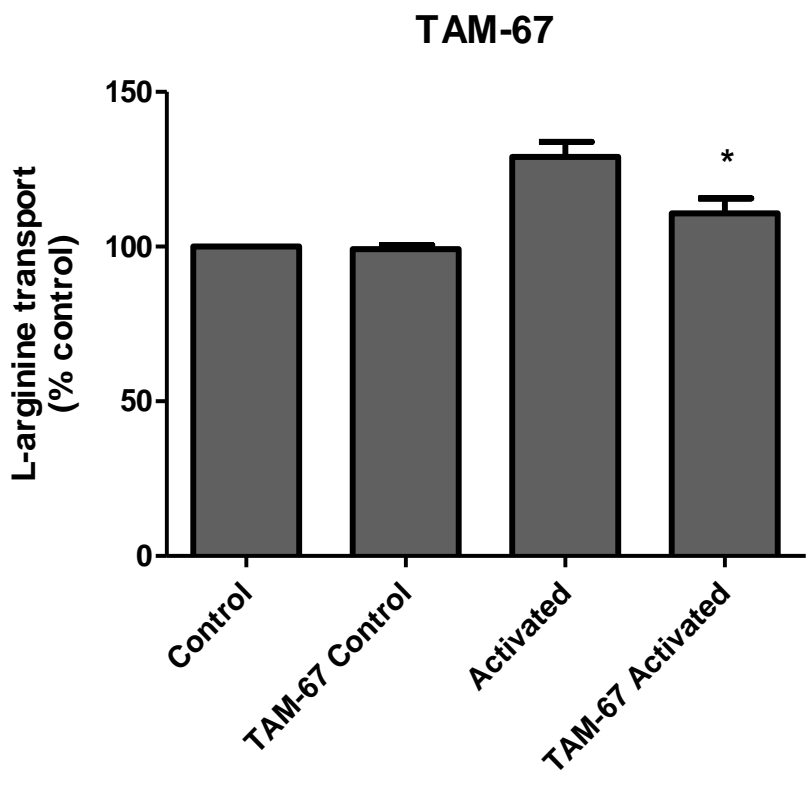
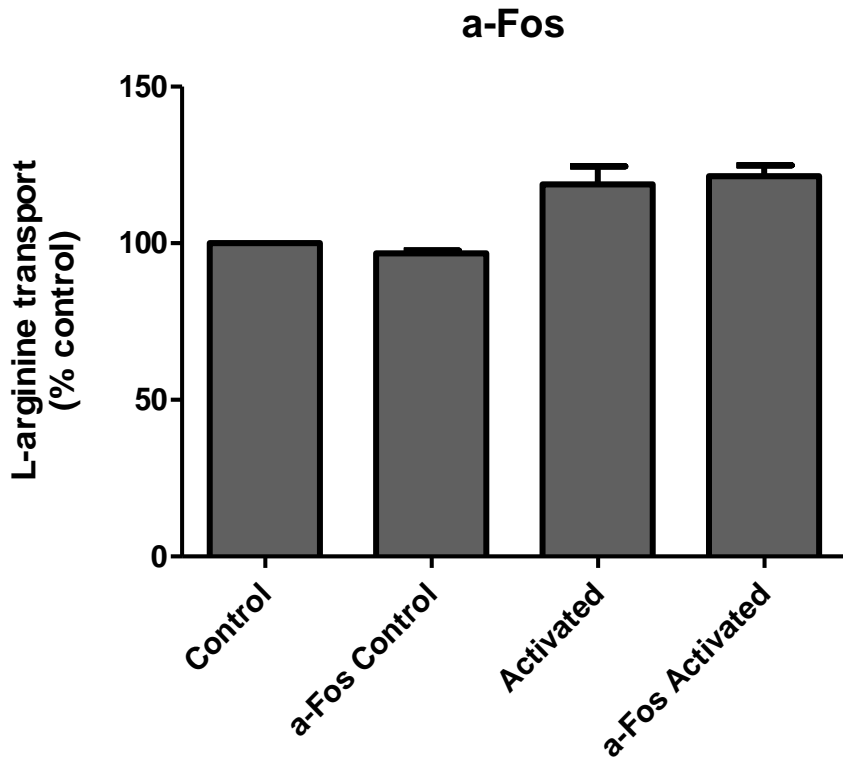


**Figure 3.32 Effect of pGFP-a-Fos and pGFP-TAM-67 on LPS and IFN- $\gamma$  induced L-arginine transport in RASMCs**

Partially confluent monolayers of RASMCs were transfected with pGFP-a-Fos or pGFP-TAM-67 and activated for 24 h with LPS ( $100 \mu\text{g ml}^{-1}$ ) and IFN- $\gamma$  ( $100 \text{ U ml}^{-1}$ ). Transport of L-arginine was measured over 2 minutes in Krebs buffer containing  $1 \mu\text{Ci ml}^{-1}$  L- $^3\text{H}$ -arginine plus  $100 \mu\text{M}$  unlabelled L-arginine. Values are expressed as the mean  $\pm$  S.E.M of 3 separate experiments with 5 replicate in each. Statistical analysis was carried out using a one way Anova followed by Dunnett's multiple comparison test. \*  $p < 0.05$  compared to activated non-transfected cells.



### **3.3.25 Effect of SP600125 on iNOS gene expression in RASMCs**

The data presented in sections 3.3.4, 3.3.5 and 3.3.6 for SP600125 on iNOS, NO synthesis and L-arginine transport would suggest that this compound does not affect the induction of the L-arginine-NO pathway in RASMCs. However, the studies conducted focused on changes in protein expression and function. To determine whether SP600125 regulated gene expression or exerted any effects at the transcriptional level, two different concentrations of SP600125 (0.3 and 3  $\mu$ M) were examined on iNOS mRNA expression. Consistent with the other data, SP600125 failed to cause any significant change in iNOS mRNA levels induced by LPS and IFN- $\gamma$  (Figure 3.33) confirming the lack of effect of this inhibitor on iNOS expression, at least in RASMCs.

### **3.3.26 Effect of SP600125 on iNOS gene expression in J774 macrophages**

In contrast to its lack of effects in RASMCs, SP600125 caused a significant inhibition of iNOS mRNA induction in J774 macrophages at the same concentration of 3  $\mu$ M that also significantly suppressed protein levels and NO production. Interestingly, there appeared to be a marginal increase in iNOS mRNA at 0.3  $\mu$ M, aligning with the small increase in nitrite levels detected with the Griess assay. The increases in mRNA levels were however not statistically significant (Figure 3.34).

### **3.3.27 Effect of pGFP-a-Fos and pGFP-TAM-67 on LPS and IFN- $\gamma$ induced iNOS gene expression in RASMCs**

To investigate the effect of AP-1 dominant negative construct on iNOS gene expression, RASMCs were transfected with a-Fos for 18 hours and activated with LPS/IFN- $\gamma$  for another 18 hours as described previously. The results of the qPCR analysis revealed a pattern reflective of those demonstrated at the expressional and functional levels in that a-Fos enhanced while TAM-67 suppressed iNOS mRNA expression when compared to the levels induced by LPS and IFN- $\gamma$  (Figures 3.35 and 3.36).

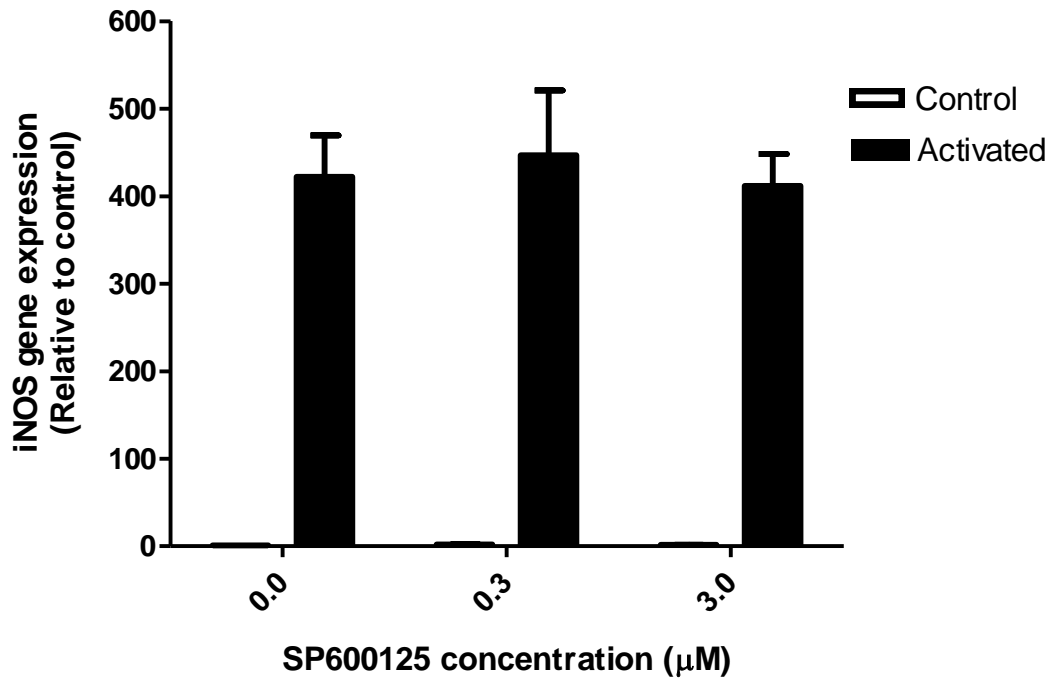


**Figure 3.33 The effect of SP600125 on iNOS gene expression in RASMCs**

Confluent monolayers of RASMCs were incubated with SP600125 (0.3-3 µM) for 30 min prior to activation with LPS (100 µg ml<sup>-1</sup>) and IFN-γ (100 U ml<sup>-1</sup>) for 18 hours. Total RNA was isolated from cells and cDNA was prepared before analysing by quantitative PCR using iNOS specific primers. The graph reflects fold changes in iNOS level in activated cells containing SP600125 compared to activated cells without SP600125. The results are representative of 3 independent experiments with 3 replicates in each and the values are expressed as the mean ± S.E.M of 3 separate experiments.

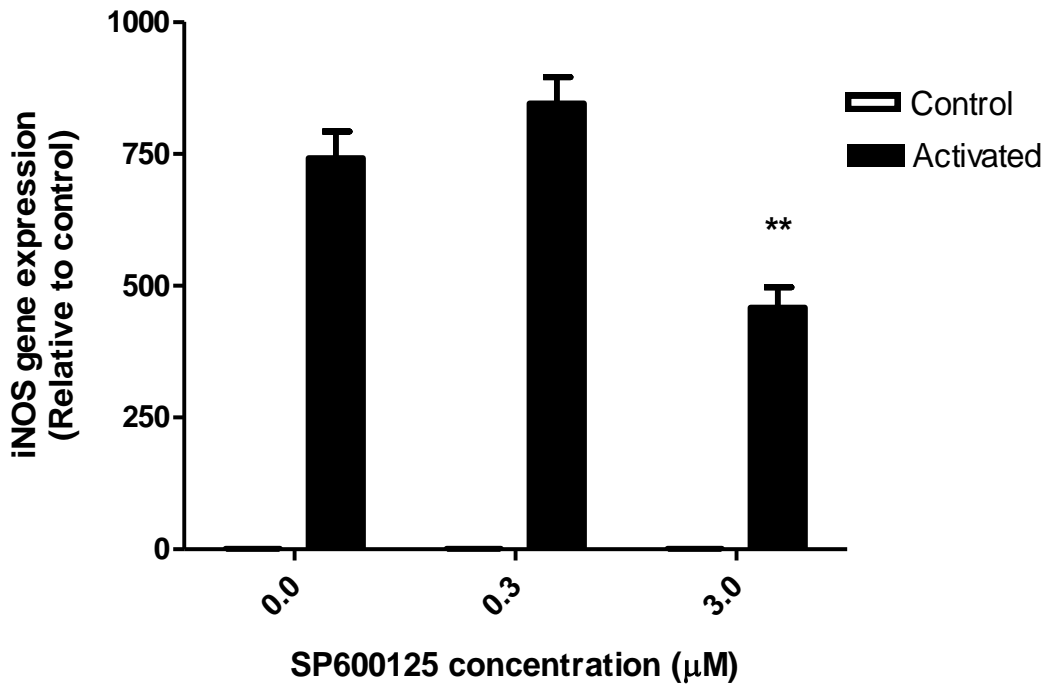


**Figure 3.34 The effect of SP600125 on iNOS gene expression in J774 macrophages**

Confluent monolayers of J774 macrophages were incubated with SP600125 (0.3-3 µM) for 30 min prior to activation with LPS (1 µg ml<sup>-1</sup>) for a further 18 hours. Total RNA was isolated from cells and cDNA was prepared before analysing by quantitative PCR using iNOS specific primers. The graph reflects fold changes in iNOS level in activated cells containing SP600125 compared to activated cells without SP600125. The results are representative of 3 independent experiments with 3 replicates in each and the values are expressed as the mean ± S.E.M of 3 separate experiments. Statistical analysis was carried out using a one way Anova followed by Dunnett's multiple comparison test. \*\* p<0.01 compared to activated non-inhibitor cells.

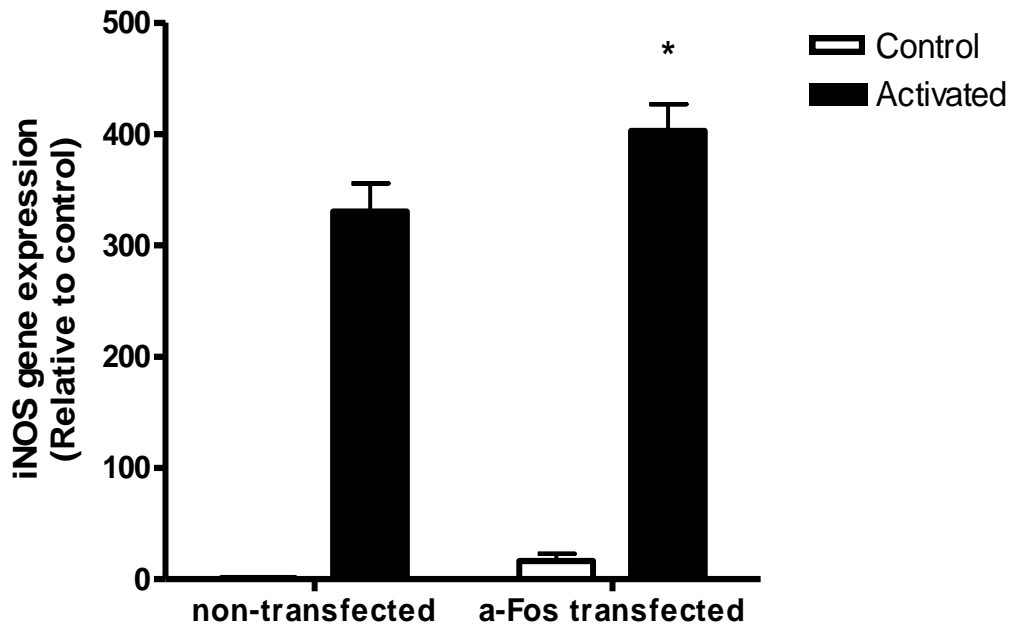


**Figure 3.35 The effect of pGFP-a-Fos construct on iNOS expression in LPS/IFN- $\gamma$  stimulated RASMCs**

Partially Confluent monolayers of RASMCs were transfected with pGFP-a-Fos for 18 hours prior to activation with LPS ( $100 \mu\text{g ml}^{-1}$ ) and IFN- $\gamma$  ( $100 \text{ U ml}^{-1}$ ) for a further 18 hours. Controls were treated with transfection mixture in the absence or presence of LPS/IFN- $\gamma$  and also another control for the experiment which was activated but without transfection. Total RNA was isolated from cells and cDNA was prepared before analysing by quantitative PCR using iNOS specific primers. Values are expressed as the mean  $\pm$  S.E.M of 3 separate experiments. Statistical analysis was carried out using a one way Anova followed by Dunnett's multiple comparison test. \*  $p < 0.05$  compared to activated non-transfected cells.

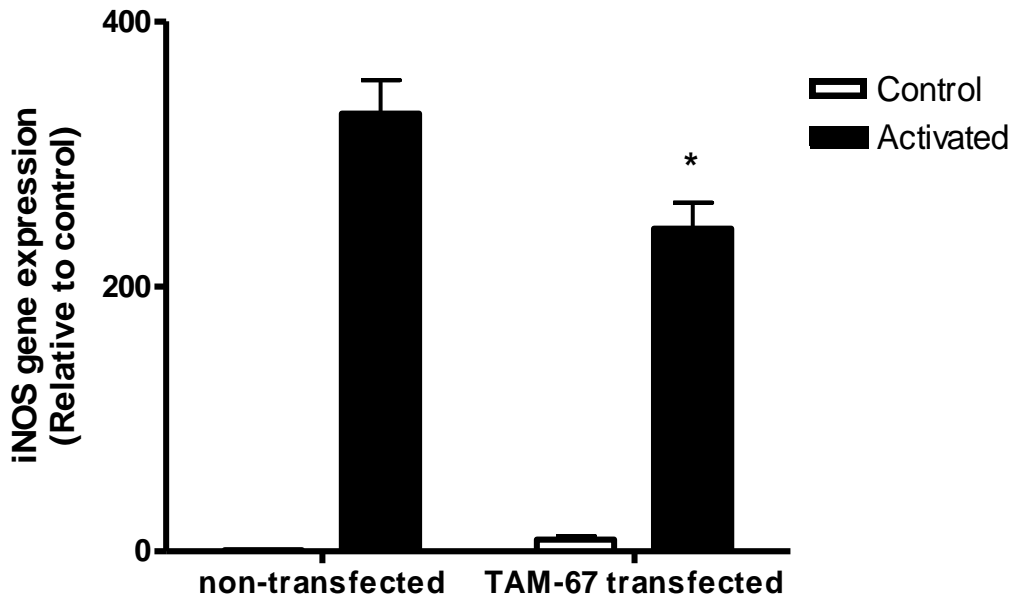


**Figure 3.36 The effect of pGFP-TAM-67 construct on iNOS expression in LPS/IFN- $\gamma$  stimulated RASMCs**

Partially Confluent monolayers of RASMCs were transfected with pGFP-TAM-67 for 18 hours prior to activation with LPS ( $100 \mu\text{g ml}^{-1}$ ) and IFN- $\gamma$  ( $100 \text{ U ml}^{-1}$ ) for a further 18 hours. Controls were treated with transfection mixture in the absence or presence of LPS/IFN- $\gamma$ . Control for the experiment was not transfected but activated. Total RNA was isolated from cells and cDNA was prepared before analysing by quantitative PCR using iNOS specific primers. Values are expressed as the mean  $\pm$  S.E.M of 3 separate experiments. Statistical analysis was carried out using a one way Anova followed by Dunnett's multiple comparison test. \*  $p < 0.05$  compared to activated non-transfected cells.

### 3.4 Discussion

The studies outlined in this thesis were carried out to establish a clear role for JNK/AP-1 pathway in the induction of iNOS and CATs in inflammatory condition. Two different cell types were chosen according to their relation to iNOS expression; Smooth muscle cells which play a key role in vascular tone regulation and are reported to be the key site for iNOS expression in vascular inflammation (Knowles *et al.*, 2004) were isolated from rat aorta, characterised and routinely used in the studies at early passage numbers (between 3 and 6 passages). J774 macrophages were the other cell type used because (i) of their role in host immunity in which iNOS derived NO plays a critical role and (ii) they have been widely characterised and used for studies on iNOS induction in a multitude of laboratories.

To determine the profile of iNOS induction, experiments were carried out in order to establish the time course of induction in response to stimulation with LPS/IFN- $\gamma$  in rat aortic smooth muscle cells or LPS in J774 macrophages. In RASMCs, iNOS expression was evident as early as 30 min after activation with LPS/IFN- $\gamma$ . The marginal levels of the enzyme protein detected at this stage increased in a time dependent manner reaching a peak at 24 hours after stimulation of cells. This pattern was also consistent for nitrite level which was detectable at significant amounts much later as this requires accumulation in the culture medium for detection. These results are consistent with other studies in which control smooth muscle cells produced little amount of nitrite (approximately  $0.01 \text{ pmol } \mu\text{g protein}^{-1} \text{ 24 h}^{-1}$ ) and activation with LPS/IFN- $\gamma$  significantly induced this process (Gross *et al.*, 1992; Petit *et al.*, 1990). In J774 macrophages the pattern was almost the same and

the cells respond to LPS stimulation by expressing iNOS and producing nitric oxide in a time-dependent manner. However with LPS, there was a marked increase in iNOS protein expression after 30 min indicating a rapid response of the cells to inflammatory stimulation. A similar effect has also been reported in macrophages (Cattell *et al.*, 1990), lung epithelial cells (Robbins *et al.*, 1994), hepatocytes (Smith *et al.*, 1997), epithelial cell line (Taylor *et al.*, 1998) and skeletal myoblasts (Adams *et al.*, 2002) showing a rapid increase in iNOS expression and NO released. Interestingly, in other *in vitro* cell culture models such as mouse astrocytes, induction of iNOS does not peak until 48 hours after stimulation (Di Rosa *et al.*, 1990; Da Silva *et al.*, 1997) while *in vivo* iNOS protein may peak within 3 hours, declining back to basal levels 24 h after stimulation (Sunday *et al.*, 2006). The reasons for these discrepancies are unclear but highlight the differences and complex nature of iNOS induction in different systems. With the rapid *in vivo* effects, it is possible that the tissues/ cells may already be primed or may have other essential components for rapid induction which are missing in the *in vitro* models.

In RASMCs two stimulants, LPS and IFN- $\gamma$  are needed for maximum iNOS induction. This may relate to the fact that LPS alone is not enough for iNOS expression and IFN- $\gamma$  is needed for iNOS mRNA stabilisation (Bergeron *et al.*, 2006; Flodstrom *et al.*, 1997; Vodovotz *et al.*, 1993). In fact LPS can induce the iNOS gene but the stability of the latter may require other elements which can be induced by IFN- $\gamma$ . By comparison, macrophages appear to require only LPS for full induction of iNOS indicating that these cells may not require IFN- $\gamma$  to stabilise the gene once induced. This area however requires further studies to fully elucidate the manner in which both message and protein expression are controlled in the two systems.

As indicated earlier, and also highlighted above, macrophages respond differently to smooth muscle cells in terms of the stimuli required for the induction of the L-arginine-NO pathway. The different stimuli used in our studies mediate different effects in the two systems with IFN- $\gamma$ , for example, failing to cause significant induction of NO synthesis when compared to LPS. Similarly, IFN- $\gamma$  caused only partial induction of iNOS mRNA expression, with transcript levels well below those seen with LPS or the combination of LPS and IFN- $\gamma$ . Worth noting is the fact that the combination did not cause much of an increase in iNOS mRNA above that seen with LPS alone strengthening the suggestion that latter is able to fully induce iNOS expression.

Apart from our data, there are several contradictory reports in the literature on the regulation of iNOS induction and NO production in different systems using either LPS and/or IFN- $\gamma$ . For instance, Hammermann *et al* (2000) have demonstrated that both LPS and IFN- $\gamma$  could independently induce expression of iNOS in rat lung macrophages but the combination of the two did not produce any additive or synergistic effects. In contrast, LPS alone (Shi *et al.*, 2006) or IFN- $\gamma$  alone (Chan *et al.*, 1998) have been shown to have little or no effect on iNOS in macrophages respectively. To further highlight these contradictions, IFN- $\gamma$  alone has been shown to induce iNOS expression in J774 macrophages (Bergeron *et al.*, 2006; Reis *et al.*, 2001) and RAW264.7 macrophages (Xiong *et al.*, 2003). Clearly the regulation of iNOS expression by inflammatory mediators is complex and effects produced may be species, cell type or even stimuli dependent. Each system should therefore be fully validated in its own right.

To determine the role of JNK/AP-1 on the induction of iNOS (and L-arginine transport), pharmacological and molecular interventions were exploited. Pharmacologically, SP600125 and JNK inhibitor VIII, which have been widely reported as being potent inhibitors of the JNK pathway, were used. SP600125, as already mentioned, is a selective and reversible inhibitor of the JNKs, inhibiting JNK-1, JNK-2 JNK-3 with relatively equal potency (IC<sub>50</sub> of 40 nM for JNK1 and 2 vs 90 nm for JNK3). It exerts its effects by inhibiting the phosphorylation of c-Jun (Bogoyevitch *et al.*, 2008). The inhibition is competitive with respect to ATP, exhibiting over 300-fold greater selectivity for JNK as compared to ERK1 and p38 MAP kinases. It is worth noting that other studies have reported that SP600125 may act on other pathways (Stempin *et al.*, 2008; Stempin *et al.*, 2004). For instance, in J774 macrophages SP600125 induces p38 MAPK phosphorylation (Stempin *et al.*, 2008). This effect is however observed at higher concentrations comparing to ours.

JNK inhibitor VIII is a cell-permeable pyridinylamide compound that also acts as an ATP-competitive, reversible inhibitor of JNK (K<sub>i</sub> = 2 nM, 4 nM and 52 nM for JNK1, 2 and 3, respectively) and displays excellent selectivity over 72 other kinases. It inhibits c-Jun phosphorylation with an IC<sub>50</sub> of 920 nM in some cell systems (Szczepankiewicz *et al.*, 2006) and at present there are no other non-selective effects reported for other pathways.

Using these inhibitors it would appear that the requirement of JNK for iNOS and CAT induction may be cell type specific since both inhibitors seem to have different effects in the different cell systems used in this thesis. SP600125 had no significant inhibitory effect on iNOS expression, NO production or L-arginine transport in smooth muscle cells; but showed a biphasic action on iNOS expression and NO

production in J774 macrophages, enhancing these processes at lower concentrations while inhibiting at higher concentrations. Transport of L-arginine however remained unaffected except at 10  $\mu$ M where induced transport rate was inhibited, suggesting that SP600125 may regulate induced but not basal/control CAT activity. In this regard experiments conducted looking at changes in CAT mRNA expression when SP600125 applied to clarify the role of JNK pathway in transport system which will discuss in chapter 4.

To ensure that the lack of effect with SP600125 in RASMCs was not simply reflective of the compound itself parallel studies were carried out using JNK inhibitor VIII, which as described above is another known selective and highly potent inhibitor the JNKs and capable of inhibiting all isoforms of the kinase. Consistent with SP600125, JNK inhibitor VIII did not cause any changes in nitric oxide production, iNOS expression or L-arginine transport in RASMCs but suppressed all three processes in J774 macrophages indicating that activation of the JNK pathway may be critical in these cells but not in the former.

At present it is not clear why SP600125 exhibited a biphasic effect in J774 macrophages. It could be speculated that the potentiation reflects the true selective inhibition of JNK since these effects were observed with low concentrations of the drug. The inhibitory effects produced at the higher concentration range may reflect actions at targets other than JNK. This would however indicate a degree of non-selectivity in the actions of SP600125 and would need further confirmation. It is worth noting however that other studies have used concentrations of SP600125 up to 50  $\mu$ M to suppress iNOS expression in Bv-2 cells (Svensson *et al.*, 2010) and in the RAW 264.7 murine macrophages (Jung *et al.*, 2007; Kim *et al.*, 2007), It is also

claimed that the inhibitions were independent of both p38 MAPK or ERKs, suggesting some degree of selectivity.

Other than differences in selectivity at the extreme concentrations, another alternative explanation for the biphasic actions of SP600125 could be that the cells express different isoforms of JNK of which one may be positively coupled to iNOS and another isoform may negatively regulate iNOS expression. Thus, inhibition of the latter would enhance LPS-induced iNOS expression while inhibition of the former would result in suppression in the induction of iNOS. Also there is a possibility that AP-1, the downstream targets for JNK, may act in a different way when JNK is inhibited in various cell system or different drugs may cause activation or suppression of different subunits of this transcription factor. This interesting speculation led us to go further and investigate the regulation by SP600125 of AP-1 and its subunits more closely and the results are discussed in chapter 5.

Biphasic responses to SP600125 have previously been reported in the macrophage cell line RAW 264 (Lahti *et al.*, 2003) where SP600125 enhanced nitrite production at 0.1  $\mu$ M but caused an inhibition at 1 $\mu$ M.

In order to conclusively confirm the role of the JNK pathway and thus AP-1 in the induction of iNOS and NO production, additional experiments were carried out using two dominant negative constructs of AP-1,  $\alpha$ -Fos and TAM-67.  $\alpha$ -Fos is a chimeric protein which belongs to a class of transcription factors containing the c-Fos leucine zipper and a designed 25 amino acid acidic protein sequence which could replace the DNA-binding region and hetero-dimerises with c-Fos dimerisation partners, to prevent AP-1 DNA binding (Gerdes *et al.*, 2006). TAM-67 is another dominant negative which blocks AP-1 activity. Deletion of the major transactivation

domain of c-Jun (amino acids 3–122) results in TAM-67 formation. However, TAM-67 does have a bZIP domain and can, therefore, dimerise with other members of the Jun and Fos families, and with other bZIP proteins. Therefore, dimers containing TAM-67 are able to bind DNA, but have little or no transactivational activity (Li *et al.*, 2000; Young *et al.*, 1999).

In this study both dominant negatives were used in RASMCs in order to establish the role of JNK and thus AP-1 in our systems. Studies in J774 macrophages have not yet been carried out as transfection of these cells appears to be more difficult, giving a very low transfection efficiency.

The transfection strategy used involved exploiting a polycationic peptide (Peptide 6) which binds DNA and introduces this into cells through specific integrin binding sites. Peptide 6 has many advantages over other transfection systems, for instance those that utilise viruses. Firstly, peptide 6 is easy to synthesise to a high degree of purity; sequences can be designed on the basis of known ligands, or new peptides can be selected for a particular cell type (Hart *et al.*, 1998).

Transfection of pGFP-a-Fos or pGFP-TAM-67 with peptide 6 caused a time dependent increase in GFP expression reaching a peak at 24 hours. However, there appear to be many dead and floating cells when the 24 h transfected cells are activated with LPS and IFN- $\gamma$  for a further 24 h. This therefore limits experiments that can be carried out in the 24 h transfected cells. To reduce the cytotoxic effect of Peptide 6 as much as possible and also have enough transfected cells before activation, a series of experiments were performed at different time point after transfection and based on the amount of GFP band and also the fact that after 24

hours the number of dead cells were increased, it was established that 18 hours after transfection may be the optimum time to activate cells.

Transfection of RASMCs with either a-Fos or TAM-67 for 18 h prior to activation modified induced iNOS expression and NO production. What is interesting is the fact that a-Fos enhanced while TAM-67 inhibited both processes. From these observations, it is likely that some components of the JNK/AP-1 pathway may down-regulate induction of iNOS and NO production under normal physiological conditions. Thus when blocked by a-Fos we get an enhancement not only in iNOS but also in NO synthesis.

TAM-67, in contrast to a-Fos, significantly reduced NO production and iNOS expression. Transport of L-arginine also declined. These observations may be of significant interest as the findings may highlight the differential regulation by the JNK/AP-1 pathway of the expression of the inducible L-arginine-NO pathway. It is not unreasonable to hypothesise that proteins targeted by a-Fos down-regulate while those targeted by TAM-67 up-regulate expression of iNOS and CATs. Thus inhibition of one enhances while inhibition of the other decreases NO synthesis and L-arginine transport. This hypothesis was further investigated by examining changes in AP-1 subunit activity in cell transfected with these dominant negatives in parallel with those treated with SP600125 in chapter 5.

One other alternative explanation that could account for the actions of TAM-67 is the fact that it may interact with bind the p65 subunit of NF- $\kappa$ B and in doing so inhibit NF- $\kappa$ B (Young *et al.*, 1999; Young *et al.*, 2003) which is reported to be critical for the induction of iNOS (Goldring *et al.*, 1995; Kone *et al.*, 1995; Xie *et al.*, 1994). This novel action of TAM-67 however remains to be confirmed in our cell system.

Not only TAM-67 but even c-Jun has been shown to interact with the p65 subunit of NF- $\kappa$ B to enhance binding to  $\kappa$ B and AP-1 sites (Stein *et al.*, 1993; Smith *et al.*, 1999).

The NF- $\kappa$ B family contains five members; p105 (constitutively processed to p50), p100 (processed to p52 under tightly regulated conditions), p65 (also known as Rel A), Rel B and c-Rel. These NF- $\kappa$ B subunits form homodimers and heterodimers to make NF- $\kappa$ B transcription factors (Simmonds *et al.*, 2008; Uwe Reuter *et al.*, 2002). These subunits may be able to cross-talk with AP-1 subunits or with the dominant negatives of AP-1.

Consistent with a role for NF- $\kappa$ B, previous work has shown that the three non-consensus AP-1 sites in the 5'-flanking region of the iNOS promoter were not involved in enhancing iNOS transcription by LPS (Lowenstein *et al.*, 1993; Xie *et al.*, 1992). It is instead suggested that an alternative transcription factor, NF- $\kappa$ B, may be the critical regulator of iNOS transcription induced by LPS. Moreover, JNK has been shown to bind the c-Rel component of NF- $\kappa$ B and to enhance NF- $\kappa$ B activation (Meyer *et al.*, 1996). Although DBD-c-Jun would be expected to inhibit AP-1 activity, it is not known whether it would also be capable of inhibiting any NF- $\kappa$ B-c-Jun interaction, because the mutated c-Jun still contains the bZIP region that is capable of binding the p65 subunit (Li *et al.*, 2000; Stein *et al.*, 1993; Young *et al.*, 1999).

More specifically in the smooth muscle cells, there is no clear evidence confirming that JNK/AP-1 has effect on iNOS induction; however it has been suggested that NF- $\kappa$ B activation alone is not sufficient for complete induction of iNOS. NF- $\kappa$ B activity was induced by TNF- $\alpha$  (Tumour necrosis factor- $\alpha$ ), but TNF- $\alpha$  alone cannot induce

iNOS promoter activity, protein expression, or nitrite production (Perrella *et al.*, 1996; Zhang *et al.*, 2000). It is clear that further work looking at possible cross-talk between JNK and NF- $\kappa$ B in inducing iNOS and/or L-arginine transport in our cell systems is required.

To confirm that the inhibitors and dominant negatives of the AP-1 pathway regulate iNOS induction, additional studies were carried out examining changes in gene expression. The data confirm that in smooth muscle cells, SP600125 caused no significant change in mRNA or protein level. On the other hand in macrophages, higher concentration of SP600125 down regulated iNOS mRNA levels which is in agreement with the data on protein expression. The dominant negatives also exhibited the same effect on gene induction as those seen on protein level. a-Fos caused up-regulation while TAM-67 decreased iNOS transcript levels.

### 3.5 Summary

Taken together our data demonstrate the regulation of the expression profile of iNOS gene and protein, as well as nitric oxide production and L-arginine transport by LPS and IFN- $\gamma$  in both RASMCs and J774 macrophages. Of importance is the fact that these were regulated differently in the two cell systems in terms of the stimulus needed and of the potential cellular events that lead to the inductions. In RASMCs, both LPS and IFN- $\gamma$  are required while in the macrophages only LPS was essential. Moreover, IFN- $\gamma$  even when added was without significant effect when compared to LPS. In RASMCs, the induction of iNOS and NO synthesis was insensitive to pharmacological inhibition while sensitive to AP-1 dominant negatives. Even with these constructs the effects produced varied and was dependent on the dominant negative used. TAM-67 which inhibits c-Jun activation partially blocked enzyme protein and mRNA expression while a-Fos which blocks c-Fos enhanced both processes. In J774 macrophages the pharmacological inhibitors did show their inhibitory effects and confirm the role of JNK/AP-1 in these cells. All the data obtained, reveal a different regulation mechanism in various cell systems. The importance of these observations is further discussed in Chapter 5 and the findings in their entirety put into context to explain these divergent actions.

# Results

## **Chapter 4**

**The expression profile of Cationic Amino acid Transporters and their regulation by JNK/AP-1 inhibition**

## 4.1 Introduction

This chapter has focused on establishing the profile of expression of CATs in RASMCs and J774 macrophages and has further explored how the induction of these proteins may be regulated by SP600125,  $\alpha$ -Fos or TAM-67 at the transcriptional level. These studies parallel those on iNOS mRNA expression described in Chapter 3 and should further shed light on the transporters that may be involved with L-arginine entry and thus substrate supply for iNOS in the two cell types.

As highlighted in the main introductory chapter, L-arginine uptake into cells may be mediated by several different carrier proteins of which the CATs may be the most predominant. While CAT-2A is generally associated with uptake of cationic amino acids (CAAs) into the liver (where it functions to pool these amino acids into the liver after meals), CAT-1 has often been known as the key physiological transporter of the CAAs within the vasculature; with CAT-2B associated with L-arginine uptake into cell under pathological/inflammatory conditions. Indeed, there was a consensus that CAT-1 is ubiquitous while CAT-2B may only be expressed in select cells and tissues following exposure to pro-inflammatory mediators. Previous studies in our group have, however, revealed the presence of all three cationic amino acid transporters (CAT-1, 2A and 2B) in control RASMCs (Baydoun *et al.*, 1999), suggesting that these transporters may be present as a family within the same cell systems under normal physiological conditions. Whether they respond in the same way to stimulation by inflammatory mediators or whether the induction of their respective genes occurs in a similar manner remains to be elucidated. Studies described in this chapter were therefore aimed at addressing these issues, at least

in part, by exploring how transcripts for each protein may be regulated by LPS and IFN- $\gamma$  and by inhibitors of the JNK/AP-1 pathway.

## **4.2 Methods**

### **4.2.1 Time course of CAT gene expression in RASMCs and J774 macrophages**

Cells were cultured to confluency in T-25 flasks and treated either with LPS ( $100 \mu\text{g ml}^{-1}$ ) / IFN- $\gamma$  ( $100 \text{ U ml}^{-1}$ ) (RASMCs) or LPS ( $1 \mu\text{g ml}^{-1}$ ) alone (J774 macrophages) for periods of 3, 6, 12, 18 and 24 hours. Control cells were incubated with complete culture medium alone. Total RNA was subsequently extracted, cDNAs generated using RT-PCR reaction and qPCR performed using  $1 \mu\text{g/ml}$  of cDNA template, employing CAT-1, CAT-2A or CAT-2B specific primers (Tables 2.1 and 2.2). Expression of RPL-13 or GAPDH was also determined using its specific primers and these were used to standardise the loading and expression levels of the CATs in RASMCs and J774 macrophages respectively.

### **4.2.2 Effect of different stimuli on CAT gene expression in J774 macrophages**

Confluent monolayers of J774 macrophages in T-25 culture flasks were incubated for 18 hours with either LPS ( $1 \mu\text{g ml}^{-1}$ ), IFN- $\gamma$  ( $1 \text{ U ml}^{-1}$ ) or LPS plus IFN- $\gamma$  together. Changes in CAT-1, CAT-2A or CAT-2B expression were determined on isolated RNA by qPCR analysis using individual CAT specific primers (Tables 2.1 and 2.2).

#### **4.2.3 Effect of SP600125 on CAT gene expression in RASMCs and J774 macrophages**

Confluent monolayers of cells were treated with SP600125 (0.3 and 3  $\mu\text{M}$ ) for 30 min prior to an 18 hour activation with LPS (100  $\mu\text{g ml}^{-1}$ ) and IFN- $\gamma$  (100 U  $\text{ml}^{-1}$ ) for RASMCs or LPS (1  $\mu\text{g ml}^{-1}$ ) for macrophages. The control cells were incubated in complete culture medium in the absence and presence of SP600125 for the same period of time but without activation with LPS and IFN- $\gamma$ . The incubations were terminated at the end of this period, total RNA extracted and analysed using CAT-1, CAT-2A or CAT-2B specific primers in the qPCR reaction.

#### **4.2.4 Effect of a-Fos and TAM-67 on CAT gene expression in RASMCs**

To determine the effect of AP-1 dominant negative construct on CATs expression in the RASMCs, the cells were cultured in T-25 cultured flask to partial confluency (60-70%) before being transfected with pGFP-aFos or pGFP-TAM-67 for 18 hours and then activated with LPS (100  $\mu\text{g ml}^{-1}$ ) and IFN- $\gamma$  (100 U  $\text{ml}^{-1}$ ) for a further 18 hours. The total RNA was extracted and analysed using CAT-1, CAT-2A or CAT-2B specific primers in a qPCR reaction.

## 4.3 Results

### 4.3.1 Time course of CAT mRNA expression induced by LPS and IFN- $\gamma$ in RASMCs

Time course of CAT mRNA induction was conducted in parallel with the studies on iNOS gene expression. Changes in CATs expression were determined on isolated total RNA by qPCR analysis using CAT specific primers (Tables 2.1 and 2.2). The association curve for primers shows the melting temperature for each primer and also revealed if there is just one product in the PCR. Figure 4.1 revealed different melting temperature for each CAT primers which were: 81.5°C for CAT-1 (panel A), 81°C for CAT-2A (Panel B) and 77.5°C for CAT-2B (Panel C). Moreover, there was only the existence of one detectable peak in the association curves, confirming the existence of just one PCR product.

Figure 4.2 demonstrate that after stimulation with LPS and IFN- $\gamma$ , there was a reduction in CAT-1 expression, which was evident as early as 3h reaching a minimum level at 12 hours and staying reduced over 24 hours in the continued presence of LPS. In contrast, mRNA expression of CAT-2A and CAT-2B increased following LPS stimulation. Interestingly, the CAT-2A gene increased only marginally (less than 2 Fold increase) (Figure 4.3) while CAT-2B mRNA increased significantly after 6 hours, reaching a peak of about 14 fold increase above basal levels at 18 hours and remaining at the elevated level over 24 hours of induction (Figure 4.4). These findings confirm that CAT-2B may be the main transporter of L-arginine in the

induced cells and this could potentially also be the case in inflammatory condition where iNOS and L-arginine transport are induced.

#### **4.3.2 Time course of CAT mRNA expression induced by LPS in J774 macrophages**

As with the RASMCs, time course of CAT mRNA induction was conducted in parallel with the studies for iNOS in J774 macrophages. Figure 4.5 is the association curve confirming the presence of just one product for each primer (Panel A for CAT-1; Panel B for CAT-2A; Panel C for CAT-2B). It also reveals a different melting temperature for each CAT primer which were: 86°C for CAT-1, 80.5°C for CAT-2A and 78°C for CAT-2B.

Figures 4.6 to 4.8 demonstrate the trends for CAT expression in time point assays and reveal that CAT-1 mRNA was not significantly altered by incubations with LPS over the time course studied (Figure 4.6). In contrast, both CAT-2A and CAT-2B transcripts were significantly elevated by LPS from 3 hours onwards reaching peak expression after 24 hours of induction (Figure 4.7 and 4.8). Worth noting is the fact that in these cells induction of CAT-2A was much higher (80 Fold above basal; Figure 4.7) than that seen for CAT-2B which was only elevated 30 fold above the basal control levels (Figure 4.8).

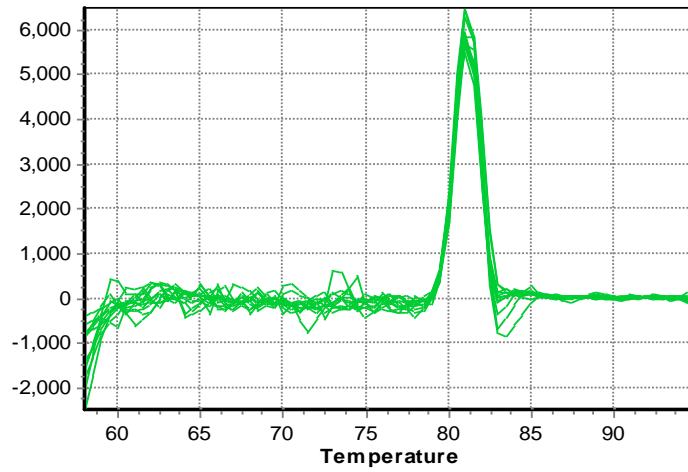
### **4.3.3 Effect of different stimuli on CATs mRNA expression in J774 macrophages**

To verify whether different stimuli show varying profiles of CAT gene expression in J774 macrophages, the cells were incubated for 18 hours with either LPS ( $1 \mu\text{g ml}^{-1}$ ), IFN- $\gamma$  ( $1 \text{ U ml}^{-1}$ ) or LPS plus IFN- $\gamma$  together. The total RNA isolated was subjected to qPCR analysis using specific primer for each CAT. As shown in Figure 4.9 Panel A, after stimulation with LPS, there was no significant changes in the CAT-1 gene expression and this trend was the same when IFN- $\gamma$  was used independently. The combination of both also failed to cause any changes in the CAT-1 gene expression levels. Panels B and C reveal that while LPS, as already reported above, was able to enhance CAT-2A and CAT-2B mRNA expression, IFN- $\gamma$  alone failed to cause significant changes in CAT-2A mRNA but enhanced that for CAT-2B by approximately 10 % of the levels caused by LPS or the combination of both LPS and IFN- $\gamma$  (Figure 4.9).

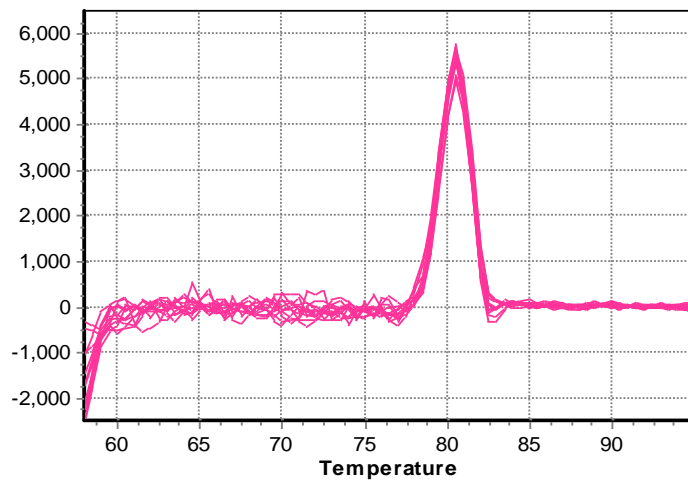
**Figure 4.1 Representative association curves for CAT-1, CAT-2A and CAT-2B**

Using a specific primer for each cationic amino acid transporters in RASMCs, qPCR was conducted and association curves obtained. Each product has its specific melting temperature which also indicates the existence of just one product. Panel A reveals the melting temperature for CAT-1, Panel B for CAT-2A and Panel C for CAT-2B.

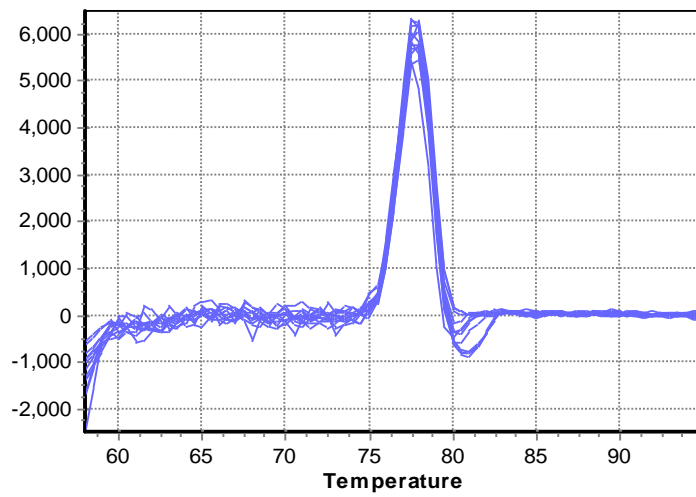
(A)



(B)



(C)



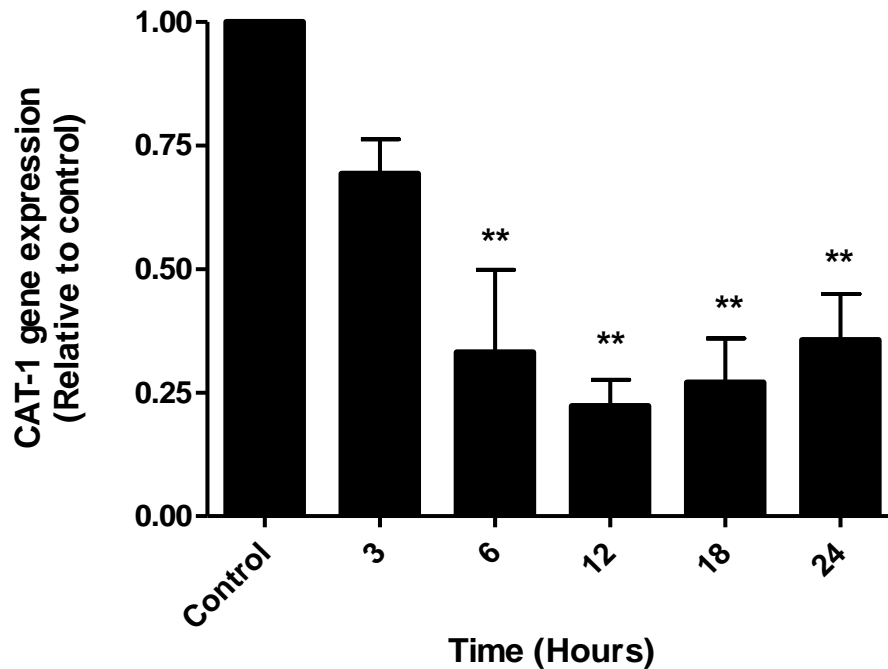


**Figure 4.2 CAT-1 gene expression profile in RASMCs following treatment with LPS and IFN- $\gamma$**

Confluent monolayer of RASMCs were stimulated with LPS ( $100 \mu\text{g ml}^{-1}$ ) and IFN- $\gamma$  ( $100 \text{ U ml}^{-1}$ ) for different time periods. Total RNA was isolated from cells and the cDNA prepared before analysing by quantitative PCR using CAT-1 specific primers. The graph reflects fold changes in CAT-1 level in activated cells compared to control. Expression of RPL-13 was also determined and used to standardise the loading and expression levels of CAT-1. The data is the mean  $\pm$  SEM of three separate experiments. Statistical analysis was carried out using a one way Anova followed by Dunnett's multiple comparison test. \*\* $p < 0.01$  compared to control, non-activated results.

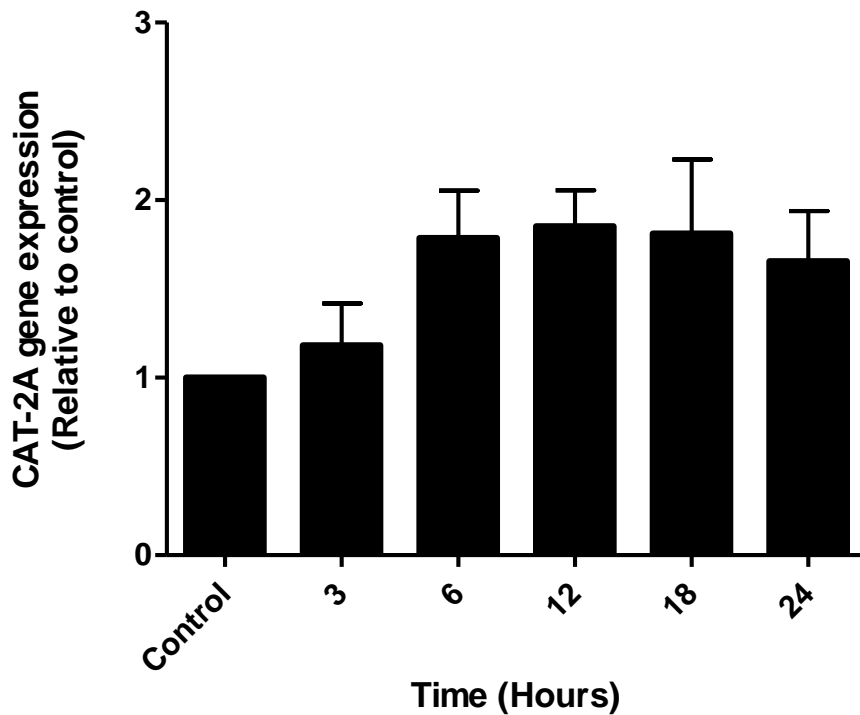


**Figure 4.3 Time course of CAT-2A gene expression induced by LPS and IFN- $\gamma$  in RASMCs**

Confluent monolayer of RASMCs were stimulated with LPS ( $100 \mu\text{g ml}^{-1}$ ) and IFN- $\gamma$  ( $100 \text{ U ml}^{-1}$ ) for different time periods. Total RNA was isolated from cells and the cDNA prepared before analysing by quantitative PCR using CAT-2A specific primers. The graph reflects fold changes in CAT-2A level in activated cells compared to control. Expression of RPL-13 was also determined and used to standardise the loading and expression levels of CAT-2A. The data is the mean  $\pm$  SEM of three separate experiments.

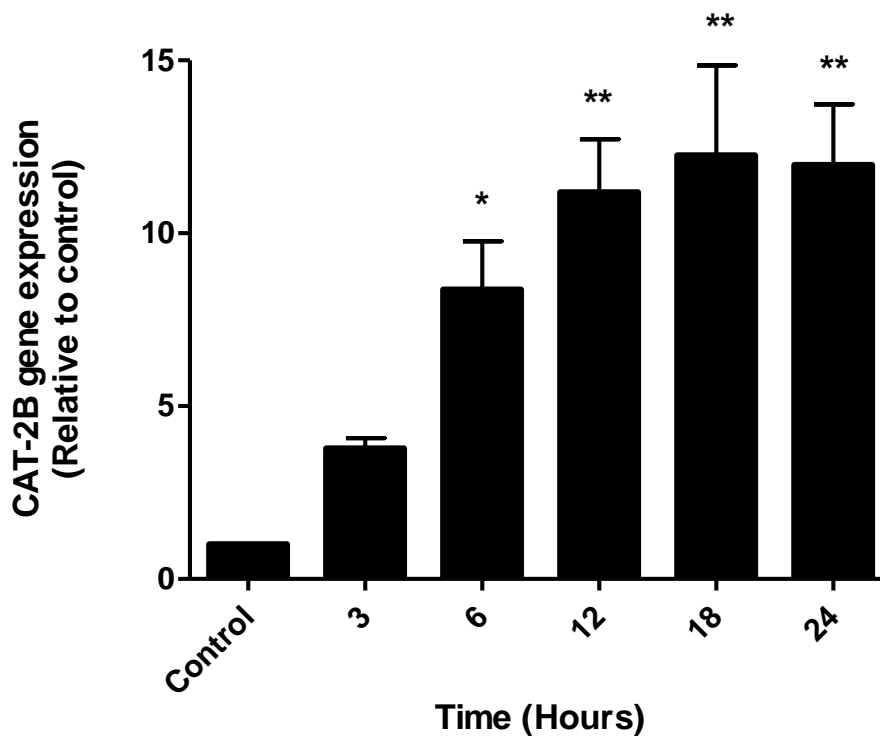
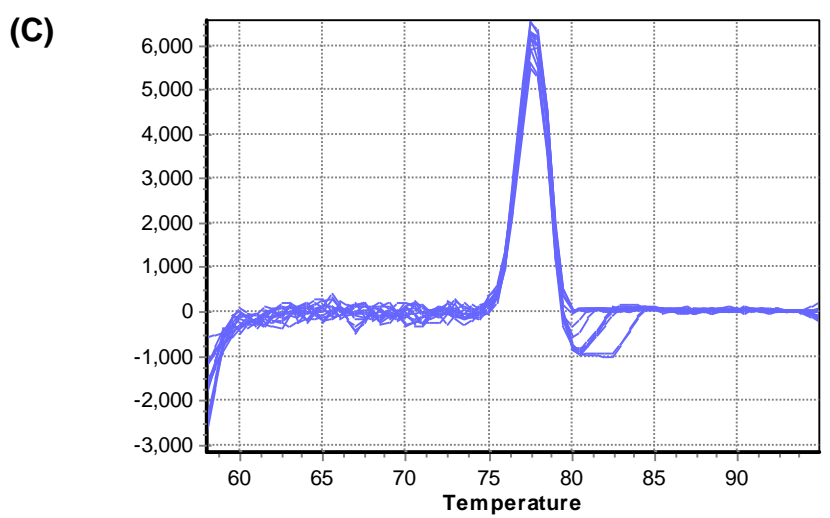
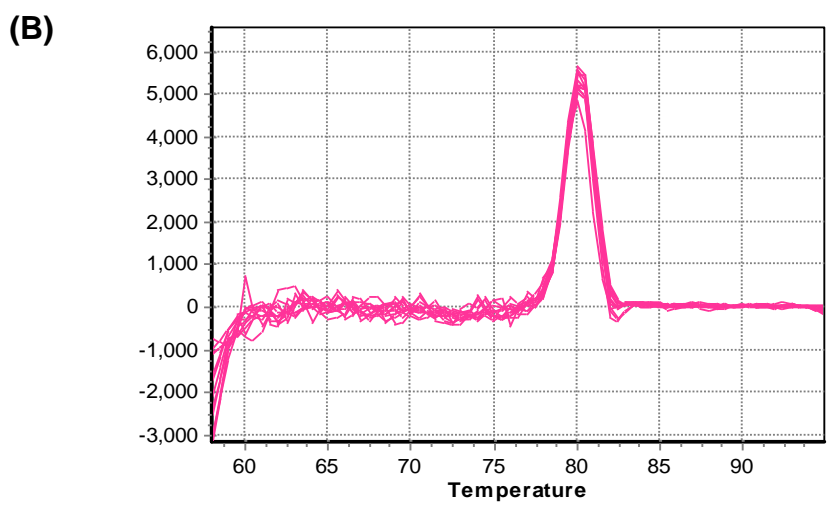
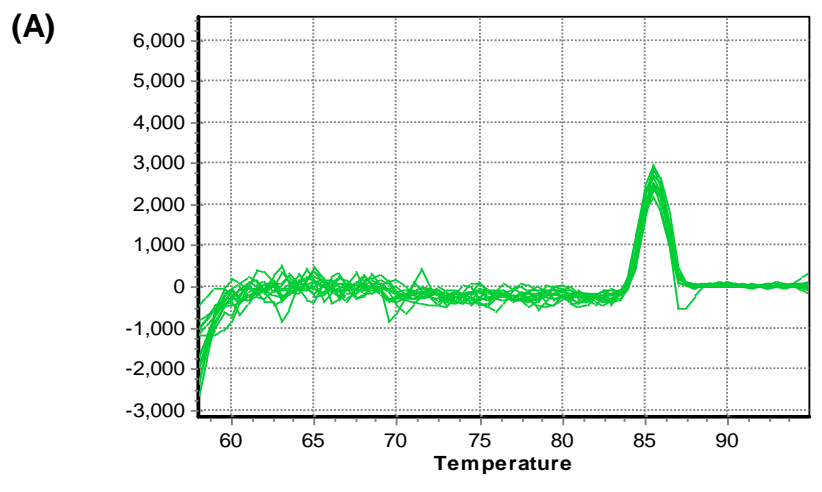


**Figure 4.4 Time course of CAT-2B gene expression induced by LPS and IFN- $\gamma$  in RASMCs**

Confluent monolayer of RASMCs were stimulated with LPS ( $100 \mu\text{g ml}^{-1}$ ) and IFN- $\gamma$  ( $100 \text{ U ml}^{-1}$ ) for different time periods. Total RNA was isolated from cells and the cDNA prepared before analysing by quantitative PCR using CAT-2B specific primers. The graph reflects fold changes in CAT-2B level in activated cells compared to control. Expression of RPL-13 was also determined and used to standardise the loading and expression levels of CAT-2B. The data is the mean  $\pm$  SEM of three separate experiments. Statistical analysis was carried out using a one way Anova followed by Dunnett's multiple comparison test. \* $p < 0.05$  and \*\* $p < 0.01$  compared to control, non-activated results.

**Figure 4.5 Representative association curves for CAT-1, CAT-2A and CAT-2B**

Using a specific primer for each cationic amino acid transporters in J774 macrophages, qPCR was conducted and association curves obtained. Each product has its specific melting temperature which also indicates the existence of just one product. Panel A reveals the melting temperature for CAT-1, Panel B for CAT-2A and Panel C for CAT-2B.



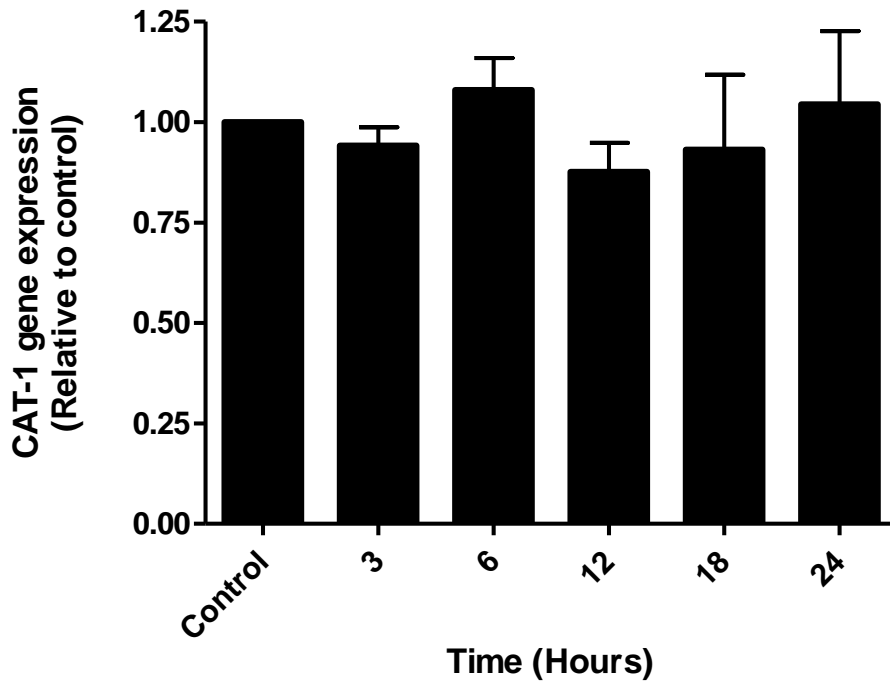


**Figure 4.6 CAT-1 gene expression profile in J774 macrophages following treatment with LPS**

Confluent monolayer of J774 macrophages were stimulated with LPS ( $1 \mu\text{g ml}^{-1}$ ) for different time periods. Total RNA was isolated from cells and the cDNA prepared before analysing by quantitative PCR using CAT-1 specific primers. The graph reflects fold changes in CAT-1 level in activated cells compared to control. Expression of GAPDH was also determined and used to standardise the loading and expression levels of CAT-1. The data is the mean  $\pm$  SEM of three separate experiments. Statistical analysis was carried out using a one way Anova followed by Dunnett's multiple comparison test.

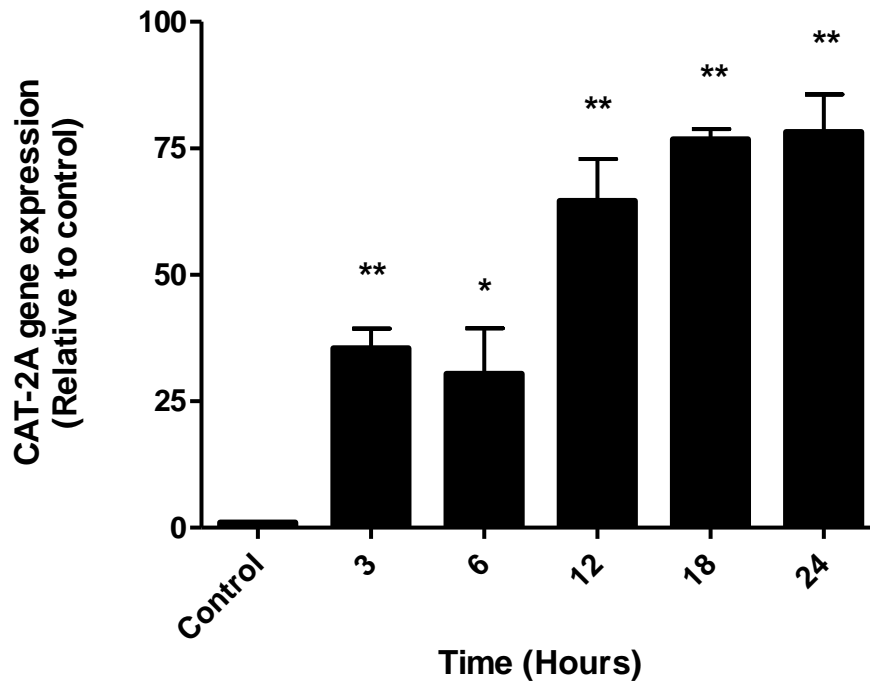


**Figure 4.7 CAT-2A gene expression profile in J774 macrophages following treatment with LPS**

Confluent monolayer of J774 macrophages were stimulated with LPS ( $1 \mu\text{g ml}^{-1}$ ) for different time periods. Total RNA was isolated from cells and the cDNA prepared before analysing by quantitative PCR using CAT-2A specific primers. The graph reflects fold changes in CAT-2A level in activated cells compared to control. Expression of GAPDH was also determined and used to standardise the loading and expression levels of CAT-2A. The data is the mean  $\pm$  SEM of three separate experiments. Statistical analysis was carried out using a one way Anova followed by Dunnett's multiple comparison test. \* $p < 0.05$  and \*\* $p < 0.01$  compared to control, non-activated results.

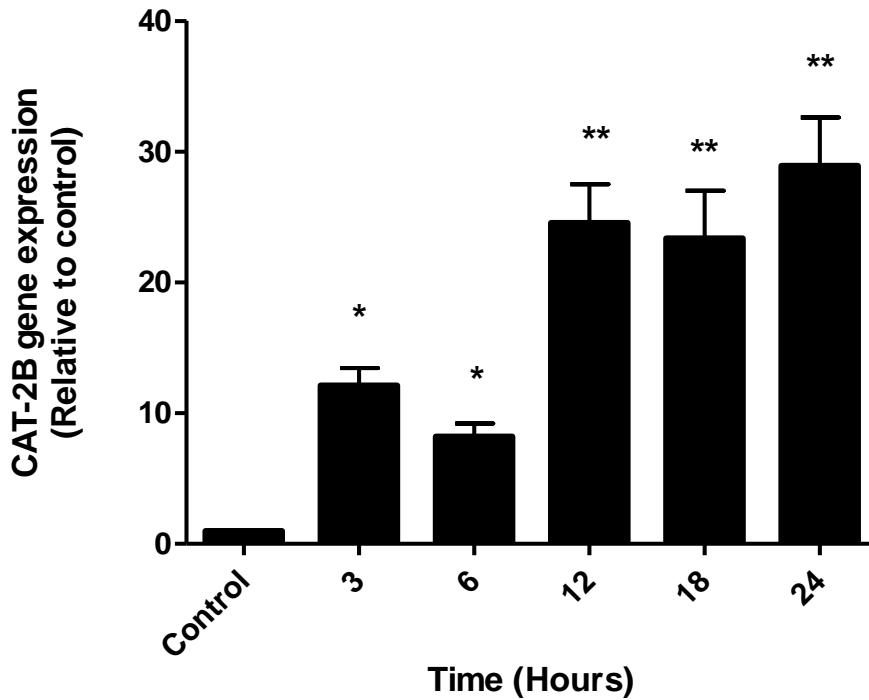
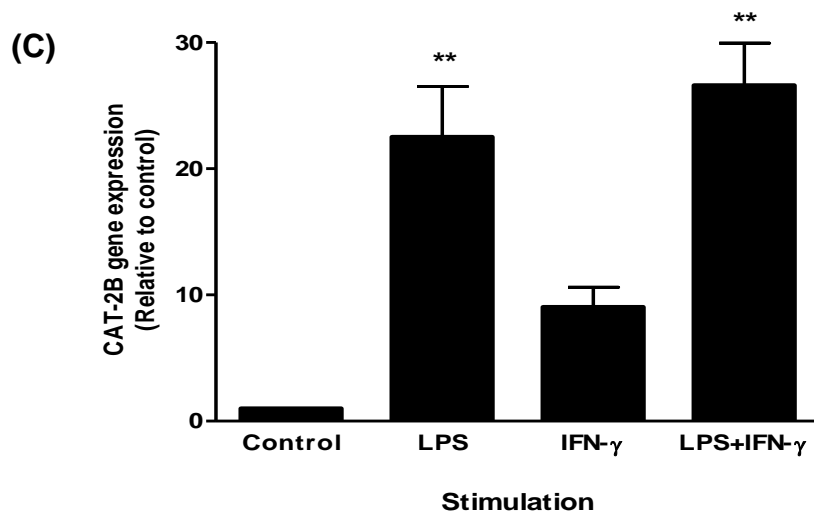
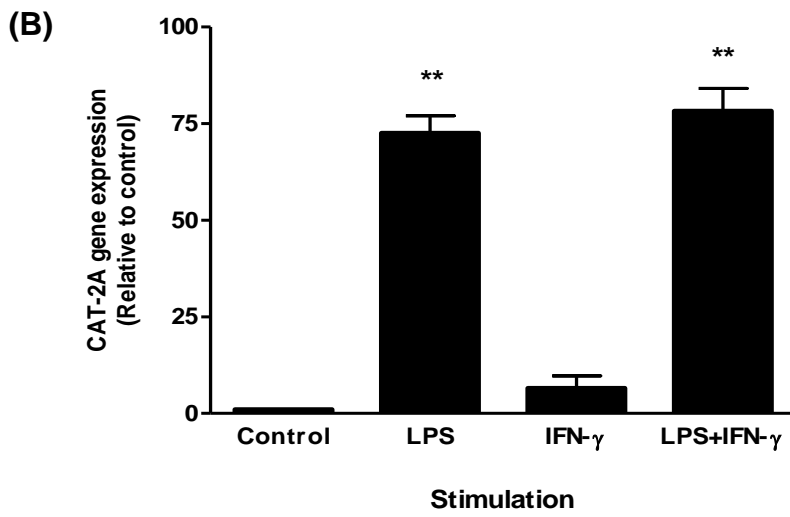
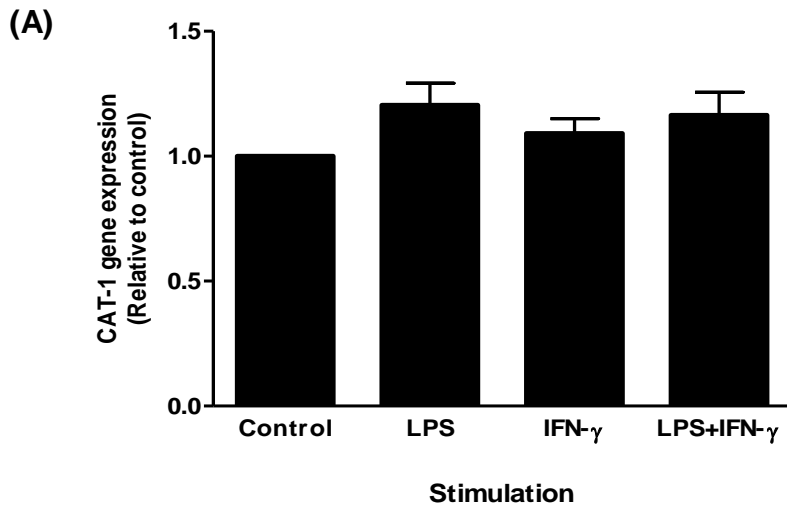


**Figure 4.8 CAT-2B gene expression profile in J774 macrophages following treatment with LPS**

Confluent monolayer of J774 macrophages were stimulated with LPS ( $1 \mu\text{g ml}^{-1}$ ) for different time periods. Total RNA was isolated from cells and the cDNA prepared before analysing by quantitative PCR using CAT-2B specific primers. The graph reflects fold changes in CAT-2B level in activated cells compared to control. Expression of GAPDH was also determined and used to standardise the loading and expression levels of CAT-2B. The data is the mean  $\pm$  SEM of three separate experiments. Statistical analysis was carried out using a one way Anova followed by Dunnett's multiple comparison test. \* $p < 0.05$  and \*\* $p < 0.01$  compared to control, non-activated results.

**Figure 4.9 Effect of different stimuli on CAT gene expression in J774 macrophages**

Confluent monolayers of J774 macrophages were incubated with either LPS ( $1 \mu\text{g ml}^{-1}$ ), IFN- $\gamma$  ( $1 \text{ U ml}^{-1}$ ) or a combination of both for 18 hours. RNA was generated at the end of the incubation period and the cDNA prepared before analysing by quantitative PCR using CAT-1 (panel A), CAT-2A (panel B) or CAT-2B (panel C) specific primers. Expression of GAPDH was also determined and used to standardise the loading and expression levels of CATs. The data is the mean  $\pm$  SEM of three separate experiments. Statistical analysis was carried out using a one way Anova followed by Dunnett's multiple comparison test. \*\* $p < 0.01$  compared to control, non-activated results.



#### **4.3.4 Effect of SP600125 on CAT gene expression in RASMCs and J774 macrophages**

To determine the effect of JNK inhibition on CAT mRNA expression, both RASMCs and J774 macrophages were incubated with two different concentrations of SP600125 (0.3 and 3  $\mu\text{M}$ ) for 30 min prior to stimulation with LPS (100  $\mu\text{g ml}^{-1}$ ) and IFN- $\gamma$  (100 U  $\text{ml}^{-1}$ ) or LPS (1  $\mu\text{g ml}^{-1}$ ) for RASMCs and J774 macrophages respectively. The total RNA was extracted and the cDNA prepared by reverse transcription before subjecting to quantitative PCR analysis using CAT specific primers. In RASMCs, stimulation with LPS and IFN- $\gamma$  caused a reduction in the CAT-1 gene expression as already reported earlier but of importance is the fact that SP600125 did not cause any significant changes to transcript levels in control or activated cells at both 0.3  $\mu\text{M}$  and 3  $\mu\text{M}$  (Figure 4.10). Although there appeared to be a marginal increase with 0.3  $\mu\text{M}$  this was statistically not significant. Similarly, SP600125 did not alter CAT-2A or CAT-2B mRNA expression either in controls or in LPS and IFN- $\gamma$  treated cells (Figure 4.11 and Figure 4.12). In J774 macrophages neither CAT-1 (Figure 4.13) nor CAT-2A (Figure 4.14) mRNA levels were affected by SP600125 (0.3-3  $\mu\text{M}$ ) in control and activated cells. In contrast CAT-2B mRNA induction was suppressed by approximately 34 % at 3  $\mu\text{M}$  SP600125 (Figure 4.15).

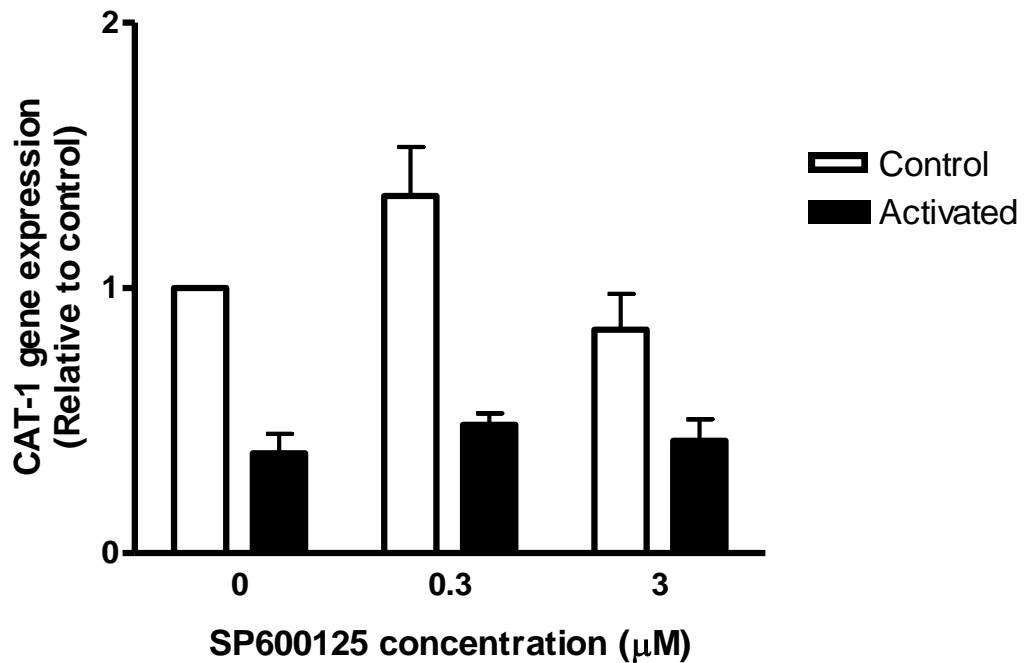


**Figure 4.10 Effect of SP600125 on CAT-1 expression in RASMCs**

Confluent monolayers of RASMCs were incubated with SP600125 (0.3-3 µM) for 30 min followed by activation with LPS (100 µg ml<sup>-1</sup>) and IFN-γ (100 U ml<sup>-1</sup>) for a further 18 hours. The controls were in the absence and presence of SP600125 without stimulation with LPS/IFN-γ. The total RNA was extracted and the cDNA prepared by reverse transcription before subjecting to quantitative PCR analysis using CAT-1 specific primer. Expression of RPL-13 was also determined and used to standardise the loading and expression levels of CAT-1. The data is the mean ± SEM of three separate experiments. Each control and activated group was analysed separately using one-way ANOVA.

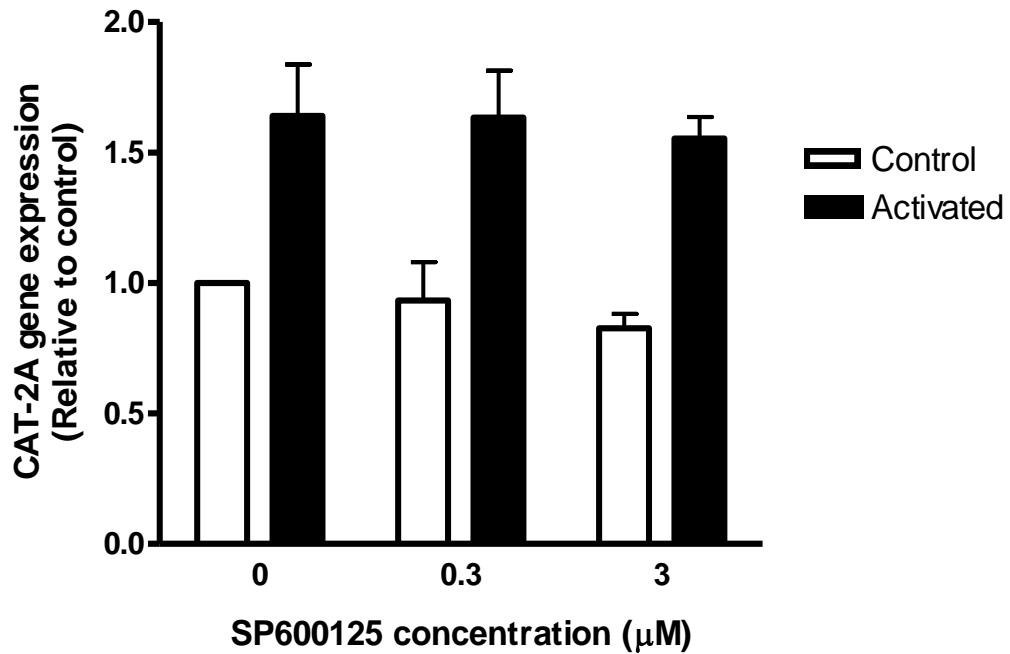


**Figure 4.11 Effect of SP600125 on CAT-2A expression in RASMCs**

Confluent monolayers of RASMCs were incubated with SP600125 (0.3-3 µM) for 30 min followed by activation with LPS (100 µg ml<sup>-1</sup>) and IFN-γ (100 U ml<sup>-1</sup>) for a further 18 hours. The controls were in the absence and presence of SP600125 without stimulation with LPS/IFN-γ. The total RNA was extracted and the cDNA prepared by reverse transcription before subjecting to quantitative PCR analysis using CAT-2A specific primers. Expression of RPL-13 was also determined and used to standardise the loading and expression levels of CAT-2A. The data is the mean ± SEM of three separate experiments. Each control and activated group was analysed separately using a one-way ANOVA.

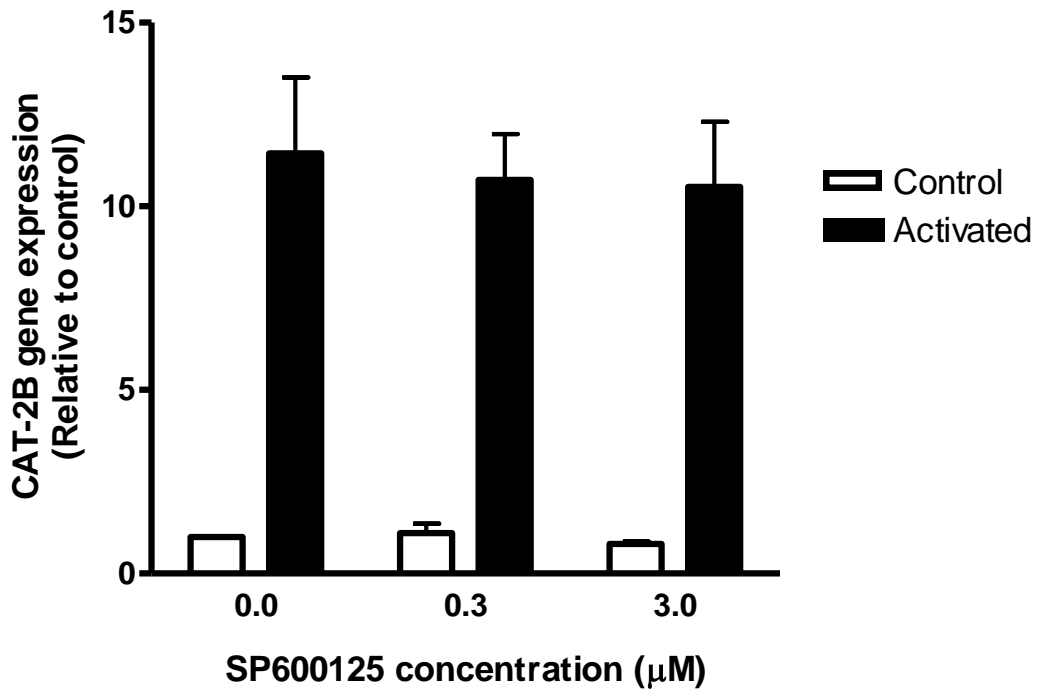


**Figure 4.12 Effect of SP600125 on CAT-2B expression in RASMCs**

Confluent monolayers of RASMCs were incubated with SP600125 (0.3-3 µM) for 30 min followed by activation with LPS (100 µg ml<sup>-1</sup>) and IFN-γ (100 U ml<sup>-1</sup>) for a further 18 hours. The controls were in the absence and presence of SP600125 without stimulation with LPS/ IFN-γ. The total RNA was extracted and the cDNA prepared by reverse transcription before subjecting to quantitative PCR analysis using CAT-2B specific primers. Expression of RPL-13 was also determined and used to standardise the loading and expression levels of CAT-2B. The data is the mean ± SEM of three separate experiments. Each control and activated group was analysed separately using a one-way ANOVA.

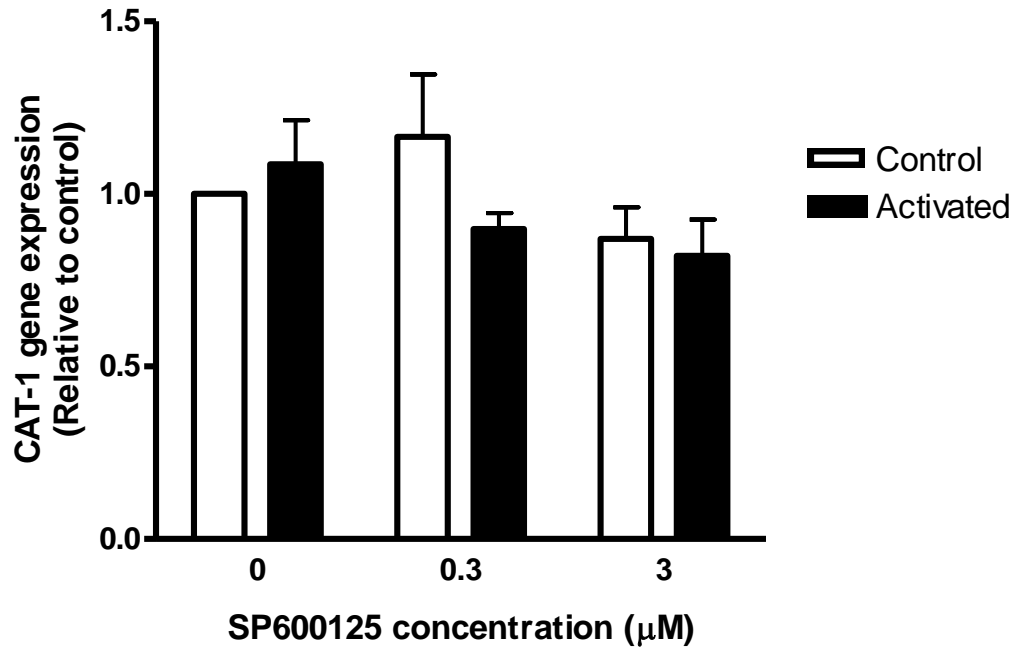


**Figure 4.13 Effect of SP600125 on CAT-1 expression in J774 macrophages**

Confluent monolayers of J774 macrophages were incubated with SP600125 (0.3-3 µM) for 30 min followed by activation with LPS ( $1 \mu\text{g ml}^{-1}$ ) for a further 18 hours. The controls were in the absence and presence of SP600125 without stimulation with LPS/IFN- $\gamma$ . The total RNA was extracted and the cDNA prepared by reverse transcription before subjecting to quantitative PCR analysis using CAT-1 specific primer. Expression of GAPDH was also determined and used to standardise the loading and expression levels of CAT-1. The data is the mean  $\pm$  SEM of three separate experiments. Each control and activated group was analysed separately using a one-way ANOVA.

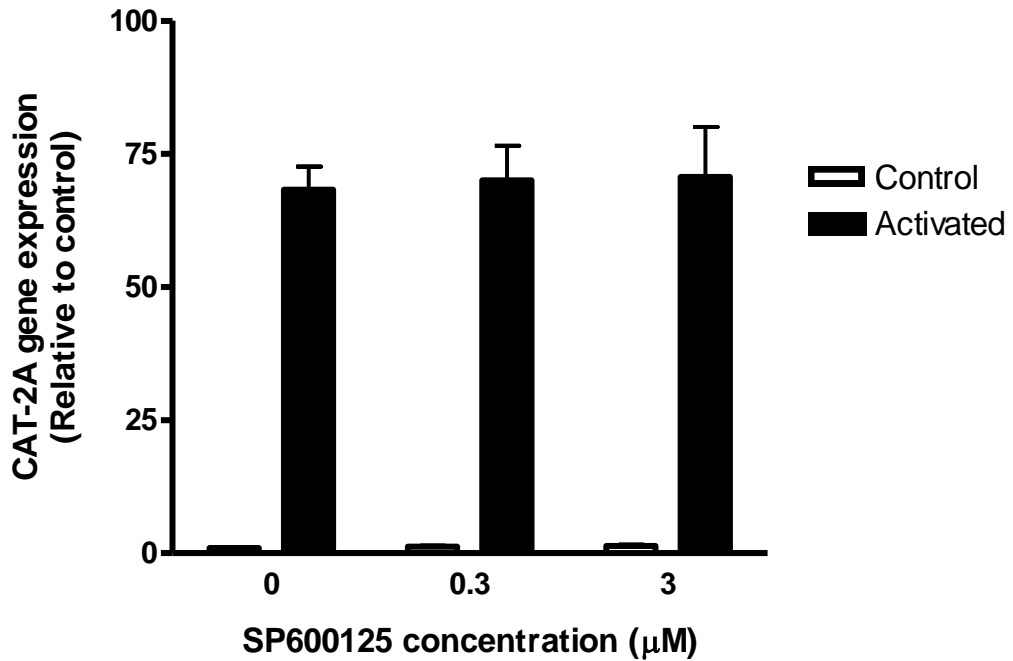


**Figure 4.14 Effect of SP600125 on CAT-2A expression in J774 macrophages**

Confluent monolayers of J774 macrophages macrophages were incubated with SP600125 (0.3-3 µM) for 30 min followed by activation with LPS (1 µg ml<sup>-1</sup>) for a further 18 hours. The controls were in the absence and presence of SP600125 without stimulation with LPS/IFN-γ. The total RNA was extracted and the cDNA prepared by reverse transcription before subjecting to quantitative PCR analysis using CAT-2A specific primer. Expression of GAPDH was also determined and used to standardise the loading and expression levels of CAT-2A. The data is the mean ± SEM of three separate experiments. Each control and activated group was analysed separately using a one-way ANOVA.

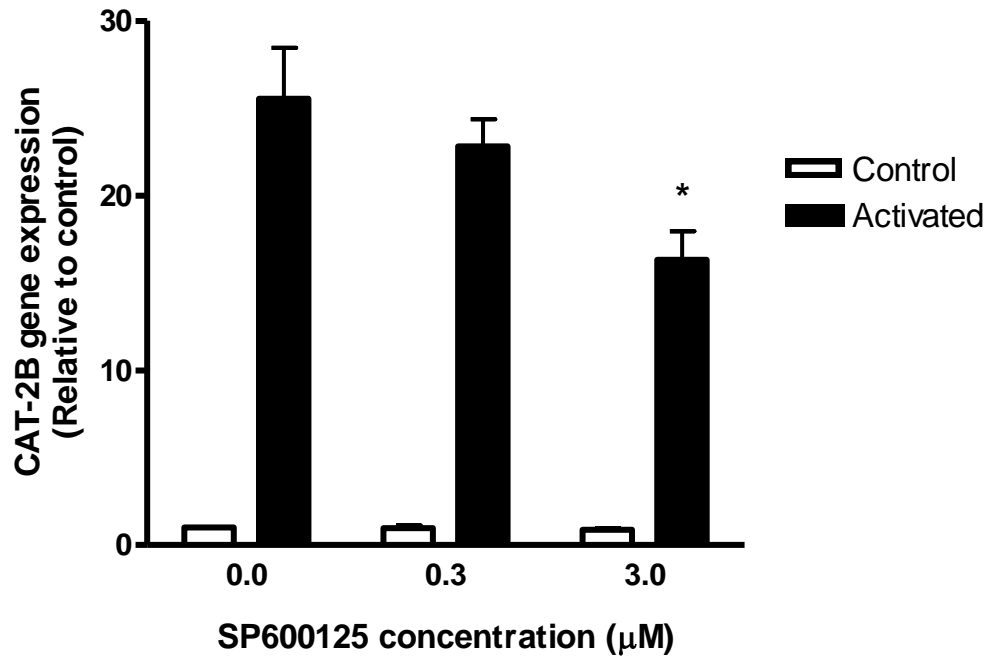


**Figure 4.15 Effect of SP600125 on CAT-2B expression in J774 macrophages**

Confluent monolayers of J774 macrophages macrophages were incubated with SP600125 (0.3-3 µM) for 30 min followed by activation with LPS ( $1 \mu\text{g ml}^{-1}$ ) for a further 18 hours. The controls were in the absence and presence of SP600125 without stimulation with LPS/IFN- $\gamma$ . The total RNA was extracted and the cDNA prepared by reverse transcription before subjecting to quantitative PCR analysis using CAT-2B specific primer. Expression of GAPDH was also determined and used to standardise the loading and expression levels of CAT-2B. The data is the mean  $\pm$  SEM of three separate experiments. Each control and activated group was analysed separately using a one-way ANOVA. \* $p < 0.05$  compared to activated, non SP600125 results.

#### 4.3.5 Effect of a-Fos and TAM-67 on CAT gene expression in RASMCs

To determine the effect of the AP-1 dominant negative construct on CAT mRNA expression in RASMCs, cells were transfected with pGFP-a-Fos or pGFP-TAM-67 for 18 hours prior to activation with LPS ( $100 \mu\text{g ml}^{-1}$ ) and IFN- $\gamma$  ( $100 \text{ U ml}^{-1}$ ) for a further 18 hours. The RNA was extracted and the cDNA prepared by reverse transcription before subjecting to qPCR analysis applying specific CAT primers. Figure 4.16 reveals the effect of a-Fos (panel A) and TAM-67 (panel B) on CAT-1 expression. Consistent with the findings above, activated cells expressed less amount of CAT-1 compared to controls and these trends were not altered by either a-Fos (Figure 4.16, panel A) or TAM-67 (Figure 4.16, panel B) were the levels of expression changed. Similarly, CAT-2A mRNA in control and activated cells was also unaffected by transfection with either a-Fos (Figure 4.17, panel A) or TAM-67 (Figure 4.17, panel B). CAT-2B which is highly expressed when cells were activated with LPS and IFN- $\gamma$  was not affected by transfection with a-Fos (Figure 4.18, panel A), but suppressed following transfections with TAM-67. This was however only evident in activated cells and was not statistically significant when compared to the non transfected cells (Figure 4.18, panel B).

#### **Figure 4.1 Effect of a-Fos and TAM-67 on CAT-1 gene expression in RASMCs**

Partially confluent monolayers of RASMCs were transfected with either a-Fos or TAM-67 for 18 hour prior to activation with LPS ( $100 \mu\text{g ml}^{-1}$ ) and IFN- $\gamma$  ( $100 \text{ U ml}^{-1}$ ) for a further 18 hours. The control cells were obtained in the absence and presence of dominant negative construct with or without activation. The total RNA was extracted and the cDNA prepared by reverse transcription before subjecting to quantitative PCR analysis using CAT-1 specific primers. Expression of RPL-13 was also determined and used to standardise the loading and expression levels of CAT-1. The data is the mean  $\pm$  SEM of three separate experiments. Each control and activated group was analysed separately using a one-way ANOVA program followed by Dunnett's multiple comparison test.

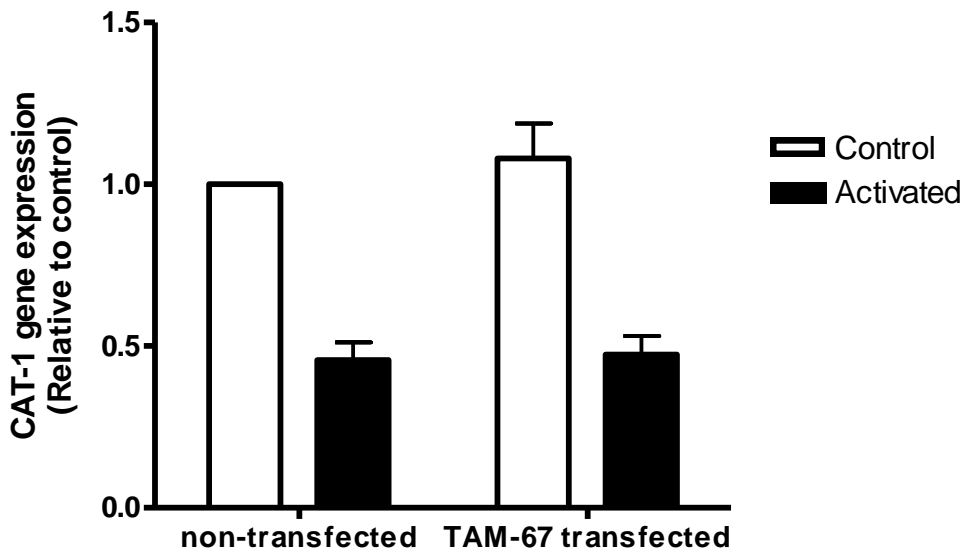
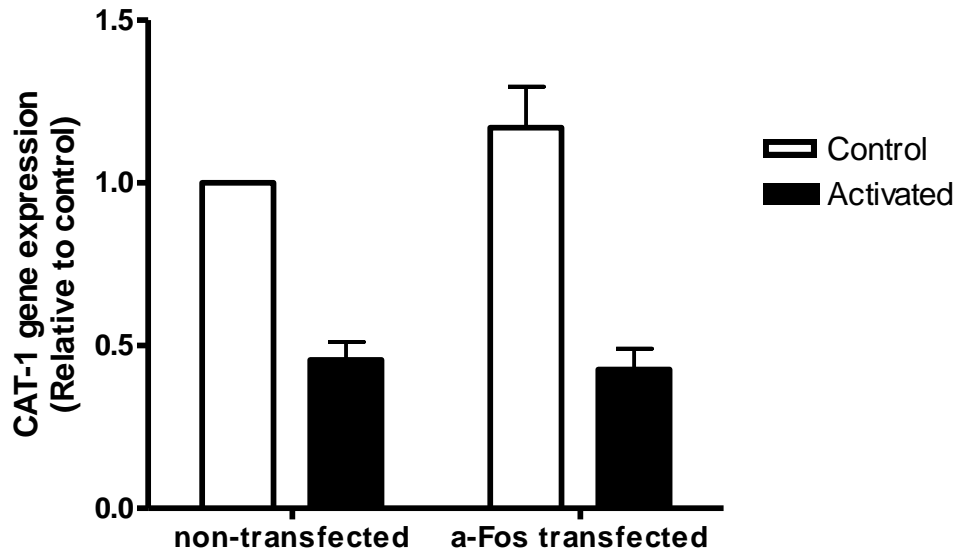


**Figure 4.2 Effect of a-Fos and TAM-67 on CAT-2A gene expression in RASMCs**

Partially confluent monolayers of RASMCs were transfected with either a-Fos or TAM-67 for 18 hour prior to activation with LPS ( $100 \mu\text{g ml}^{-1}$ ) and IFN- $\gamma$  ( $100 \text{ U ml}^{-1}$ ) for a further 18 hours. The control cells were obtained in the absence and presence of dominant negative construct with or without activation. The total RNA was extracted and the cDNA prepared by reverse transcription before subjecting to quantitative PCR analysis using CAT-2A specific primers. Expression of RPL-13 was also determined and used to standardise the loading and expression levels of CAT-2A. The data is the mean  $\pm$  SEM of three separate experiments. The data is the mean  $\pm$  SEM of three separate experiments. Each control and activated group was analysed separately using a one-way ANOVA followed by Dunnett's multiple comparison test.

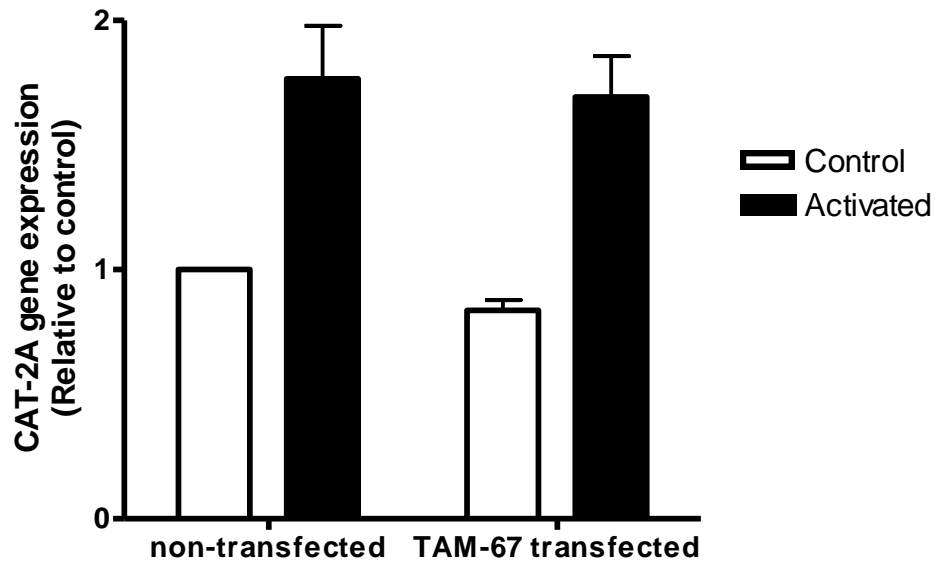
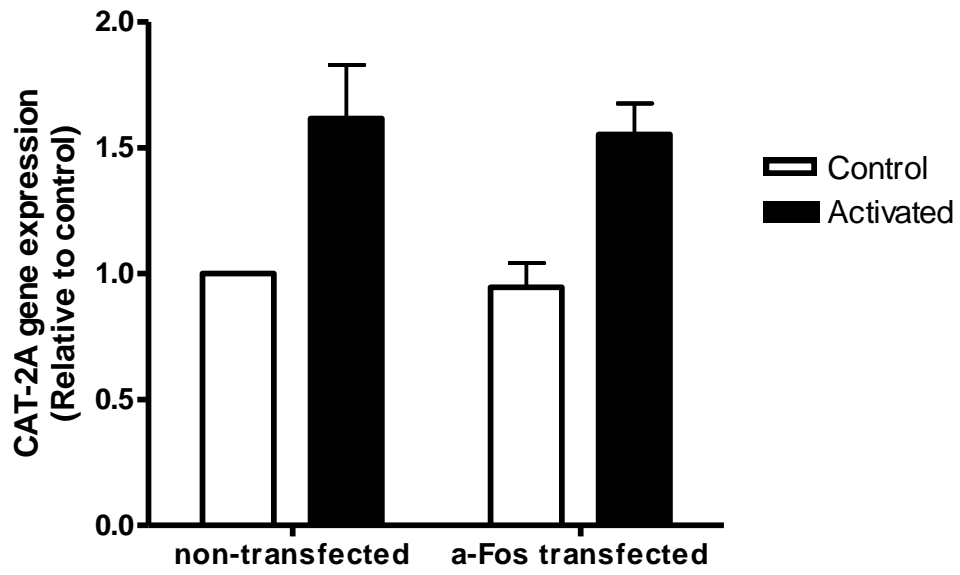
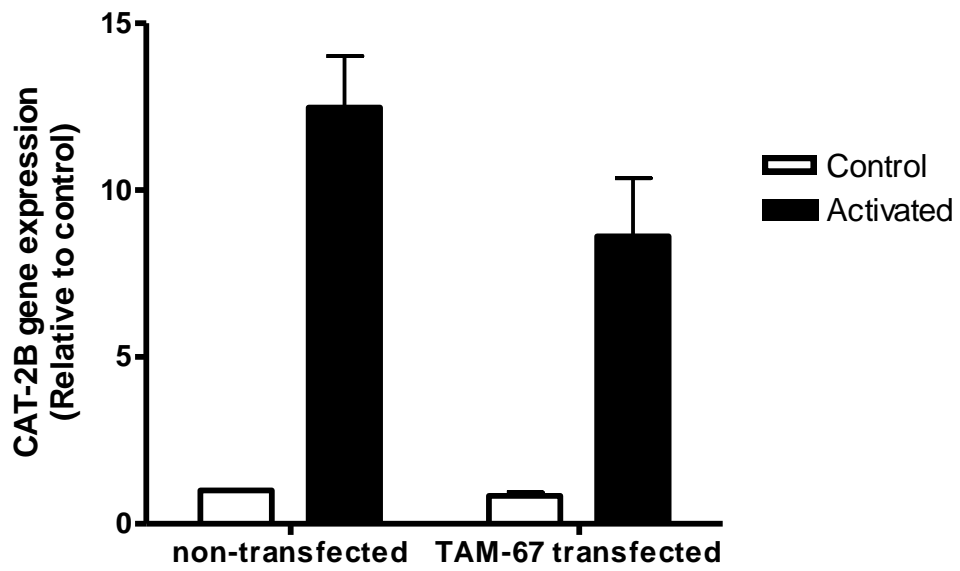
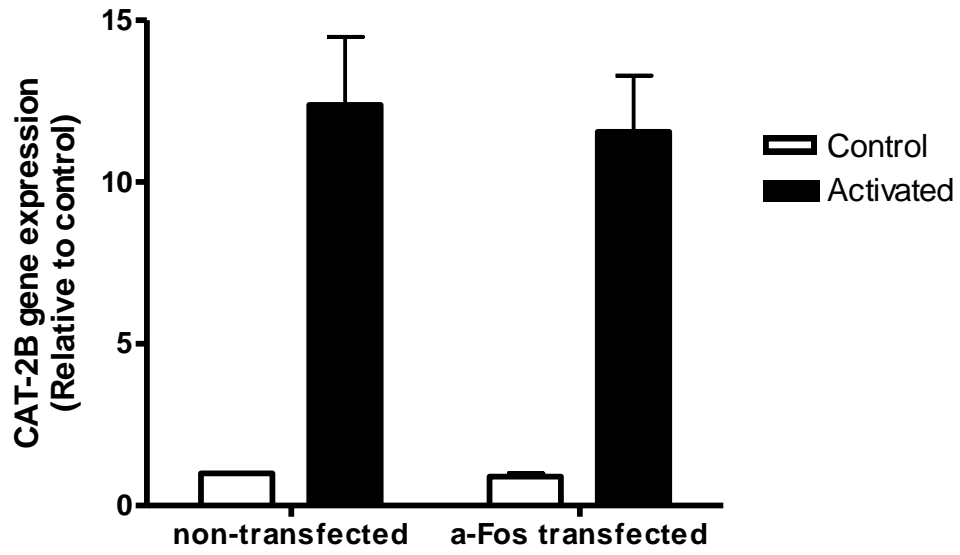


**Figure 4.3 Effect of a-Fos and TAM-67 on CAT-2B gene expression in RASMCs**

Partially confluent monolayers of RASMCs were transfected with either a-Fos or TAM-67 for 18 hour prior to activation with LPS ( $100 \mu\text{g ml}^{-1}$ ) and IFN- $\gamma$  ( $100 \text{ U ml}^{-1}$ ) for a further 18 hours. The control cells were obtained in the absence and presence of dominant negative construct with or without activation. The total RNA was extracted and the cDNA prepared by reverse transcription before subjecting to quantitative PCR analysis using CAT-2B specific primers. Expression of RPL-13 was also determined and used to standardise the loading and expression levels of CAT-2B. The data is the mean  $\pm$  SEM of three separate experiments. The data is the mean  $\pm$  SEM of three separate experiments. Each control and activated group was analysed separately using a one-way ANOVA followed by Dunnett's multiple comparison test.



## 4.4 Discussion

The signalling mechanism that regulates iNOS expression and L-arginine transport in different cell systems may not be similar. The differential regulation of these two processes is however not unusual since previous studies have shown that upstream signalling molecules such as tyrosine kinases can regulate the expression of iNOS whilst having no effect on the increase in the transport of L-arginine although the latter was induced in parallel with iNOS by the same activating agents (Baydoun *et al.*, 1999). However in smooth muscle cells for example it has been shown that increase in L-arginine transport activity and nitrite accumulation occurred in parallel (Wileman *et al.*, 1995). This up-regulation in L-arginine transport is correlated with enhanced expression of cationic amino acid transporters (CATs) which provides substrate supply during enhanced synthesis of nitric oxide (Cui *et al.*, 2005). To clarify the transporter responsible for L-arginine transport in inflammatory condition in our experiments, the expression profile of CATs was studied. In the next step the role of JNK/AP-1 pathway on the expression of the CATs was established.

To determine the profile of CATs gene expression, it should be noted that *Cat1* and *Cat2* genes have distinct expression patterns from one another (Kakuda *et al.*, 1998). *Cat2* is expressed from multiple promoters (Finley *et al.*, 1995) and encodes two spliced variants (MacLeod, 1996) that are different in their transport kinetic properties (Van Winkle *et al.*, 1995).

Many of studies have been performed to identify the role of different CATs in the various cell types. In this thesis we have established the profile of expression of the different CATs in both smooth muscle cell and in J774 macrophages and further

explored how these are regulated by different stimuli used in the studies. The data obtained has confirmed previous studies showing that RASMCs express transcript for CAT-1, CAT-2A and CAT-2B under basal condition (Baydoun *et al.*, 1999). However these observations are in contrast with those made in other cell systems such as J774 macrophages (Kakuda *et al.*, 1999), astrocytes (Stevens *et al.*, 1996) and cardiac Myocytes (Simmons *et al.*, 1996a) where CAT-1 was the only constitutively expressed isoform. In these systems CAT-2A (cardiac myocytes) and/or CAT-2B (macrophages, astrocytes and cardiac myocytes) were detected only after activation of the cells with pro-inflammatory mediators suggesting that CAT-1 may be the physiological transporters while CAT-2A and CAT-2B may be responsible for L-arginine entry into the cells under inflammatory condition.

In the current studies, CAT-2B was augmented when the cells were stimulated with LPS/IFN- $\gamma$ , which has the same trend as iNOS expression (chapter 3) and confirms the parallel regulation of iNOS and L-arginine transporters but more importantly indicates that CAT-2B may be the critical carrier for L-arginine in the induced cells. This inducible carrier is usually co-expressed with CAT-1, and its expression has been documented in lung, brain (Deves *et al.*, 1998), activated cells such as macrophages (Closs *et al.*, 2000), astrocytes (Stevens *et al.*, 1996) and aortic vascular smooth muscle cells (Baydoun *et al.*, 1999). Its up-regulation in our system is consistent with other reports showing its induction together with iNOS (Hattori *et al.*, 1999; Schwartz *et al.*, 2002) and the claims that CAT-2B may have a specific role in delivering substrate to iNOS (Closs *et al.*, 2000; Hammermann *et al.*, 2001).

In smooth muscle cells CAT-2A expression was also increased but using one way ANOVA statistical analysis, the change was not significant. It can be concluded that

CAT-2A may make a negligible contribution to the total entry of L-arginine into RASMCs. This may not be surprising since CAT-2A, when compared to CAT-2B or even CAT-1, has a lower affinity for L-arginine (Closs *et al.*, 1993a; Closs *et al.*, 1997).

The change in the expression profile of CATs in RASMCs activated with LPS/IFN- $\gamma$  is interesting since the current data indicate a down regulation in CAT-1 expression. The consequences of these changes would be that CAT-1 makes a small contribution to L-arginine uptake in activated RASMCs while CAT-2B plays the critical role in maintaining substrate supply into the cells and play a considerable role in parallel when iNOS is expressed. In this regard, it has been suggested that after stimulation with LPS or cytokines, iNOS and CAT-2 genes are co-induced and BH4 acts as a co-factor that up-regulates both iNOS and CAT-2 mRNA (Schwartz *et al.*, 2002). It has also been reported that iNOS activity may be reduced in macrophages from CAT-2 knockout mice (Nicholson *et al.*, 2001). This has led to the suggestion that there may be a clear cooperation between CAT-2 and iNOS in that sustained production of NO the latter may be controlled by CAT activity. It is worth noting however that our previous studies have shown that this may not be the case. Our group has demonstrated that over expression of iNOS in cells (HEK-293 cells) which do not constitutively express the enzyme does not necessarily result in enhanced transporter activity (Cui *et al.*, 2005). Thus while continued substrate supply to NOS may be essential for sustaining NO production, enhanced NOS activity does not necessarily result in increased substrate supply into the cells. This is at least the case in the transfected cells but the expression levels of iNOS in this model may be different to those attained following induction of cell/tissues *in vitro* and/or *in vivo*.

Moreover, induction with inflammatory mediators may also co-induce other factors such as BH<sub>4</sub> that are essential for optimal NOS activity. This may not be the case for cells transfected with the iNOS construct.

The decline in CAT-1 mRNA expression is of interest as it indicates that this particular transcript may not be stable when cells are induced by inflammatory mediators. The findings are consistent with other studies indicating the fact that CAT-1 mRNA is completely abolished or reduced in parallel with the augmentation in CAT-2 mRNA expression (Schwartz *et al.*, 2002). These authors have also suggested that up-regulation of an individual CAT may cause a decline on the other transporters' mRNA (Schwartz *et al.*, 2002). The decrease in CAT-1 expression following induction of rat cardiac myocytes suggests that CAT-2B may be the more important carrier of L-arginine in these cells.

Unlike RASMCs, the pattern of expression and regulation of CATs in J774 macrophages was different in some aspects. For instance, CAT-1 did not alter after stimulation with LPS while CAT-2A and CAT-2B both revealed a significant increase in mRNA expression level. These findings are in agreement with the data obtained in RAW264.7 macrophages (Huang *et al.*, 2006) and in rat mesangial kidney cells in which stimulation with LPS did not cause any up or down regulation in CAT-1 gene expression (Schwartz *et al.*, 2003).

It may be speculated that in J774 macrophages both CAT-2A and CAT-2B are required for complete substrate supply of L-arginine but the low affinity of CAT-2A for L-arginine strongly implies that CAT-2B is again the critical carrier in induced cells. Similar data was obtained in macrophages previously revealing a role for CAT-2 but

not CAT-1 in L-arginine transport when cells were exposed to *Helicobacter pylori*. Moreover, knockdown of *Cat-2* gene in macrophages was shown to prevent stimulated L-arginine uptake (Chaturvedi *et al.*, 2010). There are several studies also emphasising the important role of CAT-2 in macrophages and this protein is now widely accepted as the key transporter for substrate supply at least into induced cells expressing iNOS (Lai *et al.*, 2008; Niese *et al.*, 2010; Rothenberg *et al.*, 2006; Thompson *et al.*, 2008). To further support this notion, it has been shown that in macrophages induction of CAT-2B occurs in parallel with the marked decrease in the expression of CAT-1 suggesting that the former may be the critical transporter of L-arginine and may act as the main supplier of substrate into the cells (Kakuda *et al.*, 1999). In addition, it has been shown that NO production was significantly decreased in macrophages obtained from *Cat-2*<sup>-/-</sup> mice (Nicholson *et al.*, 2001).

In the J774 macrophages, additional studies were carried out to determine the manner in which CAT expression was modulated by LPS, IFN- $\gamma$  and the combination of both. The reason for wanting to do these experiments is because IFN- $\gamma$  in preliminary studies did not appear to significantly regulate basal L-arginine transport in J774 cells but yet was critical in RASMCs. We therefore questioned whether in the macrophages IFN- $\gamma$  does in fact control CAT gene expression. These studies were in parallel with the same study on iNOS and NO induction discussed in chapter 3. Consistent with the functional data, there was no significant change in CAT-1 expression when cells were subjected to IFN- $\gamma$  alone and this is consistent with the report by Wanasen *et al.* (2007) in murine macrophages showing that CAT-1 mRNA is not affected by IFN- $\gamma$  treatment. Interestingly, in our studies, LPS but not IFN- $\gamma$  caused an up-regulation in CAT-2A expression. It seems that even in the same cell

system, various pro-inflammatory conditions do not have the same effect. At the same time, CAT-2B showed an up-regulation with all three different stimulations but still lower for IFN- $\gamma$  treated alone.

The effect of IFN- $\gamma$  on CAT-2B was shown previously where this stimulant alone increases CAT-2B expression (Wanassen *et al.*, 2007). On the other hand, some studies suggested no effect for IFN- $\gamma$  on CAT-2 expression in macrophages (Sweet *et al.*, 1998). Again, it always should be noted that which stimulants in which cell system is being used.

Following the initiation of the preliminary studies, complementary experiments were conducted to identify the role of JNK/AP-1 on cationic amino acid transporters expression in both RASMCs and J77 macrophages. The findings showed that in RASMCs, SP600125 had little effect on CAT function and transcript expression. This suggests that the JNK-AP-1 pathway may not be critical for the activity of these proteins in either controls or induced cells. However in J77 macrophages the drug caused a significant decline in CAT-2B induction without affecting levels of CAT-1 or CAT-2A and this effect was seen only at the concentration of 3  $\mu$ M which also partially blocked L-arginine transport rates in induced cells. Thus, taken together, these findings now clearly demonstrate that CAT-2B may be the critical transporter of L-arginine following induction of cells with pro-inflammatory mediators. Moreover, these results show for the first time the selective regulation of CAT-2B but not CAT-1 or CAT-2A induction by the JNK-AP-1 pathway.

Not very much is known about the promoter region of CAT-1, CAT-2A and CAT-2B, as these have not been fully characterised. Because NF- $\kappa$ B plays an essential role in

the iNOS expression, there are some studies on the role of this transcription factor which suggested that NF- $\kappa$ B is an essential transcription factor not only for the induction of iNOS, but also for the L-arginine transport system (Kagemann *et al.*, 2007) which may relate to up-regulation of CATs specifically CAT-2B (Chu *et al.*, 2005; Hammermann *et al.*, 2000; Yang *et al.*, 2005). Also two NF- $\kappa$ B sites were identified on mouse CAT-2 gene promoter (Finley *et al.*, 1995) which can indicate a role for NF- $\kappa$ B in transport system. It should also be noted that in most of these studies there was no significant effect of NF- $\kappa$ B on CAT-1 or CAT-2A (Chu *et al.*, 2005; Hammermann *et al.*, 2000; Huang *et al.*, 2004; Visigalli *et al.*, 2004; Yang *et al.*, 2005) which again reveals the important role of NF- $\kappa$ B in parallel with induction of iNOS. Still there is not much evidence available on the full control of CATs induction or on the role of different MAPKs on these transporters. There are some studies in macrophages which indicate a role for ERK1/2 and p38 MAPK in transport of L-arginine and CAT-2B regulation (Caivano, 1998) and in RASMCs it shown that p38 MAPK but not ERK may regulate CATs expression (Baydoun *et al.*, 1999). On the other hand, there are studies suggesting a role for ERK (p42/44 MAPK) in CAT-1 expression (Casanello *et al.*, 2007; Vasquez *et al.*, 2004).

In contrast to ERK and p38 MAPK, there is little data on the requirement of JNK/AP-1 signalling in CATs regulation. Parallel studies were therefore conducted to determine the role of this pathway in CAT expression and function using a-Fos and TAM-67. The a-Fos construct did not alter expression profile of the CATs nor did it cause any effect on L-arginine transport (Chapter 3, results). This observation, at glance, indicates that AP-1 may not be involved in regulating transport of L-arginine in RASMCs. This may indeed be the case since TAM-67 also causes little change in

either CAT-1 or CAT-2A mRNA expression and only marginally altered that for CAT-2B. This trend is consistent with the functional changes reported in Chapter 3 and would indicate that induction of L-arginine transport is not only dependent on CAT-2B upregulation but also partially regulated by the JNK-AP-1 pathway at the very best. At the moment there is just one study available that shows PKC-dependent stimulation of CAT2 expression. This apparently requires the activation of MEK/ERK1/2 signalling which in turns leads to the activation of AP-1 (visigalli *et al.*, 2010).

## 4.5 Summary

In this chapter the profile of CAT expression and their regulation by SP600125, TAM-67 and a-Fos were examined. The data has generated some interesting findings, showing in RASMCs CAT-1 mRNA declined when cells were exposed to LPS and IFN- $\gamma$  while that for CAT-2B was enhanced with no effect on CAT-2A. In addition none of the transcripts were affected by the JNK inhibitor SP600125 or a-Fos but CAT-2B was marginally reduced by TAM-67 and this is consistent with the reductions in transport rates seen under identical conditions.

In J774 macrophages, CAT-2A and CAT-2B mRNA increased after stimulation with LPS while CAT-1 decreased. JNK inhibition with SP600125 reduced CAT-2B without affecting CAT-1 or CAT2A levels which strongly confirming that the transporter for enhanced L-arginine transport in these cells is again CAT-2B and that the induction of this protein may be critically regulated, at least in part, by JNK activation. Further studies with the AP-1 dominant negatives were not carried out because of limitations in transfecting macrophages but these studies are essential.

# Results

## **Chapter 5**

**The expression and activation profile of JNK isoforms and AP-1 subunits in RASMCs and J774 macrophages**

## 5.1 Introduction

As observed in chapters 3 and 4 there was a difference in responses of smooth muscle cells and macrophages to JNK inhibition using pharmacological inhibitors or to AP-1 suppression using dominant negative constructs.

In order to get a clearer understanding of the role of the JNK/AP-1 pathway in the induction of iNOS and/or CATs in the two cell systems, further studies were carried out determining the expression and activation profile of both JNK isoforms and of the different AP-1 subunits. Moreover, the effects of SP6000125 on these proteins were also investigated in both cell types but studies exploring the effects of the AP-1 dominant negative constructs ( $\alpha$ -Fos and TAM-67) were limited to the smooth muscle cells as J774 macrophages could not be transfected.

As it mentioned earlier there are three JNK isoforms in which two of them are present in most cell systems, therefore we first explored the expression profile of these two isoforms and meantime the phosphorylation of JNK when using LPS/LPS-IFN- $\gamma$  in RASMCs and J774 macrophages. After this stage using an ELISA based kit we determined the activation of all seven AP-1 subunits (c-Jun, JunB, JunD, c-Fos, FosB, Fra-1 and Fra-2). This study helps to clarify the pattern of how these subunits work together in our cell systems.

## **5.2 Methods**

### **5.2.1 Detection of JNK1, JNK2 and phospho-JNK expression in RASMCs and J774 macrophages**

Confluent monolayers of RASMCs or J774 macrophages were plated in 6 well plates and activate with LPS ( $100 \mu\text{g ml}^{-1}$ ) and IFN- $\gamma$  ( $100 \text{ U ml}^{-1}$ ) or with LPS ( $1 \mu\text{g ml}^{-1}$ ) alone respectively for the period of 1, 5, 15, 30, 60, 120 min. Control cells were incubated with complete culture medium alone. The incubation was terminated by lysaing the cells and western blot analysis was performed using anti-JNK1 or anti-JNK2 or anti-phospho-JNK. The membrane was stripped and re-probed for detection of  $\beta$ -actin as a control of loading.

### **5.2.2 Effect of SP600125 on JNK phosphorylation status in RASMCs and J774 macrophages**

Confluent monolayers of RASMCs or J774 macrophages were plated in 6 well plates and treated with SP600125 ( $0.3\text{-}3 \mu\text{M}$ ) for 30 min following activation with LPS ( $100 \mu\text{g ml}^{-1}$ ) and IFN- $\gamma$  ( $100 \text{ U ml}^{-1}$ ) or with LPS ( $1 \mu\text{g ml}^{-1}$ ) alone respectively for a further 30 min. The control cells were incubated in medium alone or treated with the same concentrations of SP600125 in the absence of any stimulants. The incubation was terminated by lysaing the cells and western blot analysis was performed using an anti-JNK1, anti-JNK2 or anti-phospho-JNK antibody. The membrane was stripped and re-probed for  $\beta$ -actin which was used as a control of loading.

### **5.2.3 Expression profile of AP-1 subunits in RASMCs and J774 macrophages stimulated with LPS/IFN- $\gamma$ or LPS**

Confluent monolayers of RASMCs or J774 macrophages were serum starved for 24 hours prior to activation. The cells were then subjected for 5, 15, 30, 60, 120 min to LPS ( $100 \mu\text{g ml}^{-1}$ ) and IFN- $\gamma$  ( $100 \text{ U ml}^{-1}$ ) for RASMCs or LPS ( $1 \mu\text{g ml}^{-1}$ ) alone for macrophages. The control cells did not contain any stimulants. The incubations were terminated and nuclear extractions carried out as described in the methods (section 2.2.23).  $10 \mu\text{g}$  of nuclear extract was analysed using a TransAM AP-1 family kit from Active Motif (Belgium) as described.

### **5.2.4 The effect of JNK inhibitor (SP600125) on the activity of AP-1 subunits in RASMCs and J774 macrophages**

Confluent monolayers of RASMCs or J774 macrophages were serum starved for 24 hours prior to 30 min incubation with SP600125 ( $0.3\text{-}3 \mu\text{M}$ ). The cells were then stimulated with LPS ( $100 \mu\text{g ml}^{-1}$ ) and IFN- $\gamma$  ( $100 \text{ U ml}^{-1}$ ) for RASMCs or LPS ( $1 \mu\text{g ml}^{-1}$ ) for macrophages for either 30 min or 2 hours. Parallel controls were set up in the presence and absence of SP600125. Nuclear extracts were subsequently prepared as described in the methods.  $10 \mu\text{g}$  of nuclear extract was analysed using a TransAM AP-1 family kit from Active Motif (Belgium).

### **5.2.5 The effect of pGFP-a-Fos and pGFP-TAM-67 on the activation of AP-1 subunits in RASMCs**

Partially confluent (60-70%) monolayers of RASMCs were serum starved for 24 hours before transfection with pGFP-a-Fos or pGFP-TAM-67 for another 18 hours. The cells were then activated with LPS ( $100 \mu\text{g ml}^{-1}$ ) and IFN- $\gamma$  ( $100 \text{ U ml}^{-1}$ ) for a further 30 min or 2 hours. Nuclear extracts were subsequently prepared as described in the methods. 10  $\mu\text{g}$  of nuclear extract was analysed using a TransAM AP-1 family kit from Active Motif (Belgium).

## 5.3 Results

### 5.3.1 Detection of JNK1, JNK2 and phospho-JNK expression in RASMCs

To determine which JNK isoform is expressed and phosphorylated in RASMCs, western blot was performed on lysates generated from controls and from cells activated with LPS ( $100 \mu\text{g ml}^{-1}$ ) and IFN- $\gamma$  ( $100 \text{ U ml}^{-1}$ ) at time points of 1, 5, 15, 30, 60 and 120 min. The data revealed the presence of both JNK1 and JNK2; with JNK1 showing one isoform at 46 kDa and JNK2 shows two band at 46 and 54 kDa. JNK1 appeared to be more predominantly expressed when compared to JNK2 (Figure 5.1). During the time course the total level of JNK1 and JNK2 remained unaffected. There was also very low and almost undetectable phospho-JNK in controls but this increased time-dependently in activated cells after 15 min, reaching a peak within 30 min and sustained over 60 min before declining 2 hours after activation (Figure 5.1).

### 5.3.2 Effect of SP600125 on JNK phosphorylation status in RASMCs

To determine whether SP600125 can affect phosphorylation of JNK in RASMCs, cells were pre-incubated with the drug at 0.3 and 3  $\mu\text{M}$  for 30 min prior to activation with LPS ( $100 \mu\text{g ml}^{-1}$ ) and IFN- $\gamma$  ( $100 \text{ U ml}^{-1}$ ) for a further 30 min. Lysates generated were subjected to western blotting for phospho-JNK. Expression of total JNK1 and JNK2 were also determined in parallel. Under these conditions, the total level of JNK1 and JNK2 remain unaffected but SP600125 significantly decreased phospho-JNK at 0.3  $\mu\text{M}$  and virtually abolished its expression at 3  $\mu\text{M}$  (Figure 5.2).

### **5.3.3 Detection of JNK1, JNK2 and phospho-JNK in J774 macrophages**

In parallel with the studies carried on RASMCs, experiments were conducted in J774 macrophages to determine which JNK isoform may be expressed and activated through phosphorylation. Western blot analysis confirmed the expression of JNK1 at 46 kDa and two isoforms of JNK2 at 46 and 54 kDa respectively. There was marginal expression of phospho-JNK in controls and this was increased in a time-dependent manner following activation with LPS (1 µg/ml). The increase was significant after 15 min reaching a peak at 30 min but beginning to decline after 60 min of activation (Figure 5.3).

### **5.3.4 The effect of SP600125 on JNK phosphorylation status in J774 macrophages**

The effect of SP600125 on JNK phosphorylation in macrophages was studied using two concentrations of the inhibitor (0.3 and 3 µM) prior to stimulation with LPS (1 µg ml<sup>-1</sup>) for 30 min. Consistent with the findings in RASMCs, SP600125 significantly reduced phosphorylation of JNK at 0.3 µM and virtually abolished its expression at 3 µM (Figure 5.4). Thus, in both cell types, JNK isoforms are expressed and activated following stimulation with inflammatory mediators and this was sensitive to inhibition by SP600125 but with the latter only able to regulate iNOS and induced NO production in the macrophages.

**Figure 5.1 Expression and activation of JNK in control and LPS/IFN- $\gamma$  activated RASMCs**

Confluent monolayers of RASMCs were incubated in culture medium alone or in medium supplemented with LPS (100  $\mu\text{g ml}^{-1}$ ) and IFN- $\gamma$  (100 U  $\text{ml}^{-1}$ ). Incubations were carried out over the time points indicated and lysates generated for western blotting using an anti-phospho-JNK and a non phospho-antibody selective for JNK1 or JNK2.  $\beta$ -actin expression was routinely determined to establish loading variability. The blots are representative of 3 experiments and the bar graphs are scanning densitometry of the bands expressed as a % of the maximum levels obtained after 30 min activated.

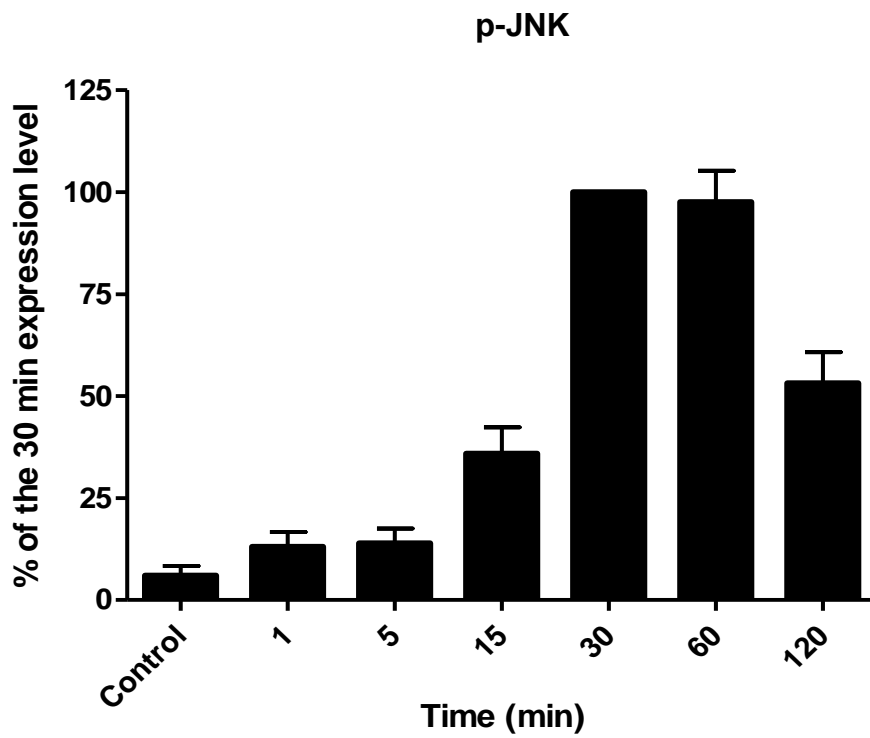
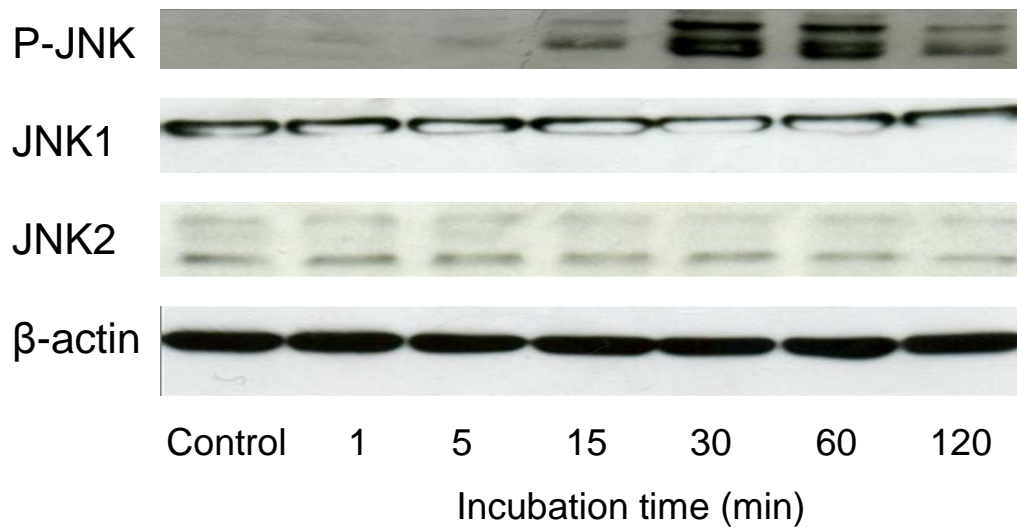


### **Figure 5.2 The effect of SP600125 on JNK phosphorylation in RASMCs**

Confluent monolayers of RASMCs were incubated with SP600125 (0.3 -3  $\mu\text{M}$ ) for 30 min prior to stimulation with LPS (100  $\mu\text{g ml}^{-1}$ ) and IFN- $\gamma$  (100 U  $\text{ml}^{-1}$ ) for a further 30 min. Lysates were generated at the end of the incubation period and subjected to western blotting using an anti-phospho-JNK or a non-phospho-JNK1 or JNK2 selective antibodies.  $\beta$ -actin expression was routinely determined to establish loading variability. The blots are representative of 3 experiments and the bar graphs are scanning the bands comparing the data with activated no SP600125 group.

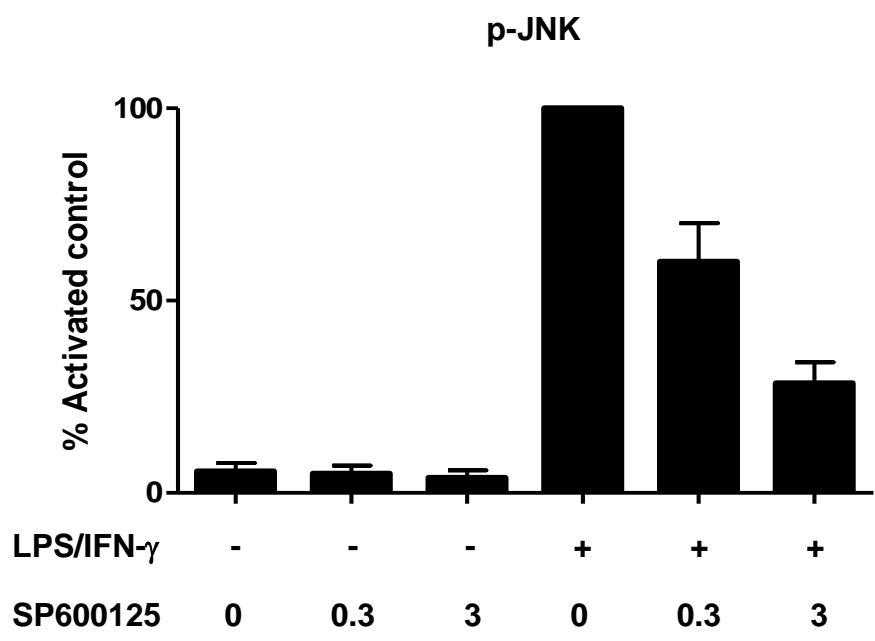
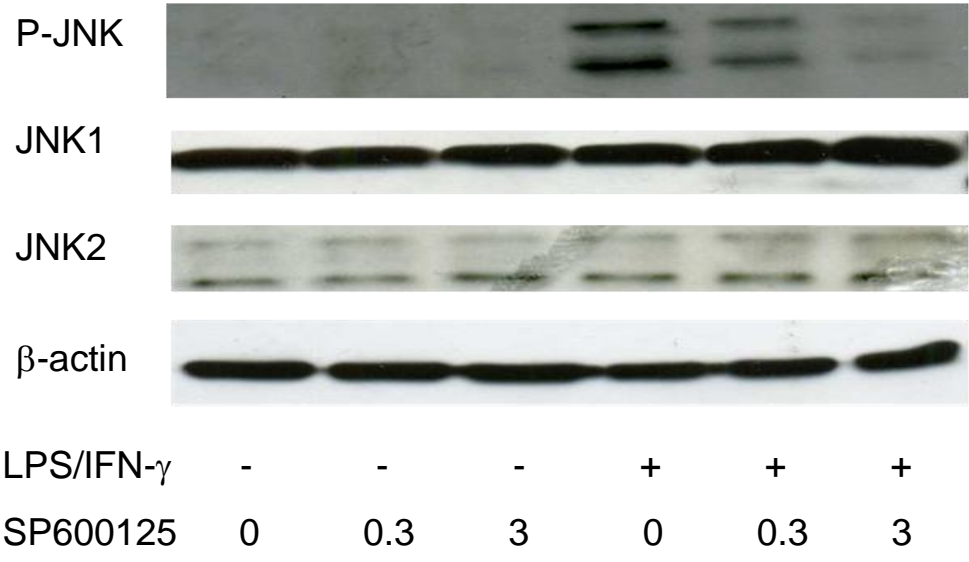


**Figure 5.3 The time point study of JNK phosphorylation following LPS activation of J774 macrophages**

Confluent monolayers of J774 macrophages were incubated in culture medium alone or in medium supplemented with LPS ( $1 \mu\text{g ml}^{-1}$ ). Incubations were carried out over the time points indicated and lysates generated for western blotting using an anti-phospho-JNK or a non phospho-antibody selective for JNK1 or JNK2.  $\beta$ -actin expression was routinely determined to establish loading variability. The blots are representative of 3 experiments and the bar graphs are scanning densitometry of the bands expressed as a % of the maximum levels obtained after 30 min activated.

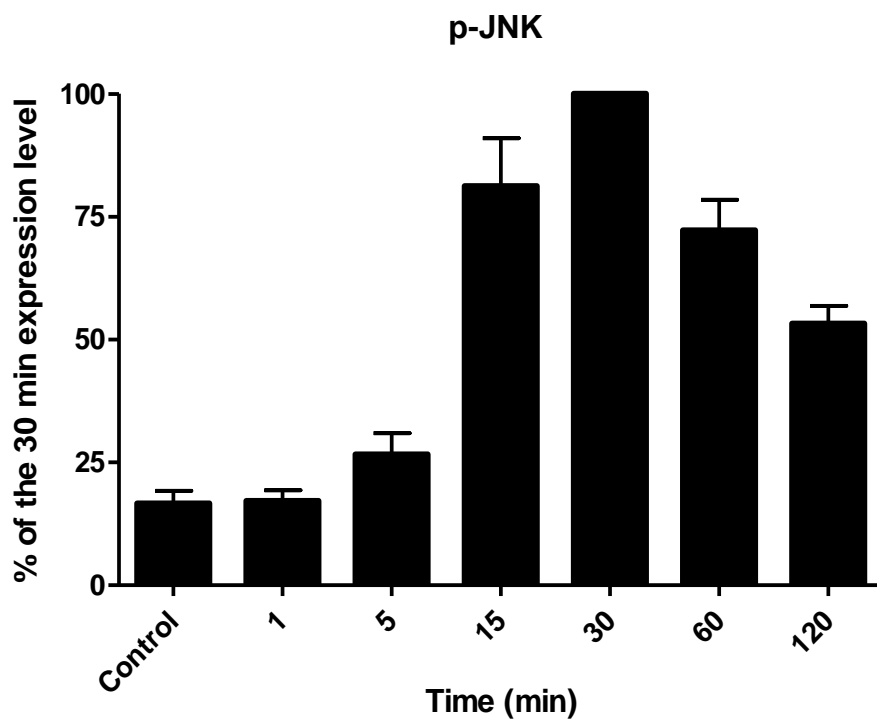
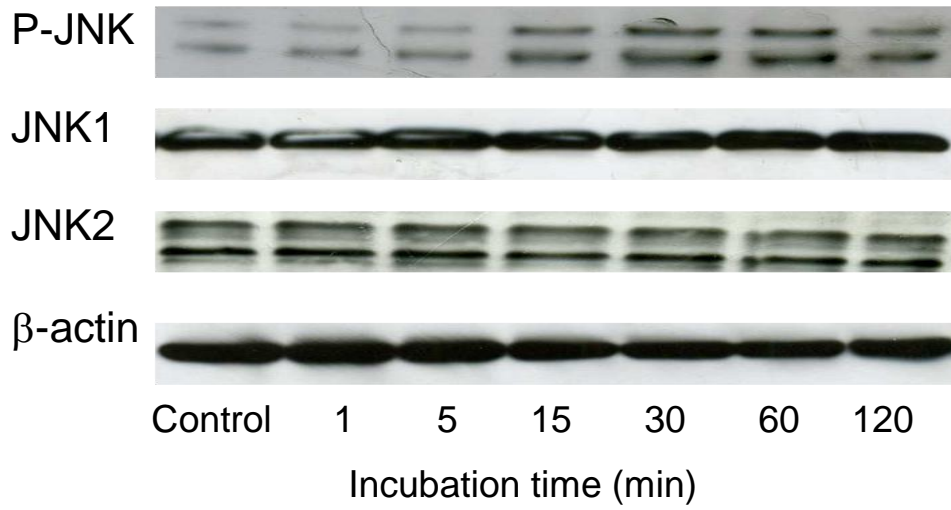
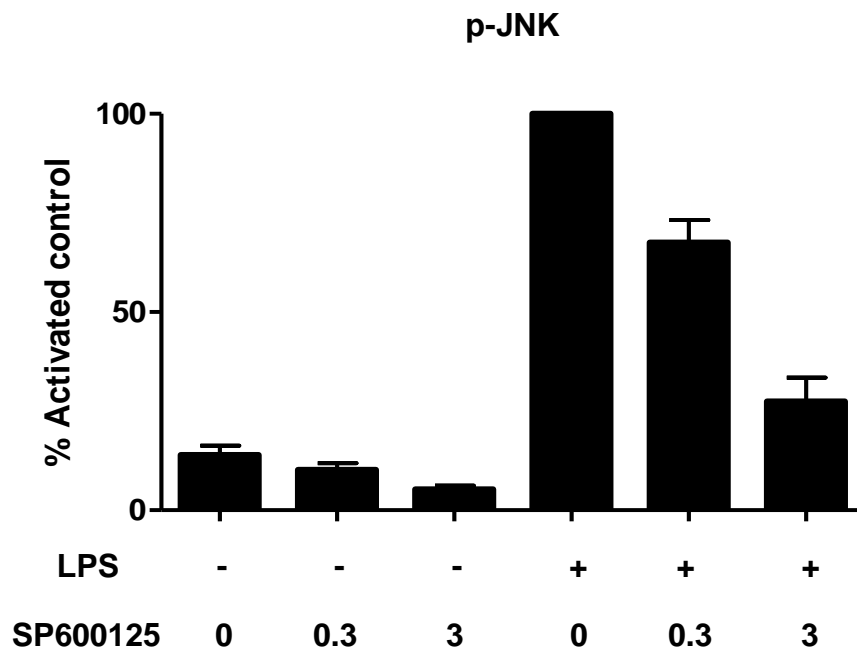
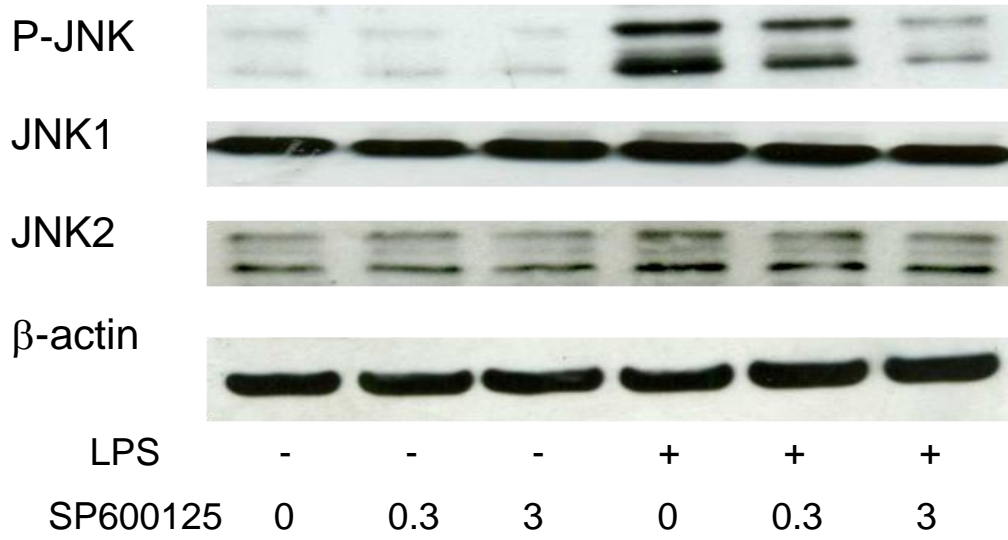


**Figure 5.4 The effect of SP600125 on JNK phosphorylation in J774 macrophages**

Confluent monolayers of J774 macrophages were incubated with SP600125 (0.3 -3  $\mu\text{M}$ ) for 30 min prior to stimulation with LPS ( $1 \mu\text{g ml}^{-1}$ ) for a further 30 min. Lysates were generated at the end of the incubation period and subjected to western blotting using an anti-phospho-JNK or a non-phospho-JNK1 or JNK2 selective antibodies.  $\beta$ -actin expression was routinely determined to establish loading variability. The blots are representative of 3 experiments and the bar graphs are scanning the bands comparing the data with activated no SP600125 group.



### 5.3.5 Expression profile of AP-1 subunits in activated RASMCs and J774 macrophages

As an extension to the studies above, further experiments were conducted looking at the expression and activation profile of different AP-1 subunits with a view to understanding how the subunits may be regulated under our experimental conditions and potentially identify AP-1 components that may mediate the divergent results already highlighted. Confluent monolayers of cells were activated with LPS ( $100 \mu\text{g ml}^{-1}$ ) and IFN- $\gamma$  ( $100 \text{ U ml}^{-1}$ ) for RASMCs and LPS ( $1 \mu\text{g ml}^{-1}$ ) for J774 macrophages at different time points ranging from 5 min to 2 hours. The cells were then harvested for nuclear extraction (methods, section 2.2.23) and the latter used to identify different AP-1 subunits and their activated status using the TransAM kit as described in the methods (section 2.2.24).

The assays carried out confirm the expression of c-Jun, Jun-B, Jun-D, c-Fos, Fos-B, Fra-1 and Fra-2 in both cell types. Of these, only c-Jun, Jun-D and Fra-1 showed clear evidence of significant activation when cells were exposed to either LPS and IFN- $\gamma$  (RASMCs) or LPS alone (J774 macrophages). Activation of c-Jun was evident after 30 min in RASMCs and after 15 min in the macrophages. Activation was sustained over 60 min, declining thereafter (Figure 5.5 and 5.12). Similarly, Jun-D activation was prominent after 30 min in macrophages (Figure 5.14) and 1 hour in RASMCs (Figure 5.7). Jun-D remained activated for up to 2 hours after stimulation in both cell systems as did Fra-1 (Figures 5.10 and 5.17). Interestingly, Jun-B which may play a prominent role in the induction of iNOS in some systems, did not appear to be activated in either cell type as its activation and DNA binding was not significantly different between control and activated samples analysed (Figures 5.6

and 5.13). Similarly, c-Fos, Fos-B and Fra-2 did not show any significant changes in activation from control basal levels especially in RASMCs (Figure 5.8, 5.9 and 5.11). There were no significant changes in both c-Fos and Fra-2 (Figure 5.15 and 5.18) but FosB on the other hand was highly activated after 1 hour in J774 macrophages (Figure 5.16).

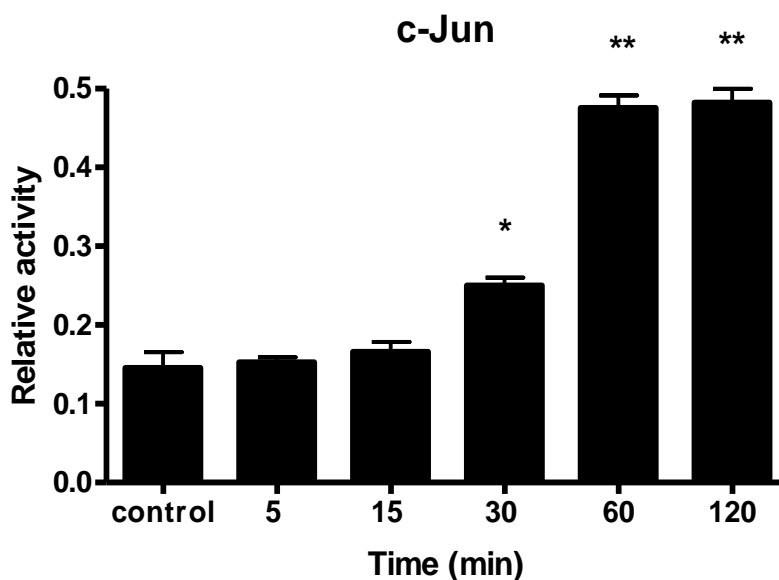


**Figure 5.5 The effect of LPS/IFN- $\gamma$  stimulation on c-Jun activation in RASMCs**

RASMCs were activated with LPS ( $100 \mu\text{g ml}^{-1}$ ) and IFN- $\gamma$  ( $100 \text{ U ml}^{-1}$ ) over the time periods indicated on the graph. Nuclear extracts were prepared and subjected to analysis as described in the methods (Section 2.2.23).  $10 \mu\text{g}$  of nuclear content was used in an AP-1 family DNA binding kit using phospho-c-Jun antibody and HRP-conjugated secondary. The absorbance was read at 450 nm. The results are representative of 3 independent experiments. Statistical analysis using a one way Anova followed by Dunnett's multiple comparison test was performed. \* $p < 0.05$  and \*\* $p < 0.01$  compared to control, non-activated results.

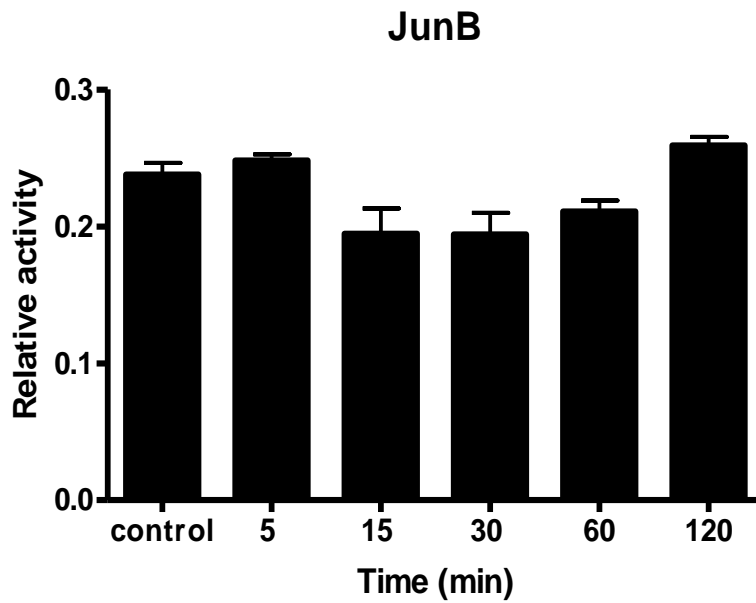


**Figure 5.6 The effect of LPS/IFN- $\gamma$  stimulation on JunB activation in RASMCs**

RASMCs were activated with LPS ( $100 \mu\text{g ml}^{-1}$ ) and IFN- $\gamma$  ( $100 \text{ U ml}^{-1}$ ) over the time periods indicated on the graph. Nuclear extracts were prepared and subjected to analysis as described in the methods (Section 2.2.23).  $10 \mu\text{g}$  of nuclear content was used in an AP-1 family DNA binding kit using JunB antibody and HRP-conjugated secondary. The absorbance was read at 450 nm. The results are representative of 3 independent experiments. Statistical analysis using a one way Anova followed by Dunnett's multiple comparison test was performed.

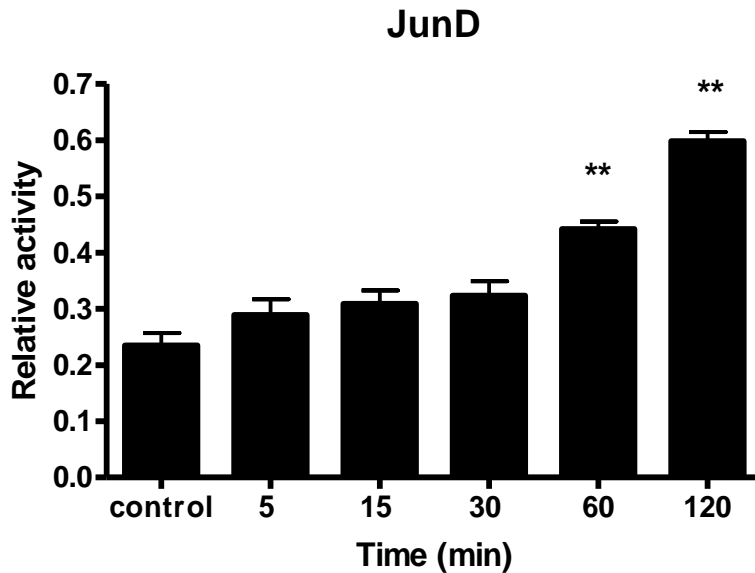


**Figure 5.7 The effect of LPS/IFN- $\gamma$  stimulation on JunD activation in RASMCs**

RASMCs were activated with LPS ( $100 \mu\text{g ml}^{-1}$ ) and IFN- $\gamma$  ( $100 \text{ U ml}^{-1}$ ) over the time periods indicated on the graph. Nuclear extracts were generated and subjected to analysis as described in the methods (Section 2.2.23).  $10 \mu\text{g}$  of nuclear content were used in an AP-1 family DNA binding kit using JunD antibody and HRP-conjugated secondary. The absorbance was read at 450 nm. The results are representative of 3 independent experiments. Statistical analysis using a one way Anova followed by Dunnett's multiple comparison test was performed. \*\* $p < 0.01$  compared to control, non-activated results.

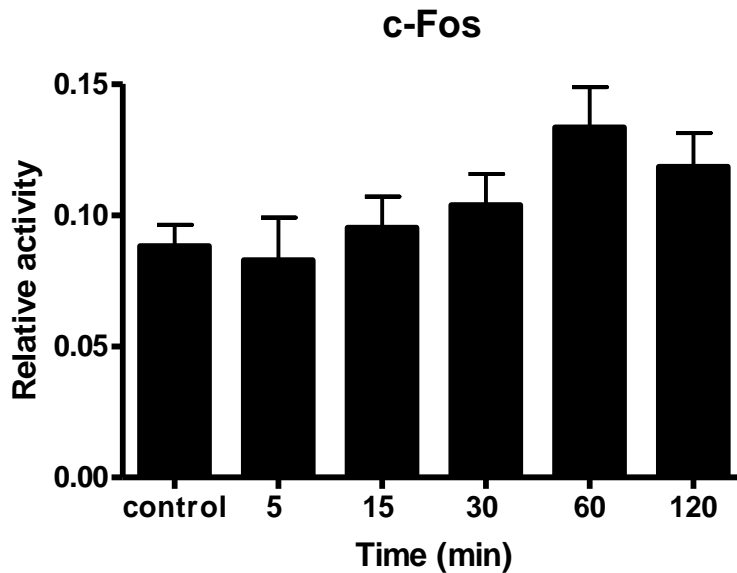


**Figure 5.8 The effect of LPS/IFN- $\gamma$  stimulation on c-Fos activation in RASMCs**

RASMCs were activated with LPS ( $100 \mu\text{g ml}^{-1}$ ) and IFN- $\gamma$  ( $100 \text{ U ml}^{-1}$ ) over the time periods indicated on the graph. Nuclear extracts were generated and subjected to analysis as described in the methods (Section 2.2.23).  $10 \mu\text{g}$  of nuclear content was used in an AP-1 family DNA binding kit using c-Fos antibody and HRP-conjugated secondary. The absorbance was read at 450 nm. The results are representative of 3 independent experiments. Statistical analysis using a one way Anova followed by Dunnett's multiple comparison test was performed.

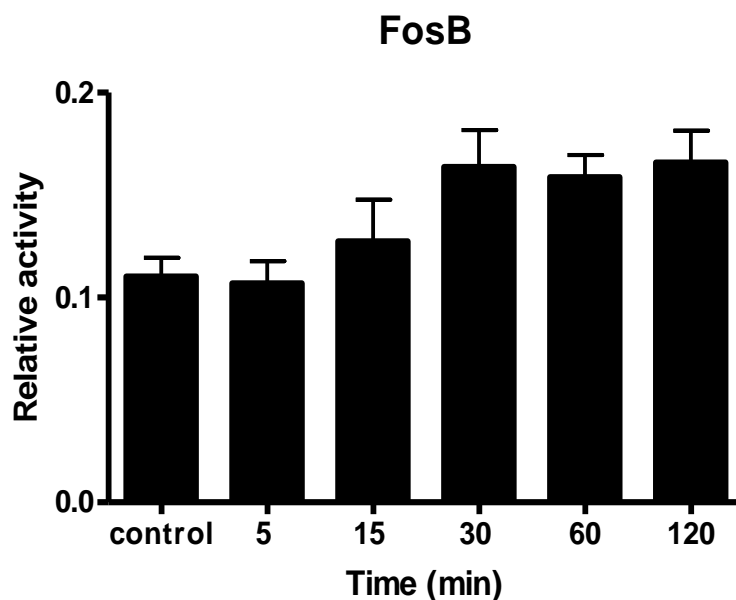


**Figure 5.9 The effect of LPS/IFN- $\gamma$  stimulation on FosB activation in RASMCs**

RASMCs were activated with LPS ( $100 \mu\text{g ml}^{-1}$ ) and IFN- $\gamma$  ( $100 \text{ U ml}^{-1}$ ) over the time periods indicated on the graph. Nuclear extracts were generated and subjected to analysis as described in the methods (Section 2.2.23).  $10 \mu\text{g}$  of nuclear content was used in an AP-1 family DNA binding kit using FosB antibody and HRP-conjugated secondary. The absorbance was read at 450 nm. The results are representative of 3 independent experiments. Statistical analysis using a one way Anova followed by Dunnett's multiple comparison test was performed.

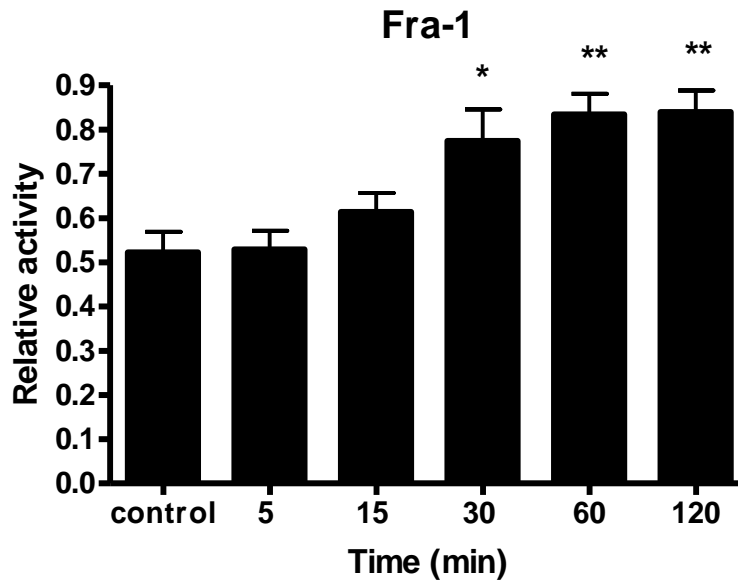


**Figure 5.10** The effect of LPS/IFN- $\gamma$  stimulation on Fra-1 activation in RASMCs

RASMCs were activated with LPS ( $100 \mu\text{g ml}^{-1}$ ) and IFN- $\gamma$  ( $100 \text{ U ml}^{-1}$ ) over the time periods indicated on the graph. Nuclear extracts were prepared and subjected to analysis as described in the methods (Section 2.2.23).  $10 \mu\text{g}$  of nuclear content was used in an AP-1 family DNA binding kit using Fra-1 antibody and HRP-conjugated secondary. The absorbance was read at 450 nm. The results are representative of 3 independent experiments. Statistical analysis using a one way Anova followed by Dunnett's multiple comparison test was performed. \* $p < 0.05$  and \*\* $p < 0.01$  compared to control, non-activated results.

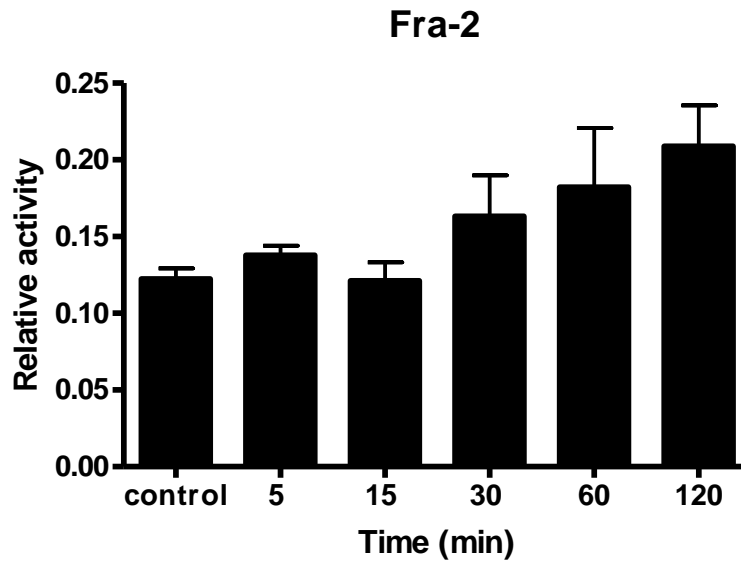


**Figure 5.11 The effect of LPS/IFN- $\gamma$  stimulation on Fra-2 activation in RASMCs**

RASMCs were activated with LPS ( $100 \mu\text{g ml}^{-1}$ ) and IFN- $\gamma$  ( $100 \text{ U ml}^{-1}$ ) over the time periods indicated on the graph. Nuclear extracts were prepared and subjected to analysis as described in the methods (Section 2.2.23).  $10 \mu\text{g}$  of nuclear content was used in an AP-1 family DNA binding kit using Fra-2 antibody and HRP-conjugated secondary. The absorbance was read at 450 nm. The results are representative of 3 independent experiments. Statistical analysis using a one way Anova followed by Dunnett's multiple comparison test was performed.

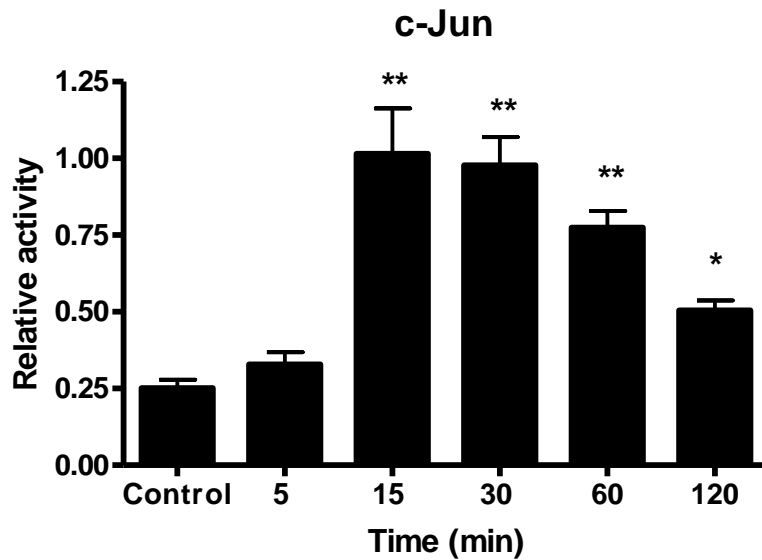


**Figure 5.12** The effect of LPS stimulation on c-Jun activation in J774 macrophages

J774 macrophages were activated with LPS ( $1 \mu\text{g ml}^{-1}$ ) over the time periods indicated on the graph. Nuclear extracts were prepared and subjected to analysis as described in the methods (Section 2.2.23).  $10 \mu\text{g}$  of nuclear content was used in an AP-1 family DNA binding kit using phospho-c-Jun antibody and HRP-conjugated secondary. The absorbance was read at 450 nm. The results are representative of 3 independent experiments. Statistical analysis using a one way Anova followed by Dunnett's multiple comparison test was performed. \* $p < 0.05$  and \*\* $p < 0.01$  compared to control, non-activated results.

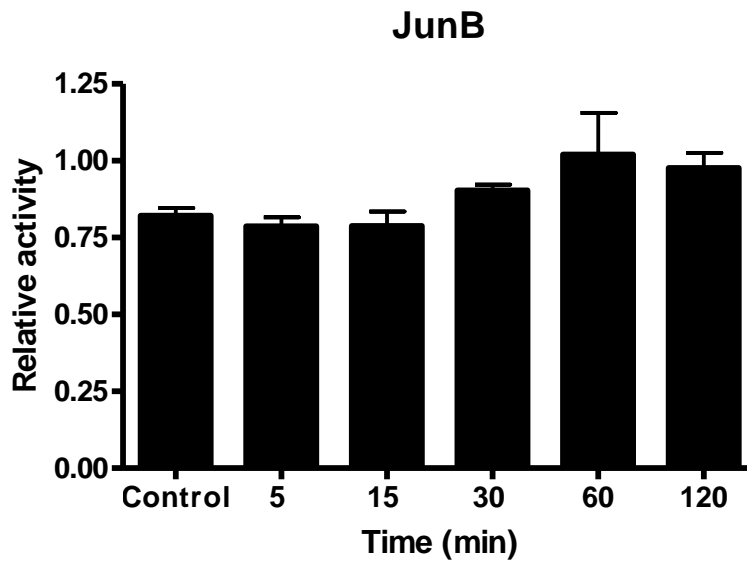


**Figure 5.13 The effect of LPS stimulation on JunB activation in J774 macrophages**

J774 macrophages were activated with LPS ( $1 \mu\text{g ml}^{-1}$ ) over the time periods indicated on the graph. Nuclear extraction prepared and subjected to analysis as described in the methods (Section 2.2.23).  $10 \mu\text{g}$  of nuclear content was used in an AP-1 family DNA binding kit using JunB antibody and HRP-conjugated secondary. The absorbance was read at 450 nm. The results are representative of 3 independent experiments. Statistical analysis using a one way Anova followed by Dunnett's multiple comparison test was performed.

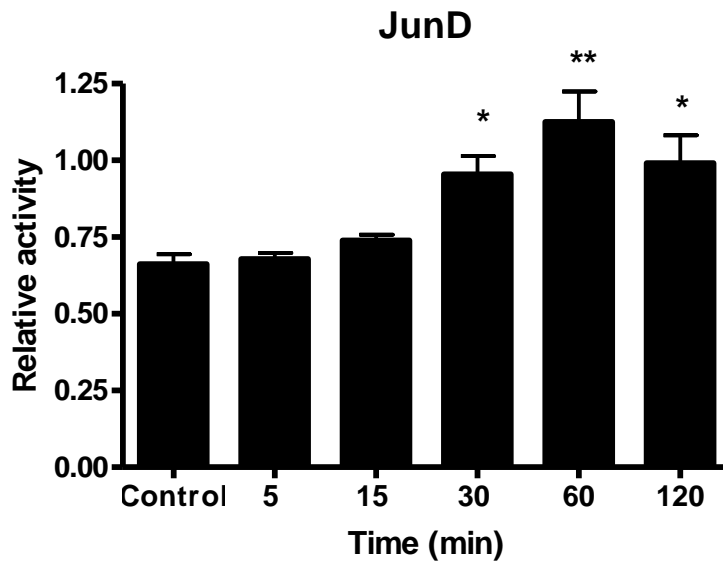


**Figure 5.14 The effect of LPS stimulation on JunD activation in J774 macrophages**

J774 macrophages were activated with LPS ( $1 \mu\text{g ml}^{-1}$ ) over the time periods indicated on the graph. Nuclear extracts were prepared and subjected to analysis as described in the methods (Section 2.2.23).  $10 \mu\text{g}$  of nuclear content was used in an AP-1 family DNA binding kit using JunD antibody and HRP-conjugated secondary. The absorbance was read at 450 nm. The results are representative of 3 independent experiments. Statistical analysis using a one way Anova followed by Dunnett's multiple comparison test was performed. \* $p < 0.05$  and \*\* $p < 0.01$  compared to control, non-activated results.

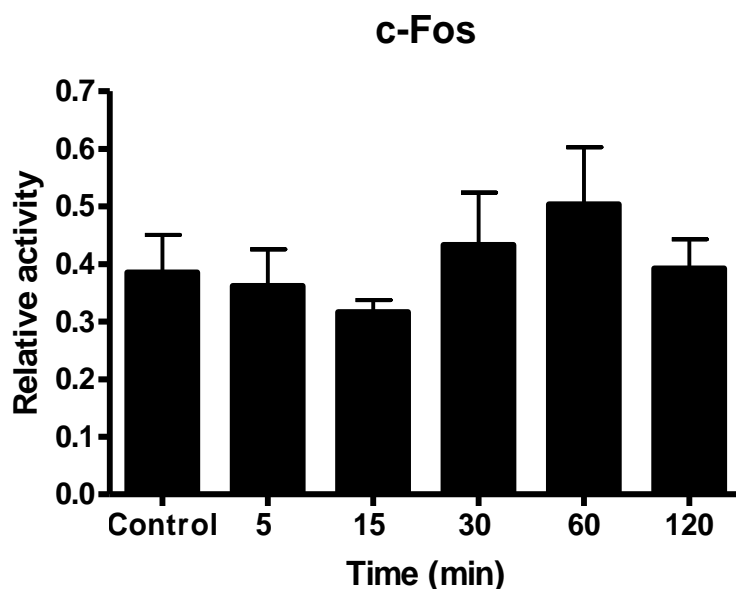


**Figure 5.15 The effect of LPS stimulation on c-Fos activation in J774 macrophages**

J774 macrophages were activated with LPS ( $1 \mu\text{g ml}^{-1}$ ) over the time periods indicated on the graph. Nuclear extracts were prepared and subjected to analysis as described in the methods (Section 2.2.23).  $10 \mu\text{g}$  of nuclear content was used in an AP-1 family DNA binding kit using c-Fos antibody and HRP-conjugated secondary. The absorbance was read at 450 nm. The results are representative of 3 independent experiments. Statistical analysis using a one way Anova followed by Dunnett's multiple comparison test was performed.

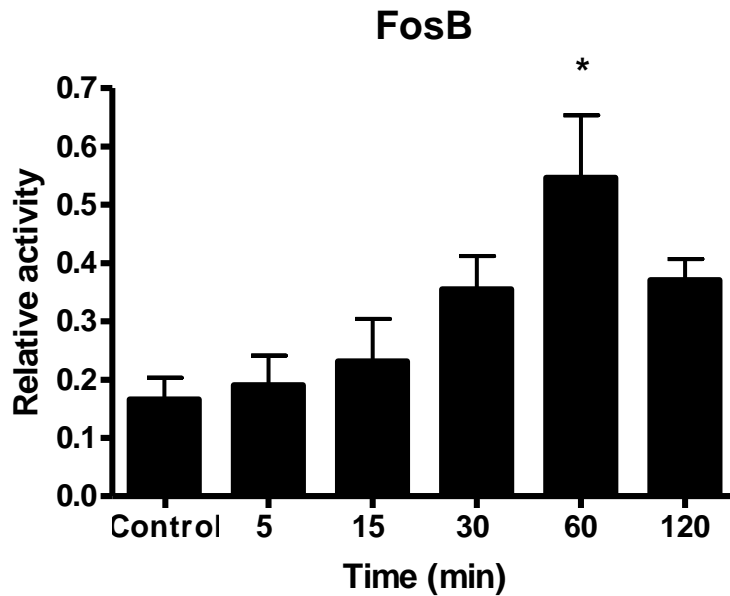


**Figure 5.16 The effect of LPS stimulation on FosB activation in J774 macrophages**

J774 macrophages were activated with LPS ( $1 \mu\text{g ml}^{-1}$ ) over the time periods indicated on the graph. Nuclear extracts were prepared and subjected to analysis as described in the methods (Section 2.2.23).  $10 \mu\text{g}$  of nuclear content was used in an AP-1 family DNA binding kit using FosB antibody and HRP-conjugated secondary. The absorbance was read at 450 nm. The results are representative of 3 independent experiments. Statistical analysis using a one way Anova followed by Dunnett's multiple comparison test was performed. \* $p < 0.05$  compared to control, non-activated results.

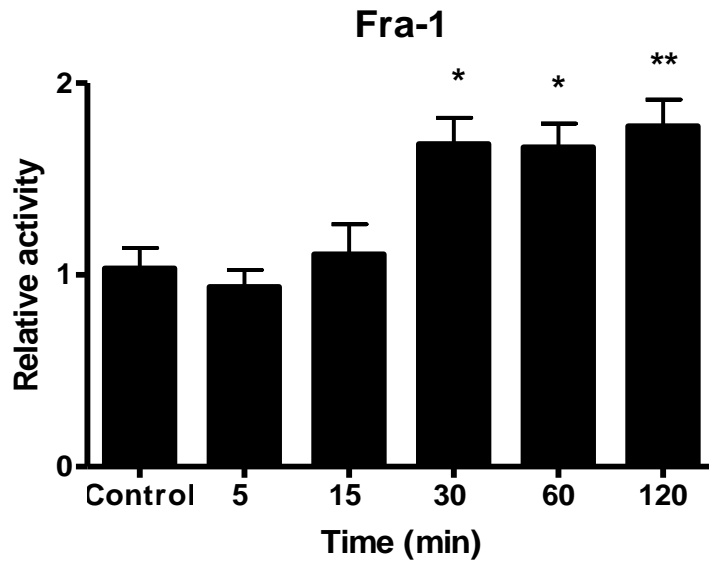


**Figure 5.17 The effect of LPS stimulation on Fra-1 activation in J774 macrophages**

J774 macrophages were activated with LPS ( $1 \mu\text{g ml}^{-1}$ ) over the time periods indicated on the graph. Nuclear extracts were prepared and subjected to analysis as described in the methods (Section 2.2.23).  $10 \mu\text{g}$  of nuclear content was used in an AP-1 family DNA binding kit using Fra-1 antibody and HRP-conjugated secondary. The absorbance was read at 450 nm. The results are representative of 3 independent experiments. Statistical analysis using a one way Anova followed by Dunnett's multiple comparison test was performed.  $*p < 0.05$  and  $**p < 0.01$  compared to control, non-activated results.

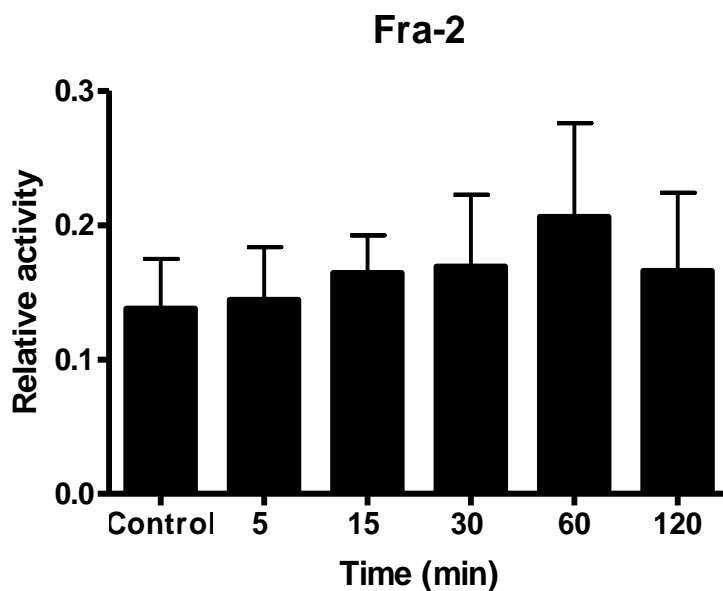


**Figure 5.18 The effect of LPS stimulation on Fra-2 activation in J774 macrophages**

J774 macrophages were activated with LPS ( $1 \mu\text{g ml}^{-1}$ ) over the time periods indicated on the graph. Nuclear extracts were prepared and subjected to analysis as described in the methods (Section 2.2.23).  $10 \mu\text{g}$  of nuclear content was used in an AP-1 family DNA binding kit using Fra-2 antibody and HRP-conjugated secondary. The absorbance was read at 450 nm. The results are representative of 3 independent experiments. Statistical analysis using a one way Anova followed by Dunnett's multiple comparison test was performed.

### 5.3.6 The effect of JNK inhibition on AP-1 subunits activity in RASMCs and J774 macrophages

Following from the above observations, studies were subsequently carried out investigating the effects of SP600125 at concentration of 0.3  $\mu\text{M}$  and 3  $\mu\text{M}$  on the activation of various AP-1 subunits by LPS (100  $\mu\text{g ml}^{-1}$ ) and IFN- $\gamma$  (100 U  $\text{ml}^{-1}$ ) in RASMCs or LPS alone (1  $\mu\text{g ml}^{-1}$ ) in J774 macrophages. Nuclear fractions were extract at different time point (30 min and 2 hours). The extracts were then used to identify different AP-1 subunits and their activated status using the TransAM kit as described in the methods (section 2.2.24).

SP600125 significantly inhibited c-Jun activation in both RASMCs and J774 macrophages. This was seen at the concentrations used and in both controls and activated cells (Figure 5.19 and 5.26). In contrast to its effects on c-Jun, SP600125 up-regulated Fra-1 in both cell systems (Figures 5.24 and 5.31) but selectively increased JunD (Figures 5.21) and c-Fos (Figures 5.22) in RASMCs. Fos-B on the other hand was selectively up-regulated in a non-concentration-dependent manner in control J774 macrophages (Figures 5.30) while Fra-2 remained unaffected in both cell types (Figures 5.25 and 5.32). What is even more interesting is the observation that JunB activity was significantly enhanced by SP600125 in both control and activated RASMCs (Figure 5.20) and J774 macrophages (Figure 5.27) even though the activity of this subunit was not altered by LPS or LPS and IFN- $\gamma$ . In RASMCs, FosB (Figure 5.23) and in J774 macrophages JunD (Figure 5.28) and c-Fos (Figure 5.29) did not reveal any changes after incubation with SP600125.

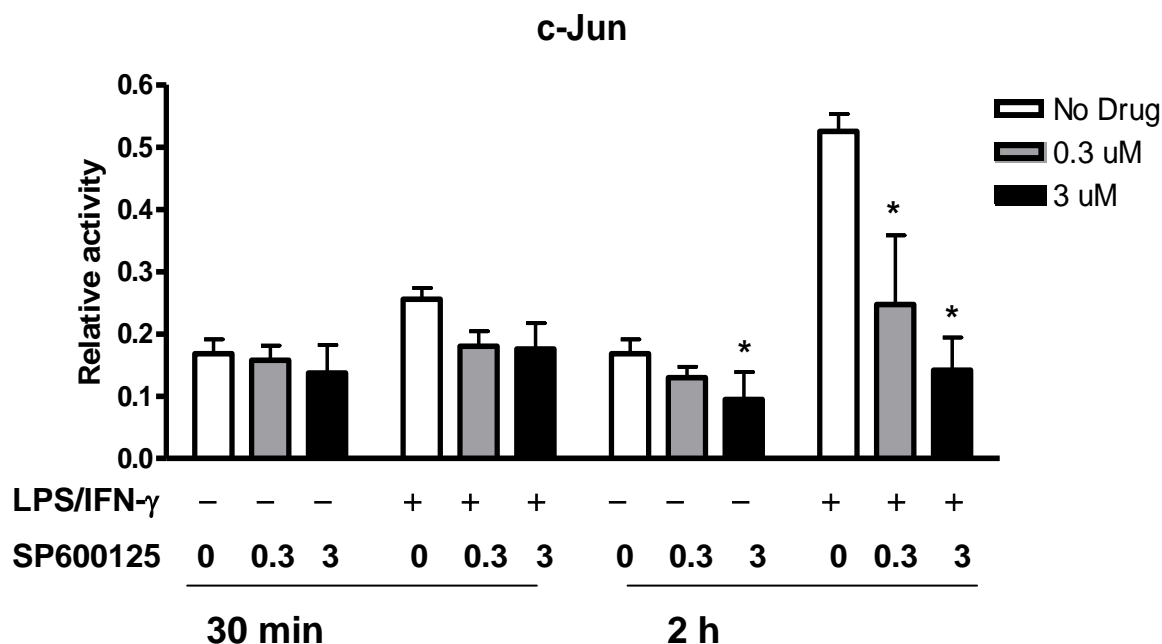


**Figure 5.19 Effect of SP600125 on activation of c-Jun in RASMCs**

RASMCs were incubated with SP600125 (0.3  $\mu\text{M}$  and 3  $\mu\text{M}$ ) for 30 min prior to activation with LPS (100  $\mu\text{g ml}^{-1}$ ) and IFN- $\gamma$  (100 U  $\text{ml}^{-1}$ ) for either 30 min or 2 hours. Nuclear extracts were prepared and analysed using the TransAM kit as described in the methods using a phospho-c-Jun antibody (methods, section 2.2.24). The activity of the subunit was measured and expressed as relative activity. Results are the mean  $\pm$  SEM of 3 independent experiments. Statistical analysis using two way Anova followed by multiple comparison test performed. \*  $p < 0.05$  and \*\* $p < 0.01$  compared to control or activated, non-drug results.

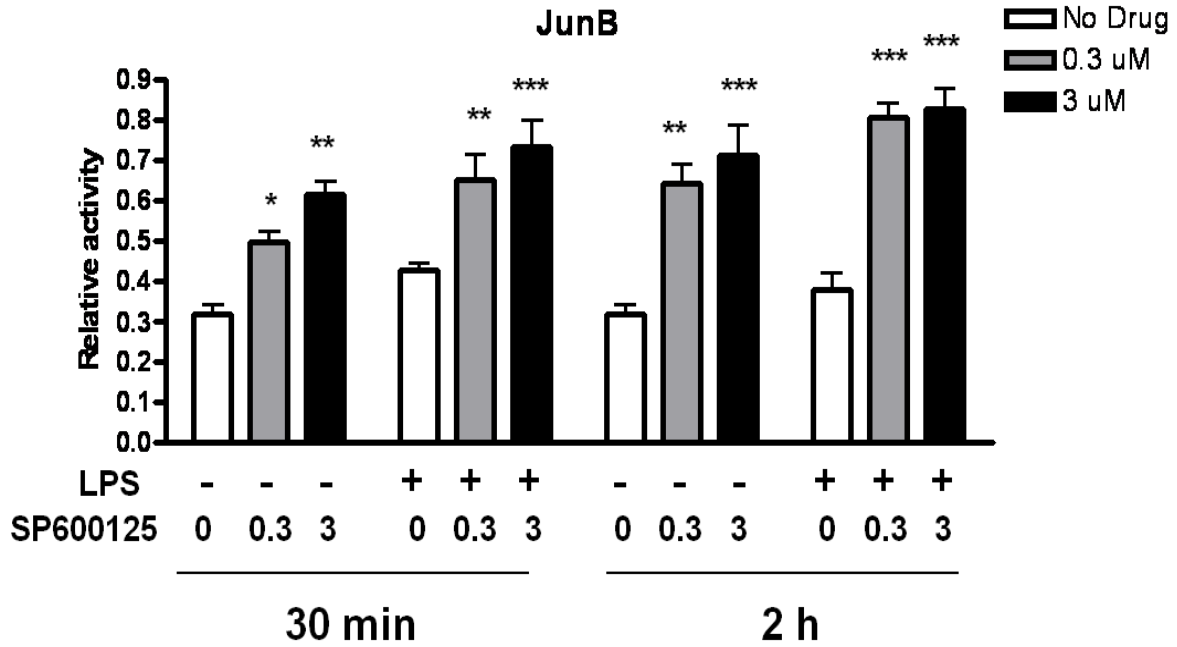


**Figure 5.20 Effect of SP600125 on activation of JunB in RASMCs**

RASMCs were incubated with SP600125 (0.3  $\mu$ M and 3  $\mu$ M) for 30 min prior to activation with LPS (100  $\mu$ g ml<sup>-1</sup>) and IFN- $\gamma$  (100 U ml<sup>-1</sup>) for either 30 min or 2 hours. Nuclear extracts were prepared and analysed using the TransAM kit as described in the methods using a JunB antibody. The activity of the subunit was measured and expressed as relative activity. The results are the mean  $\pm$  SEM of 3 independent experiments. Statistical analysis using two way Anova followed by multiple comparison test performed. \*  $p < 0.05$ , \*\* $p < 0.01$  and \*\*\* $p < 0.001$  compared to control or activated, non-drug results.

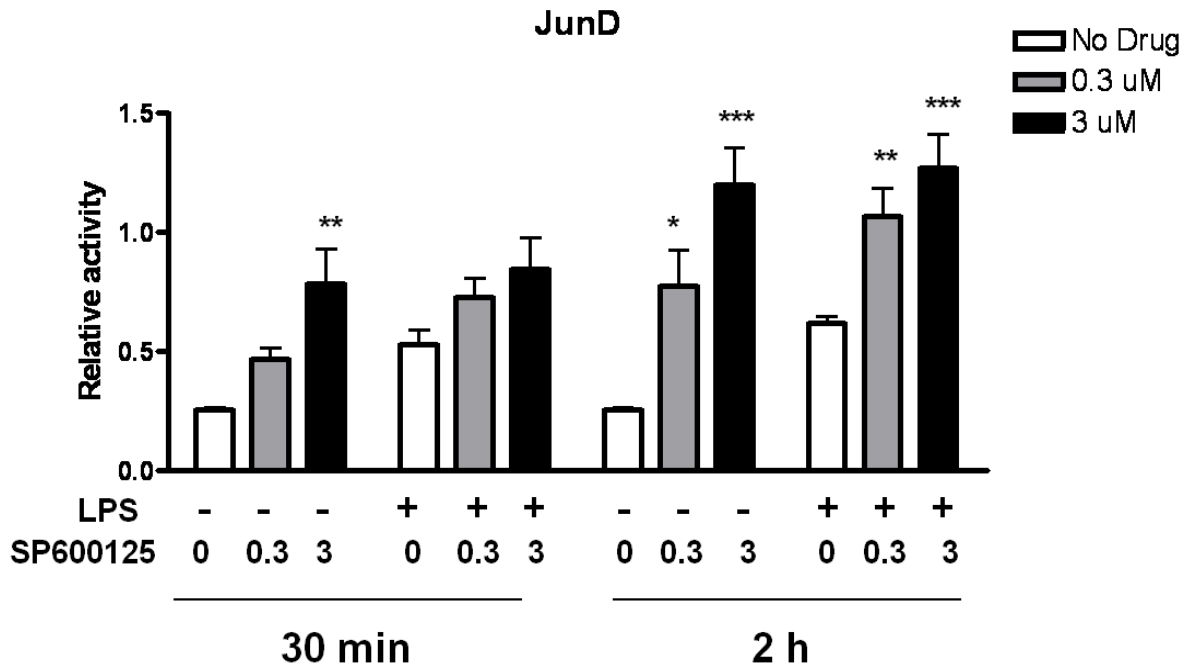


**Figure 5.21 Effect of SP600125 on activation of JunD in RASMCs**

RASMCs were incubated with SP600125 (0.3 μM and 3 μM) for 30 min prior to activation with LPS (100 μg ml<sup>-1</sup>) and IFN-γ (100 U ml<sup>-1</sup>) for either 30 min or 2 hours. Nuclear extracts were prepared and analysed using the TransAM kit as described in the methods using a JunD antibody. The activity of the subunit was measured and expressed as relative activity. The results are the mean ± SEM of 3 independent experiments. Statistical analysis using two way Anova followed by multiple comparison test performed. \* p<0.05, \*\*p<0.01 and \*\*\*p<0.001 compared to control or activated, non-drug results.

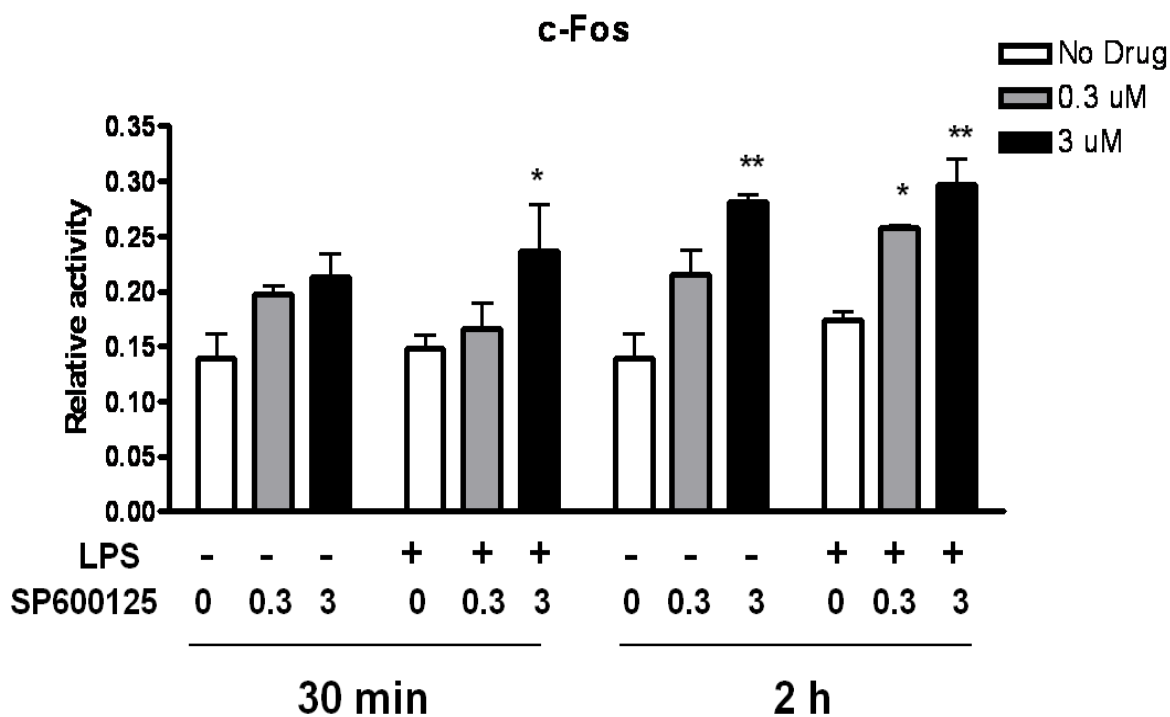


**Figure 5.22 Effect of SP600125 on activation of c-Fos in RASMCs**

RASMCs were incubated with SP600125 (0.3  $\mu\text{M}$  and 3  $\mu\text{M}$ ) for 30 min prior to activation with LPS (100  $\mu\text{g ml}^{-1}$ ) and IFN- $\gamma$  (100 U  $\text{ml}^{-1}$ ) for either 30 min or 2 hours. Nuclear extracts were prepared and analysed as described in the methods (Section 2.2.23). TransAM kit was run using c-Fos antibody. The activity of the subunit was measured and expressed as relative activity. The results are the mean  $\pm$  SEM of 3 independent experiments. Statistical analysis using two way Anova followed by multiple comparison test performed. \*  $p < 0.05$  and \*\* $p < 0.01$  compared to control or activated, non-drug results.

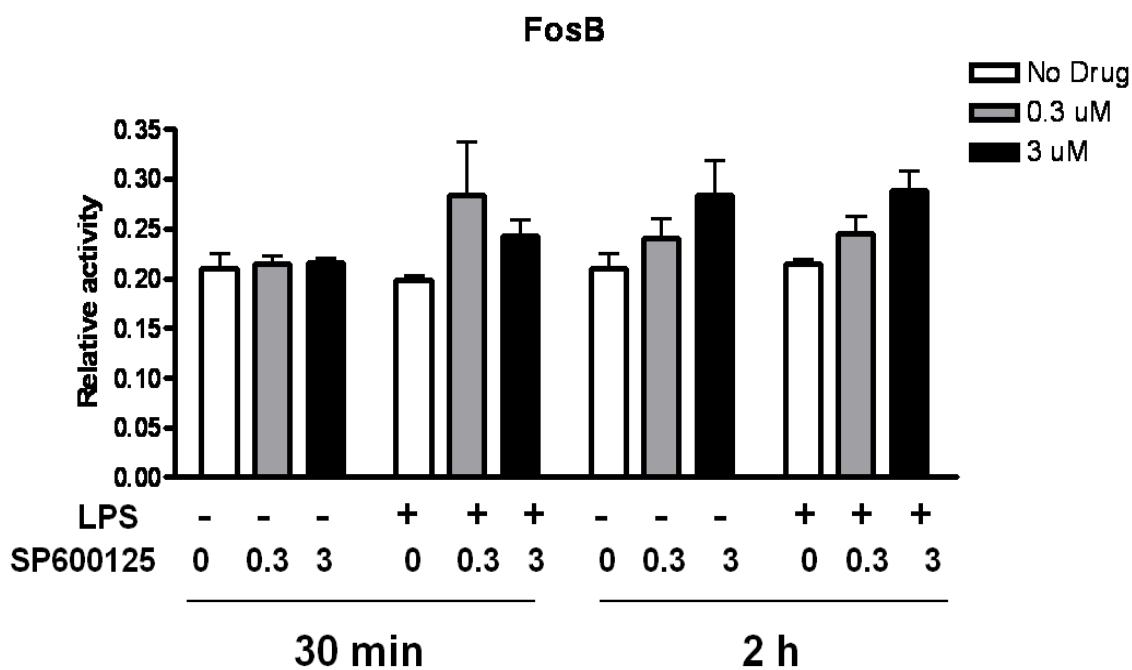


**Figure 5.23 Effect of SP600125 on activation of FosB in RASMCs**

RASMCs were incubated with SP600125 (0.3  $\mu\text{M}$  and 3  $\mu\text{M}$ ) for 30 min prior to activation with LPS (100  $\mu\text{g ml}^{-1}$ ) and IFN- $\gamma$  (100 U  $\text{ml}^{-1}$ ) for either 30 min or 2 hours. Nuclear extracts were prepared and analysed as described in the methods (Section 2.2.23). TransAM kit was run using FosB antibody. The activity of the subunit was measured and expressed as relative activity. The results are the mean  $\pm$  SEM of 3 independent experiments. Statistical analysis using two way Anova followed by multiple comparison test performed.

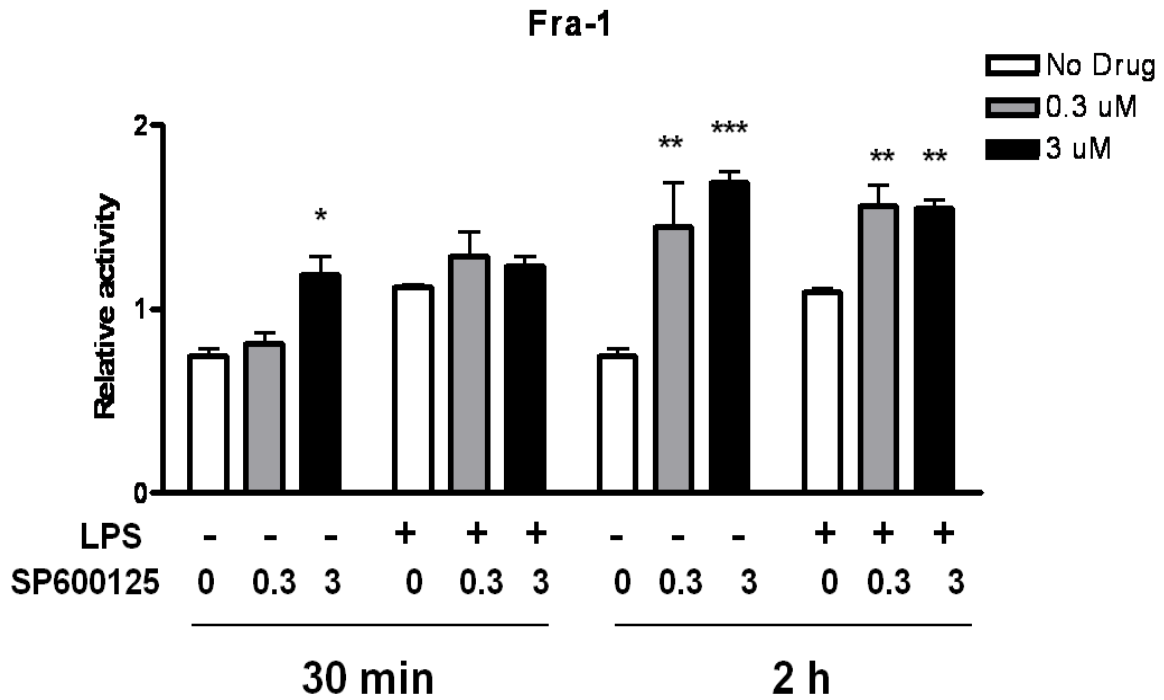


**Figure 5.24 Effect of SP600125 on activation of Fra-1 in RASMCs**

RASMCs were incubated with SP600125 (0.3  $\mu\text{M}$  and 3  $\mu\text{M}$ ) for 30 min prior to activation with LPS (100  $\mu\text{g ml}^{-1}$ ) and IFN- $\gamma$  (100 U  $\text{ml}^{-1}$ ) for either 30 min or 2 hours. Nuclear extracts were prepared and analysed as described in the methods (Section 2.2.123). TransAM kit was run using Fra-1 antibody. The activity of the subunit was measured and expressed as relative activity. The results are the mean  $\pm$  SEM of 3 independent experiments. Statistical analysis using two way Anova followed by multiple comparison test performed. \*  $p < 0.05$ , \*\* $p < 0.01$  and \*\*\* $p < 0.001$  compared to control or activated, non-drug results.

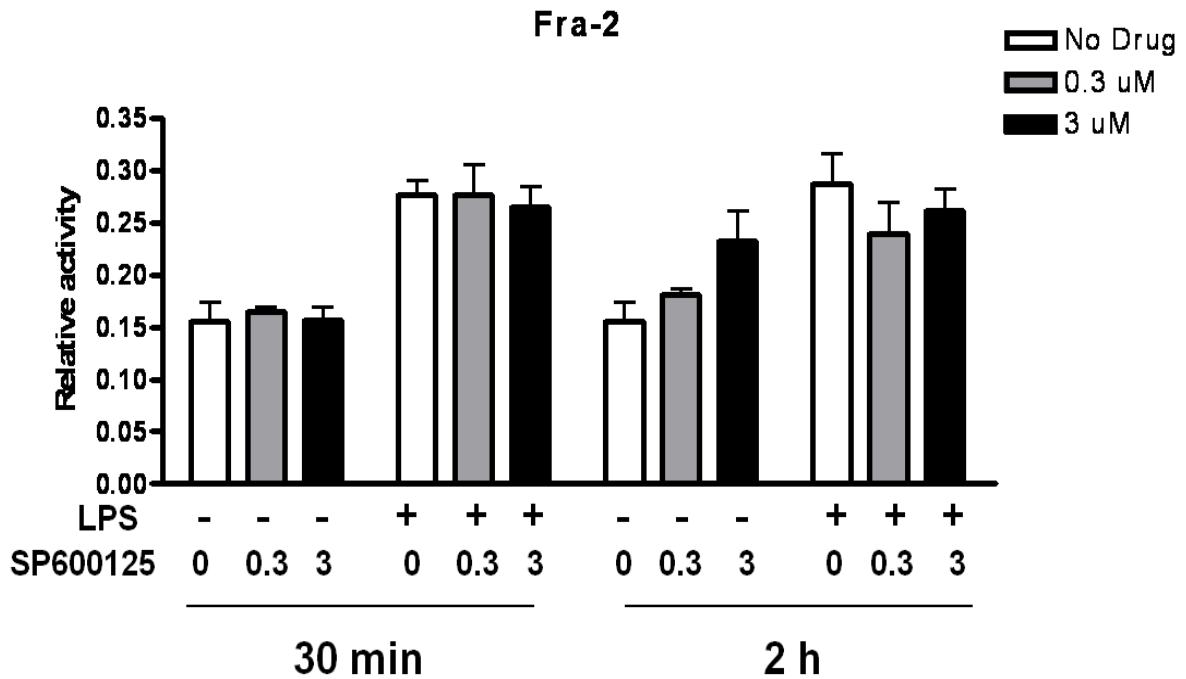


**Figure 5.25 Effect of SP600125 on activation of Fra-2 in RASMCs**

RASMCs were incubated with SP600125 (0.3  $\mu\text{M}$  and 3  $\mu\text{M}$ ) for 30 min prior to activation with LPS (100  $\mu\text{g ml}^{-1}$ ) and IFN- $\gamma$  (100 U  $\text{ml}^{-1}$ ) for either 30 min or 2 hours. Nuclear extracts were prepared and analysed as described in the methods (Section 2.2.23). TransAM kit was run using Fra-2 antibody. The activity of the subunit was measured and expressed as relative activity. The results are the mean  $\pm$  SEM of 3 independent experiments. Statistical analysis using two way Anova followed by multiple comparison test performed.

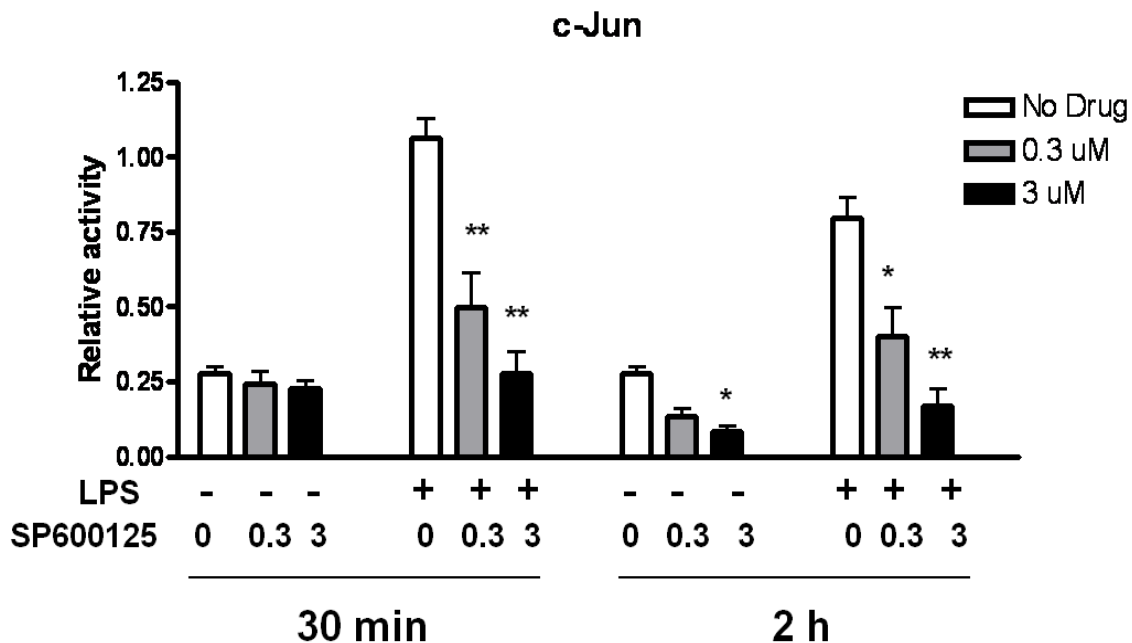


**Figure 5.26 Effect of SP600125 on activation of c-Jun in J774 macrophages**

J774 macrophages were incubated with SP600125 (0.3  $\mu\text{M}$  and 3  $\mu\text{M}$ ) for 30 min prior to activation with LPS (1  $\mu\text{g ml}^{-1}$ ) for either 30 min or 2 hours. Nuclear extracts were prepared and analysed as described in the methods (Section 2.2.23). TransAM kit was run using phospho-c-Jun antibody (Section 2.2.24). The activity of the subunit was measured and expressed as relative activity. The results are the mean  $\pm$  SEM of 3 independent experiments. Statistical analysis using two way Anova followed by multiple comparison test performed. \*  $p < 0.05$ , and \*\* $p < 0.01$  compared to control or activated, non-drug results.

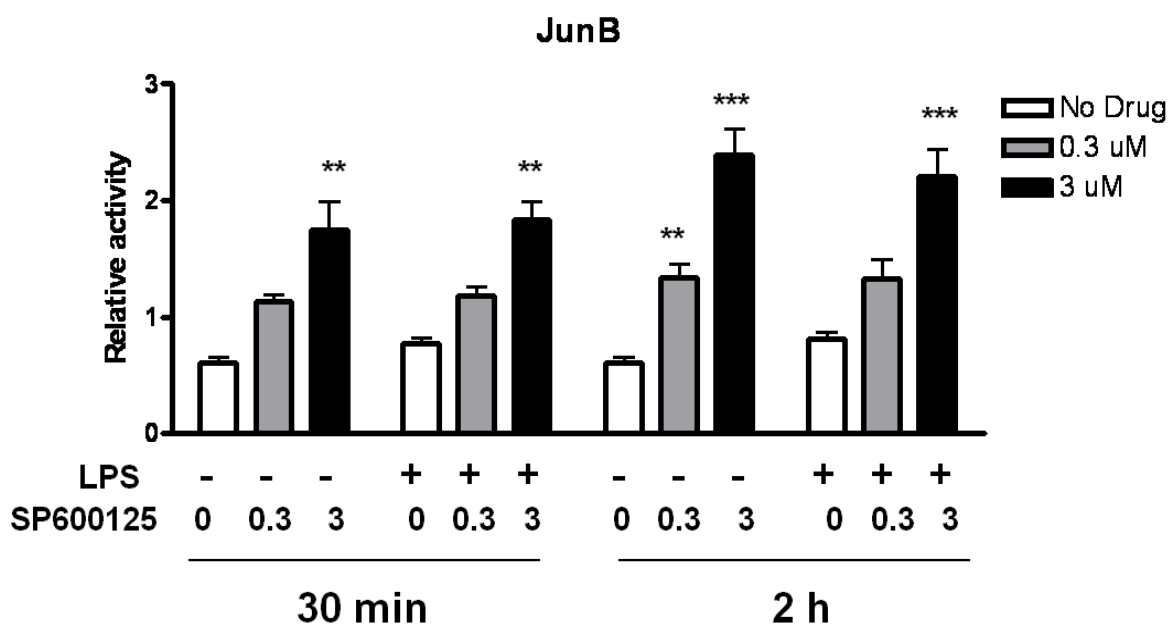


**Figure 5.27 Effect of SP600125 on activation of JunB in J774 macrophages**

J774 macrophages were incubated with SP600125 (0.3  $\mu$ M and 3  $\mu$ M) for 30 min prior to activation with LPS (1  $\mu$ g ml<sup>-1</sup>) for either 30 min or 2 hours. Nuclear extracts were prepared and analysed as described in the methods (Section 2.2.23). TransAM kit was run using JunB antibody (Section 2.2.24). The activity of the subunit was measured and expressed as relative activity. The results are the mean  $\pm$  SEM of 3 independent experiments. Statistical analysis using two way Anova followed by multiple comparison test performed. \*\*  $p < 0.01$ , and \*\*\*  $p < 0.001$  compared to control or activated, non-drug results.

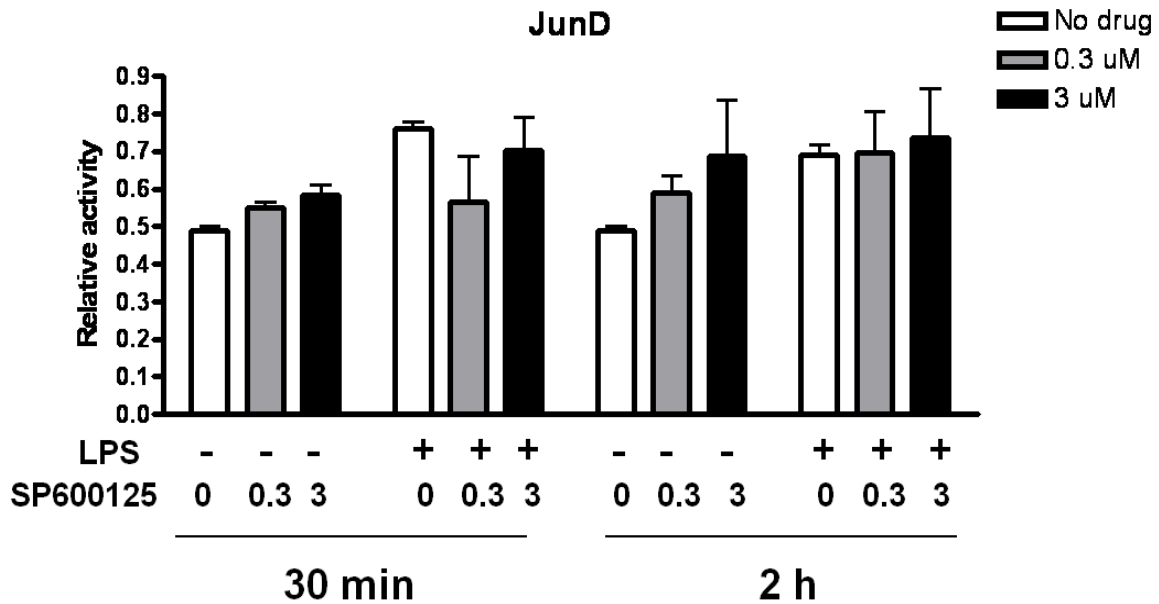


**Figure 5.28 Effect of SP600125 on activation of JunD in J774 macrophages**

J774 macrophages were incubated with SP600125 (0.3 μM and 3 μM) for 30 min prior to activation with LPS (1 μg ml<sup>-1</sup>) for either 30 min or 2 hours. Nuclear extracts were prepared and analysed as described in the methods (Section 2.2.23). TransAM kit was run using JunD antibody (Section 2.2.24). The activity of the subunit was measured and expressed as relative activity. The results are the mean ± SEM of 3 independent experiments. Statistical analysis using two way Anova followed by multiple comparison test performed.

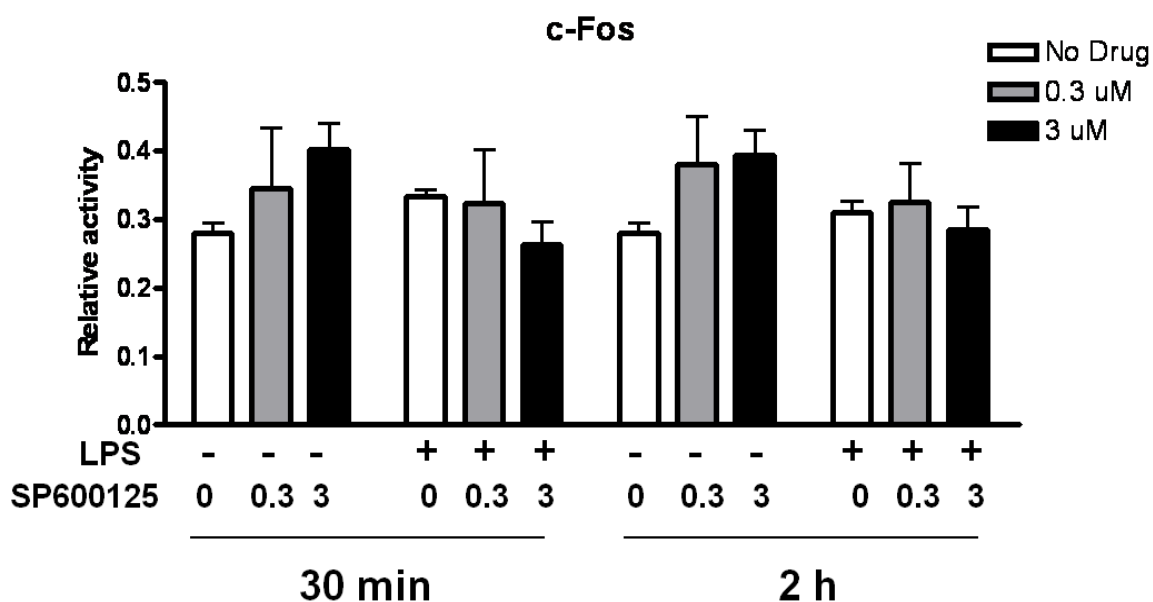


**Figure 5.29 Effect of SP600125 on activation of c-Fos in J774 macrophages**

J774 macrophages were incubated with SP600125 (0.3  $\mu$ M and 3  $\mu$ M) for 30 min prior to activation with LPS (1  $\mu$ g ml<sup>-1</sup>) for either 30 min or 2 hours. Nuclear extracts were prepared and analysed as described in the methods (Section 2.2.23). TransAM kit was run using c-Fos antibody (Section 2.2.24). The activity of the subunit was measured and expressed as relative activity. The results are the mean  $\pm$  SEM of 3 independent experiments. Statistical analysis using two way Anova followed by multiple comparison test performed.

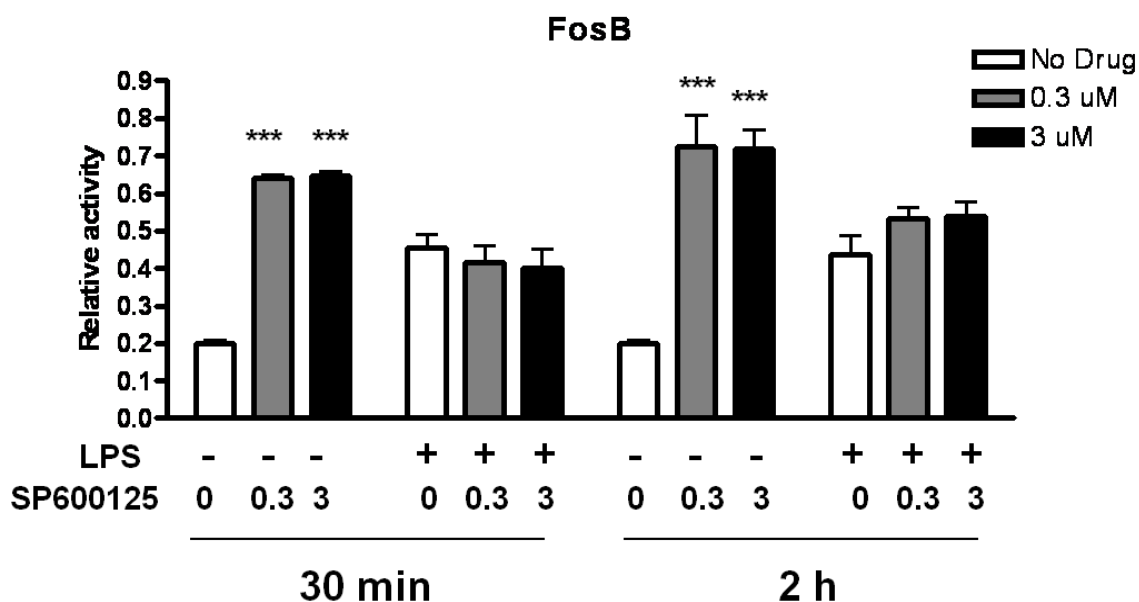


**Figure 5.30 Effect of SP600125 on activation of FosB in J774 macrophages**

J774 macrophages were incubated with SP600125 (0.3  $\mu$ M and 3  $\mu$ M) for 30 min prior to activation with LPS (1  $\mu$ g ml<sup>-1</sup>) for either 30 min or 2 hours. Nuclear extracts were prepared and analysed as described in the methods (Section 2.2.23). TransAM kit was run using FosB antibody (Section 2.2.24). The activity of the subunit was measured and expressed as relative activity. The results are the mean  $\pm$  SEM of 3 independent experiments. Statistical analysis using two way Anova followed by multiple comparison test performed. \*\*\* $p$ <0.001 compared to control or activated, non-drug results.

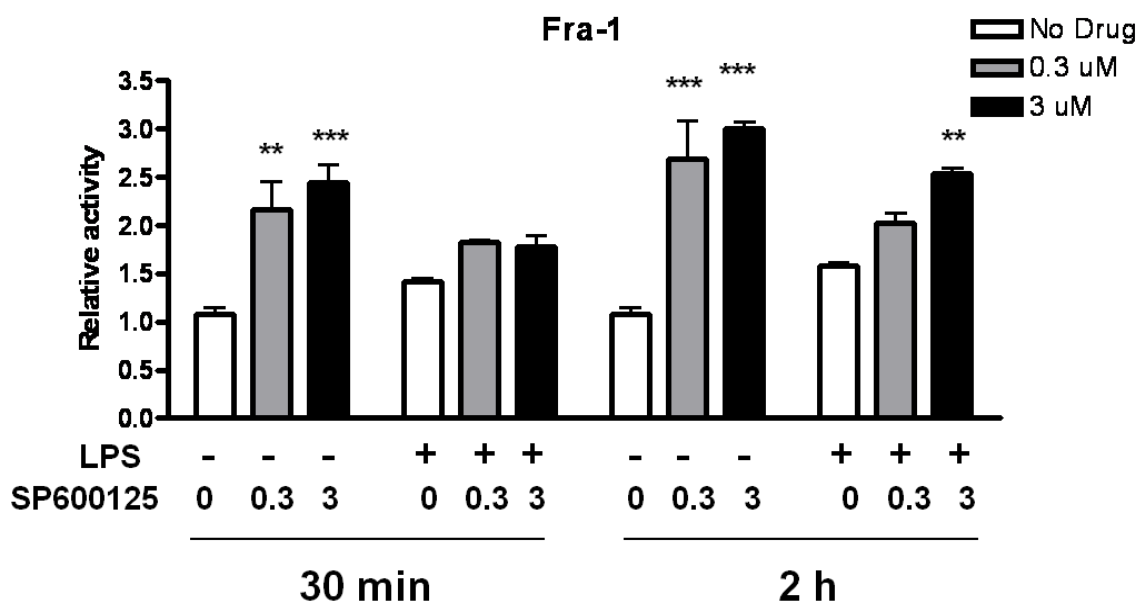


**Figure 5.31 Effect of SP600125 on activation of Fra-1 in J774 macrophages**

J774 macrophages were incubated with SP600125 (0.3  $\mu$ M and 3  $\mu$ M) for 30 min prior to activation with LPS (1  $\mu$ g ml<sup>-1</sup>) for either 30 min or 2 hours. Nuclear extracts were prepared and analysed as described in the methods (Section 2.2.23). TransAM kit was run using Fra-1 antibody (Section 2.2.24). The activity of the subunit was measured and expressed as relative activity. The results are the mean  $\pm$  SEM of 3 independent experiments. Statistical analysis using two way Anova followed by multiple comparison test performed. \*\*p<0.01 and \*\*\*p<0.001 compared to control or activated, non-drug results.

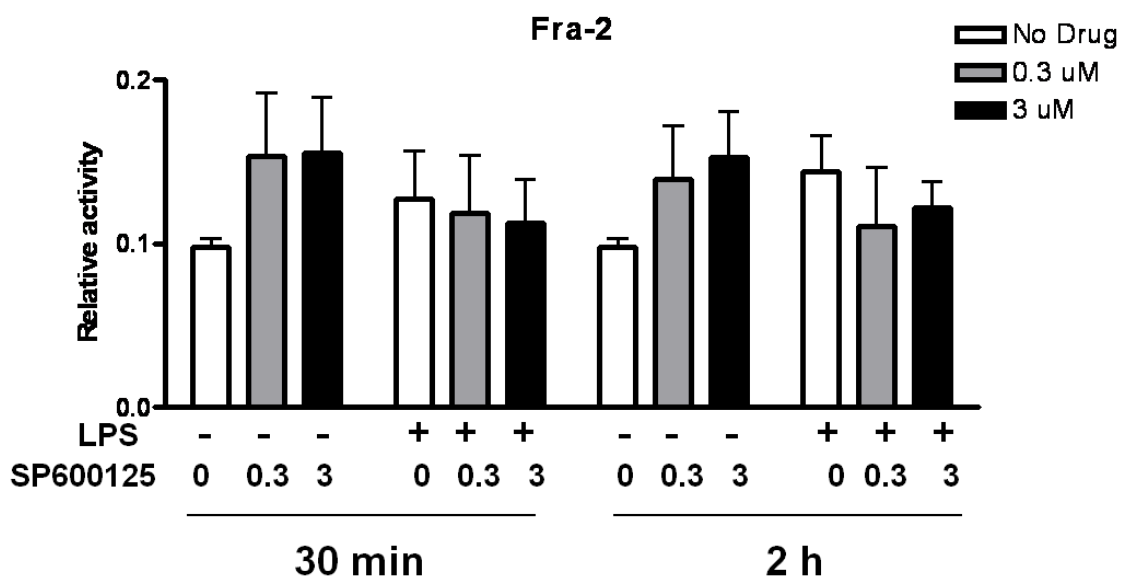


**Figure 5.32 Effect of SP600125 on activation of Fra-2 in J774 macrophages**

J774 macrophages were incubated with SP600125 (0.3  $\mu\text{M}$  and 3  $\mu\text{M}$ ) for 30 min prior to activation with LPS (1  $\mu\text{g ml}^{-1}$ ) for either 30 min or 2 hours. Nuclear extracts were prepared and analysed as described in the methods (Section 2.2.23). TransAM kit was run using Fra-2 antibody (Section 2.2.24). The activity of the subunit was measured and expressed as relative activity. The results are the mean  $\pm$  SEM of 3 independent experiments. Statistical analysis using two way Anova followed by multiple comparison test performed.

### **5.3.7 The effect of a-Fos and TAM-67 on activation of AP-1 subunits in RASMCs**

To determine the effect of AP-1 dominant negatives construct on DNA binding activity of each subunit in RASMCs, the cells were transfected with either pGFP-a-Fos or pGFP-TAM-67 for 18 hours as described before. The cells were then activated with LPS ( $100 \mu\text{g ml}^{-1}$ ) and IFN- $\gamma$  ( $100 \text{ U ml}^{-1}$ ) for a further 30 min or 2 hours and nuclear extract generated for analysis using the TransAM AP-1 family kit as described in the methods (section 2.2.24).

In these studies, transfection of RASMCs with a-Fos caused a reduction in the activation of c-Jun (Figure 5.33), c-Fos (Figure 5.36) and FosB (Figure 5.37) but did not alter JunB (Figure 5.34), JunD (Figure 5.35), Fra-1 (Figure 5.38) or Fra-2 (figure 5.39). By comparison, TAM-67 had no effect on the activation of JunB (Figure 5.41), JunD (Figure 5.42), FosB (Figure 5.44), or Fra-2 (Figure 5.46) but inhibited c-Jun (Figure 5.40) and c-Fos (Figure 5.43) while enhancing the activation of Fra-1 but only in control non-activated cells (Figure 5.45).

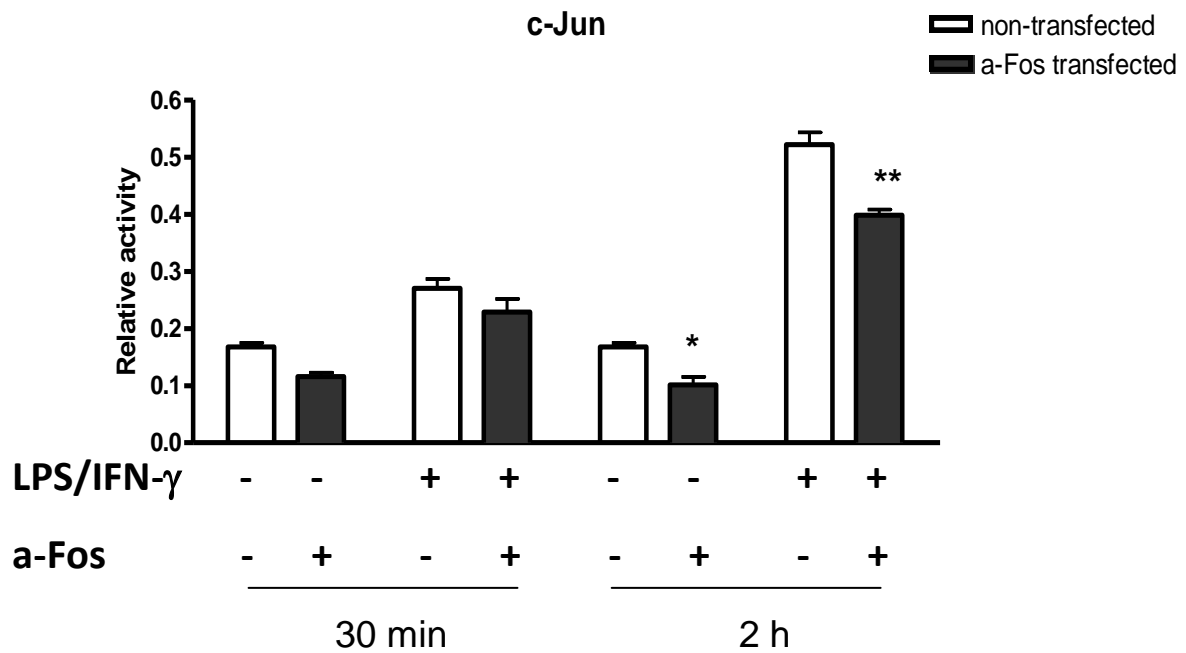


**Figure 5.33 Effects of a-Fos on c-Jun activation in RASMCs**

Partially confluent monolayers of RASMCs were transfected with a-Fos for 18 hours. The cells were then activated with LPS ( $100 \mu\text{g ml}^{-1}$ ) and IFN- $\gamma$  ( $100 \text{ U ml}^{-1}$ ) for a further 30 min or 2 hours. The nuclear extracts were prepared and analysed using a TransAM kit as described in the methods (section 2.2.24). The results are representative of 3 independent experiments. Statistical analysis using two way Anova followed by multiple comparison test was performed. \* $p < 0.05$  and \*\* $p < 0.01$  compared to non-transfected results.

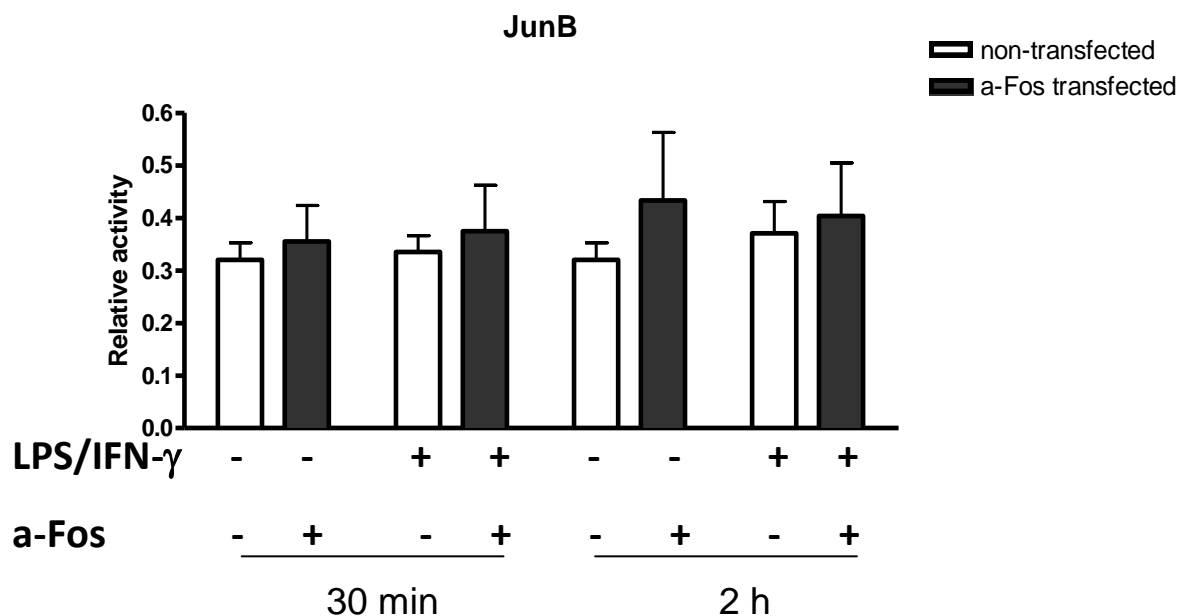


**Figure 5.34 Effects of a-Fos on JunB activation in RASMCs**

Partially confluent monolayers of RASMCs were transfected with a-Fos for 18 hours. The cells were then activated with LPS ( $100 \mu\text{g ml}^{-1}$ ) and IFN- $\gamma$  ( $100 \text{ U ml}^{-1}$ ) for a further 30 min or 2 hours. The nuclear extracts were prepared and analysed using a TransAM kit as described in the methods (section 2.2.24). The results are representative of 3 independent experiments. Statistical analysis using two way Anova followed by multiple comparison test was performed.

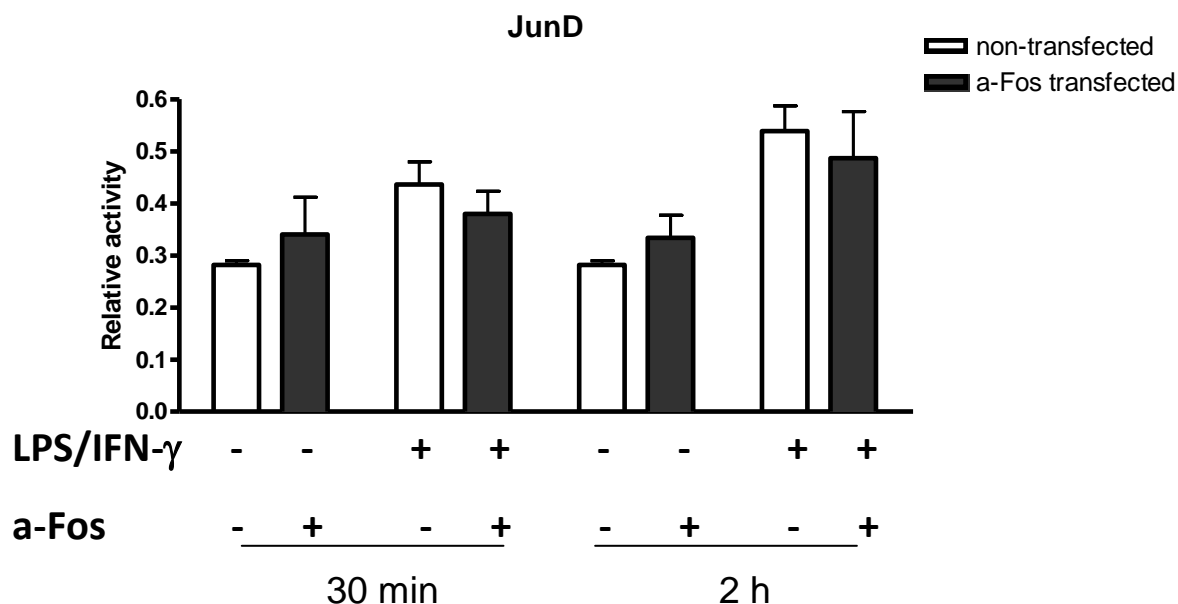


**Figure 5.35 Effects of a-Fos on JunD activation in RASMCs**

Partially confluent monolayers of RASMCs were transfected with a-Fos for 18 hours. The cells were then activated with LPS ( $100 \mu\text{g ml}^{-1}$ ) and IFN- $\gamma$  ( $100 \text{ U ml}^{-1}$ ) for a further 30 min or 2 hours. The nuclear extracts were prepared and analysed using a TransAM kit as described in the methods (section 2.2.24). The results are representative of 3 independent experiments. Statistical analysis using two way Anova followed by multiple comparison test was performed.

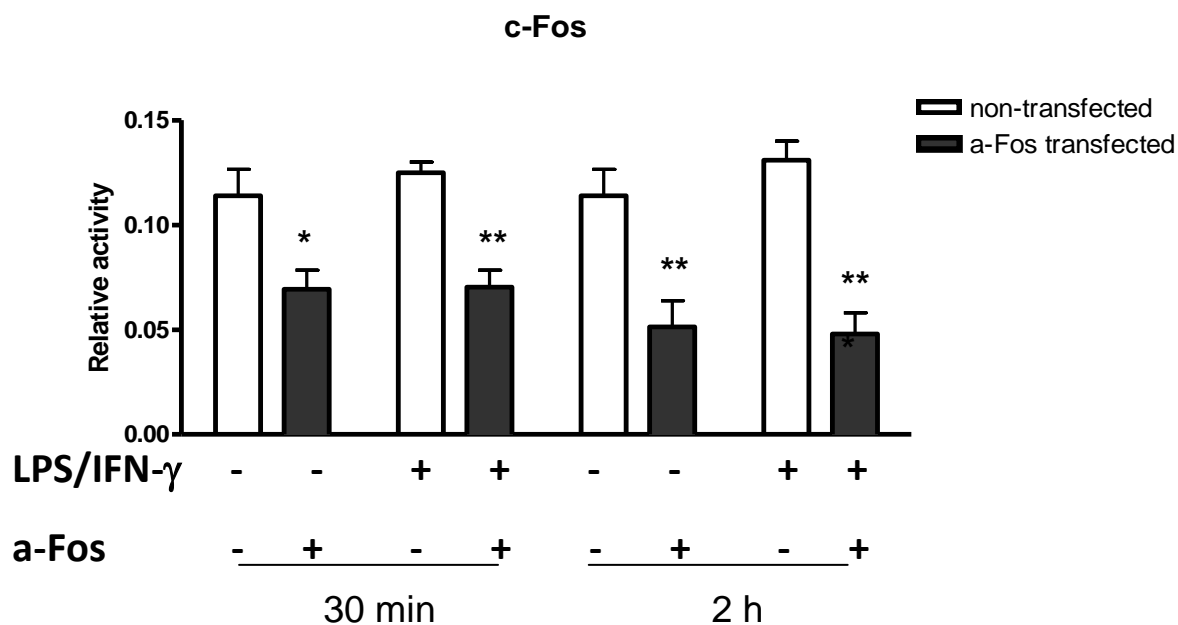


**Figure 5.36 Effects of a-Fos on c-Fos activation in RASMCs**

Partially confluent monolayers of RASMCs were transfected with a-Fos for 18 hours. The cells were then activated with LPS ( $100 \mu\text{g ml}^{-1}$ ) and IFN- $\gamma$  ( $100 \text{ U ml}^{-1}$ ) for a further 30 min or 2 hours. The nuclear extracts were prepared and analysed using a TransAM kit as described in the methods (section 2.2.24). The results are representative of 3 independent experiments. Statistical analysis using two way Anova followed by multiple comparison test performed. \* $p < 0.05$ , \*\* $p < 0.01$  and \*\*\* $p < 0.001$  compared to non-transfected results.

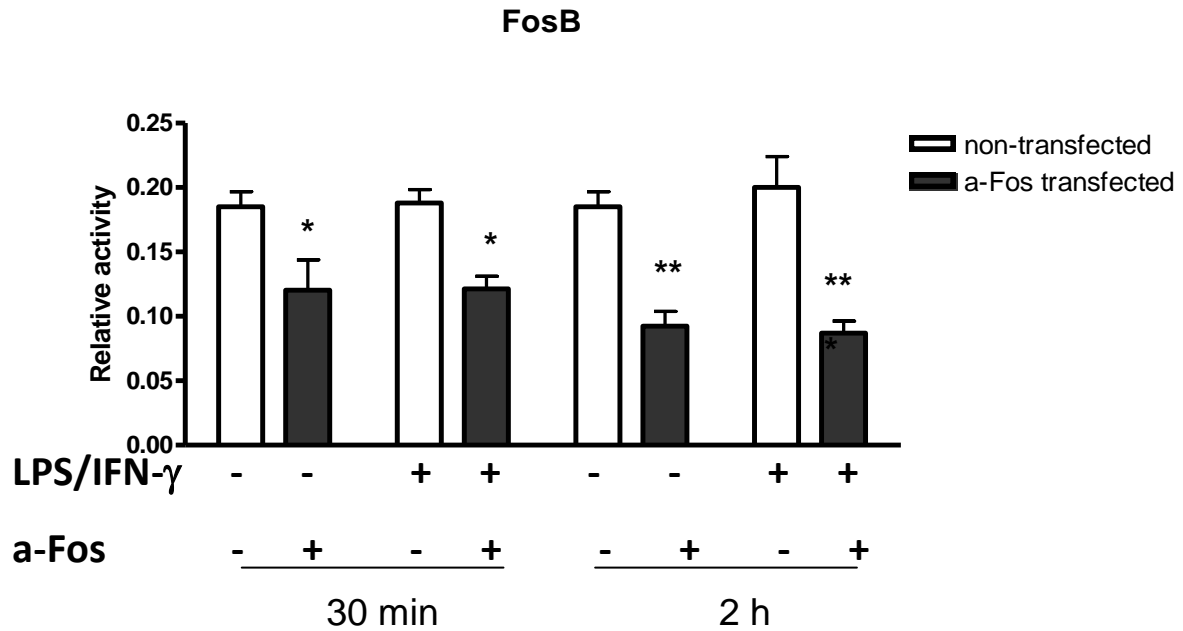


**Figure 5.37 Effects of a-Fos on FosB activation in RASMCs**

Partially confluent monolayers of RASMCs were transfected with a-Fos for 18 hours. The cells were then activated with LPS ( $100 \mu\text{g ml}^{-1}$ ) and IFN- $\gamma$  ( $100 \text{ U ml}^{-1}$ ) for a further 30 min or 2 hours. The nuclear extracts were prepared and analysed using a TransAM kit as described in the methods (section 2.2.24). The results are representative of 3 independent experiments. Statistical analysis using two way Anova followed by multiple comparison test was performed. \* $p < 0.05$ , \*\* $p < 0.01$  and \*\*\* $p < 0.001$  compared to non-transfected results.

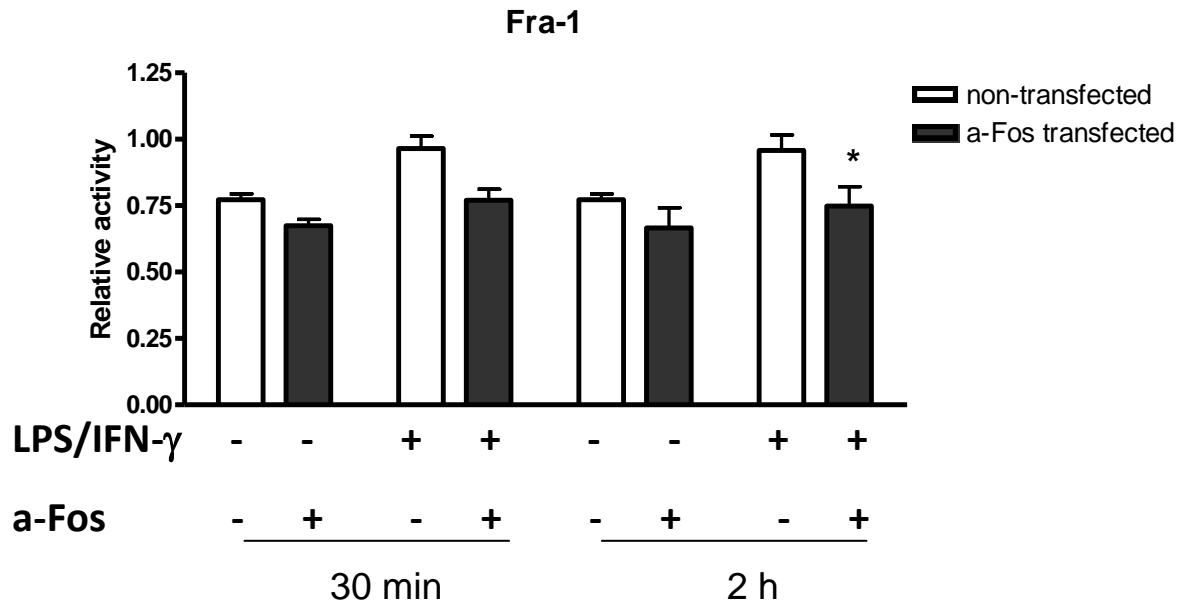


**Figure 5.38 Effects of a-Fos on Fra-1 activation in RASMCs**

Partially confluent monolayers of RASMCs were transfected with a-Fos for 18 hours. The cells were then activated with LPS ( $100 \mu\text{g ml}^{-1}$ ) and IFN- $\gamma$  ( $100 \text{ U ml}^{-1}$ ) for a further 30 min or 2 hours. The nuclear extracts were prepared and analysed using a TransAM kit as described in the methods (section 2.2.24) and the activity of Fra-1 was measured using the specific antibody. The results are representative of 3 independent experiments. Statistical analysis using two way Anova followed by multiple comparison test was performed. \* $p < 0.05$  compared to non-transfected results.

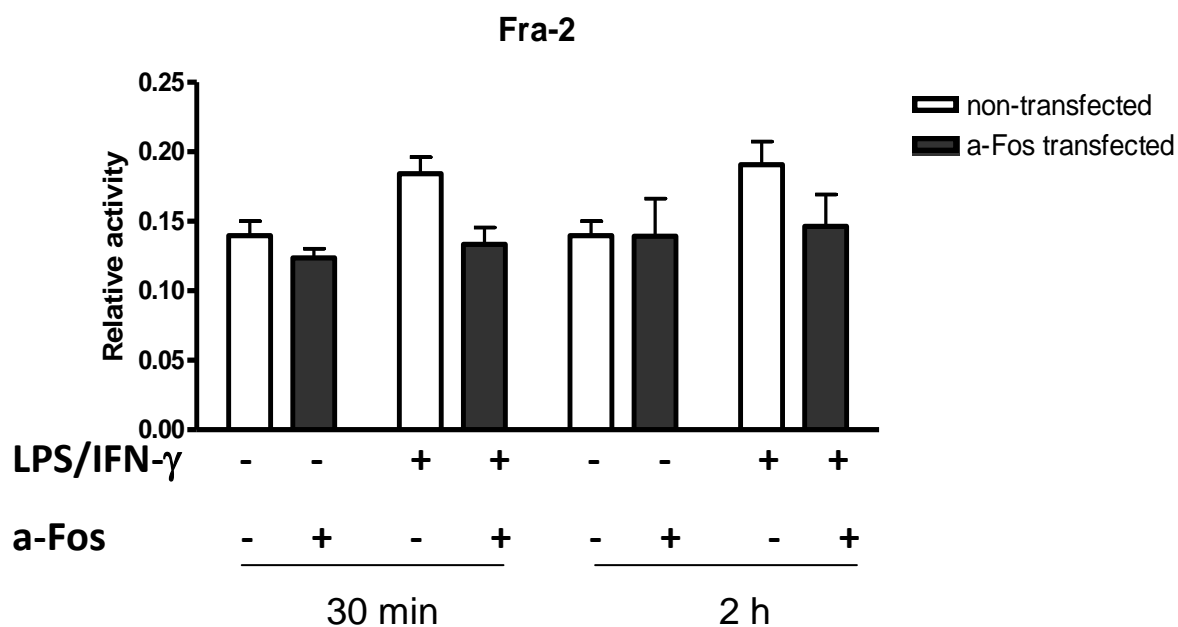


**Figure 5.39 Effects of a-Fos on Fra-2 activation in RASMCs**

Partially confluent monolayers of RASMCs were transfected with a-Fos for 18 hours. The cells were then activated with LPS ( $100 \mu\text{g ml}^{-1}$ ) and IFN- $\gamma$  ( $100 \text{ U ml}^{-1}$ ) for a further 30 min or 2 hours. The nuclear extracts were prepared and analysed using a TransAM kit as described in the methods (section 2.2.24) and the activity of Fra-2 was measured using the specific antibody. The results are representative of 3 independent experiments. Statistical analysis using two way Anova followed by multiple comparison test was performed.

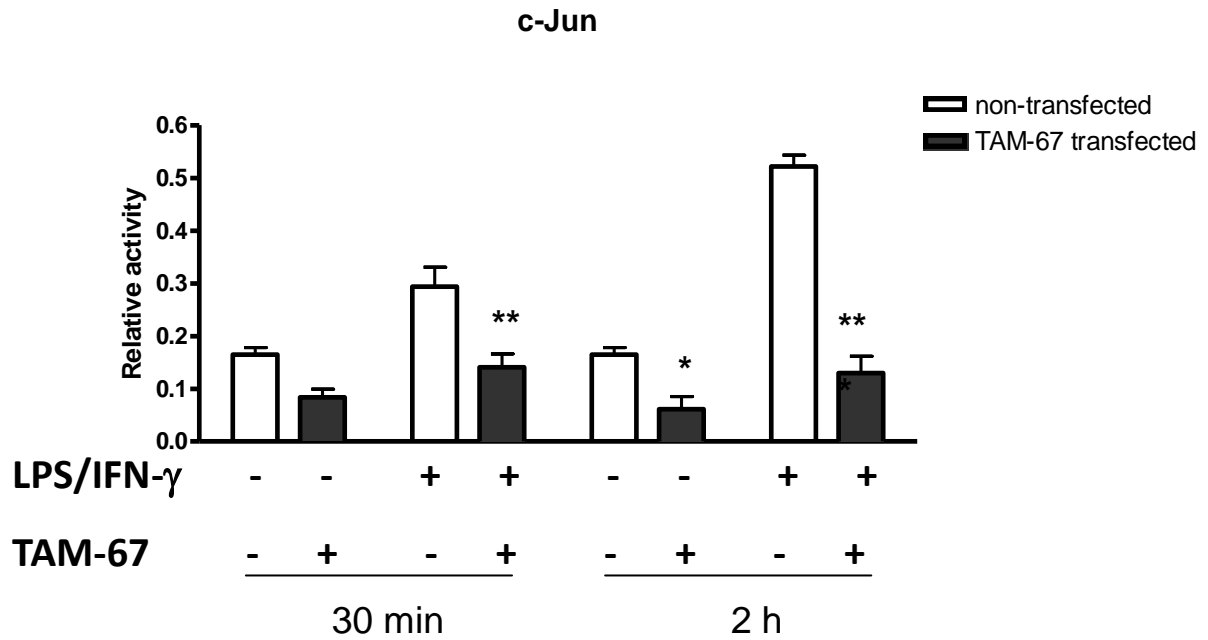


**Figure 5.40 Effects of TAM-67 on c-Jun activation in RASMCs**

Partially confluent monolayers of RASMCs were transfected with TAM-67 for 18 hours. The cells were then activated with LPS ( $100 \mu\text{g ml}^{-1}$ ) and IFN- $\gamma$  ( $100 \text{ U ml}^{-1}$ ) for a further 30 min or 2 hours. The nuclear extracts were prepared and analysed using a TransAM kit as described in the methods (section 2.2.24). The results are representative of 3 independent experiments. Statistical analysis using two way Anova followed by multiple comparison test was performed. \* $p < 0.05$ , \*\* $p < 0.01$  and \*\*\* $p < 0.001$  compared to non-transfected results.

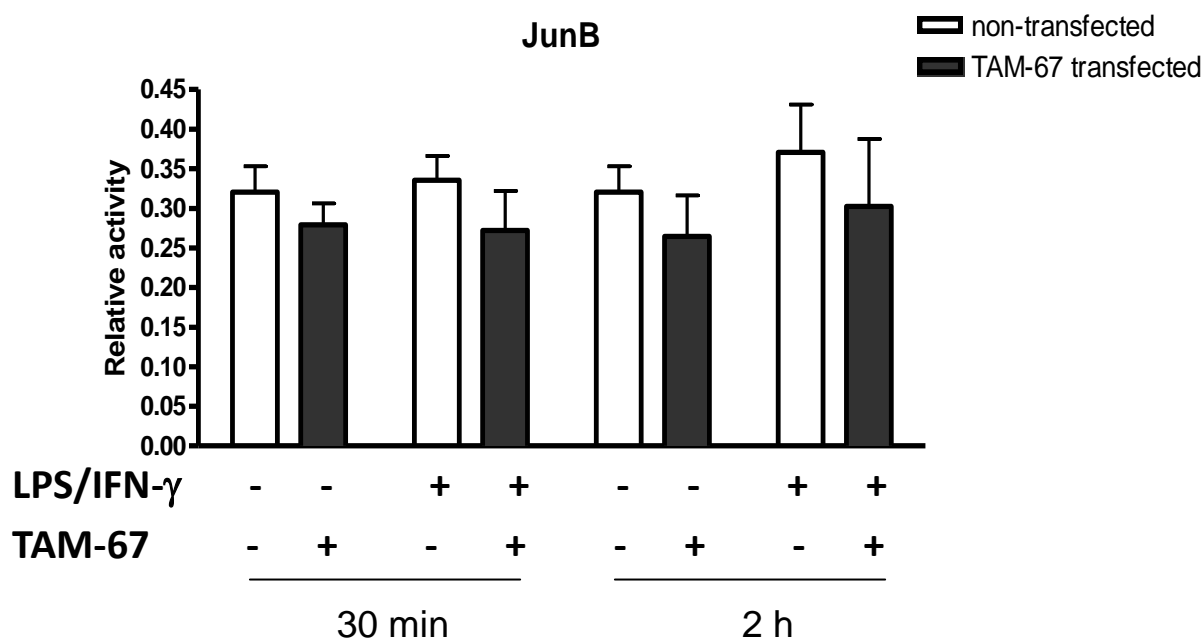


**Figure 5.41 Effects of TAM-67 on JunB activation in RASMCs**

Partially confluent monolayers of RASMCs were transfected with TAM-67 for 18 hours. The cells were then activated with LPS ( $100 \mu\text{g ml}^{-1}$ ) and IFN- $\gamma$  ( $100 \text{ U ml}^{-1}$ ) for a further 30 min or 2 hours. The nuclear extracts were prepared and analysed using a TransAM kit as described in the methods (section 2.2.24). The results are representative of 3 independent experiments. Statistical analysis using two way Anova followed by multiple comparison test was performed.

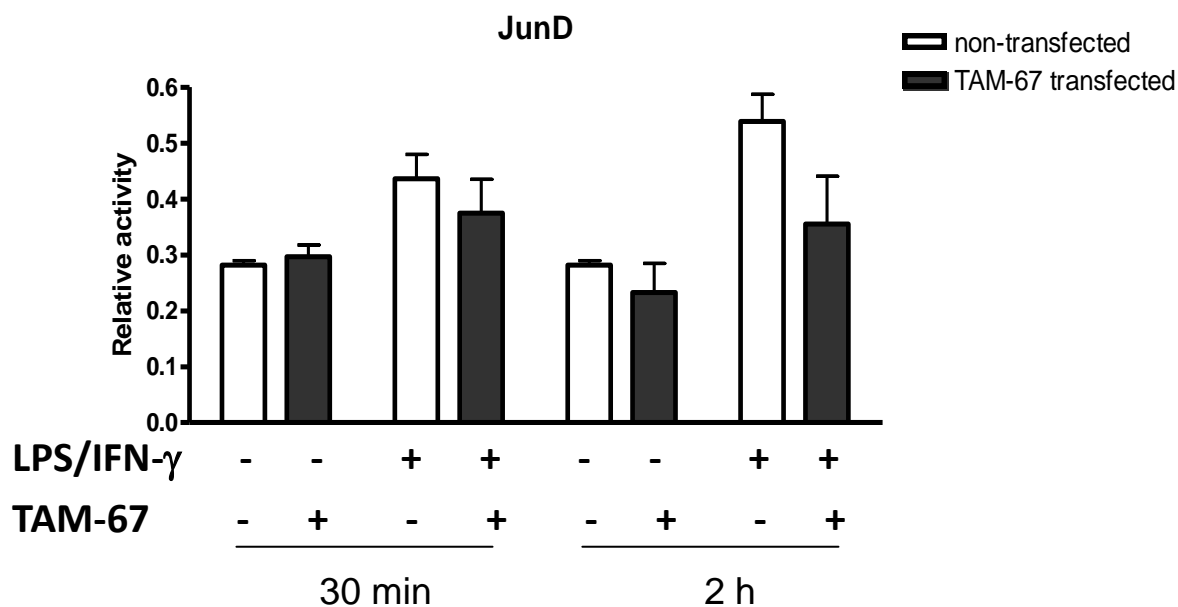


**Figure 5.42 Effects of TAM-67 on JunD activation in RASMCs**

Partially confluent monolayers of RASMCs were transfected with TAM-67 for 18 hours. The cells were then activated with LPS ( $100 \mu\text{g ml}^{-1}$ ) and IFN- $\gamma$  ( $100 \text{ U ml}^{-1}$ ) for a further 30 min or 2 hours. The nuclear extracts were prepared and analysed using a TransAM kit as described in the methods (section 2.2.24). The results are representative of 3 independent experiments. Statistical analysis using two way Anova followed by multiple comparison test was performed.

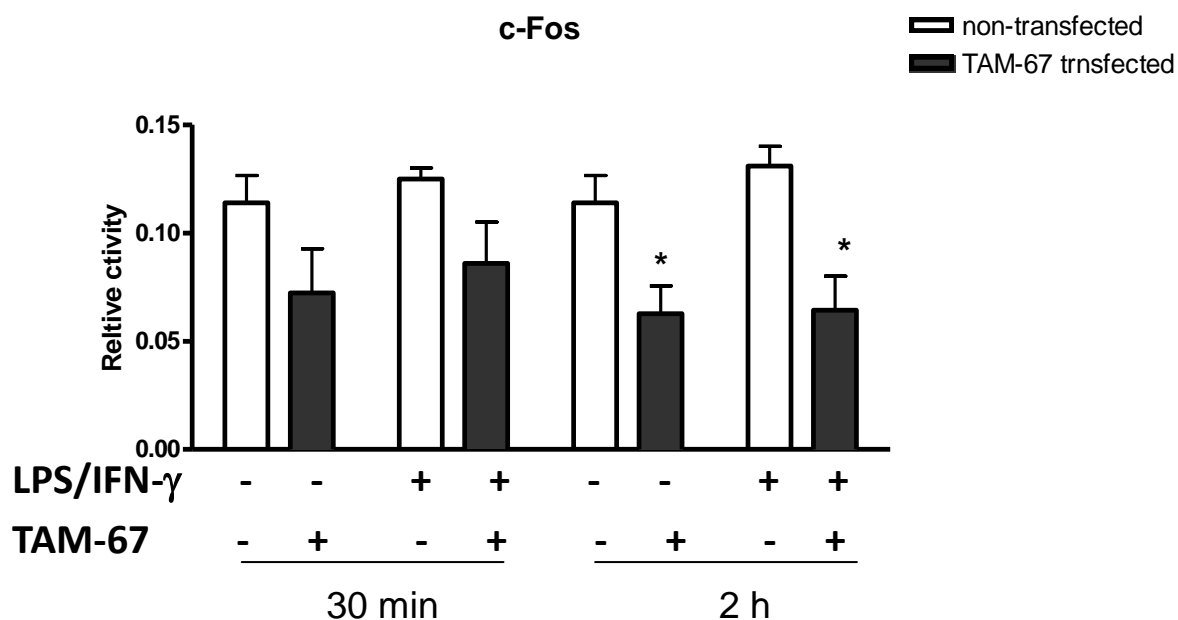


**Figure 5.43 Effects of TAM-67 on c-Fos activation in RASMCs**

Partially confluent monolayers of RASMCs were transfected with TAM-67 for 18 hours. The cells were then activated with LPS ( $100 \mu\text{g ml}^{-1}$ ) and IFN- $\gamma$  ( $100 \text{ U ml}^{-1}$ ) for a further 30 min or 2 hours. The nuclear extracts were prepared and analysed using a TransAM kit as described in the methods (section 2.2.24). The results are representative of 3 independent experiments. Statistical analysis using two way Anova followed by multiple comparison test was performed. \* $p < 0.05$  compared to non-transfected results.

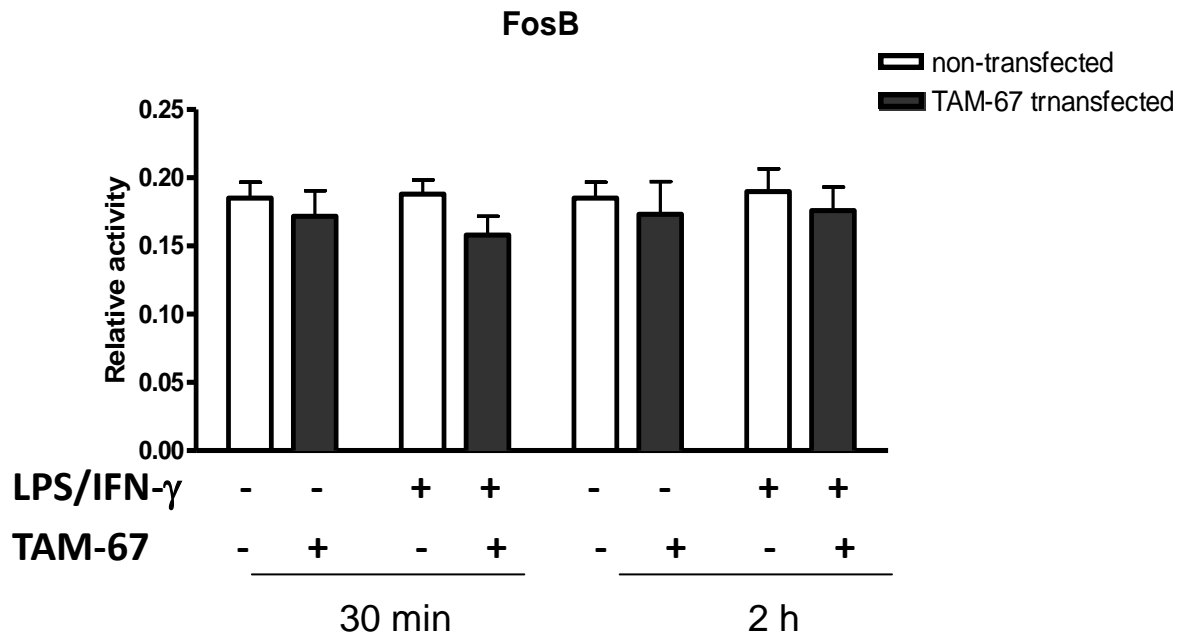


**Figure 5.44 Effects of TAM-67 on FosB activation in RASMCs**

Partially confluent monolayers of RASMCs were transfected with TAM-67 for 18 hours. The cells were then activated with LPS ( $100 \mu\text{g ml}^{-1}$ ) and IFN- $\gamma$  ( $100 \text{ U ml}^{-1}$ ) for a further 30 min or 2 hours. The nuclear extracts were prepared and analysed using a TransAM kit as described in the methods (section 2.2.24) and the activity of FosB was measured using the specific antibody. The results are representative of 3 independent experiments. Statistical analysis using two way Anova followed by multiple comparison test was performed.

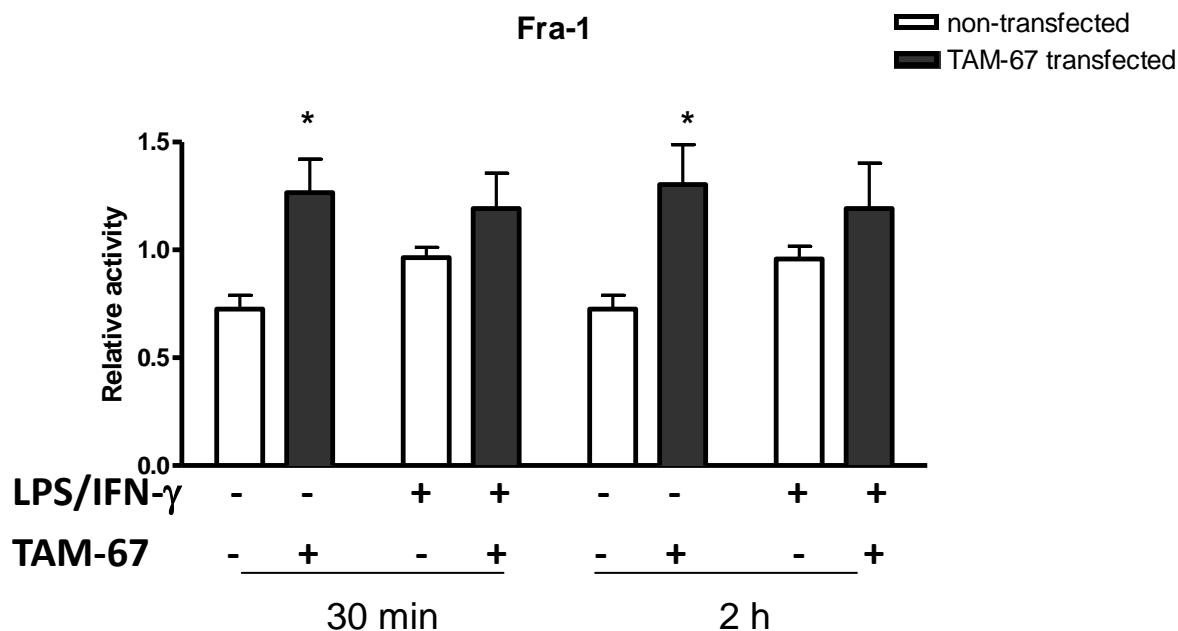


**Figure 5.45 Effects of TAM-67 on Fra-1 activation in RASMCs**

Partially confluent monolayers of RASMCs were transfected with TAM-67 for 18 hours. The cells were then activated with LPS ( $100 \mu\text{g ml}^{-1}$ ) and IFN- $\gamma$  ( $100 \text{ U ml}^{-1}$ ) for a further 30 min or 2 hours. The nuclear extracts were prepared and analysed using a TransAM kit as described in the methods (section 2.2.24) and the activity of Fra-1 was measured using the specific antibody. The results are representative of 3 independent experiments. Statistical analysis using two way Anova followed by multiple comparison test was performed. \* $p < 0.05$  compared to non-transfected results.

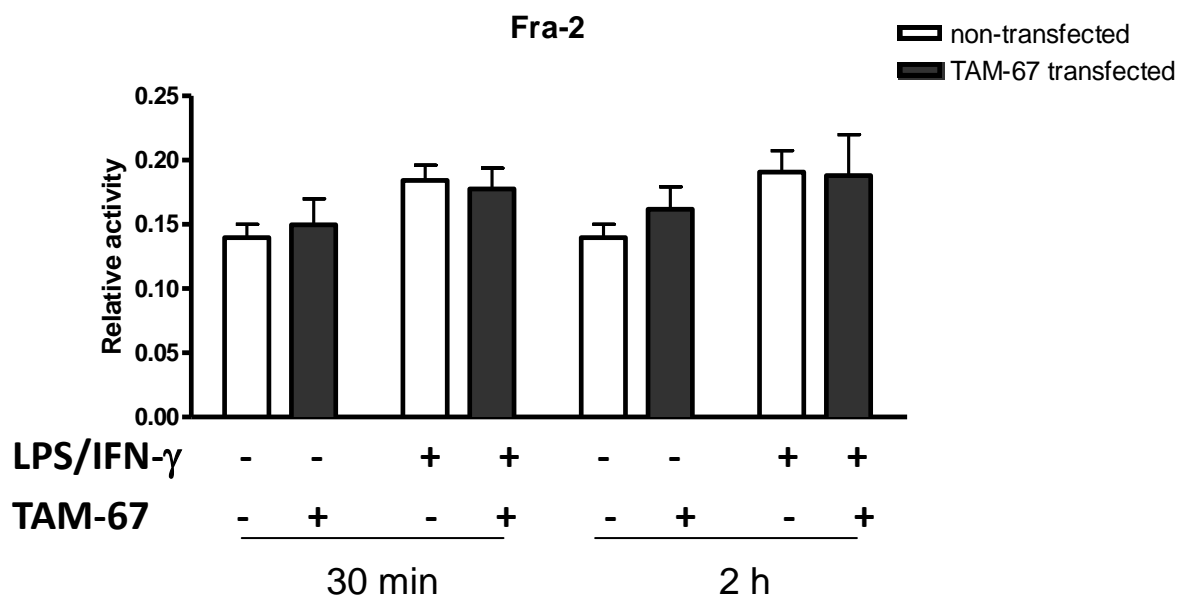


**Figure 5.46 Effects of TAM-67 on Fra-2 activation in RASMCs**

Partially confluent monolayers of RASMCs were transfected with TAM-67 for 18 hours. The cells were then activated with LPS ( $100 \mu\text{g ml}^{-1}$ ) and IFN- $\gamma$  ( $100 \text{ U ml}^{-1}$ ) for a further 30 min or 2 hours. The nuclear extracts were prepared and analysed using a TransAM kit as described in the methods (section 2.2.24) and the activity of Fra-2 was measured using the specific antibody. The results are representative of 3 independent experiments. Statistical analysis using two way Anova followed by multiple comparison test was performed.

## 5.4 Discussion

The JNK pathway plays important roles in many different cellular processes, including apoptosis as well as enhancing cell survival and proliferation (Bode *et al.*, 2007; Gupta *et al.*, 1996). Furthermore, the JNKs have also been implicated in a variety of pathologic conditions, like cancer (Wagner *et al.*, 2009), cardiac hypertrophy and heart failure (Ramirez *et al.*, 1997), neurodegenerative disorders such as Parkinson's and Alzheimer's disease (Saporito *et al.*, 2002), type I diabetes, arthritis and asthma (Sumara *et al.*, 2005). Other than the above, the JNKs have also been implicated in inflammation especially under conditions associated with the over production of nitric oxide where JNK activation has been examined. Interestingly the data presented in Chapter 3 of this thesis however failed to implicate JNK signalling in smooth muscle cells but did confirm a role for these kinases in the J774 macrophage cell line. The observations in the latter cell type would be in agreement with other studies showing that JNK regulates iNOS expression for example in RAW 264.7 macrophages (Ci *et al.*, 2010; Jung *et al.*, 2007), glial cells (Pawate *et al.*, 2006), human vascular smooth muscle cells (Sinha-Hikim *et al.*, 2010) and murine microglia BV-2 cells (Yoshioka *et al.*, 2010) and one study at least has shown that JNK is necessary for IL-1 $\beta$  induced iNOS and NO production in rat glomerular mesangial cells (Guan *et al.*, 1999). Consistent with our findings however is the report by Finder *et al.* (2001) which failed to implicate JNK in the induction of iNOS using IL-1 $\beta$  in the same smooth muscle cell type.

There are clearly inconsistencies in the findings from various laboratories and the reasons for these discrepancies are unclear but raise questions about the

experimental approaches used or even the possibility that expression and activation of various JNKs may vary under different experimental conditions.

Most cells express two JNK genes, *jnk1* and *jnk2*, which are alternatively spliced variants and yield both the p54 and p46 proteins of the  $\alpha$  and  $\beta$  isoforms (Davis, 2000b; Gupta *et al.*, 1996). These are activated by the MAPK kinase 4 (MKK4) and MAPK kinase 7 (MKK7) which are upstream of JNK1 and JNK2 respectively. The latter are activated through phosphorylation at threonine (Thr-183) and tyrosine (Tyr-185) residues (Chen *et al.*, 2002; Davis, 2000a; Lawler *et al.*, 1998; Takatori *et al.*, 2008, Derljard *et al.*, 1994) and translocation into the nucleus, where JNK phosphorylates its target transcription factors including AP-1 (Dong *et al.*, 1998).

Recent studies have demonstrated that the JNK isoforms differ in their functions (Chen *et al.*, 2002; Singh *et al.*, 2009). Some studies have shown that JNK2 has a 25-fold higher binding affinity for c-Jun than JNK1, suggesting that JNK2 is the major c-Jun activator (Kallunki *et al.*, 1994). However, other experiments have suggested that the JNK1 isoform may be slightly more efficient in phosphorylating c-Jun (Gupta *et al.*, 1996; Hochedlinger *et al.*, 2002). It seems that the different JNK isoforms may have evolved for specific biological functions, probably depending on the stimulation and responding tissue/cell type (Sabapathy *et al.*, 2004). Moreover it has been suggested that different JNKs may show varied regulatory effects on c-Jun, with JNK1 acting as a positive regulator of c-Jun while JNK2 may negatively regulate the same protein *in vivo* (Sabapathy *et al.*, 2004b). This is however contradicted by reports claiming that JNK2 normally increases the expression of c-Jun and JunD mRNA and can play a positive role in c-Jun expression in 1MN-PP1 and three MEF

lines. Thus, it also suggested that JNK1 and JNK2 are positive regulators of c-Jun expression in some but not all cell systems (Jaeschke *et al.*, 2006).

This could explain, at least in part, some of the discrepancies already highlighted relating to iNOS expression and additional experiments were therefore undertaken to determine the expression profile of the JNKs in both RASMCs and J774 macrophages. These studies were to confirm whether these proteins are indeed expressed and, more importantly, activated following stimulation of cells with pro-inflammatory mediators. In addition, the effect of the JNK inhibitor SP600125 was also examined to ascertain whether this compound did inhibit JNK activation. It was important to establish this in RASMC as the lack of effect of the SP600125 in these cells could reflect a lack of inhibition of JNK activation. Parallel experiments in RAMSCs examined the effects of the dominant negatives a-Fos and TAM-67.

In response to stress, JNK phosphorylation on both Thr-183 and Thr-185 residues by MKK4/7 (Derijard *et al.*, 1994) leads to phosphorylation of JNK substrates, include c-Jun (Verheij *et al.*, 1996; Xia *et al.*, 1995), ATF-2 (Westwick *et al.*, 1995), c-Myc (Yamamoto *et al.*, 1999), Bcl2 (Deng *et al.*, 2001; Kim *et al.*, 1999) and p53 (Fuchs *et al.*, 1998; Milne *et al.*, 1995) which among them c-Jun participate in the activation and formation of the AP-1 complex (Karin *et al.*, 1995; Shaulian *et al.*, 2002). The JNKs were shown to bind to the delta domain of c-Jun and phosphorylate it on serines 63 and 73, leading to its activation (Kallunki *et al.*, 1994).

In our studies, western blots showed that both RASMCs and J774 macrophages expressed JNK1 at 46 kDa and two isoforms of JNK2 at 46 and 54 kDa. Activation of both cell types resulted in the time-dependent expression of phospho-JNK which was detected using a phospho-specific antibody against Thr-183 and Tyr-185

residues. Phosphorylation was rapid with the phospho proteins becoming detectable as early as 5 min and peaking after 30 min of activation. This is consistent with other findings in human lung carcinoma A549 cells (Chittezhath *et al.*, 2008), J774 macrophages (Lahti *et al.*, 2003; Nieminen *et al.*, 2006) and pancreatic stellate cells (Masamune *et al.*, 2004); however, interestingly, other reports have demonstrated rapid peak phosphorylation of JNK in rat vascular smooth muscle cells within 5 minutes of stimulation with interleukin-1 $\beta$  (Jiang *et al.*, 2004) or after balloon injury (Kim *et al.*, 1998).

What is important however, are the observations that JNK is indeed expressed in RASMCs as well as J774 cells and can be phosphorylated by pro-inflammatory mediators that induce iNOS expression. It is therefore even more curious that the latter could not be inhibited by SP600125 in RASMCs and the next series of experiments examined whether JNK phosphorylation could be blocked by this compound.

In these studies, both cell types were incubated with the inhibitor at two different concentrations (0.3 and 3  $\mu$ M) and then activated 30 min later for a further 30 min (peak JNK phosphorylation time point) before generating lysates for western blotting. The reason for choosing these concentrations was because at 0.3  $\mu$ M SP600125 enhanced while at 3  $\mu$ M inhibited NO production and iNOS expression in the macrophages. Thus we wanted to see if this biphasic effect correlated with any biphasic regulation of JNK phosphorylation. Interestingly, phospho-JNK expression was partially inhibited at 0.3  $\mu$ M and completely abolished at 3  $\mu$ M SP600125. This is not consistent with the biphasic trends seen with iNOS and NO and it is unclear why SP600125 would enhance iNOS/NO production, albeit marginally, at lower

concentrations and suppress at higher concentrations but yet inhibit JNK phosphorylation at both concentrations. The possibility that SP600125 may affect other pathways distinct from the JNKs which are perhaps positively or negatively coupled to iNOS expression and/or NO production remains to be established. The effect of this inhibitor on p38 MAPK or ERK was previously discussed and reveals a certain degree of non-specificity for SP600125.

Our findings however support other studies which have reported the inhibitory effect of SP600125 on JNK phosphorylation for instance in J774 macrophages (Nieminen *et al.*, 2006) or other cell types (Chansard *et al.*, 2007; Saito *et al.*, 2010; Wang *et al.*, 2007) and this effect may, at least in part, account for the inhibitions seen in the macrophages. It was intriguing however why despite inhibiting JNK phosphorylation in RASMCs, SP600125 was without any significant effect on either iNOS expression or NO synthesis in these cells. Further studies were therefore carried out examining the expression profile and changes in the activated status of different AP-1 subunits in the presence and absence of SP600125. This was to determine whether SP600125 did regulate the sequential activation of AP-1 and, more importantly, the pattern of activation of the different subunits which could have an impact on the actual biological response produced.

As already explained earlier (Chapter 1), AP-1 consists of distinct subunits which include members of Jun (c-Jun, JunB, JunD) and the Fos families (c-Fos, FosB, Fra-1 and Fra-2). These proteins have different transactivation potentials and each may be linked with various specific stages of a cellular process, rather than the entire process (Keklikoglu, 2004). There is a vast amount of data suggesting various roles for each AP-1 subunits and their effects may vary between different cell types and/or

affected differently by different stimulants, experimental approaches and various other factors (Young *et al.*, 2003).

AP-1 responds to a wide range of physiological and pathological extracellular stimuli encountered by the cell. Stimuli such as hormones, cytokines, growth factors, stress signals, infections, and radiation or chemical carcinogens activate AP-1 (Angel *et al.*, 2002; Hess *et al.*, 2004). AP-1 activity plays critical roles in the activation of several cytokines (Linard *et al.*, 2003). AP-1 member proteins have different transactivation potentials and each protein may be linked with various specific stages of a cellular process, rather than the entire process (Keklikoglu, 2004). There is a huge amount of different studies suggesting various roles for each AP-1 subunits. The differences may reflect variations between different cell types, stimulant used, experimental approaches and various other factors.

Of the different AP-1 subunits, c-Jun is activated by JNKs through phosphorylation on serines 63 and 73 following binding of JNK to its delta domain (Kallunki *et al.*, 1994). Once activated c-Jun regulates various cellular processes including growth, proliferation, differentiation and apoptosis, and also contribute to basal and stimulus-activated gene expression including that for iNOS (Young *et al.*, 2003).

By comparison, JunB exhibits weaker DNA binding and homo-dimerization affinity than c-Jun and has been shown, depending on the promoter sequence and dimerization partner, to act both as a transactivator or transrepressor (Passegue *et al.*, 2000). JunD on the other hand mediates some functions such as inhibition of fibroblast proliferation and although activated by JNK (Yazgan *et al.*, 2002) may not be entirely dependent on the latter for its activation. In fact there are reports that JNK

may not completely drive JunD phosphorylation but rather requires the activation of the ERKs to induce full JunD activity (Smart *et al.*, 2006). Similarly, Kuntzen *et al.* (2005) showed that JunD activation may not be mediated through JNK as this was insensitive to SP600125 inhibition.

In our studies, both RASMCs and J774 macrophages expressed all subunits of AP-1. What was interesting however was the pattern of activation of each following stimulation of cells and also the manner in which each subunit was modified by SP600125. These experiments were carried out using the TransAM AP-1 family kit to measure the DNA-binding activity of the subunits based on an ELISA assay. Basically, AP-1 subunits in the nuclear extracts would bind to specific oligonucleotides containing TPA-responsive elements (TREs) immobilized into a 96-well plate and since this only occurs with activated proteins, the assay allows for the detection of the active phosphorylated subunits (Ahmad *et al.*, 2007; Mukhopadhyay *et al.*, 2008; Shimizu *et al.*, 2008; Xie *et al.*, 2005; Zhang *et al.*, 2009).

The results obtained from these studies revealed that the activity of c-Jun increased rapidly in J774 macrophages following 15 min stimulation with LPS and reached a maximum level at 30 min, declining gradual thereafter. The trend of c-Jun activation in J774 macrophages was similar to that seen in RASMCs with the only difference being that responses in RAMSCs were delayed, peaking at 60 min after activation. This time frame is consistent with similar activation of c-Jun observed in smooth muscle cells following mechanical stretch (Mitchell *et al.*, 2004). Similarly, the rapid activation of c-Jun in J774 macrophages has been reported previously not only in response to LPS but also to IL-1 and TNF- $\alpha$  (Tengku-Muhammad *et al.*, 2000). LPS has also been shown to enhance c-Jun activity in RAW264.7 cells (Chen *et al.*,

2008; Dudhgaonkar *et al.*, 2009; Lee *et al.*, 2009a) as well as in HCT-116 (Lee *et al.*, 2007), microglia cells (Jung *et al.*, 2006), smooth muscle cells (Gonzalo *et al.*, 2011; Lin *et al.*, 2009) and RASMCs (MacKenzie *et al.*, 2003). More importantly, the rapid induction of c-Jun demonstrate its critical role in inflammatory conditions and since its activation may be JNK dependent, it indicates that JNK could be an “immediate early gene” along with other AP-1 family members (Franciscovich *et al.*, 2008; Guo *et al.*, 2007; Hartwig *et al.*, 2008) especially c-Jun (Wainford *et al.*, 2009).

JunD, the other subunit of AP-1 was also rapidly activated in J774 macrophages at the 30 min time point, reaching a maximum at 1 hour and a slight decline was observed after 2 hours. Similarly, Fra-1 and FosB DNA-binding activities were also enhanced at 30 min with that for FosB peaking at 60 min and declining thereafter while Fra-1 remained elevated over two hours. JunB, c-Fos and Fra-2 were unaltered. In parallel with these observations, RASMCs exposed to LPS and IFN- $\gamma$  showed increased Fra-1 activation after 30 min and that of JunD after 1 hour, increasing to a maximum at 2 hours. Interestingly, c-Fos was virtually unaltered as was JunB and FosB; and although Fra-2 appeared to be enhanced, this was not statistically significant when compared to the non-activated cells. These findings summarised in Tables 5.1 and 5.2 for clarity, highlight a sequential activation and further indicate differences in the activation pattern of the different subunits.

The consequence of the sequential activation is unclear but there is at least one report that JunD, which we found was activated after c-Jun, can stabilise c-Jun mRNA expression. Also worth noting is the fact that the basal levels of both JunB and c-Fos in macrophages were significantly higher than in RASMCs which may

relate to the roles of these proteins in normal physiological cellular functions such as differentiation and proliferation in macrophages (Cho *et al.*, 2002).

These observations are the first to report the expression and activation profile of these sub-components of AP-1 in vascular smooth muscle cells. Indeed there is very little published literature on either the profile of expression or activation of any of the AP-1 subunits we have investigated and the data we have generated for this thesis should therefore further enhance our understanding of the role and activation of these subunits.

Some of our observations described above are consistent with, for instance the activation of JunD in cytokine stimulated A549 cells (Chittezhath *et al.*, 2008); the activation of FosB in RAW264.7 macrophages by LPS and IFN- $\gamma$  (Okada *et al.*, 2003) and the lack of c-Fos stimulation by IL-6 (Tengku-Muhammad *et al.*, 2000). The activation of JunD in the J774 macrophages has been reported but others studies which have looked at changes in JunD mRNA expression level have shown no changes when cells were exposed to LPS (Tengku-Muhammad *et al.*, 2000); and the activation of FosB contrasts with its lack of activation in human aortic smooth muscle cells exposed to LPS and CD14 (Patel *et al.*, 2006) as does the lack of stimulation of c-Fos which Tengku-Muhammad *et al.* (2000) claims is enhanced by LPS stimulation of J774 macrophages. Similarly, our findings for JunB contracts with those reported by Tengku-Muhammad *et al.* (2000) who claimed the induction of JunB mRNA in macrophages within 1 hour of exposure to LPS (Tengku-Muhammad *et al.*, 2000) and with others in rat myometrial smooth muscle cells (Mitchell *et al.*, 2004) or in human aortic smooth muscle cells where JunB activation and expression

was elevated respectively by mechanical stretch and by exposure to LPS and CD14 (Patel *et al.*, 2006).

However it should be noted that in some of these studies the induction or mRNA expression and not activation was measured. The reasons for these discrepancies are unclear but highlight the need for establishing the actual changes that occur to the AP-1 subunits under different conditions, especially when trying to correlate this with changes in biological functions.

The important point about the findings discussed above is the fact that various AP-1 subunits that may be critical for the induction of iNOS are not only expressed but also activated in both RASMCs and J774 macrophages. Thus the fact that SP600125 selectively blocked this process in the macrophages but not in the smooth muscle cells raises a critical question of whether the AP-1 subunits are regulated differentially by this compound in the two cell systems.

SP600125 is known to inhibit the c-Jun transactivation domain (Bogoyevitch *et al.*, 2008) and acts as a reversible ATP-competitive inhibitor with equal potency towards JNK1, JNK2 and JNK3. It has a high degree of selectivity (300-fold) for these proteins when compared to its effects on the extracellular signal regulated kinases (ERKs) and p38 MAPKs (Bogoyevitch *et al.*, 2004; Maroney *et al.*, 2001). To determine the effects of SP600125 on the activation of the various AP-1 subunits, the drug was used at the two concentrations of 0.3  $\mu$ M and 3  $\mu$ M discussed previously and at two incubation time points which covered the peak activation time points (30 min and 2 hours) of the different subunits. In these studies, SP600125 concentration-dependently blocked c-Jun DNA binding activity without affecting FosB or Fra-2 in RASMCs and JunD, c-Fos or Fra-2 in J774 macrophages. Interestingly,

SP600125 significantly enhanced JunB, JunD, c-Fos and Fra-1 activity in RASMCs while in activated macrophages JunB was the most affected. In these cells SP600125 caused an increase in JunB activity which was not further enhanced by LPS, suggesting that SP600125, on its own, is able to activate JunB significantly. Similarly, the up-regulation of Fra-1 in RASMCs and FosB and Fra-1 in J774 macrophages again appear to be a direct response to SP600125. These changes in both cell types are again summarised in Tables 5.1 and 5.2 and summarised diagrammatically in Figure 6.1 for clarity.

**Table 5.1 Changes in activation of AP-1 subunits, iNOS and L-arginine transport in RASMCs treated with LPS + IFN- $\gamma$ , SP600125, a-Fos or TAM-67.**

( $\uparrow$  = increase;  $\downarrow$  = decrease and – = no changes)

LPS/IFN- $\gamma$  treatment up-regulated c-Jun, JunD and Fra-1 as well as induce iNOS expression and L-arginine transport. Addition of SP600125 in the presence of LPS/IFN- $\gamma$  caused a significant decline in c-Jun, enhanced JunD and c-Fos level but did not reveal any effect on basal iNOS or L-arginine transport. SP600125 independently elevated level of JunB and Fra-1 in the absence of LPS and IFN- $\gamma$  treatment. Transfection of RASMCs with a-Fos or TAM-67 and incubation with LPS/IFN- $\gamma$ , caused reductions respectively in c-Jun, c-Fos, FosB and Fra-1 and in c-Jun, c-Fos. However TAM-67 up-regulated the induction of Fra-1. a-Fos transfection resulted in iNOS/L-arg enhancement while TAM-67 reduced these processes.

<b>RASMCs</b>	LPS/INF- $\gamma$	SP600125 -LPS/INF- $\gamma$	SP600125 +LPS/INF- $\gamma$	a-Fos +LPS/INF- $\gamma$	TAM-67 +LPS/INF- $\gamma$
c-Jun	↑	—	↓	↓	↓
JunB	—	↑	↑	—	—
JunD	↑	—	↑	—	—
c-Fos	—	—	↑	↓	↓
FosB	—	—	—	↓	—
Fra-1	↑	↑	↑	↓	↑
Fra-2	—	—	—	—	—
<b>iNOS</b>	↑	—	↑	—	↓
<b>L-arginine</b>	↑	—	↑	—	↓

**Table 5.2 Changes in activation of AP-1 subunits, iNOS and L-arginine transport in J774 macrophages treated with LPS, SP600125.**

(↑ = increase; ↓ = decrease and – = no changes)

LPS treatment up-regulates c-Jun, JunD, FosB and Fra-1 and resulted in the induction of iNOS expression and L-arginine transport. Addition of SP600125 caused a significant decline in c-Jun and in iNOS expression and L-arginine transport. The other AP-1 subunits were not affected. Treatment with SP600125 alone elevated level of JunB, FosB and Fra-1 above basal. No changes were observed in JunD, c-Fos and Fra-2 expression.

<b>J774 macrophages</b>	LPS	SP600125 -LPS	SP600125 +LPS
c-Jun	↑	—	↓
JunB	—	↑	↑
JunD	↑	—	—
c-Fos	—	—	—
FosB	↑	↑	—
Fra-1	↑	↑	↑
Fra-2	—	—	—
<b>iNOS</b>	↑	—	↓
<b>L-arginine</b>	↑	—	↓

The significance of the observations described above and how they relate to the regulation of iNOS or NO production are as yet unclear. It has, however, been reported that the activation of c-Jun may be essential for these processes to occur and inhibition of this molecule could result in the blockade of iNOS expression and subsequently NO synthesis. This could explain the results obtained in the J774 macrophages where inhibition of c-Jun activation by SP600125 was clearly demonstrated. Should this argument hold, the same outcome should also have been observed in RASMCs where c-Jun DNA-binding activity was evidently blocked by SP600125. However, there was no suppression of iNOS expression or NO production in smooth muscle cells despite the inhibition of c-Jun activity.

In RASMCs, the situation may be more complex because inhibition of c-Jun was accompanied by a parallel up-regulation in the activity of several other subunits including JunD and c-Fos while in LPS-activated J774 macrophages there were no notable changes or increase in any other subunits. It is therefore possible that in RASMCs there may be some compensation for the inhibition of c-Jun by subunits with enhanced activity. As a result of this, any inhibitory actions that may have been mediated by the blockade of c-Jun may be masked by opposing compensatory actions of others especially where these are positively coupled to the induction of iNOS. Some of the key candidates for consideration include JunB, JunD, c-Fos and Fra-1. In this regard, it is worth noting that there is at least one report in cytokine-treated C<sub>6</sub> glial cells claiming that JunD and Fra-1 may be the critical AP-1 subunits required for iNOS gene expression (Giri *et al.*, 2002). Both of these are not only activated by LPS and IFN- $\gamma$  in the RASMCs but their activities were also further enhanced by SP600125. Thus even with c-Jun inhibited the activation of JunD and

Fra-1 may compensate for the effects of SP600125 on c-Jun especially as they can both dimerise into an active AP-1 complex (Nadori *et al.*, 1997; Tkach *et al.*, 2003). JunD can also complex with Fra-2 and has been implicated in the induction of iNOS following LPS and IFN- $\gamma$  treatment of the A549 human lung epithelial cells (Kristof *et al.*, 2001).

Interestingly, in C<sub>6</sub> cells it would appear Fra-1 and JunB rather than c-Jun and c-Fos may be required following stimulation of these cells with LPS and TNF- $\alpha$  (Lee *et al.* 2003). We can however discount an involvement of Fra-2 or complexes involving this subunit as it was not activated by LPS and IFN- $\gamma$  nor was its activity induced by SP600125. Similarly, although activated by SP600125, JunB was not altered in the presence of LPS and IFN- $\gamma$  and unlikely to be associated with the induction of iNOS in this cell system. Other active complexes which could be formed and potentially regulate the activation of the iNOS gene include complexes with c-Fos that do not involve c-Jun which could be just as critical for the induction of iNOS and will be addressed further below when discussing the effects of the dominant negative a-Fos.

The discussions above although largely speculative, could be substantiated using more direct and selective approaches such as exploiting siRNA technology, over expression of individual AP-1 subunits or both. However, these experiments although identified could not be carried out because of the time limitation. Instead further studies were conducted by investigating the effects of dominant negative constructs of AP-1. One of the dominant negatives used was a-Fos which is an engineered chimeric protein containing the c-Fos leucine-zipper and a designed 25 amino acid acidic protein sequence that replaces the DNA-binding region (Bobrovnikova-Marjon *et al.*, 2004; Bonovich *et al.*, 2002; Gerdes *et al.*, 2006). It has

also been shown to inactivate the DNA binding of the Fos-Jun hetero-dimer and potentially inhibit Jun-dependent transactivation (Manna *et al.*, 2004; Olive *et al.*, 1997).

Transactivation minus *c-jun* dominant negative AP-1 (TAM-67) is the other dominant negative construct which acts against c-Jun and has the ability to form dimers with wild-type AP-1 proteins because of its DNA binding domain and leucine-zipper region (bZIP). However TAM-67 lacks the transactivation domain of c-Jun (amino acids 1–122) and thus functions as a dominant negative to block wild-type c-Jun activity (Dhar *et al.*, 2004; Feng *et al.*, 2002; Wu *et al.*, 2003; Young *et al.*, 2006). In exerting its effects, TAM-67 can act by (i) forming a homo-dimer which binds to DNA and blocks the 12-O-tetradecanoylphorbol-13-acetate response element (TRE), (ii) quenching DNA activation by directly binding to the latter but without activating transcription and (iii) squelching through formation of a heterodimer with wild-type transcription factors with the complex formed failing to bind to DNA (Thompson *et al.*, 2002).

In this thesis, each dominant negative was transfected into RASMCs using an integrin binding peptide with an RGD domain for integrin and a poly-lysine tail for DNA binding (Hart *et al.*, 1998). The non-transfected or cells incubated with the transfection mix lacking the cDNA construct were used as controls. The data from these studies confirm that a-Fos could significantly suppress both c-Fos and FosB activity with a smaller but significant inhibition of c-Jun. In contrast JunB, JunD, Fra-1 and Fra-2 remained virtually unaltered. These results show a good degree of selectivity of a-Fos for the Fos subunits and the fact that when transfected into cells enhanced both iNOS and NO production strongly suggests that the Fos proteins may

be negatively coupled to these processes and their inhibition results in enhanced expression of iNOS and thus NO synthesis. This would indeed agree with the report by Okada *et al.* (2003) showing that over expression of c-Fos in macrophages suppressed rather than enhanced iNOS expression, indicating that c-Fos may be negatively coupled to the induction of iNOS. In contrast, other reports have indicated that c-Fos rather than c-Jun may be more relevant for inducing the expression of iNOS in some cell systems. This is further supported by observation in terminal bronchiole lesions in rats exposed to cigarette smoke where expression of iNOS was associated with a significant enhancement of c-Fos expression (Chang *et al.*, 2001).

In contrast to the actions of a-Fos, TAM-67 significantly inhibited c-Jun DNA-binding activity and marginally suppressed that of c-Fos without affecting any of the other subunits. These effects are not unpredictable as TAM-67 is a dominant negative of c-Jun and the latter often complexes with c-Fos. As a result, suppression of c-Jun may impact on the activation of c-Fos. In this regard, it has been reported that TAM-67 is able to interact with all proteins which combine with c-Jun (Thompson *et al.*, 2002) and can augment c-Fos activity (Brown *et al.*, 1994) as well as block the DNA binding of a Fos-Jun hetero-dimer (Olive *et al.*, 1997). Since c-Jun may be critical for iNOS induction, its inhibition by TAM-67 without any up-regulation of other subunits that could compensate for its inhibition may result in the inhibition of iNOS expression and reveals the true effects of c-Jun. This would be consistent with the inhibition of iNOS expression by TAM-67 in gastric epithelial cells (Cho *et al.*, 2009).

Finally, unlike SP600125, neither a-Fos nor TAM-67 caused any significant elevations in the activities of the AP-1 subunits. The only indication of this was with Fra-1 following transfections with TAM-67 but the increases were marginal and only

evident in control non-activated cells. Thus, the effects of the dominant negatives would appear to be more selective and less complex. This could explain the clear trends obtained and trends that perhaps were masked in RASMCs when treated with the pharmacological inhibitor (SP600125) due to induction of parallel effects that could have potentially compensated for the inhibitory actions of the compound. This raises a serious issue which is often overlooked in research exploiting purely pharmacological interventions. As demonstrated in this thesis, compounds such as SP600125 may exert effects beyond their expected pharmacological actions and this is often overlooked resulting in conclusions which may not be truly representative of their pharmacological actions. Multiple approaches that combine pharmacological and molecular tools may therefore be the preferred approach and this need to be given some attention in experimental designs. Figure 5.47 simply demonstrated this events and their role in iNOS gene induction.

As mentioned in chapter 3 and 4, the role of JNK/AP-1 on iNOS expression was studied in parallel with L-arginine transport and also cationic amino acid transporters responsible for transport of this amino acid. There are not many studies on the signalling mechanism controlling CAT expression. Visigalli *et al.* (2004) suggested a mechanism in which stimulation by PKC $\alpha$  activation through ERK1/2/AP-1 pathway lead the arginine transport through system y<sup>+</sup> and induction of CAT-2A and CAT-2B expression in endothelial cells. On the other hand Baydoun *et al.* (1999) showed no involvement of PKC on transport of L-arginine but the important role of p38 MAPKs in rat aortic smooth muscle cells.

In this thesis we have shown (Chapter 3) that transport in RASMC is not affected by SP600125 but it was in J774 macrophages even with JNK inhibitor VIII. Moreover we

have shown that in these cells, CAT-2B which is potentially the predominant CAT transporter in these cells is inhibited by SP600125 at 3  $\mu$ M. In RASMCs transport was inhibited by TAM-67 but not  $\alpha$ -Fos suggesting selective regulation by c-Jun or at least a non Fos subunit. It is clear that while in RASMC SP600125 may not have an effect, JNK/AP-1 is still involved but like iNOS the effect is masked by compensation. JNK is also clearly involved in J774 macrophages.

Data obtained in this chapter makes a vivid picture of how all the subunits of one transcription factor work alongside with all the compensatory and positive/negative effect on each other to determine the response of the cells to various stimulations.

## 5.1 Summary

In conclusion our data indicates a series of different activation patterns in AP-1 subunits whilst using LPS alone or with LPS/IFN- $\gamma$  in J774 macrophages and RASMCs respectively. The data presented is to our knowledge the first to explore the complex regulation of all seven subunits of AP-1 in RASMCs and J774 macrophages and has revealed some interesting but complex trends which may help explain the variation in responses of these two cell systems to pharmacological inhibition. Moreover, the data has contributed towards understanding the controversy that surrounds the role of JNK in the induction of iNOS. It would appear that JNK signalling is indeed critical for the latter process but may not always be evident in certain biological systems especially where the experimental approach has relied exclusively on a pharmacological intervention, or at least the use of SP600125. Furthermore, our findings have also revealed for the first time that L-arginine transport regulation in parallel with iNOS is partly dependent on JNK/AP-1 pathway. In RASMCs however this pattern is not observed using the pharmacological inhibitor which again confirms the compensatory mechanism of the other subunits which mask c-Jun up-regulation.

Using the dominant negative constructs of AP-1 help to visualize better understanding of how the individual subunits are acting independently and dependent of each other. High level of c-Jun inhibition caused a down-regulation of iNOS-NO when TAM-67 was used and this inhibition was not enough in a-Fos transfected cell to inhibit iNOS-NO. In this regard, molecular approach shows more selective way to regulate this pattern.

# **Chapter 6**

## **General Discussion**

## Discussion

The experiments described in this report were carried out to get a clear understanding of the mechanisms involved in the expression of the inducible L-arginine-NO pathway in cultured vascular smooth muscle cells and J774 macrophages focusing specifically on the JNK/AP-1 cascade.

Although there has been a good deal of work carried out investigating the role of JNK/AP-1 in the induction of iNOS, the findings are inconclusive with contradictory reports which are poorly explained. Furthermore there is currently very little information in the literature as to whether the parallel up-regulation in L-arginine transport, widely reported under conditions of induced NO synthesis, also requires activation of the JNKs. The studies reported in this thesis were therefore carried out to determine unequivocally whether JNK/AP-1 signalling is indeed critical for the induction of iNOS and/or L-arginine transport in RASMCs and also in J774 macrophages. These two cell systems were selected because they are two of the widely reported sites for iNOS expression *in vivo* and, perhaps more importantly, because of their critical role in the actions of pro-inflammatory mediators in disease states such as septic shock associated with overproduction of NO (Knowles *et al.*, 2004).

For our studies, we exploited both pharmacological and molecular approaches to regulate JNK and/or AP-1 activity. This approach is essential if we are to understand the discrepancies in the literature and gain a better understanding of how over production of NO might be regulated in biological systems.

The first task in this study was to determine the responses of our cells to inflammatory condition and subsequently establish how JNK/AP-1 might affect the responses produced. Thus, LPS and IFN- $\gamma$  were used to stimulate RASMCs and LPS alone was used in J774 macrophages at established concentrations identified in previous studies within the group (Baydoun *et al.*, 1993). Both cells were consistently activated by the stimuli used and produced significant amount of iNOS and NO as well as increase their ability to transport L-arginine. What was interesting however was the fact that in RASMCs there was little response to JNK inhibition using the pharmacological inhibitors, while in J774 macrophages both inhibitors used caused significant suppression of these processes.

It should be noted that in all the experiments conducted in this thesis different stimuli for two cell types were used. The high amount of LPS/IFN- $\gamma$  for smooth muscle cells and low LPS for macrophages may affect interpretation of the results, because of the different signalling pathways consequently activated in each cell system. In RASMCs LPS alone cannot induce iNOS and requires co-incubation with the direct activator of adenylyl cyclase, forskolin. LPS will bind to a serum derived binding protein, CD14 and activates TLR-4 receptors. But this mechanism for IFN- $\gamma$  is different. Interferon-regulatory factor-1 (IRF-1) is a protein transcription activator which is regulator of IFN system. Also two intracellular signalling pathways that have been implicated in the regulation of IRF-1 included JAK/STAT and NF-kB pathways (Liu *et al.*, 2001). In smooth muscle cells both systems are required for the complete stimulation in the system. It has been shown that IFN- $\gamma$  also can stabilise iNOS mRNA however in macrophages LPS alone is sufficient and there is no need for another factor for mRNA stabilisation (Wileman *et al.*, 1995).

The findings in RASMCs are at odds with other reports in the same cell type which have suggested that inhibition of JNK/AP-1 can cause a reduction in NO production and iNOS expression (Hattori *et al.*, 2003; Nakata *et al.*, 2005) but consistent, at least in part, with others claiming that expression of iNOS in smooth muscle cells is indeed independent of JNK activation (Jiang *et al.*, 2004). The situation in J774 macrophages appear less complicated as activation of JNK/AP-1 has been confirmed for the induction of iNOS (Chan *et al.*, 1998; Cho *et al.*, 2002) and it has been suggested that JNK may in fact be the dominant regulator of iNOS expression in these cells (Blanchette *et al.*, 2008; Chen *et al.*, 2008). It is worth noting, however, that JNK may only partially regulate the induction of iNOS and this process may in part require the ERKs in macrophage (Chan *et al.*, 1998). Interestingly, there appears to be some differences between the changes in expression of iNOS and in the degree of inhibition of the JNKs that is seen. It would appear that iNOS mRNA inhibition occurs even without complete blockade of JNK, suggesting that any inhibitory effect on iNOS transcription is only partially dependent on this MAPKs (Chan *et al.*, 1998). Other studies have suggested that depending on the stimulus and cell type, MAPKs may play a positive (Bhat *et al.*, 1998; Da Silva *et al.*, 1997; Singh *et al.*, 1996), negative (Guan *et al.*, 1997), or neutral (Chan *et al.*, 2001) regulatory role on iNOS expression. Thus, as with JNK, the critical requirement of other MAPKs like ERKs for the induction of iNOS may not be unambiguously universal.

Other than the JNKs and ERKs there is also controversy about the role of other MAPKs such as the P38 MAPK which have been shown not to be essential for NO production and iNOS expression because LPS induced iNOS expression could not

be blocked by SB203580 (Caivano, 1998). By contrast, there it has been reported that activation of p38 and ERKs may be involved in LPS-induced iNOS expression in J774 macrophages (Kim *et al.*, 2004) and in murine macrophages stimulation with LPS leads to increased phosphorylation and activation of ERK1/2, JNK, and p38 kinase (Chen *et al.*, 2008; Choi *et al.*, 2007; Nakano *et al.*, 1998). Baydoun *et al.*, (1999) showed that SB203580 can potentiate NO production at lower concentration and inhibit it at the higher range in rat vascular smooth muscle cells therefore it can be speculated that these effect may be variable at diverse concentration of the inhibitor.

With regards to JNK, it is perhaps worth pointing out again that the regulation of iNOS expression by these proteins and the interaction of JNK with its downstream targets AP-1 is complex. Such interactions may be determined by several factors, including the cell system being explored and the stimulus being applied. These do need careful consideration in experimental designs but even more important is ensuring that appropriate experiments are conducted that can unmask the full profile of drug actions at both the functional and molecular level. This point is emphasised in the findings of this thesis and discussed in further details below.

As already described in earlier chapters, using a purely pharmacological approach failed to reveal a conclusive role for JNK in RASMCs while the molecular approach used, exploiting dominant negatives of AP-1 revealed effects which were not evident with a pharmacological inhibitor. In these studies,  $\alpha$ -Fos, a dominant negative inhibitor of the Fos proteins, increased iNOS mRNA and protein as well as NO production while TAM-67, a dominant negative for c-Jun, caused down-regulation in iNOS mRNA, protein and NO synthesis.

To address the variations in the results we examined the expression profiles of the JNK isoforms and AP-1 subunits, which to our knowledge is the first time such detailed studies have been carried out. There is increasing evidence to suggest an important role for the different AP-1 subunits and their dimer formation in the control of cellular functions in diverse cell systems. These subunits may be regulated differentially by ERK, p38, and JNK, with each selectively regulating AP-1 subcomponent and their DNA binding activity (Ding *et al.*, 2008). This may depend on the cell type and stimulations used and may result in different biological outcomes.

AP-1 may act either as an inducer or as a repressor of the iNOS gene promoter (Mendes *et al.*, 2003) and these effects have been reported in cell types like J774 macrophages (Chen *et al.*, 1999; Lin *et al.*, 2007) and RAW264.7 macrophages as inducer (Park *et al.*, 2009), or repressor (Huh *et al.*, 2007; Ichikawa *et al.*, 2009), smooth muscle cells as inducer (Hattori *et al.*, 2003; Knipp *et al.*, 2004) or repressor (Chyu *et al.*, 2004), gastric epithelial AGS cells (Cho *et al.*, 2009), pancreatic beta-cells (Gurzov *et al.*, 2008) and microglia (Chang *et al.*, 2008) as inducer. However, there are other reports which suggest that AP-1 is not required for iNOS gene expression in cell types such as chondrocytes (Mendes *et al.*, 2003) or smooth muscle cells (Matsumura *et al.*, 2001). These differences are confusing however different experimental design or approach, different tissues or cell life cycle and lots of various conditions can lead to this inconsistency.

It is becoming increasingly clear that the modulation and composition of AP-1 complex formed can affect AP-1 transcriptional activity (Baskey *et al.*, 2002). For example Fos-Jun hetero-dimers have been shown to be more stable than Jun-Jun

homo-dimers (Abate *et al.*, 1991; Baskey *et al.*, 2002) or c-Jun binding complex has a greater stability than those containing JunB or JunD (Ryseck *et al.*, 1991). However, this is still controversial in terms of AP-1 composition and function and its role in iNOS induction. It is therefore important to determine the composition and the role of AP-1 under inflammatory conditions.

It has been shown that iNOS gene promoter contains binding sites for AP-1 (Chu *et al.*, 1998; Lowenstein *et al.*, 1993) but in different cells the role of this transcription factor on iNOS gene expression has been shown to differ from induction (Giri *et al.*, 2002; Kristof *et al.*, 2001) to repression (Kleinert *et al.*, 1998; Pance *et al.*, 2002) or even failing to show any effect as observed in bovine articular chondrocytes (Mendes *et al.*, 2003). This controversy raises the question of the role of each subunit in the signalling events and suggests that different AP-1 dimers may have distinct roles (Shaulian *et al.*, 2002) in the regulation of iNOS and/or CAT gene transcription. The hetero-dimer of c-Jun-c-Fos appear to be the most accepted dimer that regulate iNOS expression however recent studies have indicated that other AP-1 dimers such as JunB or JunD can participate in the regulation of iNOS gene expression (Mendes *et al.*, 2003).

In our study the activation of the transcription factors was evident as early as 15 min and optimal at 2 hrs after activation. This rapid activation may reflect the fact that these are early response genes. However there was a study on RAW 264.7 macrophages which showed that following the induction of iNOS with LPS there were either no or minor changes in AP-1 activation, but over a prolonged period of iNOS induction, nitric oxide itself caused the activation of AP-1 (von Knethen *et al.*, 2000). In our system, after activation with LPS/IFN- $\gamma$  in RASMCs and LPS in J774

macrophages, there was sequential activation of various AP-1 subunits. In the first instance, there was an increase in c-Jun, JunD and Fra-1 in both cells and FosB only in J774 macrophages. In both cell types c-Jun was the first to be activated which shows an important role for this subunit and JunD enhancement which can be an indicator of its role in stabilization of c-Jun mRNA.

The pattern of AP-1 activation was the same as for the activation of JNK which was phosphorylated within a few minutes (5-15 min) of activation. Moreover inhibition of JNK using SP600125 in both smooth muscle cells and J774 macrophages has the same effect on JNK phosphorylation; but then the activation profile of AP-1 subunits varied between smooth muscle cells and J774 macrophages. c-Jun, a proposed direct target for p-JNK had the same pattern of activation in both cells but the interaction between other subunits also determine the different response from cells; for instance as described in chapter 5, some subunits like JunB or even JunD and c-Fos can substitute for c-Jun decline.

Therefore our studies on the subunits provide strong evidence for c-Jun involvement in the signalling pathway that lead to iNOS expression in these cells especially in J774 macrophages as it showed an increase after LPS stimulation and decrease after using the JNK inhibitor SP600125. This followed the same pattern seen for iNOS/NO/L-arginine. This subunit may act as a homo-dimer of c-Jun-c-Jun or hetro-dimer of c-Jun-Fra-1 following activation with LPS and/or IFN- $\gamma$  as the time point of c-Jun and Fra-1 activation had the same pattern. The suggestion of c-Jun-Fra-1 combination has been shown previously (Singh *et al.*, 2009).

In RASMCs c-Jun activity was reduced by SP600125 but that of JunB was elevated and this subunit may substitute for the decline in c-Jun as shown previously (Passegue *et al.*, 2002). As a result iNOS gene transcription may still be initiated leading to iNOS expression and NO production even with SP600125 present. This potential compensation may explain why we could not see any blockade of iNOS when SP600125 was applied to the cells.

The above suggestion is supported by the fact that TAM-67 suppressed c-Jun activation without altering JunB and, more importantly, reduced iNOS induction and NO production. This observation is taken to indicate that when c-Jun is suppressed without any compensatory up-regulation of Jun-B, we demonstrate inhibition of iNOS. In contrast, if Jun-B (or other subunits positively coupled to iNOS expression) is induced then the inhibition of iNOS that would be associated with the suppression of c-Jun may not be evident.

It has been reported that in SK-N-SH neuroblastoma cell line, TAM-67 but not a-Fos decreased AP-1 transcriptional activation, which demonstrates the role of c-Jun as this subunit is the direct target of TAM-67; moreover c-Fos was not involved in the activated AP-1 complex and this study suggest a Jun homo-dimer format for AP-1 complex (Herdman *et al.*, 2006).

These results suggest an essential requirement of the JNK/AP-1 pathway that may not always be evident in studies when using pharmacological inhibitors because of the induction of potential compensatory mechanisms that could mask their inhibitory action in certain cell systems. Thus, when identifying pathways that regulate expression of target proteins (eg iNOS) it is important to appreciate that there may

be compensatory mechanisms involving other targets beyond that being targeted by the pharmacological molecule used. This, as clearly demonstrated in this thesis, may skew the conclusions reached and could potentially account for some of the controversies in the literature. It is possible that AP-1 components interact together in a way that in smooth muscle cells, compensatory effect of subunits like JunB, JunD, c-Fos and Fra-1 overcome effect associated with, for instance, c-Jun reduction. When there is no compensation, the consequences of c-Jun inhibition becomes evident as seen with TAM-67 which selectively blocked c-Jun-DNA binding activity without altering other AP-1 subunits. Also it seems that the level of inhibition and how much activity is inhibited is very important and determines how efficient the AP-1 complex may be at initiating gene transcription. This is perhaps evident with the data obtained for TAM-67 which showed greater inhibition of c-Jun than a-Fos and therefore showed its effect more strongly. As c-Jun is the positive regulator of iNOS expression and seems to have an important role in AP-1 complex we suggest that the c-Jun high level of inhibition and decline was the main reason for iNOS reduction level.

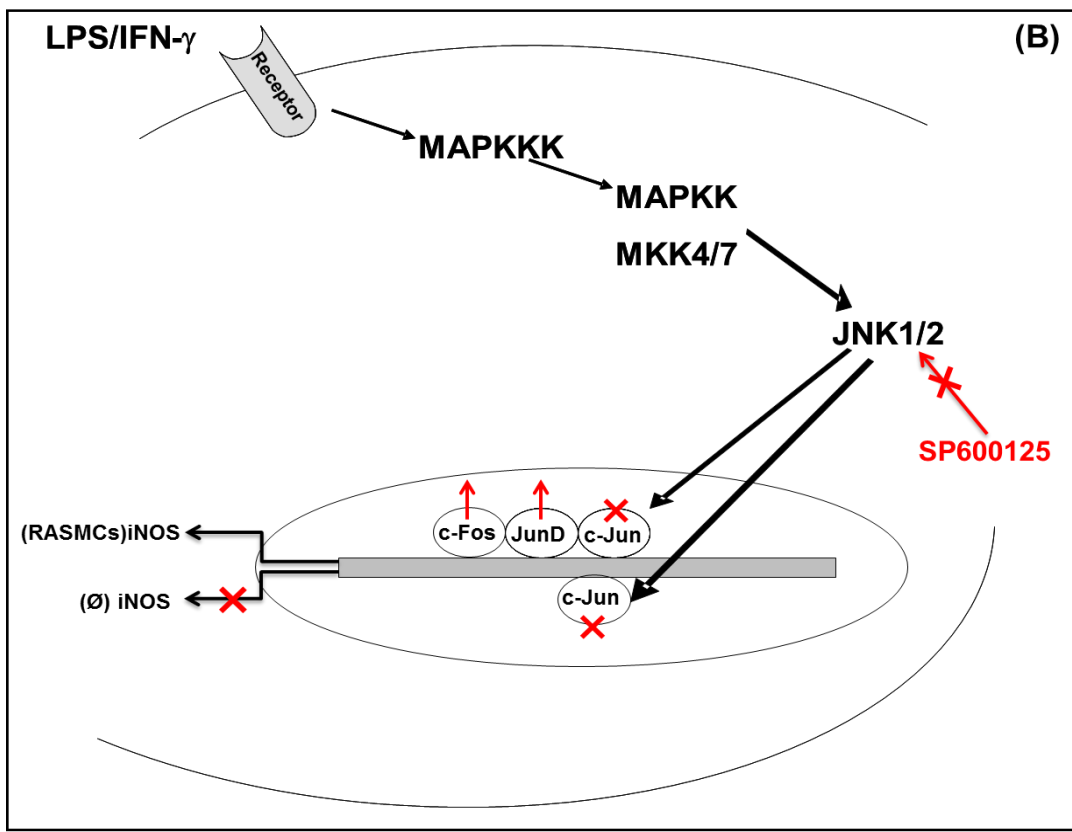
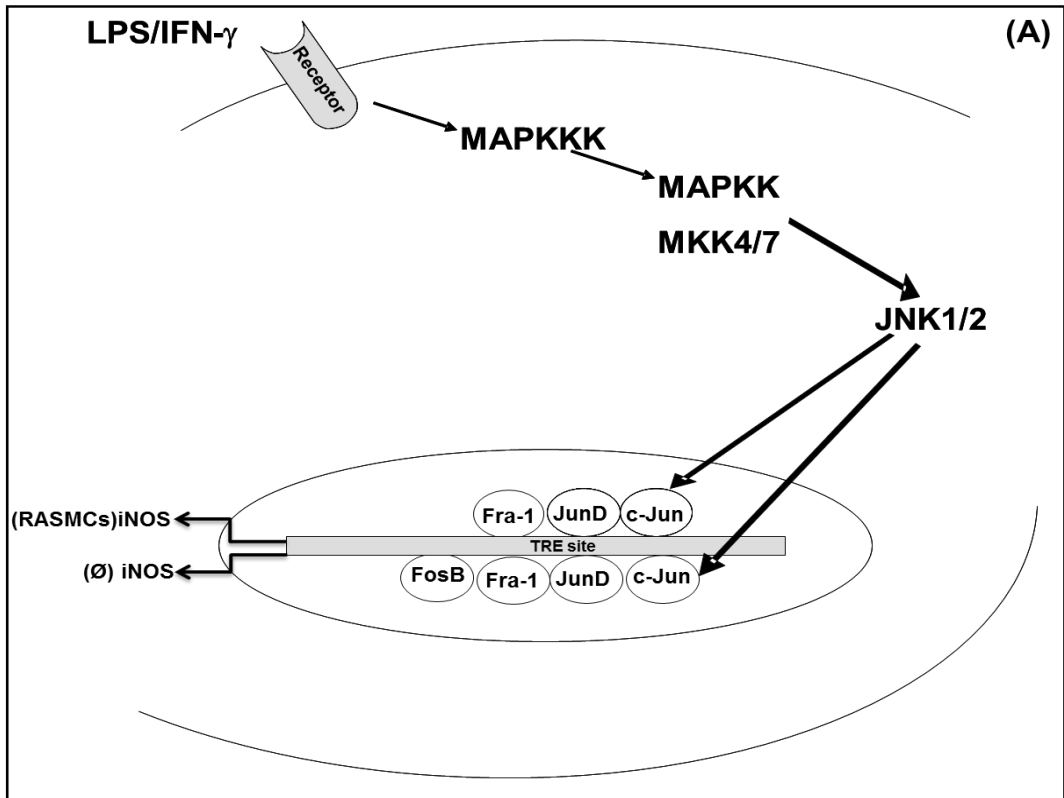
In macrophages no compensatory effect from JunD and c-Fos was observed and therefore c-Jun reduction caused a down-regulation in iNOS expression. Because as it was shown before JunB, JunD and c-Fos can compensate c-Jun reduction (Nadori *et al.*, 1997; Tkach *et al.*, 2003).

To summarise the interaction between subunits we can conclude that in macrophages c-Jun may be the main subunit. Its induction caused an increase in AP-1 positive transcriptional activity and its decline caused a down-regulation in AP-1 activity and therefore in this cell type, c-Jun is a positive regulator which regulates

iNOS gene expression. In smooth muscle cells however, the mechanism is more complex. c-Jun is a positive regulator as its increase after activation with LPS resulted in iNOS induction, however other regulators such as c-Fos may also be involved as their activity did not change when the cells were activated with LPS/IFN- $\gamma$  but altered by the pharmacological JNK inhibitor SP600125 which could have caused a compensatory response to c-Jun inhibition, thus sustaining iNOS expression. This complex mechanism, summarised in Figure 6.1, needs a more detailed examination to enable us to have a full understanding of how iNOS induction may be regulated.

**Figure 6.1 The proposed role of different AP-1 subunits in the induction of iNOS expression in RASMCs and J774 macrophages**

Classically activation of RASMCs or J774 macrophages ( $\emptyset$ ) with inflammatory mediators may induce c-Jun activation which when complexed with another AP-1 subunit initiates iNOS gene transcription and subsequent protein expression (Pannel A). This process may be blocked by SP600125 resulting in the inhibition of iNOS epxresion in J774 macrophages. In RASMCs this may be compensated for by the activation of other AP-1 subunits such as c-Fos which may complex with JunD and compensate for the loss of c-Jun activity (Pannel B). This may in turn sustain iNOS induction leading to no significant loss in NO production as reported in this thesis.



In parallel with studies on iNOS, the effect of JNK/AP-1 pathway on L-arginine transporter and its transporters was determined. Interestingly, the two dominant negatives regulated L-arginine transport differently with a-Fos showing no effect while TAM-67 partially blocked transport rates in RASMCs. These observations are the first to show that induction of transporter activity is dependent on the JNK/AP-1 pathway and perhaps more interestingly that there may be differential regulation of CATs by different AP-1 subunits. In RASMCs CAT-1 mRNA declined when cells were exposed to LPS and IFN- $\gamma$  and at the same time CAT-2B mRNA was enhanced with no effect on CAT-2A. Also, none of the transcripts for the transporters were affected by the JNK inhibitor SP600125 or a-Fos but CAT-2B was marginal reduced by TAM-67 and this is consistent with the reductions in transport rates seen under identical conditions. In J774 macrophages, CAT-2A and CAT-2B mRNA increased following stimulation with LPS but CAT-1 didn't show any changes. JNK inhibition with SP600125 reduced CAT-2B without affecting CAT-1 or CAT-2A mRNA levels which helped the conclusion that CAT-2B, one of the main transporters of L-arginine in these cells, is critically regulated at least in part by JNK activation.

It should be noted that the experiments in this study were limited to pharmacological and molecular tools and further complementary experiments can be carry out to fully establish the role of the JNK/AP-1 pathway in inflammatory condition. These could include the use of knockout animals such as JNK<sup>-/-</sup> mice (Medeiros *et al.*, 2007; Zingarelli *et al.*, 2002). In these experiments JNK 1 and JNK 2 can separately be knock-out and the animals stimulated with LPS/ IFN- $\gamma$  to reveal whether iNOS expression has been induced. These studies could be coupled with the determination of plasma nitrite levels and with changes in the expression profile of

iNOS protein in various tissues in comparison to the wild type animals. Furthermore, smooth muscle cells could be isolated and cultured *in vitro* to establish whether the cells will respond to stimulation by expressing iNOS. In relation to these studies, Wang *et al.* (2009) has already used a MAPK phosphatase 1 (MKP-1) <sup>-/-</sup> mice model to determine the changes in inflammatory response to LPS. Their results reveal that in response to LPS, MKP-1 <sup>-/-</sup> mice produced much more inflammatory cytokines and nitric oxide and severe hypotension compared to wild type. These observations already begin to indicate a critical role of JNK as MKP-1 is an inhibitor of the upstream activator of JNK.

Another approach could be the use of siRNA against AP-1 subunits to specifically knockout individual subunits component genes. The expression of each sub-unit gene could be blocked and the consequences on iNOS expression and NO production investigated. Alternatively, JNK and/or various AP-1 subunits could be overexpressed and the consequences on iNOS expression and NO production again investigated through the standard protocols described in this thesis. At the moment not much has been done on the effect of AP-1 subunits overexpression on iNOS induction and such studies would therefore be valuable. Studies by Wang *et al.* (2009) have used the co-transfection of c-Jun and c-Fos plasmids to inspect the effect of AP-1 overexpression on iNOS regulation and showed this resulted in a reduction of iNOS expression.

To support the studies above, additional experiments could be carried out correlating changes in AP-1 subunits expression using western blotting with changes in iNOS expression and NO production after incubation with LPS and/or IFN- $\gamma$ . This would confirm the trend observed in chapter 5 and give a clear indication of which subunits

may actually be critical for the induction of iNOS. Moreover all these experiments should be conducted in parallel with the experiments studying the L-arginine transport systems to verify how this system may be regulated by JNK.

Another desirable experiment would be determining the possibility of any crosstalk between AP-1 and NF- $\kappa$ B as Angel *et al.*, 1991 revealed that TAM-67 may have a regulatory effect on the p65 subunit of NF- $\kappa$ B. Therefore western blotting can detect the expression of p65 in a TAM-67 transfected system. Additionally changes in NF- $\kappa$ B activity in response to TAM-67 treatment could be monitored by ELISA. Such studies would shed light on whether the effects of TAM-67 may, in part, relate to NF- $\kappa$ B signalling.

## Summary

It has been established that JNK/AP-1 pathway has a role in iNOS induction in both RASMCs and J774 macrophages. Although this effect is not clear in RASMCs, it seems that in these cells, JNK is phosphorylated by LPS/IFN- $\gamma$  and after inhibition with SP600125, there is a down regulation in JNK which should potentially down-regulate AP-1 leading to suppression of iNOS expression. This was however not apparent, potentially because of up-regulation of other AP-1 subunits, which may be positively coupled to iNOS gene promoter and thus able to sustain iNOS expression, regulating the induction of the enzyme. These findings reveal why pharmacological tools alone may not be sufficient for illustrating the complex signalling that may be essential for iNOS induction. Researchers should therefore consider appropriate experimental approaches to their studies and should exercise caution in interpreting data for which there is no additional studies in support that could account for the proposed underlying mechanism of action of drugs.

## Future Work

- As our experiments were limited in two cell types, it will be desirable to employ different cell types to get a clear picture and determine if the diversity of response is depend on the cell type or specious. Moreover it will be ideal to isolate macrophages from rat to compare the pathways in both macrophages but different species.
- Investigate the signalling upstream of JNK to identify the diverse mechanisms that regulate iNOS and L-arginine transport. In this regard MKK4 and MKK7 specific antibody can be employ to observe any differences in JNK1 and JNK 2 from above.
- Identify any cross-talk between AP-1 and NF- $\kappa$ B pathways as TAM-67 may have regulatory effect on p65 subunit of NF- $\kappa$ B.
- Over-expression study needed for each subunit of AP-1 to observe their individual behaviour when over-expressed. Also a study with different AP-1 dimer inhibition can be performing to clarify the role of various dimer combinations.
- Investigation the role of JNK and it's upstream MKK4/7 in CAT expression and determine which MAPK is involved in the regulation of these transporters.
- Determine the role of each AP-1 subunits in CATs expression when there is over-expressed subunits system.

# References

- ABATE, C., LUK, D. & CURRAN, T. (1991). Transcriptional regulation by Fos and Jun in vitro: interaction among multiple activator and regulatory domains. *Mol Cell Biol*, **11**, 3624-32.
- ADAMS, J.W., SAKATA, Y., DAVIS, M.G., SAH, V.P., WANG, Y., LIGGETT, S.B., CHIEN, K.R., BROWN, J.H., DORN, G.W. 2nd. Enhanced Galphaq signaling: a common pathway mediates cardiac hypertrophy and apoptotic heart failure. *Proc Natl Acad Sci U S A*. 95(17), 10140-5.
- ADAWI, D., MOLIN, G., JEPPSSON, B. (1997). Inhibition of nitric oxide modulates the effect of oral arginine supplementation in acute liver injury. *Scand J Gastroenterol*. **32**, 835-40.
- ADCOCK, I.M., BROWN, C.R., KWON, O. & BARNES, P.J. (1994). Oxidative stress induces NF kappa B DNA binding and inducible NOS mRNA in human epithelial cells. *Biochem Biophys Res Commun*, **199**, 1518-24.
- AGVALD, P., ADDING, L.C., ARTLICH, A., PERSSON, M.G., GUETAFSSON, L.E. (2002). Mechanisms of nitric oxide generation from nitroglycerin and endogenous sources during hypoxia in vivo. *Br J Pharmacol*. **135**, 373-82.
- AHMAD, R., QURESHI, H.Y., EL MABROUK, M., SYLVESTER, J., AHMAD, M. & ZAFARULLAH, M. (2007). Inhibition of interleukin 1-induced matrix metalloproteinase 13 expression in human chondrocytes by interferon gamma. *Ann Rheum Dis*, **66**, 782-9.
- ALBUSZIES, G., Vogt, J., Wachter, U., Thiemermann, C., Leverve, X. M., Weber, S., et al. (2007). The effect of iNOS deletion on hepatic gluconeogenesis in hyperdynamic murine septic shock. *Intensive Care Med*, **33**(6), 1094-1101.
- ALDERTON, W.K., COOPER, C.E. & KNOWLES, R.G. (2001). Nitric oxide synthases: structure, function and inhibition. *Biochem J*, **357**, 593-615.

- ANDREW, P.J. & MAYER, B. (1999). Enzymatic function of nitric oxide synthases. *Cardiovasc Res*, **43**, 521-31.
- ANGEL, P., IMAGAWA, M., CHIU, R., STEIN, B., IMBRA, R.J., RAHMSDORF, H.J., JONAT, C., HERRLICH, P. & KARIN, M. (1987). Phorbol ester-inducible genes contain a common cis element recognized by a TPA-modulated trans-acting factor. *Cell*, **49**, 729-39.
- ANGEL, P. & KARIN, M. (1991). The role of Jun, Fos and the AP-1 complex in cell-proliferation and transformation. *Biochim Biophys Acta*, **1072**, 129-57.
- ANGEL, P. & SZABOWSKI, A. (2002). Function of AP-1 target genes in mesenchymal-epithelial cross-talk in skin. *Biochem Pharmacol*, **64**, 949-56.
- ANGELONI, C., HRELIA, S. (2012). Quercetin reduces inflammatory responses in LPS-stimulated cardiomyoblasts. *Oxid Med Cell Longev*. 2012:837104.
- ARNOLD, W.P., MITTAL, C.K., KATSUKI, S. & MURAD, F. (1977). Nitric oxide activates guanylate cyclase and increases guanosine 3':5'-cyclic monophosphate levels in various tissue preparations. *Proc Natl Acad Sci U S A*, **74**, 3203-7.
- ARSTALL, M.A., SAWYER, D.B., FUKAZAWA, R., KELLY, R.A. (1999). Cytokine-mediated apoptosis in cardiac myocytes: the role of inducible nitric oxide synthase induction and peroxynitrite generation. *Circ Res*. 85(9), 829-40.
- ASSREUY, J. & MONCADA, S. (1992). A perfusion system for the long term study of macrophage activation. *Br J Pharmacol*, **107**, 317-21.
- AVONTUUR, J.A., BUIJK, S.L., BRUINING, H.A. (1998). Distribution and metabolism of N(G)-nitro-L-arginine methyl ester in patients with septic shock. *Eur J Clin Pharmacol*. **54**, 627-31.

- BAHASSI EL, M., KARYALA, S., TOMLINSON, C.R., SARTOR, M.A., MEDVEDOVIC, M. & HENNIGAN, R.F. (2004). Critical regulation of genes for tumor cell migration by AP-1. *Clin Exp Metastasis*, **21**, 293-304.
- BASKEY, J.C., KALISCH, B.E., DAVIS, W.L., MEAKIN, S.O. & RYLETT, R.J. (2002). PC12nr5 cells expressing TrkA receptors undergo morphological but not cholinergic phenotypic differentiation in response to nerve growth factor. *J Neurochem*, **80**, 501-11.
- BAYDOUN, A.R., BOGLE, R.G., PEARSON, J.D., MANN, G.E. (1993). Selective inhibition by dexamethasone of induction of NO synthase, but not of induction of L-arginine transport, in activated murine macrophage J774 cells. *Br J Pharmacol*. **110**, 1401-6.
- BAYDOUN, A.R., EMERY, P.W., PEARSON, J.D. & MANN, G.E. (1990). Substrate-dependent regulation of intracellular amino acid concentrations in cultured bovine aortic endothelial cells. *Biochem Biophys Res Commun*, **173**, 940-8.
- BAYDOUN, A.R. & MANN, G.E. (1994). Selective targeting of nitric oxide synthase inhibitors to system  $\gamma^+$  in activated macrophages. *Biochem Biophys Res Commun*, **200**, 726-31.
- BAYDOUN, A.R., WILEMAN, S.M., WHEELER-JONES, C.P., MARBER, M.S., MANN, G.E., PEARSON, J.D. & CLOSS, E.I. (1999). Transmembrane signalling mechanisms regulating expression of cationic amino acid transporters and inducible nitric oxide synthase in rat vascular smooth muscle cells. *Biochem J*, **344 Pt 1**, 265-72.
- BEASLEY, D., SCHWARTZ, J.H. & BRENNER, B.M. (1991). Interleukin 1 induces prolonged L-arginine-dependent cyclic guanosine monophosphate and nitrite production in rat vascular smooth muscle cells. *J Clin Invest*, **87**, 602-8.

- BECK, K.F., EBERHARDT, W., WALPEN, S., APEL, M. & PFEILSCHIFTER, J. (1998). Potentiation of nitric oxide synthase expression by superoxide in interleukin 1 beta-stimulated rat mesangial cells. *FEBS Lett*, **435**, 35-8.
- BECK, K.F. & STERZEL, R.B. (1996). Cloning and sequencing of the proximal promoter of the rat iNOS gene: activation of NFkappaB is not sufficient for transcription of the iNOS gene in rat mesangial cells. *FEBS Lett*, **394**, 263-7.
- BECKMAN, J.S., BECKMAN, T.W., CHEN, J., MARSHALL, P.A. & FREEMAN, B.A. (1990). Apparent hydroxyl radical production by peroxynitrite: implications for endothelial injury from nitric oxide and superoxide. *Proc Natl Acad Sci U S A*, **87**, 1620-4.
- BECKMAN, J.S. & KOPPENOL, W.H. (1996). Nitric oxide, superoxide, and peroxynitrite: the good, the bad, and ugly. *Am J Physiol*, **271**, C1424-37.
- BENGTSSON, M., KARLSSON, H.J., WESTMAN, G. & KUBISTA, M. (2003). A new minor groove binding asymmetric cyanine reporter dye for real-time PCR. *Nucleic Acids Res*, **31**, e45.
- BERGERON, M. & OLIVIER, M. (2006). Trypanosoma cruzi-mediated IFN-gamma-inducible nitric oxide output in macrophages is regulated by iNOS mRNA stability. *J Immunol*, **177**, 6271-80.
- BERGMAN, M.R., CHENG, S., HONBO, N., PIACENTINI, L., KARLINER, J.S. & LOVETT, D.H. (2003). A functional activating protein 1 (AP-1) site regulates matrix metalloproteinase 2 (MMP-2) transcription by cardiac cells through interactions with JunB-Fra1 and JunB-FosB heterodimers. *Biochem J*, **369**, 485-96.
- BERNARDEAU, C., DERNIS-LABOUS, E., BLANCHARD, H., LAMARQUE, D. & BREBAN, M. (2001). Nitric oxide in rheumatology. *Joint Bone Spine*, **68**, 457-62.

- BERNSTEIN, H.G., Bogerts B, Keilhoff G. (2005). The many faces of nitric oxide in schizophrenia. A review. *Schizophr Res.* 78, 69-86.
- BLANCHETTE, J., DAYYEH, I.A., HASSANI, K., WHITCOMBE, L. & OLIVIER, M. (2008). Regulation of macrophage nitric oxide production by the protein tyrosine phosphatase Src homology 2 domain phosphotyrosine phosphatase 1 (SHP-1). *Immunology*.
- BOBROVNIKOVA-MARJON, E.V., MARJON, P.L., BARBASH, O., VANDER JAGT, D.L. & ABCOUWER, S.F. (2004). Expression of angiogenic factors vascular endothelial growth factor and interleukin-8/CXCL8 is highly responsive to ambient glutamine availability: role of nuclear factor-kappaB and activating protein-1. *Cancer Res*, **64**, 4858-69.
- BODE, A.M. & DONG, Z. (2007). The functional contrariety of JNK. *Mol Carcinog*, **46**, 591-8.
- BOGLE, R.G., BAYDOUN, A.R., PEARSON, J.D., MONCADA, S. & MANN, G.E. (1992). L-arginine transport is increased in macrophages generating nitric oxide. *Biochem J*, **284 ( Pt 1)**, 15-8.
- BOGOYEVITCH, M.A. & ARTHUR, P.G. (2008). Inhibitors of c-Jun N-terminal kinases: JuNK no more? *Biochim Biophys Acta*, **1784**, 76-93.
- BOGOYEVITCH, M.A., BOEHM, I., OAKLEY, A., KETTERMAN, A.J. & BARR, R.K. (2004). Targeting the JNK MAPK cascade for inhibition: basic science and therapeutic potential. *Biochim Biophys Acta*, **1697**, 89-101.
- BOGOYEVITCH, M.A. & KOBE, B. (2006). Uses for JNK: the many and varied substrates of the c-Jun N-terminal kinases. *Microbiol Mol Biol Rev*, **70**, 1061-95.

- BONOVICH, M., OLIVE, M., REED, E., O'CONNELL, B. & VINSON, C. (2002). Adenoviral delivery of A-FOS, an AP-1 dominant negative, selectively inhibits drug resistance in two human cancer cell lines. *Cancer Gene Ther*, **9**, 62-70.
- BOUGHTON-SMITH, N.K., EVANS, S.M., HAWKEY, C.J., COLE, A.T., BALSITIS, M., WHITTLE, B.J., MONCADA S. (1993). Nitric oxide synthase activity in ulcerative colitis and Crohn's disease. *Lancet*. 342, 338-40.
- BOUTROS, T., CHEVET, E. & METRAKOS, P. (2008). Mitogen-activated protein (MAP) kinase/MAP kinase phosphatase regulation: roles in cell growth, death, and cancer. *Pharmacol Rev*, **60**, 261-310.
- BROWN, P.H., CHEN, T.K. & BIRRER, M.J. (1994). Mechanism of action of a dominant-negative mutant of c-Jun. *Oncogene*, **9**, 791-9.
- Bultinck, J., Sips, P., Vakaet, L., Brouckaert, P., & Cauwels, A. (2006). Systemic NO production during (septic) shock depends on parenchymal and not on hematopoietic cells: in vivo iNOS expression pattern in (septic) shock. *FASEB J*, **20**(13), 2363-2365.
- BUTTERY, L.D., CHESTER, A.H., SPRINGALL, D.R., BORLAND, J.A., MICHEL, T., YACOUB, M.H., POLAK, J.M. (1996). Inducible nitric oxide synthase is present within human atherosclerotic lesions and promotes the formation and activity of peroxynitrite. *Lab Invest* **75**, 77-85.
- CAIVANO, M. (1998). Role of MAP kinase cascades in inducing arginine transporters and nitric oxide synthetase in RAW264 macrophages. *FEBS Lett*, **429**, 249-53.
- CASANELLO, P., ESCUDERO, C. & SOBREVIA, L. (2007). Equilibrative nucleoside (ENTs) and cationic amino acid (CATs) transporters: implications in foetal endothelial dysfunction in human pregnancy diseases. *Curr Vasc Pharmacol*, **5**, 69-84.

- CAVICCHI, M. & WHITTLE, B.J. (1999). Potentiation of cytokine induced iNOS expression in the human intestinal epithelial cell line, DLD-1, by cyclic AMP. *Gut*, **45**, 367-74.
- CHAMPION H.C., SKAF, M.W., HARE, J.M. (2003). Role of nitric oxide in the pathophysiology of heart failure. *Heart Fail Rev.* 8, 35-46.
- CHAN, E.D. & RICHES, D.W. (2001). IFN-gamma + LPS induction of iNOS is modulated by ERK, JNK/SAPK, and p38(mapk) in a mouse macrophage cell line. *Am J Physiol Cell Physiol*, **280**, C441-50.
- CHAN, E.D. & RICHES, D.W. (1998). Potential role of the JNK/SAPK signal transduction pathway in the induction of iNOS by TNF-alpha. *Biochem Biophys Res Commun*, **253**, 790-6.
- CHANG, L.C., TSAO, L.T., CHANG, C.S., CHEN, C.J., HUANG, L.J., KUO, S.C., LIN, R.H. & WANG, J.P. (2008). Inhibition of nitric oxide production by the carbazole compound LCY-2-CHO via blockade of activator protein-1 and CCAAT/enhancer-binding protein activation in microglia. *Biochem Pharmacol*, **76**, 507-19.
- CHANG, W.C., LEE, Y.C., LIU, C.L., HSU, J.D., WANG, H.C., CHEN, C.C. & WANG, C.J. (2001). Increased expression of iNOS and c-fos via regulation of protein tyrosine phosphorylation and MEK1/ERK2 proteins in terminal bronchiole lesions in the lungs of rats exposed to cigarette smoke. *Arch Toxicol*, **75**, 28-35.
- CHANSARD, M., MOLYNEUX, P., NOMURA, K., HARRINGTON, M.E. & FUKUHARA, C. (2007). c-Jun N-terminal kinase inhibitor SP600125 modulates the period of mammalian circadian rhythms. *Neuroscience*, **145**, 812-23.

- CHATURVEDI, R., ASIM, M., HOGE, S., LEWIS, N.D., SINGH, K., BARRY, D.P., DE SABLET, T., PIAZUELO, M.B., SARVARIA, A.R., CHENG, Y., CLOSS, E.I., CASERO, R.A., JR., GOBERT, A.P. & WILSON, K.T. Polyamines Impair Immunity to *Helicobacter pylori* by Inhibiting L-Arginine Uptake Required for Nitric Oxide Production. *Gastroenterology*.
- CHEN, C., CHEN, Y.H. & LIN, W.W. (1999). Involvement of p38 mitogen-activated protein kinase in lipopolysaccharide-induced iNOS and COX-2 expression in J774 macrophages. *Immunology*, **97**, 124-9.
- CHEN, C.C., TSAI, P.C., WEI, B.L. & CHIOU, W.F. (2008). 8-Prenylkaempferol suppresses inducible nitric oxide synthase expression through interfering with JNK-mediated AP-1 pathway in murine macrophages. *Eur J Pharmacol*, **590**, 430-6.
- CHEN, C.W., LEE, S.T., WU, W.T., FU, W.M., HO, F.M. & LIN, W.W. (2003). Signal transduction for inhibition of inducible nitric oxide synthase and cyclooxygenase-2 induction by capsaicin and related analogs in macrophages. *Br J Pharmacol*, **140**, 1077-87.
- CHEN, N., SHE, Q.B., BODE, A.M. & DONG, Z. (2002). Differential gene expression profiles of Jnk1- and Jnk2-deficient murine fibroblast cells. *Cancer Res*, **62**, 1300-4.
- CHEN, R.H., JUO, P.C., CURRAN, T. & BLENIS, J. (1996). Phosphorylation of c-Fos at the C-terminus enhances its transforming activity. *Oncogene*, **12**, 1493-502.
- CHIN-DUSTING, J.P.F., WILLEMS, L. & KAYE, D.M. (2007). L-Arginine transporters in cardiovascular disease: A novel therapeutic target. *Pharmacology & Therapeutics*, **116**, 428-436.

- CHIN, S.Y., PANDEY, K.N., SHI, S.J., KOBORI, H., MORENO, C. & NAVAR, L.G. (1999). Increased activity and expression of Ca(2+)-dependent NOS in renal cortex of ANG II-infused hypertensive rats. *Am J Physiol*, **277**, F797-804.
- CHINENOV, Y. & KERPPOLA, T.K. (2001). Close encounters of many kinds: Fos-Jun interactions that mediate transcription regulatory specificity. *Oncogene*, **20**, 2438-52.
- CHITTEZHATH, M., DEEP, G., SINGH, R.P., AGARWAL, C. & AGARWAL, R. (2008). Silibinin inhibits cytokine-induced signaling cascades and down-regulates inducible nitric oxide synthase in human lung carcinoma A549 cells. *Mol Cancer Ther*, **7**, 1817-26.
- CHIU, F.L. & LIN, J.K. (2008). Tomatidine inhibits iNOS and COX-2 through suppression of NF-kappaB and JNK pathways in LPS-stimulated mouse macrophages. *FEBS Lett*, **582**, 2407-12.
- CHO, M.K., SUH, S.H. & KIM, S.G. (2002). JunB/AP-1 and NF-kappa B-mediated induction of nitric oxide synthase by bovine type I collagen in serum-stimulated murine macrophages. *Nitric Oxide*, **6**, 319-32.
- CHO, S.O., LIM, J.W., KIM, K.H. & KIM, H. (2009). Involvement of Ras and AP-1 in Helicobacter pylori-Induced Expression of COX-2 and iNOS in Gastric Epithelial AGS Cells. *Dig Dis Sci*.
- CHOI, C.Y., PARK, K.R., LEE, J.H., JEON, Y.J., LIU, K.H., OH, S., KIM, D.E. & YEA, S.S. (2007). Isoeugenol suppression of inducible nitric oxide synthase expression is mediated by down-regulation of NF-kappaB, ERK1/2, and p38 kinase. *Eur J Pharmacol*, **576**, 151-9.
- CHU, L.C., TSAI, P.S., LEE, J.J., YEN, C.H. & HUANG, C.J. (2005). NF-kappaB inhibitors significantly attenuate the transcription of high affinity type-2 cationic

amino acid transporter in LPS-stimulated rat kidney. *Acta Anaesthesiol Taiwan*, **43**, 23-32.

CHU, S.C., MARKS-KONCZALIK, J., WU, H.P., BANKS, T.C. & MOSS, J. (1998). Analysis of the cytokine-stimulated human inducible nitric oxide synthase (iNOS) gene: characterization of differences between human and mouse iNOS promoters. *Biochem Biophys Res Commun*, **248**, 871-8.

CHYU, K.Y., DIMAYUGA, P.C., ZHAO, X., NILSSON, J., SHAH, P.K. & CERCEK, B. (2004). Altered AP-1/Ref-1 redox pathway and reduced proliferative response in iNOS-deficient vascular smooth muscle cells. *Vasc Med*, **9**, 177-83.

CI, X., LIANG, X., LUO, G., YU, Q., LI, H., WANG, D., LI, R. & DENG, X. (2010). Regulation of inflammatory mediators in lipopolysaccharide-stimulated RAW 264.7 cells by 2"-hydroxy-3"-en-anhydroicaritin involves down-regulation of NF-kappaB and MAPK expression. *Int Immunopharmacol*.

CLOSS, E.I., ALBRITTON, L.M., KIM, J.W. & CUNNINGHAM, J.M. (1993a). Identification of a low affinity, high capacity transporter of cationic amino acids in mouse liver. *J Biol Chem*, **268**, 7538-44.

CLOSS, E.I., BOISSEL, J.P., HABERMEIER, A. & ROTMANN, A. (2006). Structure and function of cationic amino acid transporters (CATs). *J Membr Biol*, **213**, 67-77.

CLOSS, E.I., BOREL RINKES, I.H., BADER, A., YARMUSH, M.L. & CUNNINGHAM, J.M. (1993b). Retroviral infection and expression of cationic amino acid transporters in rodent hepatocytes. *J Virol*, **67**, 2097-102.

CLOSS, E.I., GRAF, P., HABERMEIER, A., CUNNINGHAM, J.M. & FORSTERMANN, U. (1997). Human cationic amino acid transporters hCAT-1, hCAT-2A, and hCAT-2B: three related carriers with distinct transport properties. *Biochemistry*, **36**, 6462-8.

- CLOSS, E.I., LYONS, C.R., KELLY, C. & CUNNINGHAM, J.M. (1993c). Characterization of the third member of the MCAT family of cationic amino acid transporters. Identification of a domain that determines the transport properties of the MCAT proteins. *J Biol Chem*, **268**, 20796-800.
- CLOSS, E.I. & MANN, G.E. (1999). Identification of carrier systems in plasma membranes of mammalian cells involved in transport of L-arginine. *Methods Enzymol*, **301**, 78-91.
- CLOSS, E.I., SCHELD, J.S., SHARAFI, M. & FORSTERMANN, U. (2000). Substrate supply for nitric-oxide synthase in macrophages and endothelial cells: role of cationic amino acid transporters. *Mol Pharmacol*, **57**, 68-74.
- COHEN, R.I., CHEN, L., SCHARF, S.M. (1996). The effects of high dose NG-nitro-L-arginine-methyl ester on myocardial blood flow and left ventricular function in dogs. *J Crit Care*. 11(4), 206-13.
- COOKE and DAVIDGE (2002). Peroxynitrite increases iNOS through NF-kappaB and decreases prostacyclin synthase in endothelial cells. *Am J Physiol Cell Physiol* **282**(2): C395-402.
- COOKE, J.P. (1998). Is atherosclerosis an arginine deficiency disease? *J Investig Med*, **46**, 377-80.
- COOPER, R.G., & MAGWERE, T. (2008). Nitric oxide-mediated pathogenesis during nicotine and alcohol consumption. *Indian J Physiol Pharmacol* **52**(1): 11-8.
- COTTER, G., KALUSKI, E., MILO, O., BLATT, A., SALAH, A., Hendler A, Krakover R, Golick A, Vered Z. (2003). LINCS: L-NAME (a NO synthase inhibitor) in the treatment of refractory cardiogenic shock: a prospective randomized study. *Eur Heart J*. **24**, 1287-95.

- CROSS, H.R., MURPHY, E. & STEENBERGEN, C. (2002). Ca(2+) loading and adrenergic stimulation reveal male/female differences in susceptibility to ischemia-reperfusion injury. *Am J Physiol Heart Circ Physiol*, **283**, H481-9.
- CUI, Z., TULADHAR, R., HART, S.L., MARBER, M.S., PEARSON, J.D. & BAYDOUN, A.R. (2005). Rate of transport of L-arginine is independent of the expression of inducible nitric oxide synthase in HEK 293 cells. *Nitric Oxide*, **12**, 21-30.
- DALL'ASTA, V., BUSSOLATI, O., SALA, R., ROTOLI, B.M., SEBASTIO, G., SPERANDEO, M.P., ANDRIA, G. & GAZZOLA, G.C. (2000). Arginine transport through system y(+)L in cultured human fibroblasts: normal phenotype of cells from LPI subjects. *Am J Physiol Cell Physiol*, **279**, C1829-37.
- DAVIS, R.J. (2000a). Signal transduction by the JNK group of MAP kinases. *Cell*, **103**, 239-52.
- DAVIS, R.J. (2000b). Signal Transduction by the JNK Group of MAP Kinases. *Cell*, **103**, 239-252.
- DEBELDER A., ROBINSON N., RICHARDSON P., MARTIN J., MONCADA S. (1997). Expression of inducible nitric oxide synthase in human heart failure. *Circulation*, **95**, 1672-3.
- DENG, T. & KARIN, M. (1993). JunB differs from c-Jun in its DNA-binding and dimerization domains, and represses c-Jun by formation of inactive heterodimers. *Genes Dev*, **7**, 479-90.
- DENG, X., XIAO, L., LANG, W., GAO, F., RUVOLO, P. & MAY, W.S., JR. (2001). Novel role for JNK as a stress-activated Bcl2 kinase. *J Biol Chem*, **276**, 23681-8.
- DERIJARD, B., HIBI, M., WU, I.H., BARRETT, T., SU, B., DENG, T., KARIN, M. & DAVIS, R.J. (1994). JNK1: a protein kinase stimulated by UV light and Ha-Ras that binds and phosphorylates the c-Jun activation domain. *Cell*, **76**, 1025-37.

- DERIJARD, B., RAINGEAUD, J., BARRETT, T., WU, I.H., HAN, J., ULEVITCH, R.J. & DAVIS, R.J. (1995). Independent human MAP-kinase signal transduction pathways defined by MEK and MKK isoforms. *Science*, **267**, 682-5.
- DEVES, R. & BOYD, C.A. (1998). Transporters for cationic amino acids in animal cells: discovery, structure, and function. *Physiol Rev*, **78**, 487-545.
- DHAR, A., HU, J., REEVES, R., RESAR, L.M. & COLBURN, N.H. (2004). Dominant-negative c-Jun (TAM67) target genes: HMGA1 is required for tumor promoter-induced transformation. *Oncogene*, **23**, 4466-76.
- DIJKSTRA, G., MOSHAGE, H., VAN DULLEMEN, H.M., DE JAGER-KRIKKEN, A., TIEBOSCH, A.T., KLEIBEUKER, J.H., JANSEN, P.L. & VAN GOOR, H. (1998). Expression of nitric oxide synthases and formation of nitrotyrosine and reactive oxygen species in inflammatory bowel disease. *J Pathol*, **186**, 416-21.
- DING, A., HWANG, S., LANDER, H.M. & XIE, Q.W. (1995). Macrophages derived from C3H/HeJ (Lpsd) mice respond to bacterial lipopolysaccharide by activating NF-kappa B. *J Leukoc Biol*, **57**, 174-9.
- DING, S.Z., OLEKHNOVICH, I.N., COVER, T.L., PEEK, R.M., JR., SMITH, M.F., JR. & GOLDBERG, J.B. (2008). Helicobacter pylori and mitogen-activated protein kinases mediate activator protein-1 (AP-1) subcomponent protein expression and DNA-binding activity in gastric epithelial cells. *FEMS Immunol Med Microbiol*, **53**, 385-94.
- DONG, C., DAVIS, R.J., FLAVELL, R.A. (2002). MAP kinases in the immune response. *Annu Rev Immunol*. **20**, 55-72.
- DONG, C., YANG, D.D., WYSK, M., WHITMARSH, A.J., DAVIS, R.J. & FLAVELL, R.A. (1998). Defective T cell differentiation in the absence of Jnk1. *Science*, **282**, 2092-5.

- DUDHGAONKAR, S., THYAGARAJAN, A. & SLIVA, D. (2009). Suppression of the inflammatory response by triterpenes isolated from the mushroom *Ganoderma lucidum*. *Int Immunopharmacol*, **9**, 1272-80.
- DURNER, J., WENDEHENNE, D. & KLESSIG, D.F. (1998). Defense gene induction in tobacco by nitric oxide, cyclic GMP, and cyclic ADP-ribose. *Proc Natl Acad Sci U S A*, **95**, 10328-33.
- DUSTING G.J. (1996). Nitric oxide in coronary artery disease: roles in atherosclerosis, myocardial reperfusion and heart failure. *EXS, Review*. 76, 33-55.
- EFERL, R., HASSELBLATT, P., RATH, M., POPPER, H., ZENZ, R., KOMNENOVIC, V., IDARRAGA, M.H., KENNER, L. & WAGNER, E.F. (2008). Development of pulmonary fibrosis through a pathway involving the transcription factor Fra-2/AP-1. *Proc Natl Acad Sci U S A*, **105**, 10525-30.
- EFERL, R. & WAGNER, E.F. (2003). AP-1: a double-edged sword in tumorigenesis. *Nat Rev Cancer*, **3**, 859-68.
- EVGENOV, O.V., PACHER, P., SCHMIDT, P.M., HASKO, G., SCHMIDT, H.H. & STASCH, J.P. (2006). NO-independent stimulators and activators of soluble guanylate cyclase: discovery and therapeutic potential. *Nat Rev Drug Discov*, **5**, 755-68.
- FENG, Z., LI, L., NG, P.Y. & PORTER, A.G. (2002). Neuronal differentiation and protection from nitric oxide-induced apoptosis require c-Jun-dependent expression of NCAM140. *Mol Cell Biol*, **22**, 5357-66.
- FERNANDEZ, A.P., Pozo-Rodrigalvarez A, Serrano J, Martinez-Murillo R. (2010). Nitric oxide: target for therapeutic strategies in Alzheimer's disease. *Curr Pharm Des*. 16(25), 2837-50.

- FINDER, J.D., PETRUS, J.L., HAMILTON, A., VILLAVICENCIO, R.T., PITT, B.R. & SEBTI, S.M. (2001). Signal transduction pathways of IL-1beta-mediated iNOS in pulmonary vascular smooth muscle cells. *Am J Physiol Lung Cell Mol Physiol*, **281**, L816-23.
- FINLEY, K.D., KAKUDA, D.K., BARRIEUX, A., KLEEMAN, J., HUYNH, P.D. & MACLEOD, C.L. (1995). A mammalian arginine/lysine transporter uses multiple promoters. *Proc Natl Acad Sci U S A*, **92**, 9378-82.
- FLODSTROM, M. & EIZIRIK, D.L. (1997). Interferon-gamma-induced interferon regulatory factor-1 (IRF-1) expression in rodent and human islet cells precedes nitric oxide production. *Endocrinology*, **138**, 2747-53.
- FLODSTROM, M., NIEMANN, A., BEDOYA, F.J., MORRIS, S.M., JR. & EIZIRIK, D.L. (1995). Expression of the citrulline-nitric oxide cycle in rodent and human pancreatic beta-cells: induction of argininosuccinate synthetase by cytokines. *Endocrinology*, **136**, 3200-6.
- FORSTERMANN, U. & KLEINERT, H. (1995). Nitric oxide synthase: expression and expressional control of the three isoforms. *Naunyn Schmiedebergs Arch Pharmacol*, **352**, 351-64.
- FRANCISCOVICH, A.L., MORTIMER, A.D., FREEMAN, A.A., GU, J. & SANYAL, S. (2008). Overexpression screen in *Drosophila* identifies neuronal roles of GSK-3 beta/shaggy as a regulator of AP-1-dependent developmental plasticity. *Genetics*, **180**, 2057-71.
- FRANK, S., KAMPFER, H., WETZLER, C. & PFEILSCHIFTER, J. (2002). Nitric oxide drives skin repair: novel functions of an established mediator. *Kidney Int*, **61**, 882-8.
- FUCHS, S.Y., ADLER, V., BUSCHMANN, T., YIN, Z., WU, X., JONES, S.N. & RONAI, Z. (1998). JNK targets p53 ubiquitination and degradation in nonstressed cells. *Genes Dev*, **12**, 2658-63.

- FUCHS, S.Y., XIE, B., ADLER, V., FRIED, V.A., DAVIS, R.J. & RONAI, Z. (1997). c-Jun NH2-terminal kinases target the ubiquitination of their associated transcription factors. *J Biol Chem*, **272**, 32163-8.
- FURCHGOTT, R.F. & ZAWADZKI, J.V. (1980). The obligatory role of endothelial cells in the relaxation of arterial smooth muscle by acetylcholine. *Nature*, **288**, 373-6.
- GERDES, M.J., MYAKISHEV, M., FROST, N.A., RISHI, V., MOITRA, J., ACHARYA, A., LEVY, M.R., PARK, S.W., GLICK, A., YUSPA, S.H. & VINSON, C. (2006). Activator protein-1 activity regulates epithelial tumor cell identity. *Cancer Res*, **66**, 7578-88.
- GHOSH, D.K. & SALERNO, J.C. (2003). Nitric oxide synthases: domain structure and alignment in enzyme function and control. *Front Biosci*, **8**, d193-209.
- GILL, D.J., LOW, B.C. & GRIGOR, M.R. (1996). Interleukin-1 beta and tumor necrosis factor-alpha stimulate the cat-2 gene of the L-arginine transporter in cultured vascular smooth muscle cells. *J Biol Chem*, **271**, 11280-3.
- GIRI, S., JATANA, M., RATTAN, R., WON, J.S., SINGH, I. & SINGH, A.K. (2002). Galactosylsphingosine (psychosine)-induced expression of cytokine-mediated inducible nitric oxide synthases via AP-1 and C/EBP: implications for Krabbe disease. *Faseb J*, **16**, 661-72.
- GOLDRING, C.E., NARAYANAN, R., LAGADEC, P. & JEANNIN, J.F. (1995). Transcriptional inhibition of the inducible nitric oxide synthase gene by competitive binding of NF-kappa B/Rel proteins. *Biochem Biophys Res Commun*, **209**, 73-9.
- GREEN, L.C., WAGNER, D.A., GLOGOWSKI, J., SKIPPER, P.L., WISHNOK, J.S. & TANNENBAUM, S.R. (1982). Analysis of nitrate, nitrite, and [15N]nitrate in biological fluids. *Anal Biochem*, **126**, 131-8.

- GRISHAM, M.B., PAVLICK, K.P., LAROUX, F.S., HOFFMAN, J., BHARWANI, S., WOLF, R.E. (2002). Nitric oxide and chronic gut inflammation: controversies in inflammatory bowel disease. *J Investig Med*. 50, 272-83.
- GUAN, Z., BUCKMAN, S.Y., SPRINGER, L.D. & MORRISON, A.R. (1999). Both p38alpha(MAPK) and JNK/SAPK pathways are important for induction of nitric-oxide synthase by interleukin-1beta in rat glomerular mesangial cells. *J Biol Chem*, **274**, 36200-6.
- GUO, L., SANS, M.D., GURDA, G.T., LEE, S.H., ERNST, S.A. & WILLIAMS, J.A. (2007). Induction of early response genes in trypsin inhibitor-induced pancreatic growth. *Am J Physiol Gastrointest Liver Physiol*, **292**, G667-77.
- GUPTA, P. & PRYWES, R. (2002). ATF1 phosphorylation by the ERK MAPK pathway is required for epidermal growth factor-induced c-jun expression. *J Biol Chem*, **277**, 50550-6.
- GUPTA, S., BARRETT, T., WHITMARSH, A.J., CAVANAGH, J., SLUSS, H.K., DERIJARD, B. & DAVIS, R.J. (1996). Selective interaction of JNK protein kinase isoforms with transcription factors. *Embo J*, **15**, 2760-70.
- GURZOV, E.N., ORTIS, F., BAKIRI, L., WAGNER, E.F. & EIZIRIK, D.L. (2008). JunB Inhibits ER Stress and Apoptosis in Pancreatic Beta Cells. *PLoS One*, **3**, e3030.
- HAHN, C., ORR, A.W., SANDERS, J.M., JHAVERI, K.A., SCHWARTZ, M.A. (2009). The subendothelial extracellular matrix modulates JNK activation by flow. *Circ Res*. 104(8):995-1003.
- HAMMERMANN, R., DREISSIG, M.D., MOSSNER, J., FUHRMANN, M., BERRINO, L., GOTHERT, M. & RACKE, K. (2000). Nuclear factor-kappaB mediates simultaneous induction of inducible nitric-oxide synthase and Up-regulation of

the cationic amino acid transporter CAT-2B in rat alveolar macrophages. *Mol Pharmacol*, **58**, 1294-302.

HAMMERMANN, R., STICHNOTE, C., CLOSS, E.I., NAWRATH, H. & RACKE, K. (2001). Inhibition of nitric oxide synthase abrogates lipopolysaccharides-induced up-regulation of L-arginine uptake in rat alveolar macrophages. *Br J Pharmacol*, **133**, 379-86.

HAN, Z., CHANG, L., YAMANISHI, Y., KARIN, M. & FIRESTEIN, G.S. (2002). Joint damage and inflammation in c-Jun N-terminal kinase 2 knockout mice with passive murine collagen-induced arthritis. *Arthritis Rheum*, **46**, 818-23.

HART, S.L., ARANCIBIA-CARCAMO, C.V., WOLFERT, M.A., MAILHOS, C., O'REILLY, N.J., ALI, R.R., COUTELLE, C., GEORGE, A.J., HARBOTTLE, R.P., KNIGHT, A.M., LARKIN, D.F., LEVINSKY, R.J., SEYMOUR, L.W., THRASHER, A.J. & KINNON, C. (1998). Lipid-mediated enhancement of transfection by a nonviral integrin-targeting vector. *Hum Gene Ther*, **9**, 575-85.

HARTWIG, C.L., WORRELL, J., LEVINE, R.B., RAMASWAMI, M. & SANYAL, S. (2008). Normal dendrite growth in Drosophila motor neurons requires the AP-1 transcription factor. *Dev Neurobiol*, **68**, 1225-42.

HATTORI, Y., CAMPBELL, E.B. & GROSS, S.S. (1994). Argininosuccinate synthetase mRNA and activity are induced by immunostimulants in vascular smooth muscle. Role in the regeneration or arginine for nitric oxide synthesis. *J Biol Chem*, **269**, 9405-8.

HATTORI, Y., KASAI, K. & GROSS, S.S. (1999). Cationic amino acid transporter gene expression in cultured vascular smooth muscle cells and in rats. *Am J Physiol*, **276**, H2020-8.

HATTORI, Y., MATSUMURA, M. & KASAI, K. (2003). Vascular smooth muscle cell activation by C-reactive protein. *Cardiovasc Res*, **58**, 186-95.

- HAYWOOD G.A., TSAO, P.S., VON DER LEYEN, H.E., MANN, M.J., KEELING, P.J., TRINDADE, P.T., LEWIS, N.P., BYRNE, C.D., RICKENBACHER, P.R., BISHOPRIC, N.H., COOKE, J.P., MACKENNA, W.J., FOWLER, M.B. (1996). Expression of inducible nitric oxide synthase in human heart failure. *Circulation*. 93, 1087-94.
- HECKER, M., CATTARUZZA, M. & WAGNER, A.H. (1999). Regulation of inducible nitric oxide synthase gene expression in vascular smooth muscle cells. *Gen Pharmacol*, **32**, 9-16.
- HECKER, M., PREISS, C. & SCHINI-KERTH, V.B. (1997). Induction by staurosporine of nitric oxide synthase expression in vascular smooth muscle cells: role of NF-kappa B, CREB and C/EBP beta. *Br J Pharmacol*, **120**, 1067-74.
- HEINEKE, J., MOLKENTIN, J.D. (2006). Regulation of cardiac hypertrophy by intracellular signalling pathways. *Nat. Rev. Mol. Cell. Biol.* 589–600.
- HEMMRICH, K., SUSCHEK, C.V., LERZINSKI, G. K., KOLB-BACHOFEN, V. (2003). iNOS activity is essential for endothelial stress gene expression protecting against oxidative damage." *J Appl Physiol* **95**(5): 1937-46.
- HENNIGAN, R.F. & STAMBROOK, P.J. (2001). Dominant negative c-jun inhibits activation of the cyclin D1 and cyclin E kinase complexes. *Mol Biol Cell*, **12**, 2352-63.
- HERDMAN, M.L., MARCELO, A., HUANG, Y., NILES, R.M., DHAR, S. & KININGHAM, K.K. (2006). Thimerosal induces apoptosis in a neuroblastoma model via the cJun N-terminal kinase pathway. *Toxicol Sci*, **92**, 246-53.
- HERLAAR, E. & BROWN, Z. (1999). p38 MAPK signalling cascades in inflammatory disease. *Molecular Medicine Today*, **5**, 439-447.

- HESS, J., ANGEL, P. & SCHORPP-KISTNER, M. (2004). AP-1 subunits: quarrel and harmony among siblings. *J Cell Sci*, **117**, 5965-73.
- HIROSUMI, J., TUNCMAN, G., CHANG, L., GORGUN, C.Z., UYSAL, K.T., MAEDA, K., KARIN, M. & HOTAMISLIGIL, G.S. (2002). A central role for JNK in obesity and insulin resistance. *Nature*, **420**, 333-6.
- HOCHEDLINGER, K., WAGNER, E.F. & SABAPATHY, K. (2002). Differential effects of JNK1 and JNK2 on signal specific induction of apoptosis. *Oncogene*, **21**, 2441-5.
- HORIKOSHI, S., FUKUDA, K., RAY, P.E., SAWADA, M., BRUGGEMAN, L.A. & KLOTMAN, P.E. (1992). A PCR method for the quantitative assessment of mRNA for laminin A, B1, and B2 chains. *Kidney Int*, **42**, 764-9.
- HORTON, J.W., MAASS, D., WHITE, J., SANDERS, B. (2000). Nitric oxide modulation of TNF-alpha-induced cardiac contractile dysfunction is concentration dependent. *Am J Physiol Heart Circ Physiol*. 278(6), H1955-65.
- HOU, Y.C., JANCZUK, A. & WANG, P.G. (1999). Current trends in the development of nitric oxide donors. *Curr Pharm Des*, **5**, 417-41.
- HUANG, C.J., TSAI, P.S., LU, Y.T., CHENG, C.R., STEVENS, B.R., SKIMMING, J.W. & PAN, W.H. (2004). NF-kappaB involvement in the induction of high affinity CAT-2 in lipopolysaccharide-stimulated rat lungs. *Acta Anaesthesiol Scand*, **48**, 992-1002.
- HUGHES, M.N. (2008). Chemistry of nitric oxide and related species. *Methods Enzymol*, **436**, 3-19.
- HUGHES, M.N. & ROBERT, K.P. (2008). Chemistry of Nitric Oxide and Related Species. In *Methods in Enzymology*. pp. 3-19: Academic Press.

- HUH, J.E., YIM, J.H., LEE, H.K., MOON, E.Y., RHEE, D.K. & PYO, S. (2007). Prodigiosin isolated from *Hahella chejuensis* suppresses lipopolysaccharide-induced NO production by inhibiting p38 MAPK, JNK and NF-kappaB activation in murine peritoneal macrophages. *Int Immunopharmacol*, **7**, 1825-33.
- HUNOT, S., VILA, M., TEISMANN, P., DAVIS, R.J., HIRSCH, E.C., PRZEDBORSKI, S., RAKIC, P. & FLAVELL, R.A. (2004). JNK-mediated induction of cyclooxygenase 2 is required for neurodegeneration in a mouse model of Parkinson's disease. *Proc Natl Acad Sci U S A*, **101**, 665-70.
- IADECOLA, C., ZHANG, F., CASEY, R., NAGAYAMA, M. & ROSS, M.E. (1997). Delayed reduction of ischemic brain injury and neurological deficits in mice lacking the inducible nitric oxide synthase gene. *J Neurosci*, **17**, 9157-64.
- IADECOLA, C., ZHANG, F., XU, S., CASEY, R. & ROSS, M.E. (1995). Inducible nitric oxide synthase gene expression in brain following cerebral ischemia. *J Cereb Blood Flow Metab*, **15**, 378-84.
- ICHIKAWA, T., LI, J., NAGARKATTI, P., NAGARKATTI, M., HOFSETH, L.J., WINDUST, A. & CUI, T. (2009). American ginseng preferentially suppresses STAT/iNOS signaling in activated macrophages. *J Ethnopharmacol*, **125**, 145-50.
- IGNARRO, L.J. (1991). Heme-dependent activation of guanylate cyclase by nitric oxide: a novel signal transduction mechanism. *Blood Vessels*, **28**, 67-73.
- IGNARRO, L.J. (2000). The unique role of nitric oxide as a signaling molecule in the cardiovascular system. *Ital Heart J*, **1 Suppl 3**, S28-9.
- IGNARRO, L.J., BYRNS, R.E. & WOOD, K.S. (1987). Endothelium-dependent modulation of cGMP levels and intrinsic smooth muscle tone in isolated bovine intrapulmonary artery and vein. *Circ Res*, **60**, 82-92.

- ISHII, K., KERWIN, J.F., JR. & MURAD, F. (1990). N omega-nitro-L-arginine: a potent inhibitor of the L-arginine-dependent soluble guanylate cyclase activation pathway in LLC-PK1 cells. *Can J Physiol Pharmacol*, **68**, 749-51.
- ISHIMURA, Y., GAO, Y.T., PANDA, S.P., ROMAN, L.J., MASTERS, B.S. & WEINTRAUB, S.T. (2005). Detection of nitrous oxide in the neuronal nitric oxide synthase reaction by gas chromatography-mass spectrometry. *Biochem Biophys Res Commun*, **338**, 543-9.
- JAESCHKE, A., KARASARIDES, M., VENTURA, J.J., EHRHARDT, A., ZHANG, C., FLAVELL, R.A., SHOKAT, K.M. & DAVIS, R.J. (2006). JNK2 is a positive regulator of the cJun transcription factor. *Mol Cell*, **23**, 899-911.
- JIA, Y.X., LU, Z.F., ZHANG, J., PAN, C.S., YANG, J.H., ZHAO, J., YU, F., DUAN, X.H., TANG, C.S. & QI, Y.F. (2007). Apelin activates L-arginine/nitric oxide synthase/nitric oxide pathway in rat aortas. *Peptides*, **28**, 2023-9.
- JIANG, B., XU, S., HOU, X., PIMENTEL, D.R. & COHEN, R.A. (2004). Angiotensin II differentially regulates interleukin-1-beta-inducible NO synthase (iNOS) and vascular cell adhesion molecule-1 (VCAM-1) expression: role of p38 MAPK. *J Biol Chem*, **279**, 20363-8.
- JONES, SP., & BOLLI, R. (2006). The ubiquitous role of nitric oxide in cardioprotection. *J Mol Cell Cardiol*, **40**, 16-23.
- JUNG, C.H., JUNG, H., SHIN, Y.C., PARK, J.H., JUN, C.Y., KIM, H.M., YIM, H.S., SHIN, M.G., BAE, H.S., KIM, S.H. & KO, S.G. (2007). Eleutherococcus senticosus extract attenuates LPS-induced iNOS expression through the inhibition of Akt and JNK pathways in murine macrophage. *J Ethnopharmacol*, **113**, 183-7.
- JUNG, K.K., LEE, H.S., CHO, J.Y., SHIN, W.C., RHEE, M.H., KIM, T.G., KANG, J.H., KIM, S.H., HONG, S. & KANG, S.Y. (2006). Inhibitory effect of curcumin on nitric oxide production from lipopolysaccharide-activated primary microglia. *Life Sci*, **79**, 2022-31.

- KAGEMANN, G., SIES, H. & SCHNORR, O. (2007). Limited availability of L-arginine increases DNA-binding activity of NF-kappaB and contributes to regulation of iNOS expression. *J Mol Med*, **85**, 723-32.
- KAKUDA, D.K., FINLEY, K.D., MARUYAMA, M. & MACLEOD, C.L. (1998). Stress differentially induces cationic amino acid transporter gene expression. *Biochim Biophys Acta*, **1414**, 75-84.
- KAKUDA, D.K., SWEET, M.J., MAC LEOD, C.L., HUME, D.A. & MARKOVICH, D. (1999). CAT2-mediated L-arginine transport and nitric oxide production in activated macrophages. *Biochem J*, **340 ( Pt 2)**, 549-53.
- KALLUNKI, T., DENG, T., HIBI, M. & KARIN, M. (1996). c-Jun can recruit JNK to phosphorylate dimerization partners via specific docking interactions. *Cell*, **87**, 929-39.
- KALLUNKI, T., SU, B., TSIGELNY, I., SLUSS, H.K., DERIJARD, B., MOORE, G., DAVIS, R. & KARIN, M. (1994). JNK2 contains a specificity-determining region responsible for efficient c-Jun binding and phosphorylation. *Genes Dev*, **8**, 2996-3007.
- KAMINSKA, B., KACZMAREK, L., ZANGENEHPOUR, S. & CHAUDHURI, A. (1999). Rapid phosphorylation of Elk-1 transcription factor and activation of MAP kinase signal transduction pathways in response to visual stimulation. *Mol Cell Neurosci*, **13**, 405-14.
- KARIN, M. (1996). The regulation of AP-1 activity by mitogen-activated protein kinases. *Philos Trans R Soc Lond B Biol Sci*, **351**, 127-34.
- KARIN, M. & HUNTER, T. (1995). Transcriptional control by protein phosphorylation: signal transmission from the cell surface to the nucleus. *Curr Biol*, **5**, 747-57.

- KARLBERG, K.E., SALDEEN, T., WALLIN, R., HENRIKSSON, P., NYQUIST, O., SYLVEN, C. (1998). Intravenous nitroglycerin reduces ischaemia in unstable angina pectoris: a double-blind placebo-controlled study. *J Intern Med.* **243**(1), 25-31.
- KEMPIAK, S.J., HIURA, T.S., NEL, A.E. (1999). The Jun kinase cascade is responsible for activating the CD28 response element of the IL-2 promoter: proof of cross-talk with the I kappa B kinase cascade. *J Immunol.* **162**, 3176-87.
- KEKLIKOGLU, N. (2004). The localization of Fos B, a member of transcription factor AP-1 family, in rat odontoblasts and pulpal undifferentiated ectomesenchymal cells. *Folia Histochem Cytobiol*, **42**, 191-3.
- KENNEDY, N.J. & DAVIS, R.J. (2003). Role of JNK in tumor development. *Cell Cycle*, **2**, 199-201.
- KIEHL, M.G. (1998). Effects of NG-nitro-L-arginine-methyl-ester on cardiopulmonary function and biosynthesis of cyclooxygenase products. *Crit Care Med.* **26**, 1137-8.
- KIM, H.J., TSOYI, K., HEO, J.M., KANG, Y.J., PARK, M.K., LEE, Y.S., LEE, J.H., SEO, H.G., YUN-CHOI, H.S. & CHANG, K.C. (2007). Regulation of lipopolysaccharide-induced inducible nitric-oxide synthase expression through the nuclear factor-kappaB pathway and interferon-beta/tyrosine kinase 2/Janus tyrosine kinase 2-signal transducer and activator of transcription-1 signaling cascades by 2-naphthylethyl-6,7-dihydroxy-1,2,3,4-tetrahydroisoquinoline (THI 53), a new synthetic isoquinoline alkaloid. *J Pharmacol Exp Ther*, **320**, 782-9.
- KIM, J.W., CLOSS, E.I., ALBRITTON, L.M. & CUNNINGHAM, J.M. (1991). Transport of cationic amino acids by the mouse ecotropic retrovirus receptor. *Nature*, **352**, 725-8.

- KIM, S. & IWAHO, H. (2003). Stress and vascular responses: mitogen-activated protein kinases and activator protein-1 as promising therapeutic targets of vascular remodeling. *J Pharmacol Sci*, **91**, 177-81.
- KIM, S., IZUMI, Y., YANO, M., HAMAGUCHI, A., MIURA, K., YAMANAKA, S., MIYAZAKI, H. & IWAHO, H. (1998). Angiotensin blockade inhibits activation of mitogen-activated protein kinases in rat balloon-injured artery. *Circulation*, **97**, 1731-7.
- KIM, S.H., KIM, J. & SHARMA, R.P. (2004). Inhibition of p38 and ERK MAP kinases blocks endotoxin-induced nitric oxide production and differentially modulates cytokine expression. *Pharmacol Res*, **49**, 433-9.
- KIM, Y.E., PARK, J.A., NAM, K.H., KWON, H.J. & LEE, Y. (2009). Pyrrolidine dithiocarbamate-induced activation of ERK and increased expression of c-Fos in mouse embryonic stem cells. *BMB Rep*, **42**, 148-53.
- KIM, Y.H. & KIM, S.S. (1999). Increase of MnSOD expression and decrease of JNK activity determine the TNF sensitivity in bcl2-transfected L929 cells. *Cytokine*, **11**, 274-81.
- KINUGAWA, K., SHIMIZU, T., YAO, A., KOHMOTO, O., SERIZAWA, T. & TAKAHASHI, T. (1997). Transcriptional regulation of inducible nitric oxide synthase in cultured neonatal rat cardiac myocytes. *Circ Res*, **81**, 911-21.
- KLEINERT, H., WALLERATH, T., FRITZ, G., IHRIG-BIEDERT, I., RODRIGUEZ-PASCUAL, F., GELLER, D.A. & FORSTERMANN, U. (1998). Cytokine induction of NO synthase II in human DLD-1 cells: roles of the JAK-STAT, AP-1 and NF-kappaB-signaling pathways. *Br J Pharmacol*, **125**, 193-201.
- KNIPP, B.S., AILAWADI, G., FORD, J.W., PETERSON, D.A., EAGLETON, M.J., ROELOFS, K.J., HANNAWA, K.K., DEOGRACIAS, M.P., JI, B., LOGSDON, C., GRAZIANO, K.D., SIMEONE, D.M., THOMPSON, R.W., HENKE, P.K., STANLEY, J.C. & UPCHURCH, G.R., JR. (2004). Increased MMP-9 expression and activity by aortic smooth

muscle cells after nitric oxide synthase inhibition is associated with increased nuclear factor-kappaB and activator protein-1 activity. *J Surg Res*, **116**, 70-80.

KNOWELS, R.G., & MONCADA, S. (1994). Nitric oxide synthases in mammals. *Biochem J*, **298** ( Pt 2), 249-258.

KNOWELS, R.G., PALACIOS, M., PALMER, R.M., & MONCADA, S. (1989). Formation of nitric oxide from L-arginine in the central nervous system: a transduction mechanism for stimulation of the soluble guanylate cyclase. *Proc Natl Acad Sci U S A*, **86**(13), 5159-5162.

KOLLURU, G.K., BIR, S.C., KEVIL, C. G. (2012). Endothelial dysfunction and diabetes: effects on angiogenesis, vascular remodeling, and wound healing. *international journal of vascular medicine*, 918267.

KOLYADA, A.Y., SAVIKOVSKY, N. & MADIAS, N.E. (1996). Transcriptional regulation of the human iNOS gene in vascular-smooth-muscle cells and macrophages: evidence for tissue specificity. *Biochem Biophys Res Commun*, **220**, 600-5.

KOOK, S.H., HWANG, J.M., PARK, J.S., KIM, E.M., HEO, J.S., JEON, Y.M. & LEE, J.C. (2009). Mechanical force induces type I collagen expression in human periodontal ligament fibroblasts through activation of ERK/JNK and AP-1. *J Cell Biochem*, **106**, 1060-7.

KOOK, S.H., SON, Y.O., JANG, Y.S., LEE, K.Y., LEE, S.A., KIM, B.S., LEE, H.J. & LEE, J.C. (2008). Inhibition of c-Jun N-terminal kinase sensitizes tumor cells to flavonoid-induced apoptosis through down-regulation of JunD. *Toxicol Appl Pharmacol*, **227**, 468-76.

KORHONEN, R., LINKER, K., PAUTZ, A., FORSTERMANN, U., MOILANEN, E. & KLEINERT, H. (2007). Post-transcriptional regulation of human inducible nitric-oxide synthase expression by the Jun N-terminal kinase. *Mol Pharmacol*, **71**, 1427-34.

- KRISTOF, A.S., FIELHABER, J., TRIANTAFILLOPOULOS, A., NEMOTO, S. & MOSS, J. (2006). Phosphatidylinositol 3-kinase-dependent suppression of the human inducible nitric-oxide synthase promoter is mediated by FKHRL1. *J Biol Chem*, **281**, 23958-68.
- KRISTOF, A.S., MARKS-KONCZALIK, J. & MOSS, J. (2001). Mitogen-activated protein kinases mediate activator protein-1-dependent human inducible nitric-oxide synthase promoter activation. *J Biol Chem*, **276**, 8445-52.
- KUBISTA, M., ANDRADE, J.M., BENGTSSON, M., FOROOTAN, A., JONAK, J., LIND, K., SINDELKA, R., SJOBACK, R., SJOGREEN, B., STROMBOM, L., STAHLBERG, A. & ZORIC, N. (2006). The real-time polymerase chain reaction. *Mol Aspects Med*, **27**, 95-125.
- KUNTZEN, C., SONUC, N., DE TONI, E.N., OPELZ, C., MUCHA, S.R., GERBES, A.L. & EICHHORST, S.T. (2005). Inhibition of c-Jun-N-terminal-kinase sensitizes tumor cells to CD95-induced apoptosis and induces G2/M cell cycle arrest. *Cancer Res*, **65**, 6780-8.
- KUNZ, D., WALKER, G., EBERHARDT, W. & PFEILSCHIFTER, J. (1996). Molecular mechanisms of dexamethasone inhibition of nitric oxide synthase expression in interleukin 1 beta-stimulated mesangial cells: evidence for the involvement of transcriptional and posttranscriptional regulation. *Proc Natl Acad Sci U S A*, **93**, 255-9.
- KUO, P.C., SCHROEDER, R.A., LOSCALZO, J. (1997). Nitric oxide and acetaminophen-mediated oxidative injury: modulation of interleukin-1-induced nitric oxide synthesis in cultured rat hepatocytes. *J Pharmacol Exp Ther*. 282,1072-83.
- KYRIAKIS, J.M., BANERJEE, P., NIKOLAKAKI, E., DAI, T., RUBIE, E.A., AHMAD, M.F., AVRUCH, J., WOODGETT, J.R. (1994). The stress-activated protein kinase subfamily of c-Jun kinases. *Nature*. 369(6476), 156-60.

- LAHTI, A., JALONEN, U., KANKAANRANTA, H. & MOILANEN, E. (2003). c-Jun NH2-terminal kinase inhibitor anthra(1,9-cd)pyrazol-6(2H)-one reduces inducible nitric-oxide synthase expression by destabilizing mRNA in activated macrophages. *Mol Pharmacol*, **64**, 308-15.
- LAHTI, A., LAHDE, M., KANKAANRANTA, H. & MOILANEN, E. (2000). Inhibition of extracellular signal-regulated kinase suppresses endotoxin-induced nitric oxide synthesis in mouse macrophages and in human colon epithelial cells. *J Pharmacol Exp Ther*, **294**, 1188-94.
- LAI, Y.C., TSAI, P.S. & HUANG, C.J. (2008). Clonidine enhances type-2 cationic amino acid transporter transcription in endotoxin-activated murine macrophages. *Acta Anaesthesiol Taiwan*, **46**, 118-23.
- LAMATTINA, L., GARCIA-MATA, C., GRAZIANO, M. & PAGNUSSAT, G. (2003). Nitric oxide: the versatility of an extensive signal molecule. *Annu Rev Plant Biol*, **54**, 109-36.
- LAMB, J.A., VENTURA, J.J., HESS, P., FLAVELL, R.A. & DAVIS, R.J. (2003). JunD mediates survival signaling by the JNK signal transduction pathway. *Mol Cell*, **11**, 1479-89.
- LAPU-BULA, R., OFILI, E. (2007). From hypertension to heart failure: role of nitric oxide-mediated endothelial dysfunction and emerging insights from myocardial contrast echocardiography. *Am J Cardiol*.99(6B), 7D-14D.
- LAWLER, S., FLEMING, Y., GOEDERT, M. & COHEN, P. (1998). Synergistic activation of SAPK1/JNK1 by two MAP kinase kinases in vitro. *Curr Biol*, **8**, 1387-90.
- LEE, C.J., TAI, Y.T., LIN, Y.L. & CHEN, R.M. (2009a). Molecular mechanisms of propofol-involved suppression of nitric oxide biosynthesis and inducible nitric

oxide synthase gene expression in lipopolysaccharide-stimulated macrophage-like Raw 264.7 cells. *Shock*.

LEE, J., JUNG, E., LEE, J., HUH, S., KIM, Y.S., KIM, Y.W., KIM, Y.S. & PARK, D. (2010). Anti-adipogenesis by 6-thioinosine is mediated by downregulation of PPAR gamma through JNK-dependent upregulation of iNOS. *Cell Mol Life Sci*, **67**, 467-81.

LEE, J.K., CHOI, S.S., WON, J.S. & SUH, H.W. (2003). The regulation of inducible nitric oxide synthase gene expression induced by lipopolysaccharide and tumor necrosis factor-alpha in C6 cells: involvement of AP-1 and NFkappaB. *Life Sci*, **73**, 595-609.

LEE, S.J. & LIM, K.T. (2009b). Inhibitory effect of ZPDC glycoprotein on the expression of inflammation-related cytokines through p38 MAP kinase and JNK in lipopolysaccharide-stimulated RAW 264.7 cells. *Inflamm Res*, **58**, 184-91.

LEE, S.J. & LIM, K.T. (2007). UDN glycoprotein regulates activities of manganese-superoxide dismutase, activator protein-1, and nuclear factor-kappaB stimulated by reactive oxygen radicals in lipopolysaccharide-stimulated HCT-116 cells. *Cancer Lett*, **254**, 274-87.

LI, B., TOURNIER, C., DAVIS, R.J. & FLAVELL, R.A. (1999). Regulation of IL-4 expression by the transcription factor JunB during T helper cell differentiation. *Embo J*, **18**, 420-32.

LI, J.J., CAO, Y., YOUNG, M.R. & COLBURN, N.H. (2000). Induced expression of dominant-negative c-jun downregulates NFkappaB and AP-1 target genes and suppresses tumor phenotype in human keratinocytes. *Mol Carcinog*, **29**, 159-69.

- LI, J.J., RHIM, J.S., SCHLEGEL, R., VOUSDEN, K.H. & COLBURN, N.H. (1998). Expression of dominant negative Jun inhibits elevated AP-1 and NF-kappaB transactivation and suppresses anchorage independent growth of HPV immortalized human keratinocytes. *Oncogene*, **16**, 2711-21.
- LI, L., FENG, Z. & PORTER, A.G. (2004). JNK-dependent phosphorylation of c-Jun on serine 63 mediates nitric oxide-induced apoptosis of neuroblastoma cells. *J Biol Chem*, **279**, 4058-65.
- LI, M., MOSSMAN, B.T., KOLPA, E., TIMBLIN, C.R., SHUKLA, A., TAATJES, D.J. & FUKAGAWA, N.K. (2003). Age-related differences in MAP kinase activity in VSMC in response to glucose or TNF-alpha. *J Cell Physiol*, **197**, 418-25.
- LIANG, Q., BUENO, O.F., WILKINS, B.J., KUAN, C.Y., XIA, Y., MOLKENTIN, J.D. (2003). c-Jun N-terminal kinases (JNK) antagonize cardiac growth through cross-talk with calcineurin-NFAT signaling. *EMBO J*. **22**, 5079–5089.
- LIANG, Q. & MOLKENTIN, J.D. (2003). Redefining the roles of p38 and JNK signaling in cardiac hypertrophy: dichotomy between cultured myocytes and animal models. *J Mol Cell Cardiol*, **35**, 1385-94.
- LIANG, F., WU, J., GARAMI, M., GARDNER, D.G. (1997). Mechanical strain increases expression of the brain natriuretic peptide gene in rat cardiac myocytes. *J Biol Chem*. 272(44), 28050-6.
- LIAUDET, L., ROSSELET, A., SCHALLER, M.D., MARKERT, M., PERRET, C., FEIHL, F. (1998). Nonselective versus selective inhibition of inducible nitric oxide synthase in experimental endotoxic shock. *J Infect Dis*. 177(1), 127-32.
- LIN, H.I., CHOU, S.J., WANG, D., FENG, N.H., FENG, E. & CHEN, C.F. (2006). Reperfusion liver injury induces down-regulation of eNOS and up-regulation of iNOS in lung tissues. *Transplant Proc*, **38**, 2203-6.

- LIN, S.K., KOK, S.H., LIN, L.D., WANG, C.C., KUO, M.Y., LIN, C.T., HSIAO, M. & HONG, C.Y. (2007). Nitric oxide promotes the progression of periapical lesion via inducing macrophage and osteoblast apoptosis. *Oral Microbiol Immunol*, **22**, 24-9.
- LINARD, C., ROPENGA, A., VOZENIN-BROTONS, M.C., CHAPEL, A. & MATHE, D. (2003). Abdominal irradiation increases inflammatory cytokine expression and activates NF-kappaB in rat ileal muscularis layer. *Am J Physiol Gastrointest Liver Physiol*, **285**, G556-65.
- LOWENSTEIN, C.J., ALLEY, E.W., RAVAL, P., SNOWMAN, A.M., SNYDER, S.H., RUSSELL, S.W. & MURPHY, W.J. (1993). Macrophage nitric oxide synthase gene: two upstream regions mediate induction by interferon gamma and lipopolysaccharide. *Proc Natl Acad Sci U S A*, **90**, 9730-4.
- MACKENZIE, A. & WADSWORTH, R.M. (2003). Extracellular L-arginine is required for optimal NO synthesis by eNOS and iNOS in the rat mesenteric artery wall. *Br J Pharmacol*, **139**, 1487-97.
- MACLEOD, C.L. (1996). Regulation of cationic amino acid transporter (CAT) gene expression. *Biochem Soc Trans*, **24**, 846-52.
- MAEDA, H., AKAIKE, T., YOSHIDA, M. & SUGA, M. (1994). Multiple functions of nitric oxide in pathophysiology and microbiology: analysis by a new nitric oxide scavenger. *J Leukoc Biol*, **56**, 588-92.
- MANNA, P.R., EUBANK, D.W. & STOCCO, D.M. (2004). Assessment of the role of activator protein-1 on transcription of the mouse steroidogenic acute regulatory protein gene. *Mol Endocrinol*, **18**, 558-73.
- MARION, R., COEFFIER, M., LEPLINGARD, A., FAVENNEC, L., DUCROTTE, P. & DECHELOTTE, P. (2003). Cytokine-stimulated nitric oxide production and

inducible NO-synthase mRNA level in human intestinal cells: lack of modulation by glutamine. *Clin Nutr*, **22**, 523-8.

MARONEY, A.C., FINN, J.P., CONNORS, T.J., DURKIN, J.T., ANGELES, T., GESSNER, G., XU, Z., MEYER, S.L., SAVAGE, M.J., GREENE, L.A., SCOTT, R.W. & VAUGHT, J.L. (2001). Cep-1347 (KT7515), a semisynthetic inhibitor of the mixed lineage kinase family. *J Biol Chem*, **276**, 25302-8.

MARTIN, E., NATHAN, C. & XIE, Q.W. (1994). Role of interferon regulatory factor 1 in induction of nitric oxide synthase. *J Exp Med*, **180**, 977-84.

MASAMUNE, A., KIKUTA, K., SUZUKI, N., SATOH, M., SATOH, K. & SHIMOSEGAWA, T. (2004). A c-Jun NH2-terminal kinase inhibitor SP600125 (anthra[1,9-cd]pyrazole-6 (2H)-one) blocks activation of pancreatic stellate cells. *J Pharmacol Exp Ther*, **310**, 520-7.

MATSUMURA, M., KAKISHITA, H., SUZUKI, M., BANBA, N. & HATTORI, Y. (2001). Dexamethasone suppresses iNOS gene expression by inhibiting NF-kappaB in vascular smooth muscle cells. *Life Sci*, **69**, 1067-77.

MATSUZAKI, H., TAMATANI, M., MITSUDA, N., NAMIKAWA, K., KIYAMA, H., MIYAKE, S. & TOHYAMA, M. (1999). Activation of Akt kinase inhibits apoptosis and changes in Bcl-2 and Bax expression induced by nitric oxide in primary hippocampal neurons. *J Neurochem*, **73**, 2037-46.

MEDEIROS, R., PREDIGER, R.D., PASSOS, G.F., PANDOLFO, P., DUARTE, F.S., FRANCO, J.L., DAFRE, A.L., DI GIUNTA, G., FIGUEIREDO, C.P., TAKAHASHI, R.N., CAMPOS, M.M., CALIXTO, J.B. (2007). Connecting TNF-alpha signaling pathways to iNOS expression in a mouse model of Alzheimer's disease: relevance for the behavioral and synaptic deficits induced by amyloid beta protein. *J Neurosci*. **27**, 5394-404.

MENDELSON, K. G., CONTOIS, L.-R., TEVOSIAN, S. G., DAVIS, R. J. & PAULSON, K. E. (1996) *Proc. Natl. Acad. Sci. USA* **93**, 12908–12913.

- MENDES, A.F., CARAMONA, M.M., CARVALHO, A.P. & LOPES, M.C. (2003). Hydrogen peroxide mediates interleukin-1beta-induced AP-1 activation in articular chondrocytes: implications for the regulation of iNOS expression. *Cell Biol Toxicol*, **19**, 203-14.
- MENDES RIBEIRO, A.C., BRUNINI, T.M., ELLORY, J.C. & MANN, G.E. (2001). Abnormalities in L-arginine transport and nitric oxide biosynthesis in chronic renal and heart failure. *Cardiovasc Res*, **49**, 697-712.
- MERCER, B.A., & D'ARMIENTO, J.M. (2006). Emerging role of MAP kinase pathways as therapeutic targets in COPD. *Int J Chron Obstruct Pulmon Dis*. 2006;1(2):137-50.
- MEYER, C.F., WANG, X., CHANG, C., TEMPLETON, D. & TAN, T.H. (1996). Interaction between c-Rel and the mitogen-activated protein kinase kinase kinase 1 signaling cascade in mediating kappaB enhancer activation. *J Biol Chem*, **271**, 8971-6.
- MIDDLETON, S.J., SHORTHOUSE, M., HUNTER, J.O. (1993). Increased nitric oxide synthesis in ulcerative colitis. *Lancet*. 341, 465-6.
- MILLER, A.D., CURRAN, T. & VERMA, I.M. (1984). c-fos protein can induce cellular transformation: a novel mechanism of activation of a cellular oncogene. *Cell*, **36**, 51-60.
- MILNE, D.M., CAMPBELL, L.E., CAMPBELL, D.G. & MEEK, D.W. (1995). p53 is phosphorylated in vitro and in vivo by an ultraviolet radiation-induced protein kinase characteristic of the c-Jun kinase, JNK1. *J Biol Chem*, **270**, 5511-8.
- MITCHELL, J.A., HECKER, M., ANGGARD, E.E. & VANE, J.R. (1990). Cultured endothelial cells maintain their L-arginine level despite the continuous release of EDRF. *Eur J Pharmacol*, **182**, 573-6.

- MITCHELL, J.A., SHYNLOVA, O., LANGILLE, B.L. & LYE, S.J. (2004). Mechanical stretch and progesterone differentially regulate activator protein-1 transcription factors in primary rat myometrial smooth muscle cells. *Am J Physiol Endocrinol Metab*, **287**, E439-45.
- MITCHELL, P.J. & TJIAN, R. (1989). Transcriptional regulation in mammalian cells by sequence-specific DNA binding proteins. *Science*, **245**, 371-8.
- MONCADA, S. (1997). Nitric oxide in the vasculature: physiology and pathophysiology. *Ann N Y Acad Sci*, **811**, 60-7; discussion 67-9.
- MONCADA, S., HIGGS, E.A. (1995). Molecular mechanisms and therapeutic strategies related to nitric oxide. *FASEB J.* **9**(13), 1319-30.
- MONCADA, S. & ERUSALIMSKY, J.D. (2002). Does nitric oxide modulate mitochondrial energy generation and apoptosis. *Nat Rev Mol Cell Biol.* **3**, 214-20.
- MONCADA, S. & HIGGS, E.A. (2006). The discovery of nitric oxide and its role in vascular biology. *Br J Pharmacol*, **147 Suppl 1**, S193-201.
- MORI, M. (2007). Regulation of nitric oxide synthesis and apoptosis by arginase and arginine recycling. *J Nutr*, **137**, 1616S-1620S.
- MORI, M. & GOTOH, T. (2004). Arginine metabolic enzymes, nitric oxide and infection. *J Nutr*, **134**, 2820S-2825S; discussion 2853S.
- MORI, M. & GOTOH, T. (2000). Regulation of nitric oxide production by arginine metabolic enzymes. *Biochem Biophys Res Commun*, **275**, 715-9.
- MOSMANN, T. (1983). Rapid colorimetric assay for cellular growth and survival: Application to proliferation and cytotoxicity assays. *Journal of Immunological Methods*, **65**, 55-63.

- MUKHOPADHYAY, S., MUKHERJEE, S., SMITH, M. & DAS, S.K. (2008). Activation of MAPK/AP-1 signaling pathway in lung injury induced by 2-chloroethyl ethyl sulfide, a mustard gas analog. *Toxicol Lett*, **181**, 112-7.
- MURPHY, L.D., HERZOG, C.E., RUDICK, J.B., FOJO, A.T. & BATES, S.E. (1990). Use of the polymerase chain reaction in the quantitation of *mdr-1* gene expression. *Biochemistry*, **29**, 10351-6.
- MUSLIN, A., (2008). MAPK Signaling in Cardiovascular Health and Disease: Molecular Mechanisms and Therapeutic Targets. *Clin Sci* **115(7)**. 203-218.
- NAKAHARA, T., MOROI, Y., UCHI, H., FURUE, M. (2006). Differential role of MAPK signaling in human dendritic cell maturation and Th1/Th2 engagement. *J Dermatol Sci*. **42(1)**, 1-11.
- NAKAMURA, T., DATTA, R., KHARBANDA, S. & KUFEL, D. (1991). Regulation of *jun* and *fos* gene expression in human monocytes by the macrophage colony-stimulating factor. *Cell Growth Differ*, **2**, 267-72.
- NAKANO, H., SHINDO, M., SAKON, S., NISHINAKA, S., MIHARA, M., YAGITA, H. & OKUMURA, K. (1998). Differential regulation of I $\kappa$ B kinase  $\alpha$  and  $\beta$  by two upstream kinases, NF- $\kappa$ B-inducing kinase and mitogen-activated protein kinase/ERK kinase kinase-1. *Proc Natl Acad Sci U S A*, **95**, 3537-42.
- NAKATA, S., TSUTSUI, M., SHIMOKAWA, H., TAMURA, M., TASAKI, H., MORISHITA, T., SUDA, O., UENO, S., TOYOHIRA, Y., NAKASHIMA, Y. & YANAGIHARA, N. (2005). Vascular neuronal NO synthase is selectively upregulated by platelet-derived growth factor: involvement of the MEK/ERK pathway. *Arterioscler Thromb Vasc Biol*, **25**, 2502-8.
- NANRI, K., MONTECOT, C., SPRINGHETTI, V., SEYLAZ, J. & PINARD, E. (1998). The selective inhibitor of neuronal nitric oxide synthase, 7-nitroindazole, reduces

the delayed neuronal damage due to forebrain ischemia in rats. *Stroke*, **29**, 1248-53; discussion 1253-4.

NANETTI, L., TAFFI, R., VIGINI, A., MORONI, C., RAFFAELLI, F., BACCHETTI, T., SILVESTRINI, M., PROVINCIALI, L., MAZZANTI, L. (2007). Reactive oxygen species plasmatic levels in ischemic stroke. *Mol Cell Biochem.* **303**(1-2), 19-25.

NATH, P., EYNOTT, P., LEUNG, S.Y., ADCOCK, I.M., BENNETT, B.L. & CHUNG, K.F. (2005). Potential role of c-Jun NH2-terminal kinase in allergic airway inflammation and remodelling: effects of SP600125. *Eur J Pharmacol*, **506**, 273-83.

NATHAN, C. (1997). Inducible nitric oxide synthase: what difference does it make? *J Clin Invest*, **100**, 2417-23.

NAVA, E., PALMER, R.M. & MONCADA, S. (1991). Inhibition of nitric oxide synthesis in septic shock: how much is beneficial? *Lancet*, **338**, 1555-7.

NELIN, L.D., WANG, X., ZHAO, Q., CHICOINE, L.G., YOUNG, T.L., HATCH, D.M., ENGLISH, B.K. & LIU, Y. (2007). MKP-1 switches arginine metabolism from nitric oxide synthase to arginase following endotoxin challenge. *Am J Physiol Cell Physiol*, **293**, C632-40.

NEWMAN, E., SPRATT, D.E., MOSHER, J., CHEYNE, B., MONTGOMERY, H.J., WILSON, D.L., WEINBERG, J.B., SMITH, S.M., SALERNO, J.C., GHOSH, D.K. & GUILLEMETTE, J.G. (2004). Differential activation of nitric-oxide synthase isozymes by calmodulin-troponin C chimeras. *J Biol Chem*, **279**, 33547-57.

NICHOLSON, B., MANNER, C.K., KLEEMAN, J. & MACLEOD, C.L. (2001). Sustained nitric oxide production in macrophages requires the arginine transporter CAT2. *J Biol Chem*, **276**, 15881-5.

- NIEMINEN, R., LAHTI, A., JALONEN, U., KANKAANRANTA, H. & MOILANEN, E. (2006). JNK inhibitor SP600125 reduces COX-2 expression by attenuating mRNA in activated murine J774 macrophages. *Int Immunopharmacol*, **6**, 987-96.
- NIESE, K.A., CHIARAMONTE, M.G., ELLIES, L.G., ROTHENBERG, M.E. & ZIMMERMANN, N. The cationic amino acid transporter 2 is induced in inflammatory lung models and regulates lung fibrosis. *Respir Res*, **11**, 87.
- NUSSLER, A.K., BILLIAR, T.R., LIU, Z.Z. & MORRIS, S.M., JR. (1994). Coinduction of nitric oxide synthase and argininosuccinate synthetase in a murine macrophage cell line. Implications for regulation of nitric oxide production. *J Biol Chem*, **269**, 1257-61.
- NUSSLER, A.K., DI SILVIO, M., BILLIAR, T.R., HOFFMAN, R.A., GELLER, D.A., SELBY, R., MADARIAGA, J. & SIMMONS, R.L. (1992). Stimulation of the nitric oxide synthase pathway in human hepatocytes by cytokines and endotoxin. *J Exp Med*, **176**, 261-4.
- OKADA, S., OBATA, S., HATANO, M. & TOKUHISA, T. (2003). Dominant-negative effect of the c-fos family gene products on inducible NO synthase expression in macrophages. *Int Immunol*, **15**, 1275-82.
- OLIVE, M., KRYLOV, D., ECHLIN, D.R., GARDNER, K., TAPAROWSKY, E. & VINSON, C. (1997). A dominant negative to activation protein-1 (AP1) that abolishes DNA binding and inhibits oncogenesis. *J Biol Chem*, **272**, 18586-94.
- ORLANDO, C., PINZANI, P. & PAZZAGLI, M. (1998). Developments in quantitative PCR. *Clin Chem Lab Med*, **36**, 255-69.
- OUYANG, J., XU, D., ZHANG, X., QI, S., MA, A., JIANG, W., CHIDA, N., SUDO, Y., TAMURA, K., DALOZE, P. & CHEN, H. (2005). Effect of a novel inducible nitric oxide synthase inhibitor in prevention of rat chronic aortic rejections. *Transplantation*, **79**, 1386-92.

- OYAMA, J., FRANTZ, S., BLAIS, J.r., KELLY, R.A., BOURCIER, T. (2002). Nitric oxide, cell death, and heart failure. *Heart Fail Rev.* 7(4), 327-34.
- PACHER, P., BECKMAN, J.S., LIAUDET, L. (2007). Nitric oxide and peroxynitrite in health and disease. *Physiol Rev.* 87(1), 315-424.
- PALACIOS, M., KNOWELS, R. G., PALMER, R. M., & MONCADA, S. (1989). Nitric oxide from L-arginine stimulates the soluble guanylate cyclase in adrenal glands. *Biochem Biophys Res Commun*, 165(2), 802-809.
- PALMER, R.M., FERRIGE, A.G. & MONCADA, S. (1987). Nitric oxide release accounts for the biological activity of endothelium-derived relaxing factor. *Nature*, **327**, 524-6.
- PANCE, A., CHANTOME, A., REVENEAU, S., BENTRARI, F. & JEANNIN, J.F. (2002). A repressor in the proximal human inducible nitric oxide synthase promoter modulates transcriptional activation. *Faseb J*, **16**, 631-3.
- PARK, P.H., KIM, H.S., JIN, X.Y., JIN, F., HUR, J., KO, G. & SOHN, D.H. (2009). KB-34, a newly synthesized chalcone derivative, inhibits lipopolysaccharide-stimulated nitric oxide production in RAW 264.7 macrophages via heme oxygenase-1 induction and blockade of activator protein-1. *Eur J Pharmacol*, **606**, 215-24.
- PASSEGUE, E. & WAGNER, E.F. (2000). JunB suppresses cell proliferation by transcriptional activation of p16(INK4a) expression. *Embo J*, **19**, 2969-79.
- PATEL, D.N., BAILEY, S.R., GRESHAM, J.K., SCHUCHMAN, D.B., SHELFHAMER, J.H., GOLDSTEIN, B.J., FOXWELL, B.M., STEMERMAN, M.B., MARANCHIE, J.K., VALENTE, A.J., MUMMIDI, S. & CHANDRASEKAR, B. (2006). TLR4-NOX4-AP-1 signaling mediates lipopolysaccharide-induced CXCR6 expression in human aortic smooth muscle cells. *Biochem Biophys Res Commun*, **347**, 1113-20.

- PAUL, A., CUENDA, A., BRYANT, C.E., MURRAY, J., CHILVERS, E.R., COHEN, P., GOULD, G.W. & PLEVIN, R. (1999). Involvement of mitogen-activated protein kinase homologues in the regulation of lipopolysaccharide-mediated induction of cyclo-oxygenase-2 but not nitric oxide synthase in RAW 264.7 macrophages. *Cell Signal*, **11**, 491-7.
- PAUL, A., PENDREIGH, R.H. & PLEVIN, R. (1995). Protein kinase C and tyrosine kinase pathways regulate lipopolysaccharide-induced nitric oxide synthase activity in RAW 264.7 murine macrophages. *Br J Pharmacol*, **114**, 482-8.
- PAWATE, S. & BHAT, N.R. (2006). C-Jun N-terminal kinase (JNK) regulation of iNOS expression in glial cells: predominant role of JNK1 isoform. *Antioxid Redox Signal*, **8**, 903-9.
- PENG, J. & ANDERSEN, J.K. (2003). The role of c-Jun N-terminal kinase (JNK) in Parkinson's disease. *IUBMB Life*, **55**, 267-71.
- PERRELLA, M.A., PATTERSON, C., TAN, L., YET, S.F., HSIEH, C.M., YOSHIZUMI, M. & LEE, M.E. (1996). Suppression of interleukin-1beta-induced nitric-oxide synthase promoter/enhancer activity by transforming growth factor-beta1 in vascular smooth muscle cells. Evidence for mechanisms other than NF-kappaB. *J Biol Chem*, **271**, 13776-80.
- PETROS, A., LAMB, G., LEONE, A., MONCADA, S., BENNETT, D., VALLANCE, P. (1994). Effects of a nitric oxide synthase inhibitor in humans with septic shock. *Cardiovasc Res*. **28**(1):34-9.
- PFAFFL, M.W. (2001). A new mathematical model for relative quantification in real-time RT-PCR. *Nucleic Acids Res*, **29**, e45.
- PIEPER, G.M. & ROZA, A.M. (2008). The complex role of iNOS in acutely rejecting cardiac transplants. *Free Radic Biol Med*, **44**, 1536-52.

- POTATOVA, O., GOROSPE, M., DOUGHERTY, R.H., DEAN, N.M., GAARDE, W.A., HOLBROOK, N.J. (2000). Inhibition of c-Jun N-terminal kinase 2 expression suppresses growth and induces apoptosis of human tumor cells in a p53-dependent manner. *Mol Cell Biol.* 20(5), 1713-22.
- POTATOVA, O., HAGHIGHI, A., BOST, F., LIU, C., BIRRER, M.J., GJEREST, R., MERCOLA, D. (1997). The Jun kinase/stress-activated protein kinase pathway functions to regulate DNA repair and inhibition of the pathway sensitizes tumor cells to cisplatin. *J Biol Chem.* 272(22). 14041-4.
- RAHMAN, I., SMITH, C. A., ANTONIOCELLI, F., & MACNEE, W. (1998). Characterisation of gamma-glutamylcysteine synthetase-heavy subunit promoter: a critical role for AP-1. *FEBS Lett*, 427(1), 129-133.
- RAVICH, G. & BEHRENS, A. (2006). Role of the AP-1 transcription factor c-Jun in developing, adult and injured brain. *Prog Neurobiol*, **78**, 347-63.
- RAMIREZ, M.T., SAH, V.P., ZHAO, X.L., HUNTER, J.J., CHIEN, K.R. & BROWN, J.H. (1997). The MEKK-JNK pathway is stimulated by alpha1-adrenergic receptor and ras activation and is associated with in vitro and in vivo cardiac hypertrophy. *J Biol Chem*, **272**, 14057-61.
- RAO, G.N., KATKI, K.A., MADAMANCHI, N.R., WU, Y. & BIRRER, M.J. (1999). JunB forms the majority of the AP-1 complex and is a target for redox regulation by receptor tyrosine kinase and G protein-coupled receptor agonists in smooth muscle cells. *J Biol Chem*, **274**, 6003-10.
- REDDY, S.P. & MOSSMAN, B.T. (2002). Role and regulation of activator protein-1 in toxicant-induced responses of the lung. *Am J Physiol Lung Cell Mol Physiol*, **283**, L1161-78.

- REES, D.D., PALMER, R.M. & MONCADA, S. (1989). Role of endothelium-derived nitric oxide in the regulation of blood pressure. *Proc Natl Acad Sci U S A*, **86**, 3375-8.
- REES, R.C. & WILTROUT, R.H. (1990). The biology and clinical applications of interleukin 2. *Immunol Today*, **11**, 36-8.
- REIS, D., SOUZA, M., MINEO, J. & ESPINDOLA, F. (2001). Myosin V and iNOS expression is enhanced in J774 murine macrophages treated with IFN-gamma. *Braz J Med Biol Res*, **34**, 221-6.
- RICCI, R., SUMARA, G., SUMARA, I., ROZENBERG, I., KURRER, M., AKHMEDOV, A., HERSBERGER, M., ERIKSSON, U., EBERLI, F.R., BECHER, B., BOREN, J., CHEN, M., CYBULSKY, M.I., MOORE, K.J., FREEMAN, M.W., WAGNER, E.F., MATTER, C.M., LUSCHER, T.F. (2004). Requirement of JNK2 for scavenger receptor A-mediated foam cell formation in atherogenesis. *Science*. **306**:1558–1561.
- RIKITAKE, Y., HIRATA, K., KAWASHIMA, S., AKITA, H., YOKOYAMA, M. (1998). Inhibitory effect of inducible type nitric oxide synthase on oxidative modification of low density lipoprotein by vascular smooth muscle cells. *Atherosclerosis*. **136**(1), 51-7.
- RODRIGUEZ, N., LANG, R., WANTIA, N., CIRL, C., ERTL, T., DURR, S., WAGNER, H. & MIETHKE, T. (2008). Induction of iNOS by *Chlamydomphila pneumoniae* requires MyD88-dependent activation of JNK. *J Leukoc Biol*, **84**, 1585-93.
- ROTHENBERG, M.E., DOEPKER, M.P., LEWKOWICH, I.P., CHIARAMONTE, M.G., STRINGER, K.F., FINKELMAN, F.D., MACLEOD, C.L., ELLIES, L.G. & ZIMMERMANN, N. (2006). Cationic amino acid transporter 2 regulates inflammatory homeostasis in the lung. *Proc Natl Acad Sci U S A*, **103**, 14895-900.

- RUSSWURM, M. & KOESLING, D. (2002). Isoforms of NO-sensitive guanylyl cyclase. *Mol Cell Biochem*, **230**, 159-64.
- RYSECK, R.P. & BRAVO, R. (1991). c-JUN, JUN B, and JUN D differ in their binding affinities to AP-1 and CRE consensus sequences: effect of FOS proteins. *Oncogene*, **6**, 533-42.
- SABAPATHY, K., HOCHEDLINGER, K., NAM, S.Y., BAUER, A., KARIN, M. & WAGNER, E.F. (2004a). Distinct roles for JNK1 and JNK2 in regulating JNK activity and c-Jun-dependent cell proliferation. *Mol Cell*, **15**, 713-25.
- SABAPATHY, K. & WAGNER, E.F. (2004b). JNK2: a negative regulator of cellular proliferation. *Cell Cycle*, **3**, 1520-3.
- SAITO, C., LEMASTERS, J.J. & JAESCHKE, H. c-Jun N-terminal kinase modulates oxidant stress and peroxynitrite formation independent of inducible nitric oxide synthase in acetaminophen hepatotoxicity. *Toxicol Appl Pharmacol*.
- SAKURAI, H., KOHSAKA, H., LIU, M.F., HIGASHIYAMA, H., HIRATA, Y., KANNO, K., SAITO, I. & MIYASAKA, N. (1995). Nitric oxide production and inducible nitric oxide synthase expression in inflammatory arthritides. *J Clin Invest*, **96**, 2357-63.
- SANCHEZ, I., HUGHES, R.T., MAYER, B.J., YEE, K., WOODGETT, J.R., AVRUCH, J., KYRIAKIS, J.M. & ZON, L.I. (1994). Role of SAPK/ERK kinase-1 in the stress-activated pathway regulating transcription factor c-Jun. *Nature*, **372**, 794-8.
- SAPORITO, M.S., HUDKINS, R.L. & MARONEY, A.C. (2002). Discovery of CEP-1347/KT-7515, an inhibitor of the JNK/SAPK pathway for the treatment of neurodegenerative diseases. *Prog Med Chem*, **40**, 23-62.
- SCHILLING, J., CAKMAKCI, M., BATTIG, U., GEROULANOS, S. (1993). A new approach in the treatment of hypotension in human septic shock by NG-monomethyl-L-

arginine, an inhibitor of the nitric oxide synthetase. *Intensive Care Med.* 19(4), 227-31.

SCHMIDT, N., PAUTZ, A., ART, J., RAUSCHKOLB, P., JUNG, M., ERKEL, G., GOLDRING, M.B. & KLEINERT, H. Transcriptional and post-transcriptional regulation of iNOS expression in human chondrocytes. *Biochem Pharmacol*, **79**, 722-32.

SCHMITTGEN, T.D. & LIVAK, K.J. (2008). Analyzing real-time PCR data by the comparative C(T) method. *Nat Protoc*, **3**, 1101-8.

SCHULZ, J.B., MATTHEWS, R.T., BEAL, M.F. (1995). Role of nitric oxide in neurodegenerative diseases. *Curr Opin Neurol.* 8, 480-6.

SCHWARTZ, I.F., HERSHKOVITZ, R., IAINA, A., GNESSIN, E., WOLLMAN, Y., CHERNICHOWSKI, T., BLUM, M., LEVO, Y. & SCHWARTZ, D. (2002). Garlic attenuates nitric oxide production in rat cardiac myocytes through inhibition of inducible nitric oxide synthase and the arginine transporter CAT-2 (cationic amino acid transporter-2). *Clin Sci (Lond)*, **102**, 487-93.

Schwartz IF, Schwartz D, Traskonov M, Chernichovsky T, Wollman Y, Gnessin E, Topilsky I, Levo Y, Iaina A. (2003) L-Arginine transport is augmented through up-regulation of tubular CAT-2 mRNA in ischemic acute renal failure in rats. *Kidney Int.* 2002 Nov;62(5):1700-6.

SCHWARZ, C.S., SEYFRIED, J., EVERT, B.O., KLOCKGETHER, T. & WULLNER, U. (2002). Bcl-2 up-regulates ha-ras mRNA expression and induces c-Jun phosphorylation at Ser73 via an ERK-dependent pathway in PC 12 cells. *Neuroreport*, **13**, 2439-42.

SCIPIONI, A., MAUROY, A., ZIANT, D., SAEGERMAN, C. & THIRY, E. (2008). A SYBR Green RT-PCR assay in single tube to detect human and bovine noroviruses and control for inhibition. *Virologia*, **5**, 94.

- SCOTT-BURDEN, T., ELIZONDO, E., GE, T., BOULANGER, C.M. & VANHOUTTE, P.M. (1994). Simultaneous activation of adenylyl cyclase and protein kinase C induces production of nitric oxide by vascular smooth muscle cells. *Mol Pharmacol*, **46**, 274-82.
- SEARLES, C.D. (2002). The nitric oxide pathway and oxidative stress in heart failure. *Congest Heart Fail.* 8(3), 142-7, 155.
- SHAH, AM. & MACCARTHEY, PA. (2000). Paracrine and autocrine effects of nitric oxide on myocardial function. *Pharmacol Ther*, **86**, 49-86
- SHAULIAN, E. & KARIN, M. (2002). AP-1 as a regulator of cell life and death. *Nat Cell Biol*, **4**, E131-6.
- SHI, D., DAS, J. & DAS, G. (2006). Inflammatory bowel disease requires the interplay between innate and adaptive immune signals. *Cell Res*, **16**, 70-4.
- SHIMIZU, Y., KINOSHITA, I., KIKUCHI, J., YAMAZAKI, K., NISHIMURA, M., BIRRER, M.J. & DOSAKA-AKITA, H. (2008). Growth inhibition of non-small cell lung cancer cells by AP-1 blockade using a cJun dominant-negative mutant. *Br J Cancer*, **98**, 915-22.
- SIMMONDS, R.E. & FOXWELL, B.M. (2008). Signalling, inflammation and arthritis: NF- $\kappa$ B and its relevance to arthritis and inflammation. pp. 584-590.
- SIMMONS, W.W., CLOSS, E.I., CUNNINGHAM, J.M., SMITH, T.W. & KELLY, R.A. (1996a). Cytokines and insulin induce cationic amino acid transporter (CAT) expression in cardiac myocytes. Regulation of L-arginine transport and no production by CAT-1, CAT-2A, and CAT-2B. *J Biol Chem*, **271**, 11694-702.
- SIMMONS, W.W., UNGUREANU-LONGROIS, D., SMITH, G.K., SMITH, T.W. & KELLY, R.A. (1996b). Glucocorticoids regulate inducible nitric oxide synthase by inhibiting

tetrahydrobiopterin synthesis and L-arginine transport. *J Biol Chem*, **271**, 23928-37.

SINGER, I.I., KAWAKA, D.W., SCOTT, S., WEIDNER, J.R., MUMFORD, R.A., RIEHL, T.E., STENSON, W.F. (1996). Expression of inducible nitric oxide synthase and nitrotyrosine in colonic epithelium in inflammatory bowel disease. *Gastroenterology*. 111(4), 871-85.

SINGH, K., BALLIGAND, J.L., FISCHER, T.A., SMITH, T.W. & KELLY, R.A. (1996). Regulation of cytokine-inducible nitric oxide synthase in cardiac myocytes and microvascular endothelial cells. Role of extracellular signal-regulated kinases 1 and 2 (ERK1/ERK2) and STAT1 alpha. *J Biol Chem*, **271**, 1111-7.

SINGH, R., WANG, Y., XIANG, Y., TANAKA, K.E., GAARDE, W.A. & CZAJA, M.J. (2009). Differential effects of JNK1 and JNK2 inhibition on murine steatohepatitis and insulin resistance. *Hepatology*, **49**, 87-96.

SINHA-HIKIM, I., SHEN, R., KOVACHEVA, E., CRUM, A., VAZIRI, N.D. & NORRIS, K.C. (2010). Inhibition of apoptotic signalling in spermine-treated vascular smooth muscle cells by a novel glutathione precursor. *Cell Biol Int*, **34**, 503-11.

SKALLI, O., BLOOM, W.S., ROPRAZ, P., AZZARONE, B. & GABBIANI, G. (1986). Cytoskeletal remodeling of rat aortic smooth muscle cells in vitro: relationships to culture conditions and analogies to in vivo situations. *J Submicrosc Cytol*, **18**, 481-93.

SMART, D.E., GREEN, K., OAKLEY, F., WEITZMAN, J.B., YANIV, M., REYNOLDS, G., MANN, J., MILLWARD-SADLER, H. & MANN, D.A. (2006). JunD is a profibrogenic transcription factor regulated by Jun N-terminal kinase-independent phosphorylation. *Hepatology*, **44**, 1432-40.

SMEAL, T., ANGEL, P., MEEK, J. & KARIN, M. (1989). Different requirements for formation of Jun: Jun and Jun: Fos complexes. pp. 2091-2100.

- SMITH, L.M., WISE, S.C., HENDRICKS, D.T., SABICHI, A.L., BOS, T., REDDY, P., BROWN, P.H. & BIRRER, M.J. (1999). cJun overexpression in MCF-7 breast cancer cells produces a tumorigenic, invasive and hormone resistant phenotype. *Oncogene*, **18**, 6063-70.
- SMITH, P.K., KROHN, R.I., HERMANSON, G.T., MALLIA, A.K., GARTNER, F.H., PROVENZANO, M.D., FUJIMOTO, E.K., GOEKE, N.M., OLSON, B.J. & KLENK, D.C. (1985). Measurement of protein using bicinchoninic acid. *Anal Biochem*, **150**, 76-85.
- SMITH, R.E., RADOMSKI, M.W., MONCADA, S. (1992). Nitric oxide mediates the vascular actions of cytokines in septic shock. *Eur J Clin Invest*. **22**(6):438-9.
- ST CLAIR, E.W., WILKINSON, W.E., LANG, T., SANDERS, L., MISUKONIS, M.A., GILKESON, G.S., PISETSKY, D.S., GRANGER, D.I. & WEINBERG, J.B. (1996). Increased expression of blood mononuclear cell nitric oxide synthase type 2 in rheumatoid arthritis patients. *J Exp Med*, **184**, 1173-8.
- STAMLER, J.S. (1994). Redox signaling: nitrosylation and related target interactions of nitric oxide. *Cell*, **78**, 931-6.
- STAMLER, J.S. & MEISSNER, G. (2001). Physiology of nitric oxide in skeletal muscle. *Physiol Rev*, **81**, 209-237.
- STAMLER, J.S., SINGEL, D.J. & LOSCALZO, J. (1992). Biochemistry of nitric oxide and its redox-activated forms. *Science*, **258**, 1898-902.
- STARLING R.C. (2005). Inducible nitric oxide synthase in severe human heart failure: impact of mechanical unloading. *J Am Coll Cardiol*. 45, 1425-7.

- STEIN, B., BALDWIN, A.S., JR., BALLARD, D.W., GREENE, W.C., ANGEL, P. & HERRLICH, P. (1993). Cross-coupling of the NF-kappa B p65 and Fos/Jun transcription factors produces potentiated biological function. *Embo J*, **12**, 3879-91.
- STEMPIN, C.C., GARRIDO, V.V., DULGERIAN, L.R. & CERBAN, F.M. (2008). Cruzipain and SP600125 induce p38 activation, alter NO/arginase balance and favor the survival of *Trypanosoma cruzi* in macrophages. *Acta Trop*, **106**, 119-27.
- STEMPIN, C.C., TANOS, T.B., COSO, O.A. & CERBAN, F.M. (2004). Arginase induction promotes *Trypanosoma cruzi* intracellular replication in Cruzipain-treated J774 cells through the activation of multiple signaling pathways. *Eur J Immunol*, **34**, 200-9.
- STEVENS, B.R., KAKUDA, D.K., YU, K., WATERS, M., VO, C.B. & RAIZADA, M.K. (1996). Induced nitric oxide synthesis is dependent on induced alternatively spliced CAT-2 encoding L-arginine transport in brain astrocytes. *J Biol Chem*, **271**, 24017-22.
- STUEHR, D.J. & NATHAN, C.F. (1989). Nitric oxide. A macrophage product responsible for cytostasis and respiratory inhibition in tumor target cells. *J Exp Med*, **169**, 1543-55.
- STUEHR, D.J., SANTOLINI, J., WANG, Z.Q., WEI, C.C. & ADAK, S. (2004). Update on mechanism and catalytic regulation in the NO synthases. *J Biol Chem*, **279**, 36167-70.
- SU, F., HUANG, H., AKIEDA, K., Occhipinti G, Donadello K, Piagnerelli M, De Backer D, Vincent JL. (2010). Effects of a selective iNOS inhibitor versus norepinephrine in the treatment of septic shock. *Shock*. **34**(3), 243-9.
- SUMARA, G., BELWAL, M. & RICCI, R. (2005). "Jnking" atherosclerosis. *Cell Mol Life Sci*, **62**, 2487-94.

- SVENSSON, C., FERNAEUS, S.Z., PART, K., REIS, K. & LAND, T. LPS-induced iNOS expression in Bv-2 cells is suppressed by an oxidative mechanism acting on the JNK pathway--a potential role for neuroprotection. *Brain Res*, **1322**, 1-7.
- SWEET, M.J., STACEY, K.J., KAKUDA, D.K., MARKOVICH, D. & HUME, D.A. (1998). IFN-gamma primes macrophage responses to bacterial DNA. *J Interferon Cytokine Res*, **18**, 263-71.
- SZABO, E., VIRAG, L., BAKONDI, E., GYURE, L., HASKO, G., BAI, P., HUNYADI, J., GERGELY, P., SZABO, C. (2007). Peroxynitrite production, DNA breakage, and poly(ADP-ribose) polymerase activation in a mouse model of oxazolone-induced contact hypersensitivity. *J Invest Dermatol*. 117, 74-80.
- SZCZEPANKIEWICZ, B.G., KOSOGOF, C., NELSON, L.T., LIU, G., LIU, B., ZHAO, H., SERBY, M.D., XIN, Z., LIU, M., GUM, R.J., HAASCH, D.L., WANG, S., CLAMPIT, J.E., JOHNSON, E.F., LUBBEN, T.H., STASHKO, M.A., OLEJNICZAK, E.T., SUN, C., DORWIN, S.A., HASKINS, K., ABAD-ZAPATERO, C., FRY, E.H., HUTCHINS, C.W., SHAM, H.L., RONDINONE, C.M. & TREVILLYAN, J.M. (2006). Aminopyridine-based c-Jun N-terminal kinase inhibitors with cellular activity and minimal cross-kinase activity. *J Med Chem*, **49**, 3563-80.
- TAKATORI, A., GEH, E., CHEN, L., ZHANG, L., MELLER, J. & XIA, Y. (2008). Differential transmission of MEKK1 morphogenetic signals by JNK1 and JNK2. *Development*, **135**, 23-32.
- TAMURA, T., JAMOUS, M.A., KITAZATO, K.T., YAGI, K., TADA, Y., UNO, M., NAGAIRO, S. (2009). Endothelial damage due to impaired nitric oxide bioavailability triggers cerebral aneurysm formation in female rats. *J Hypertens*. 27(6), 1284-92.

- TAYLOR, B.S., KIM, Y.M., WANG, Q., SHAPIRO, R.A., BILLIAR, T.R. & GELLER, D.A. (1997). Nitric oxide down-regulates hepatocyte-inducible nitric oxide synthase gene expression. *Arch Surg*, **132**, 1177-83.
- TENGGU-MUHAMMAD, T.S., HUGHES, T.R., FOKA, P., CRYER, A. & RAMJI, D.P. (2000). Cytokine-mediated differential regulation of macrophage activator protein-1 genes. *Cytokine*, **12**, 720-6.
- THOMPSON, E.J., GUPTA, A., STRATTON, M.S. & BOWDEN, G.T. (2002). Mechanism of action of a dominant negative c-jun mutant in inhibiting activator protein-1 activation. *Mol Carcinog*, **35**, 157-62.
- THOMPSON, R.W., PESCE, J.T., RAMALINGAM, T., WILSON, M.S., WHITE, S., CHEEVER, A.W., RICKLEFS, S.M., PORCELLA, S.F., LI, L., ELLIES, L.G. & WYNN, T.A. (2008). Cationic amino acid transporter-2 regulates immunity by modulating arginase activity. *PLoS Pathog*, **4**, e1000023.
- TITHERADGE, M.A. (1999). Nitric oxide in septic shock. *Biochim Biophys Acta*. 1411, 437-55.
- TKACH, V., TULCHINSKY, E., LUKANIDIN, E., VINSON, C., BOCK, E. & BEREZIN, V. (2003). Role of the Fos family members, c-Fos, Fra-1 and Fra-2, in the regulation of cell motility. *Oncogene*, **22**, 5045-54.
- TRAN, D.D., VISSER, J.J., POOL, M.O., CUESTA, M.A., HOEKMAN, K., PENA, A.S., MEUWISSEN, S.G. (1993). Enhanced systemic nitric oxide production in inflammatory bowel disease. *Lancet*. 341, 1150.
- TOURNIER, C., WHITMARSH, A.J., CAVANAGH, J., BARRETT, T. & DAVIS, R.J. (1997). Mitogen-activated protein kinase kinase 7 is an activator of the c-Jun NH2-terminal kinase. *Proc Natl Acad Sci U S A*, **94**, 7337-42.

- UPMACIS, R.K., CRABTREE, M.J., DEEB, R.S., SHEN, H., LANE, P.B., BENGUIGUI, L.E., MAEDA, N., HAJJAR, D.P., GROSS, S.S. (2007). Profound biopterin oxidation and protein tyrosine nitration in tissues of ApoE-null mice on an atherogenic diet: contribution of inducible nitric oxide synthase. *Am J Physiol Heart Circ Physiol* **293**(5), H2878-87.
- UWE REUTER, A.C.H.B.M.A.M. (2002). Nuclear factor-kappaB as a molecular target for migraine therapy. pp. 507-516.
- VAN DAM, H. & CASTELLAZZI, M. (2001). Distinct roles of Jun : Fos and Jun : ATF dimers in oncogenesis. *Oncogene*, **20**, 2453-64.
- VAN SEVENTER, G.A., MULLEN, M.M., VAN SEVENTER, J.M. (1998). Pyk2 is differentially regulated by beta1 integrin- and CD28-mediated co-stimulation in human CD4+ T lymphocytes. *Eur J Immunol.*28, 3867-77.
- VAN WINKLE, L.J., KAKUDA, D.K. & MACLEOD, C.L. (1995). Multiple components of transport are associated with murine cationic amino acid transporter (mCAT) expression in *Xenopus* oocytes. *Biochim Biophys Acta*, **1233**, 213-6.
- VARUGHESE, M., KOH, T.H. (2001). Successful use of topical nitroglycerine in ischaemia associated with umbilical arterial line in a neonate. *J Perinatol.* **21**, 556-8
- VASQUEZ, G., SANHUEZA, F., VASQUEZ, R., GONZALEZ, M., SAN MARTIN, R., CASANELLO, P. & SOBREVIA, L. (2004). Role of adenosine transport in gestational diabetes-induced L-arginine transport and nitric oxide synthesis in human umbilical vein endothelium. *J Physiol*, **560**, 111-22.
- VERHEIJ, M., BOSE, R., LIN, X.H., YAO, B., JARVIS, W.D., GRANT, S., BIRRER, M.J., SZABO, E., ZON, L.I., KYRIAKIS, J.M., HAIMOVITZ-FRIEDMAN, A., FUKS, Z. & KOLESNICK, R.N. (1996). Requirement for ceramide-initiated SAPK/JNK signalling in stress-induced apoptosis. *Nature*, **380**, 75-9.

- VESELY, P.W., STABER, P.B., HOEFLER, G. & KENNER, L. (2009). Translational regulation mechanisms of AP-1 proteins. *Mutat Res*, **682**, 7-12.
- VISIGALLI, R., BARILLI, A., PAROLARI, A., SALA, R., ROTOLI, B.M., BUSSOLATI, O., GAZZOLA, G.C. & DALL'ASTA, V. Regulation of arginine transport and metabolism by protein kinase Calpha in endothelial cells: stimulation of CAT2 transporters and arginase activity. *J Mol Cell Cardiol*, **49**, 260-70.
- VISIGALLI, R., BUSSOLATI, O., SALA, R., BARILLI, A., ROTOLI, B.M., PAROLARI, A., ALAMANNI, F., GAZZOLA, G.C. & DALL'ASTA, V. (2004). The stimulation of arginine transport by TNFalpha in human endothelial cells depends on NF-kappaB activation. *Biochim Biophys Acta*, **1664**, 45-52.
- VODOVOTZ, Y., BOGDAN, C., PAIK, J., XIE, Q.W. & NATHAN, C. (1993). Mechanisms of suppression of macrophage nitric oxide release by transforming growth factor beta. *J Exp Med*, **178**, 605-13.
- VON KNETHEN, A. & BRUNE, B. (2000). Superinduction of cyclooxygenase-2 by NO(\*) and agonist challenge involves transcriptional regulation mediated by AP-1 activation. *Biochemistry*, **39**, 1532-40.
- WAGNER, E.F. & EFERL, R. (2005). Fos/AP-1 proteins in bone and the immune system. *Immunol Rev*, **208**, 126-40.
- WAGNER, E.F. & NEBREDA, A.R. (2009). Signal integration by JNK and p38 MAPK pathways in cancer development. *Nat Rev Cancer*, **9**, 537-49.
- WAINFORD, R.D., WEAVER, R.J. & HAWKSWORTH, G.M. (2009). The immediate early genes, c-fos, c-jun and AP-1, are early markers of platinum analogue toxicity in human proximal tubular cell primary cultures. *Toxicol In Vitro*, **23**, 780-8.

- WALKER, G., PFEILSCHIFTER, J. & KUNZ, D. (1997). Mechanisms of suppression of inducible nitric-oxide synthase (iNOS) expression in interferon (IFN)-gamma-stimulated RAW 264.7 cells by dexamethasone. Evidence for glucocorticoid-induced degradation of iNOS protein by calpain as a key step in post-transcriptional regulation. *J Biol Chem*, **272**, 16679-87.
- WANASEN, N., MACLEOD, C.L., ELLIES, L.G. & SOONG, L. (2007). L-arginine and cationic amino acid transporter 2B regulate growth and survival of *Leishmania amazonensis* amastigotes in macrophages. *Infect Immun*, **75**, 2802-10.
- WANG, H., XIE, Z. & SCOTT, R.E. (1997). Induction of AP-1 activity associated with c-Jun and JunB is required for mitogenesis induced by insulin and vanadate in SV40-transformed 3T3T cells. *Mol Cell Biochem*, **168**, 21-30.
- WANG, X., DESTUMENT, A. & TOURNIER, C. (2009). Physiological roles of MKK4 and MKK7: insights from animal models. *Biochim Biophys Acta*, **1773**, 1349-57.
- WANG, X., ZHONG, Y.X., ZHANG, ZY, LU, J., LAN, M., MIAO, J.Y., Guo XG, Shi YQ, Zhao YQ, Ding J, Wu KC, Pan BR, Fan DM. (2002). Effect of L-NAME on nitric oxide and gastrointestinal motility alterations in cirrhotic rats. *World J Gastroenterol*. 8(2), 328-32.
- WANG, Y., JI, H.X., XING, S.H., PEI, D.S. & GUAN, Q.H. (2007). SP600125, a selective JNK inhibitor, protects ischemic renal injury via suppressing the extrinsic pathways of apoptosis. *Life Sci*, **80**, 2067-75.
- WATSON, D., GROVER, R., ANZUETO, A., LORENTE, J., SMITHIES, M., BELLOMO, R., GUNTUPALLI, K., GROSSMAN, S., DONALDSON, J., LEGALL, J.R.; Glaxo Wellcome International Septic Shock Study Group. (2004). Cardiovascular effects of the nitric oxide synthase inhibitor NG-methyl-L-arginine hydrochloride (546C88) in patients with septic shock: results of a randomized, double-blind, placebo-controlled multicenter study (study no. 144-002). *Crit Care Med*. 32(1), 13-20.

- WESTWICK, J.K., BIELAWSKA, A.E., DBAIBO, G., HANNUN, Y.A. & BRENNER, D.A. (1995). Ceramide activates the stress-activated protein kinases. *J Biol Chem*, **270**, 22689-92.
- WHITE, M.F., GAZZOLA, G.C. & CHRISTENSEN, H.N. (1982). Cationic amino acid transport into cultured animal cells. I. Influx into cultured human fibroblasts. *J Biol Chem*, **257**, 4443-9.
- WHITMARSH, A.J. & DAVIS, R.J. (1996). Transcription factor AP-1 regulation by mitogen-activated protein kinase signal transduction pathways. *J Mol Med*, **74**, 589-607.
- WHITMARSH, A.J., SHORE, P., SHARROCKS, A.D. & DAVIS, R.J. (1995). Integration of MAP kinase signal transduction pathways at the serum response element. *Science*, **269**, 403-7.
- WIDMANN, C., GIBSON, S., JARPE, M.B. & JOHNSON, G.L. (1999). Mitogen-activated protein kinase: conservation of a three-kinase module from yeast to human. *Physiol Rev*, **79**, 143-80.
- WIECHELMAN, K.J., BRAUN, R.D. & FITZPATRICK, J.D. (1988). Investigation of the bicinchoninic acid protein assay: identification of the groups responsible for color formation. *Anal Biochem*, **175**, 231-7.
- WILEMAN, S.M., MANN, G.E. & BAYDOUN, A.R. (1995). Induction of L-arginine transport and nitric oxide synthase in vascular smooth muscle cells: synergistic actions of pro-inflammatory cytokines and bacterial lipopolysaccharide. *Br J Pharmacol*, **116**, 3243-50.
- WON, J.S., IM, Y.B., SINGH, A.K. & SINGH, I. (2004). Dual role of cAMP in iNOS expression in glial cells and macrophages is mediated by differential

regulation of p38-MAPK/ATF-2 activation and iNOS stability. *Free Radic Biol Med*, **37**, 1834-44.

WONG, H.R., FINDER, J.D., WASSERLOOS, K., LOWENSTEIN, C.J., GELLER, D.A., BILLIAR, T.R., PITT, B.R. & DAVIES, P. (1996). Transcriptional regulation of iNOS by IL-1 beta in cultured rat pulmonary artery smooth muscle cells. *Am J Physiol*, **271**, L166-71.

WU, Y., ZHANG, X. & ZEHNER, Z.E. (2003). c-Jun and the dominant-negative mutant, TAM67, induce vimentin gene expression by interacting with the activator Sp1. *Oncogene*, **22**, 8891-901.

XIA, Z., DICKENS, M., RAINGEAUD, J., DAVIS, R.J. & GREENBERG, M.E. (1995). Opposing effects of ERK and JNK-p38 MAP kinases on apoptosis. *Science*, **270**, 1326-31.

XIE, Q.W., CHO, H.J., CALAYCAY, J., MUMFORD, R.A., SWIDEREK, K.M., LEE, T.D., DING, A., TROSO, T. & NATHAN, C. (1992). Cloning and characterization of inducible nitric oxide synthase from mouse macrophages. *Science*, **256**, 225-8.

XIE, Q.W., WHISNANT, R. & NATHAN, C. (1993). Promoter of the mouse gene encoding calcium-independent nitric oxide synthase confers inducibility by interferon gamma and bacterial lipopolysaccharide. *J Exp Med*, **177**, 1779-84.

XIE, S., ISSA, R., SUKKAR, M.B., OLTMANN, U., BHAVSAR, P.K., PAPI, A., CARAMORI, G., ADCOCK, I. & CHUNG, K.F. (2005). Induction and regulation of matrix metalloproteinase-12 in human airway smooth muscle cells. *Respir Res*, **6**, 148.

XIONG, H., ZHU, C., LI, H., CHEN, F., MAYER, L., OZATO, K., UNKELESS, J.C. & PLEVY, S.E. (2003). Complex formation of the interferon (IFN) consensus sequence-binding protein with IRF-1 is essential for murine macrophage IFN-gamma-induced iNOS gene expression. *J Biol Chem*, **278**, 2271-7.

- YAMAMOTO, K., ICHIJO, H. & KORSMEYER, S.J. (1999). BCL-2 is phosphorylated and inactivated by an ASK1/Jun N-terminal protein kinase pathway normally activated at G(2)/M. *Mol Cell Biol*, **19**, 8469-78.
- YANG, C.H., TSAI, P.S., LEE, J.J., HUANG, C.H. & HUANG, C.J. (2005). NF-kappaB inhibitors stabilize the mRNA of high-affinity type-2 cationic amino acid transporter in LPS-stimulated rat liver. *Acta Anaesthesiol Scand*, **49**, 468-76.
- YANG, R.B., MARK, M.R., GRAY, A., HUANG, A., XIE, M.H., ZHANG, M., GODDARD, A., WOOD, W.I., GURNEY, A.L. & GODOWSKI, P.J. (1998). Toll-like receptor-2 mediates lipopolysaccharide-induced cellular signalling. *Nature*, **395**, 284-8.
- YANG, S., McNULTY, S. & MEYSKENS, F.L., JR. (2004). During human melanoma progression AP-1 binding pairs are altered with loss of c-Jun in vitro. *Pigment Cell Res*, **17**, 74-83.
- YAZGAN, O. & PFARR, C.M. (2002). Regulation of two JunD isoforms by Jun N-terminal kinases. *J Biol Chem*, **277**, 29710-8.
- YEO, T.W., LAMPAH, D.A., GITAWATI, R., TJITRA, E., KENANGALEM, E., MCNEIL, Y.R., DARCY, C.J., Granger DL, Weinberg JB, Lopansri BK, Price RN, Duffull SB, Celermajer DS, Anstey NM. (2007). Impaired nitric oxide bioavailability and L-arginine reversible endothelial dysfunction in adults with falciparum malaria. *J Exp Med*. 204(11), 2693-704.
- YIN, Q., WANG, X., MCBRIDE, J., FEWELL, C. & FLEMINGTON, E. (2008). B-cell receptor activation induces BIC/miR-155 expression through a conserved AP-1 element. *J Biol Chem*, **283**, 2654-62.
- YIN, Y., WANG, S., SUN, Y., MATT, Y., COLBURN, N.H., SHU, Y. & HAN, X. (2009). JNK/AP-1 pathway is involved in tumor necrosis factor-alpha induced

expression of vascular endothelial growth factor in MCF7 cells. *Biomed Pharmacother.*

YOSHIOKA, Y., TAKEDA, N., YAMAMURO, A., KASAI, A. & MAEDA, S. Nitric Oxide Inhibits Lipopolysaccharide-Induced Inducible Nitric Oxide Synthase Expression and Its Own Production Through the cGMP Signaling Pathway in Murine Microglia BV-2 Cells. *J Pharmacol Sci.*

YOUNG, M.R. & COLBURN, N.H. (2006). Fra-1 a target for cancer prevention or intervention. *Gene*, **379**, 1-11.

YOUNG, M.R., LI, J.J., RINCON, M., FLAVELL, R.A., SATHYANARAYANA, B.K., HUNZIKER, R. & COLBURN, N. (1999). Transgenic mice demonstrate AP-1 (activator protein-1) transactivation is required for tumor promotion. *Proc Natl Acad Sci U S A*, **96**, 9827-32.

YOUNG, M.R., YANG, H.-S. & COLBURN, N.H. (2003). Promising molecular targets for cancer prevention: AP-1, NF-[kappa]B and Pcd4. *Trends in Molecular Medicine*, **9**, 36-41.

ZHANG, H., CHEN, X., TENG, X., SNEAD, C. & CATRAVAS, J.D. (1998). Molecular cloning and analysis of the rat inducible nitric oxide synthase gene promoter in aortic smooth muscle cells. *Biochem Pharmacol*, **55**, 1873-80.

ZHANG, H., TENG, X., SNEAD, C. & CATRAVAS, J.D. (2000). Non-NF-kappaB elements are required for full induction of the rat type II nitric oxide synthase in vascular smooth muscle cells. *Br J Pharmacol*, **130**, 270-8.

ZHANG, H.W., WANG, X., ZONG, Z.H., HUO, X. & ZHANG, Q. (2009). AP-1 inhibits expression of MMP-2/9 and its effects on rat smooth muscle cells. *J Surg Res*, **157**, e31-7.

- ZHANG, X., LAUBACH, V.E., ALLEY, E.W., EDWARDS, K.A., SHERMAN, P.A., RUSSELL, S.W. & MURPHY, W.J. (1996). Transcriptional basis for hyporesponsiveness of the human inducible nitric oxide synthase gene to lipopolysaccharide/interferon-gamma. *J Leukoc Biol*, **59**, 575-85.
- ZHANG, Y., JANSSENS, S.P., WINGLER, K., SCHMIDT, H.H., MOENS, A.L. (2011). Modulating endothelial nitric oxide synthase: a new cardiovascular therapeutic strategy. *Am J Physiol Heart Circ Physiol*. **301**(3):H634-46.
- ZINGARELLI, B., HAKE, P.W., YANG, Z., O'CONNOR, M., DENENBERG, A., WONG, H.R. (2002). Nitric oxide and acetaminophen-mediated oxidative injury: modulation of interleukin-1-induced nitric oxide synthesis in cultured rat hepatocytes. *J Pharmacol Exp Ther*. **282**, 1072-83
- ZIPPER, H., BRUNNER, H., BERNHAGEN, J. & VITZTHUM, F. (2004). Investigations on DNA intercalation and surface binding by SYBR Green I, its structure determination and methodological implications. *Nucleic Acids Res*, **32**, e103.

# Appendix

## Appendix 1

Griess reagent A (1000 ml): 2% Sulfanilamideamine in 10% Phosphoric acid ( $\text{H}_3\text{PO}_4$ )

Griess reagent B (1000 ml): 2% Naphthylethylenediamine in  $\text{dH}_2\text{O}$

On the day, mix them in equal volume

## Appendix 2

### Solutions for western blot

#### 1. Sample buffer: (50 ml):

Ingredients	Function
1.51g Tris (250 $\mu\text{M}$ ) and adjust the pH to 6.8	Maintains pH
2g SDS (4%)	Makes protein linear and provides negative charge
5 ml glycerol (10%)	Thickening agent
1 ml $\beta$ -mercaptoethanol (2%)	Breaks bonds to make proteins linear
0.003g Bromophenol blue (0.006%)	Colouring dye

First dissolve Tris in about 25 ml of water and adjust the pH to 6.8 and then add other ingredients and make up the final volume to 50 ml with DDW (double distilled water).

#### 2. Ammonium Persulfate (APS) 10%

- Dissolve 2g of APS (10%) in to 20 ml of DDW.

Aliquot in 150 $\mu\text{l}$  each and store at  $-20^\circ\text{C}$ .

Ammonium persulfate is used as starting agent to make polyacrylamide gel and it is quite unstable so, it should be stored at -20°C.

### 3. Resolving Buffer: (1.5 M Tris-HCl)

- Dissolve 91.05g of Tris in 500ml DDW and adjust the pH to 8.8.

### 4. Stacking Buffer: (0.5 M Tris).

- Dissolve 30.275g of Tris in 500ml of DDW and adjust the pH to 6.8.

### 5. 10% SDS:

- Dissolve 10g of SDS in 100ml of DDW. (keep it at room temperature)

### 6. Transfer Buffer :( 10X)

Ingredients	Function
29.3g glycine(39mM)	
58.2g Tris (48mM)	Maintains pH
3.75g SDS (0.0375%)	Provides negative charge to proteins.

First, dissolve all the ingredients and then adjust the pH to 8.3 and make it up to 1 litre in DDW. On the day, take 100 ml of transfer buffer+200 ml methanol and make it up to 1 litre with DDW. Methanol prevents gel expansion and keeps protein absorbed on the membrane.

## 7. Washing Buffer: (10X)

Ingredients	Function
12.1g Tris(10mM)	Maintains pH
58.4g NaCl(100mM)	Removes weakly attached proteins from the membrane by electrically binding.

Dissolve Tris and adjust the pH to 7.5 and then dissolve NaCl and make up to 1 litre in DDW. On the day, make it 1% and add 2 ml of Tween-20 for 2 litres of 1X washing buffer.

## 8. Stripping Buffer: (1X)

- Tris-7.578g/100ml (62.5 mM)
- $\beta$ -mercaptoethanol- 700 $\mu$ l/100ml (0.7%v/v)
- SDS-2g/100ml (0.2%w/v)

Note: Add  $\beta$ -mercaptoethanol and SDS on the day in the stock solution made up with Tris.

## 9. Staining solution: (1X) (Store at room temperature)

- Coomassine brilliant blue R-250-1g
- Methanol-450ml
- DDW-450ml
- Acetic acid-100ml

## 10. Destaining solution: (1X) (Store at room temperature)

- Methanol-500ml(20%)
- Acetic acid-175ml(7%)
- DDW-1825ml(73%)

### 11. Tank Buffer: (10X) (Store at room temperature)

- Tris-30.27g/l
- Glycine-144.14g/l
- SDS-10g/l

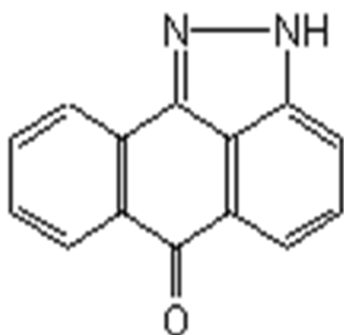
<b>Resolving gel</b>	<b>10ml (2gels)</b>	<b>20ml (4gels)</b>	<b>30ml (6gels)</b>	<b>50ml</b>
Ultra pure water from BDH	4.64ml	9.28ml	13.92ml	23.2ml
30% Acrylamide bisacrylamide mixture	2.66ml	5.32ml	7.98ml	12.5ml
Resolving buffer	2.5ml	5ml	7.5ml	12.5ml
10% SDS solution	100µl	200µl	300µl	500µl
10% Ammonium persulphate (starting agent)	100µl	200µl	300µl	500µl
TEMED (catalytic agent)	6µl	12µl	18µl	30µl

<b>Stacking gel</b>	<b>4ml (2 gels)</b>	<b>10ml (4 gels)</b>	<b>20ml (6 gels)</b>	<b>30ml</b>
Ultra pure water from BDH	2.44ml	6.1ml	12.2ml	18.3ml
30% Acrylamide bisacrylamide mixture	0.52ml	1.3ml	2.6ml	3.9ml
Stacking buffer	1ml	2.5ml	5ml	7.5ml
10% SDS solution	40µl	100µl	200µl	300µl
10% Ammonium persulphate	20µl	50µl	100µl	150µl
TEMED	4µl	10µl	20µl	30µl

Reagent for Blocking Buffer	Quantity
Washing buffer	10ml
Tween 20	100µl
5% fat free milk	5g
DDW	90ml

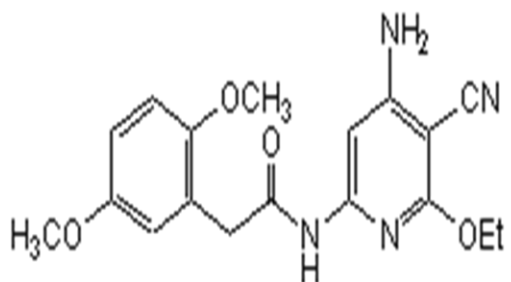
### Appendix 3

#### The JNK inhibitor structure



**JNK Inhibitor II (SP600125)**

Anthra[1,9-*cd*]pyrazol-6(2*H*)-one, 1,9-pyrazoloanthrone, SP600125, SAPK Inhibitor II

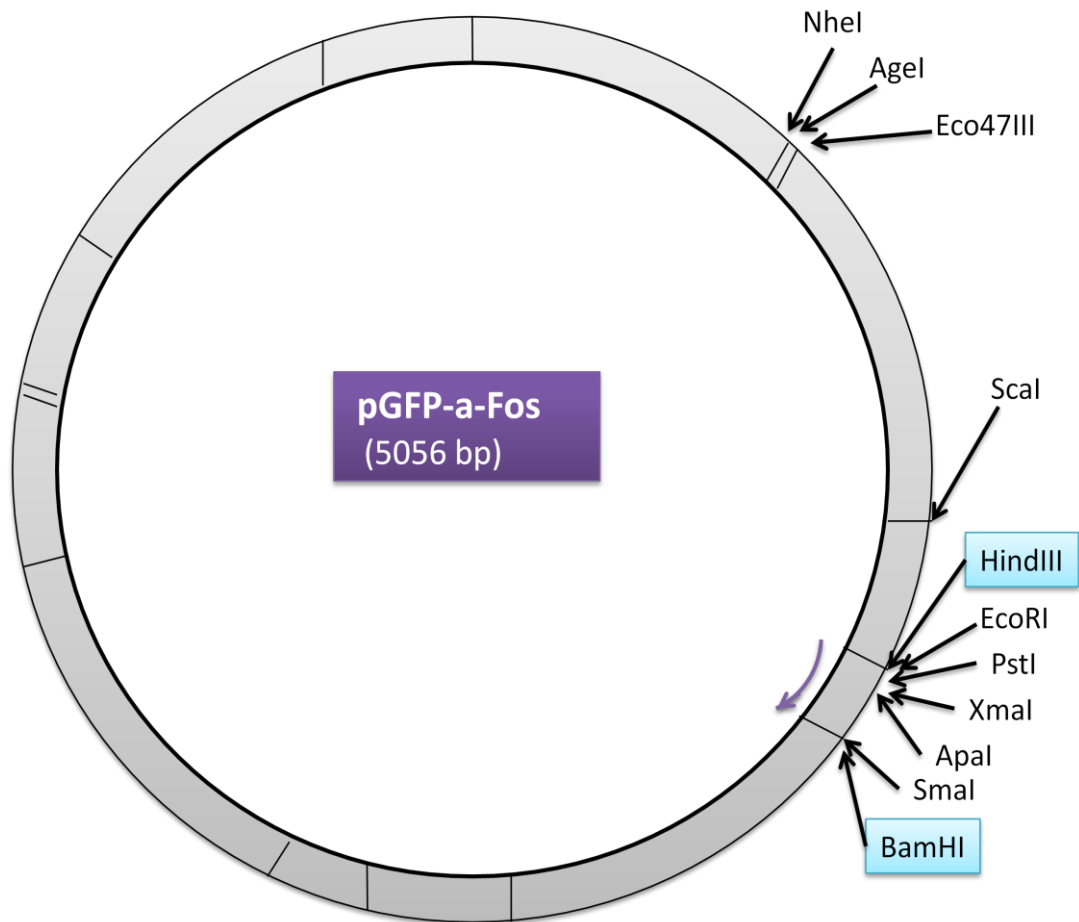


**JNK Inhibitor VIII**

N-(4-Amino-5-cyano-6-ethoxypyridin-2-yl)-2-(2,5-dimethoxyphenyl)acetamide

## The Plasmid map

### a-Fos

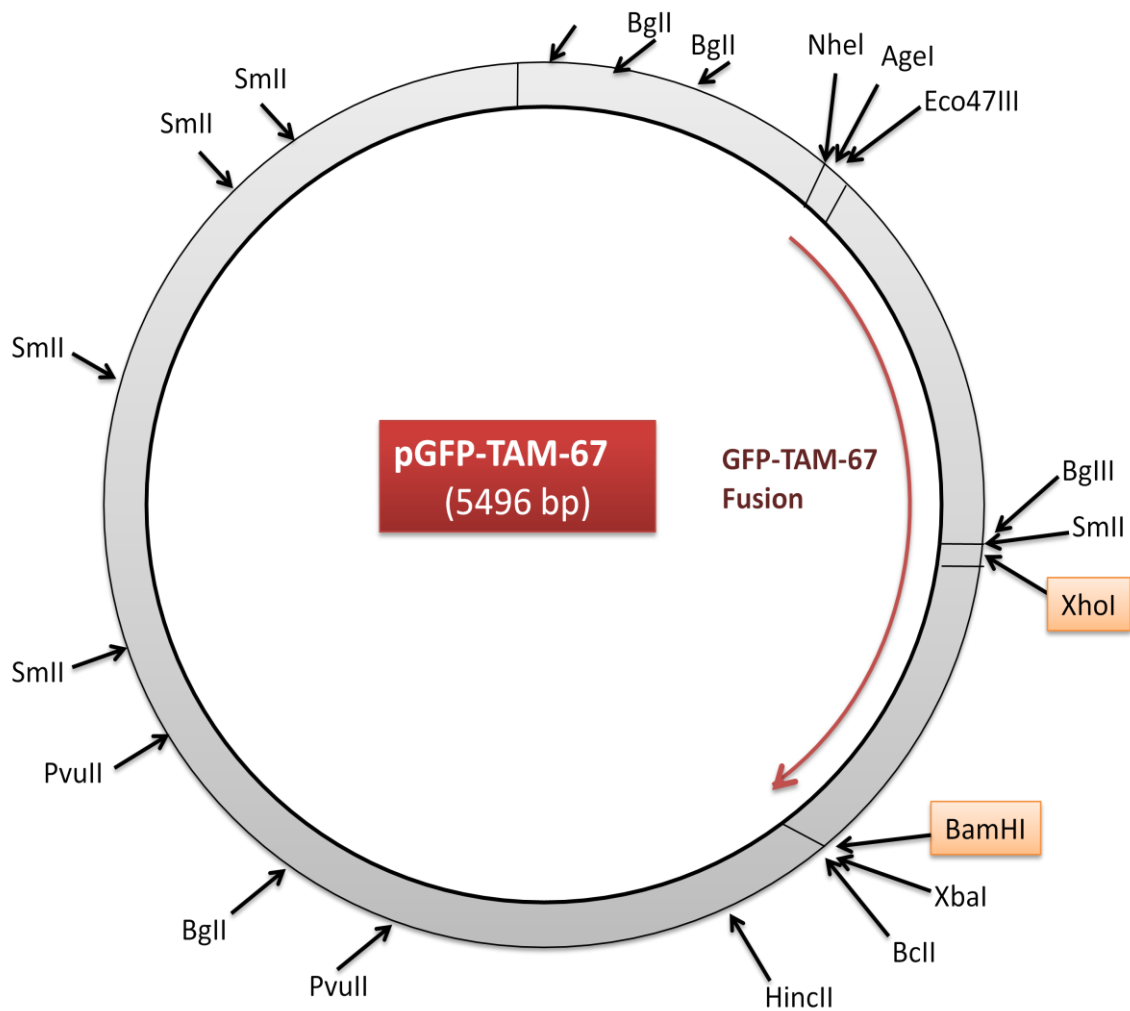


### The pGFP-a-Fos plasmid map

BamHI-HindIII fragment of pCMV a-Fos cloned into the BglIII-HindIII site of pEGFP-C3 Kanamycin resistance in *E. Coli*.

## The plasmid map

### TAM-67



### The pGFP-TAM-67 plasmid map

TAM-67 was subcloned as described (Hennigan *et al.*, 2001). The plasmid pGFP-TAM-67 encodes Kanamycin resistance in *E. Coli*.

## Materials

Absolute ethanol	Fluka
Acrylamide, ProtoGel	National Diagnostics
Agarose	Sigma
Ammonium persulphate	Acros Organics
Anti- $\alpha$ monoclonal smooth muscle actin	Sigma
Anti-biotin, HRP-linked antibody, Detection Pack	Cell Signalling
Anti-mouse IgG, FITC Conjugate developed in rabbit	Sigma
Anti-iNOS monoclonal antibody	Transduction Laboratories
Anti- $\beta$ actin monoclonal antibody	Sigma
Anti-mouse secondary antibody, Goat anti-mouse HRP	Transduction Labs
BamHI	Promega
BCA Protein Assay Reagents	Pierce Perbio
BSA (Bovine Albumin Serum) essentially fatty acid free	Sigma
Calcium chloride 2-hydrate	AnalaR
Chloroform >99.8 %	Sigma-Aldrich
Coomassie brilliant blue	Fluka
Developer (GBX) Kodak Replenisher	Sigma
D(+)-Glucose	AnalaR
DMEM, Dulbecco's Modified Eagle's Medium	GIBCO

ECL Western Blotting Detection Reagents	GE Healthcare / Amersham
EDTA	Sigma
Ethanol	BDH
Extra Thick Blot Paper	BIO-RAD
Fixer (GBX) Kodak Replenisher	Sigma
Foetal Bovine Serum	GIBCO Invitrogen
Formaldehyde	Sigma
Glycerol	Sigma
Glycine	Fisher Scientific
Goat anti-mouse HRP	Transduction Labs
JNK Inhibitor VIII	Calbiochem
HEPES	Fisher Scientific
Hyperfilm (ECK & X-ray)	Amersham
Horseradish Peroxidase-linked Antibody	Cell Signalling
[H3]L-arginine (2 $\mu$ Ci/ml)	Amersham Biosciences
IMS, Industrial Methylated Spirit	BDH
Isopropanol	BDH Biochemical AnalaR
Interferon-gamma, Rat, Recombinant, E. Coli	Calbiochem
Kanamycin	Sigma
KCl, potassium chloride	BDH
L-(+)-Arginin Hydrochloride	ALDRICH

Lipofectamine2000 Reagent	Invitrogen
LPS (Lipopolysaccharide from <i>E.Coli</i> )	Fluka
Liquiscint Scintillation Liquid	National Diagnostics
Magnesium chloride 6-hydrate	AnalaR
2-Mercaptoethanol	Sigma
Methanol	Fisher Scientific
MTT (5-Dimethylthiazol-2-yl)-2,5-diphenyltetrazolium bromide)	Sigma
NNN'N'-tetramethylethylenediamine (TEMED)	Electran
Na <sub>3</sub> VO <sub>4</sub> , Sodium Orthovanadate	Sigma
NaCl, Sodium Chloride	BDH
NaF, Sodium Fluoride	Sigma
NaH <sub>2</sub> PO <sub>4</sub> , Sodium Dihydrogen Orthophosphate 1-hydrate	BDH
NaHCO <sub>3</sub> , Sodium Bicarbonate	BDH
NaOH, Sodium hydroxide	Sigma
NaNO <sub>3</sub> , Sodium Nitrate	Sigma
Optimem 1	Invitrogen Corporation
PBS, Phosphate Buffered Saline	GIBCO
Penicillin-Streptomycin	GIBCO Invitrogen
Phosphate buffered saline tablet (PBS)	Sigma
Potassium chloride	AnalaR
PVDF membrane, Membrane Immobilon-P transfere	Millipore

Scintillation Liquid (Liquiscint)	National Diagnostics
SDS, Sodium Dodecyl Sulphate	Sigma
SP600125	Calbiochem
TRIS Base	Fisher Scientific
Tween 20	Sigma
Trypsin-EDTA	GIBCO
XhoI (Restriction Enzyme)	Promega